INFORMATION TO USERS

This manuscript has been reproduced from the microfilm master. UMI films the text directly from the original or copy submitted. Thus, some thesis and dissertation copies are in typewriter face, while others may be from any type of computer printer.

The quality of this reproduction is dependent upon the quality of the copy submitted. Broken or indistinct print, colored or poor quality illustrations and photographs, print bleedthrough, substandard margins, and improper alignment can adversely affect reproduction.

In the unlikely event that the author did not send UMI a complete manuscript and there are missing pages, these will be noted. Also, if unauthorized copyright material had to be removed, a note will indicate the deletion.

Oversize materials (e.g., maps, drawings, charts) are reproduced by sectioning the original, beginning at the upper left-hand corner and continuing from left to right in equal sections with small overlaps.

Photographs included in the original manuscript have been reproduced xerographically in this copy. Higher quality 6" x 9" black and white photographic prints are available for any photographs or illustrations appearing in this copy for an additional charge. Contact UMI directly to order.

ProQuest Information and Learning
300 North Zeeb Road, Ann Arbor, MI 48106-1346 USA
800-521-0600

Université d'Ottawa · University of Ottawa

HCO_3^-/Cl^- Exchanger Activity is Cell Cycle Dependent During Mouse Oocyte Meiotic Maturation and Egg Activation.

Karen P. Phillips

A thesis submitted to the School of Graduate Studies and Research, University of Ottawa, in partial fulfilment of the requirements for the degree of Doctor of Philosophy.

Department of Cellular and Molecular Medicine. Faculty of Medicine.

ABSTRACT

In the sea urchin, some other marine invertebrates, and the frog, *Xenopus*, egg activation at fertilization is accompanied by an increase in intracellular pH (pH_i) resulting from activation of a pH_i regulatory transporter. As pH_i regulation had not been studied in a mammalian model, I investigated pH_i regulation in the mouse egg during meiotic maturation and egg activation. Steady-state pH_i was measured using the pH_i sensitive fluorophore SNARF-1-AM in germinal vesicle (GV) oocytes, ovulated eggs, and zygotes. No sustained changes in pH_i occurred after germinal vesicle breakdown (GVBD), fertilization or during parthenogenetic egg activation.

HCO_3^-/Cl^- exchanger activity was measured in unfertilized eggs and zygotes. Zygotes exhibited a marked intracellular alkalinization and Cl^- efflux upon external Cl^- removal, which is indicative of active HCO_3^-/Cl^- exchangers, in contrast to the very small response observed in eggs. Furthermore, while zygotes quickly recovered from an induced alkalosis, eggs exhibited only a slow, incomplete recovery. HCO_3^-/Cl^- exchanger activity was upregulated following in vitro fertilization (IVF) becoming maximal after 7-9 h. Activation of HCO_3^-/Cl^- exchanger activity appeared to occur by activation of existing, inactive exchangers upregulation of activity was unaffected by inhibition of protein synthesis or by disruption of the Golgi apparatus or the cytoskeleton. HCO_3^-/Cl^- exchanger upregulation was also independent of PKC and cAMP-dependent pathways. Using cycloheximide-activated eggs, HCO_3^-/Cl^- exchanger activation was independent of the repetitive $Ca^{2+}{}_i$ transients.

HCO_3^-/Cl^- exchanger activity, measured during the cell cycle, was robust in GV

eggs, becoming downregulated during meiotic maturation. Low HCO_3^-/Cl^- exchanger activity was a feature of meiotic metaphase only, as activity was not downregulated during metaphase of the first cell cycle. HCO_3^-/Cl^- exchanger upregulation was dependent on an intact metaphase II spindle and could be blocked by the phosphatase inhibitor okadaic acid following Sr^{2+} activation. Finally, HCO_3^-/Cl^- exchanger activity could be activated in unfertilized eggs by the MEK inhibitor U0126. This suggests that HCO_3^-/Cl^- exchanger activity is upregulated at fertilization in the mouse by a cell cycle-dependent mechanism that may involve the MAPK pathway.

TABLE OF CONTENTS

LIST OF FIGURES

AUTHORIZATION

Permission was granted to include Figures 23-25, 27-29 and 30, previously published in *Intracellular pH regulation by HCO_3^-/Cl^- exchange is activated during early mouse zygote development* by K. Phillips and J. Baltz, from Developmental Biology, Volume 208, 392-405, copyright © 1999 by Academic Press, reprinted by permission of the publisher.

Permission was granted to include Figures 47-50, previously published in *Intracellular pH regulation in human preimplantation embryos* by K. Phillips, M-C Léveillé, P. Claman and J. Baltz, from Human Reproduction, Volume 15, 896-904, copyright © 2000 by European Society of Human Reproduction and Embryology, reproduced by permission of Oxford University Press/Human Reproduction.

LIST OF ABBREVIATIONS

5-HT	5-hydroxtryptamine
AC	adenylate cyclase
AE1	anion exchanger isoform 1
AE2	anion exchanger isoform 2
AE3	anion exchanger isoform 3
AM	acetoxymethyl or acetate esters
AMIL	amiloride
ANK	ankyrin
ANOVA	analysis of variance
APC	anaphase promoting complex
ATP	adenosine trisphosphate
BAPTA-AM	*N,N'*[1,2-ethanediylbis(oxy-2,1-phenylene)]bis[*N*-[2-](acetyloxy)-methoxy]2-oxoethyl]]-, bis[(acetyloxy)methyl] ester
bp	base pairs
BSA	bovine serum albumin
C-terminal	carboxy terminal
CA	carbonic anhydrase
Ca^{2+}_i	intracellular Ca^{2+}
CAK	cdc2 activating kinase
CaM	calmodulin
CaMKII	Ca^{2+} calmodulin kinase II
cADPR	adenosine 5'-cyclic diphosphoribose
cAMP	adenosine 3-5-cyclic monophosphate
$cAMP_i$	intracellular cAMP
CCD	charge-coupled device
cDNA	complementary deoxyribonucleic acid
CHP	calcineurin B homolog protein
CICR	Ca^{2+}-induced Ca^{2+} release
CSF	cytostatic factor
DAG	diacylglycerol
dbcAMP	dibutyrl adenosine 3-5-cyclic monophosphate
deme	demecolcine
DIDS	4,4'-diisothiocyanostilene-2,2'-disulfonic acid
DMSO	dimethyl sulfoxide
E_2	estradiol
EIPA	5-(*N*-ethyl-*N*-isopropyl)amiloride, hydrochloride
EM	emission of excitation photons
ER	endoplasmic reticulum
ERK	extracellular signal regulated kinases
EX	absorption of excitation photons
Fig.	figure
FSH	follicle stimulating hormone

Fura-2	(5-oxazolecarboxylic acid, 2-(6-(bis(2-((acetyloxy)methoxy)-2-oxoethyl)amino)-5-(2-(2-(bis(2-((acetyloxy)methoxy)-2-oxoethyl)amino)-5methylphenoxy)ethoxy)-2-bensofuranyl)-, (acetyloxy)methyl ester
GDP	guanosine diphosphate
GDPβS	guanosine-5'-O-(2-thiodiphosphate)
GI	gastrointestinal
Glu-	glutamate
GnRH	gonadotropin releasing hormone
GV	germinal vesicle
GVBD	germinal vesicle breakdown
h	hour
H-89	N-[2-((p-Bromocinnamyl)amino)ethyl]-5-isoquinolinesulfonamide, HCl
H_2DIDS	4,4'-diisothiocyanatodihydrostilbene-2,2'-disulfonic acid, disodium salt
hCG	human chorionic gonadotropin
His	histidine
hMG	human menopausal gonadotropin
HSP	heat shock protein
HTF	Human Tubal Fluid™
Hx	hypoxanthine
IBMX	3-isobutyl-1-methylxanthine
ICM	inner cell mass
ICSI	intracytoplasmic sperm injection
IICR	IP_3-induced Ca^{2+}_i release
IP_3	inositol trisphophate
IVF	in vitro fertilization
K_i	inhibition coefficient
KSOM	K^+ supplemented optimized medium
LH	luteinizing hormone
M	number of dishes
MAPK	mitogen-activated kinase
MAPKK	mitogen-activated kinase kinase
MAS	meiosis activating sterols
MI	metaphase I
MII	metaphase II
MIII	metaphase III
min	minute
$mos^{-/-}$	mos knockout
MPF	maturation-promoting factor or metaphase-promoting factor
MQAE	(N-(6-methoxyquinolyl)acetoethyl ester
mRNA	messenger ribonucleic acid
MTOC	microtubule organizing centers
n	number of embryos

N	number of experiments
N-terminal	amino terminal
NAADP	nicotinate-adenine dinucleotide phosphate
nANOVA	non-parametric ANOVA
NBC1	Na^+-HCO_3^- cotransporter isoform
NEBD	nuclear envelope breakdown
NHE1-5	Na^+/H^+ antiporter isoform 1-5
OA	okadaic acid
OMI	oocyte maturation inhibitor
OPU	oocyte pick-up or retrieval
p	statistical significance value
PB	polar body
PB1	first polar body
PB2	second polar body
PBS	phosphate buffered saline
PDD	phorbol-12,13-didecanoate
PDE	phosphodiesterase
pH_i	intracellular pH
pH_o	extracellular pH
pHU/min	pH units per min
PIP2	phosphoinositol diphosphate
PK-X	unidentified or unknown protein kinase
PKA	protein kinase A or cAMP dependent protein kinase
PKC	protein kinase C
PLC	phospholipase C
PMA	phorbol 12-myristate 13-acetate
PMSG	pregnant mares' serum gondadotropin
PN	pronucleus/pronuclei
PP1	protein phosphatase I
PP2	protein phosphatase 2
PVP	polyvinylpyrrolidone
RER	rough endoplasmic reticulum
RT-PCR	reverse-transcribed polymerize chain reaction
RyR	ryanodine receptor
s.e.m.	standard error of the mean
S_0	ground energy state
S_1	singlet excited state
sAC	soluble adenylate cyclase
SD	standard deviation
Ser	serine
SNARF-1-AM	carboxyseminaphthorhodafluor-1-acetoxymethyl ester
TE	trophectoderm
Thr	threonine
Tyr	tyrosine
wks	weeks

ZGA	zygotic gene activation
ZP2 and ZP3	zona sperm binding receptors

ACKNOWLEDGEMENTS

This work was conducted in the laboratory of Dr. Jay Baltz. I would like to thank him for his guidance, experience and insight during this research project. He has challenged me time and time again with his dizzying intellect and unfortunate superiority in all things grammatical and electrical! Very right *and* left-brained is he! With his quick wit and wry sense of humour, my laboratory mix-ups and conference hangovers quickly became legendary foibles. Jay has provided many opportunities, rewarded my successes and has not appeared to dwell too heavily on the failures. The embodiment of the word "obstreperous", he has defended my right to play loud music in the lab at 7:00 am and will even tolerate YMCA, although only in very low doses.

I would like to thank the members of my advisory committee, Dr. Richard Hébert (Department of Cellular and Molecular Medicine, University of Ottawa), Dr. Paul Morley (Senior Scientist, National Research Council, Ottawa, ON) and Dr. Barbara Vanderhyden (Departments of Obstetrics & Gynecology and Cellular and Molecular Medicine, University of Ottawa) who provided significant suggestions concerning the direction and scope of this work. I would particularly like to thank Dr. Barbara Vanderhyden for her incredible enthusiasm and love of science. I was happy to be a part of her Let's Talk Science program which contributed significantly to my own interests in science and confidence in public speaking.

I would like to thank the medical and laboratory staff at the Human IVF Clinic, Ottawa Hospital-Civic Site. The opportunity to work as an embryologist at the IVF clinic has provided a focus for my scientific interest and a definite career objective. Special

thanks to the embryology staff, Dianne Hoppe, Carole Lawrence, Robert Heudes and Korinne Hutt, Peggy Philion, Michele Schonfeldt and Alena Spacek for their support and encouragement. The nursing and support staff of the IVF clinic are incredibly genuine, caring and competent individuals who have always made me feel at home in the IVF family. I would also like to acknowledge the medical staff, Drs. Paul Claman, Art Leader, Delani Kotarba and Jay Spence for their patience during my embryology training and their valuable experience. Finally, this incredible opportunity would not have been possible without Dr. Marie-Claude Léveillé, Laboratory Director of the Human IVF Clinic. Her tireless devotion to excellence in the field of embryology has produced a world class IVF laboratory with exacting standards of perfection. Her organizational skills and attention to detail balanced with flawless techniques has set the standard I hope to one day follow.

This research project could not have been possible without the excellent technical support in the laboratory. Ms. Kerri Dawson contributed significantly to this project by providing not only superb technical support but also a laboratory that was well organized. Her adage "a well-stocked lab is a happy lab" was all too true because of this. Additionally, Kerri contributed to many helpful discussions, shared much over countless coffee breaks and celebrated many victories and defeats.

This torch was next passed to Mrs. Mary-Anne Hammer whose own graduate student days enabled her to identify with much of this process. Thank you for understanding that the crazy night and early morning schedule required to complete most of experiments precluded my participation in the mouse superovulation injections. Thanks also to Mrs. Marika Kolajova for her support and her computer!

I would also like to acknowledge the contributions of Jennifer (Collins) Roberts. As a summer student there is no equal. Jen's work ethic is surpassed by none. She has challenged traditional limitations of working during her summer breaks. She has applied her love of science and dedication to the craft until her goals were achieved, tailoring her schedule to my requests to begin experiments at dawn. Her involvement in the U0126 experiments, media preparation and morphology assessments is greatly appreciated.

This research could not have been completed without the guiding patience and understanding of Dr. Yuyuan Zhao. Yuyuan began his post-doc at the same time I began my graduate studies with Dr. Jay Baltz. While I struggled to adapt to this foreign lab environment, Yuyan patiently, ever so patiently, answered my questions, improved my techniques and shared his culture and his family with me. It was with great sadness that I learned of Yuyuan's untimely death and I mourn with many others this gentle father and scientist who will be greatly missed.

I also thank the staff of the Ottawa Hospital Loeb Research Institute Animal Care Unit for their excellent care of the mice used in this study. Thanks also the computer support staff at the Loeb for their quick responses to many computer emergencies. I would also like to thank Terri VanGulik, Alana Summers and Donna Mulder for their invaluable adminstrative assistance.

As I thank many individuals for knowledge and experience they have imparted to me, I must also thank those whom I have met at the Loeb Institute who have shared in my struggles as I have shared in theirs. Thanks to David Boone, Ron Booth, Danielle Schneiderman, Jon Soboloff, Candace Steeves and Tanya Taylor. Together with Kerri Dawson, these people became my friends, my confidantes, my coffee buddies, my

sounding boards and my baseball/basketball teammates. Just as many of them have graduated and found a life on 'the outside', now it is my turn.

This work was supported by a grant from the Medical Research Council of Canada (MT-12040; to Jay M. Baltz). The human embryo pH_i project was supported by the Division of Reproductive Medicine, Department of Obstetrics and Gynecology, University of Ottawa. I gratefully acknowledge the support of the Bombardier Fondation for Higher Education, Ontario Graduate Science and Technology Studentship and Ontario Graduate Scholarship programs.

While I was blessed with many friends on the 'inside', I was equally blessed with friends and family on the outside. How can I acknowledge the tremendous friendships I have made during these past few years that will continue to provide a touchstone of support, encouragement, laughter and tears in everything that I do. Thank you to my friend David Silverman for his support, many late night chats and the benefit of his own graduate school experience.

Thank you to my friend Jacqui Synard for the endless conversations about research and ethics, about integrity and about life. She strives for balance in her life and provides an excellent example of what can be achieved if one is willing to be flexible and creative.

Thank you to my friend Lisa Orr, who has passionately disagreed with the use of animals in this research, but because she is my friend, has tempered her beliefs with understanding. Her encouragement, support, humour and love of all things furry has led me to question the ethics of animal research and value the sacrifices made on behalf of this project. It is the ability to question which lies at the heart of an individual's tenets

and beliefs. I thank her for asking the question, for it is the question which has made me a more responsible and ethical scientist.

Thanks to my friend Carolyn Stanzel. I am rich indeed to have her friendship and support for the past 25 years and counting. Her courage and resiliance in the face of such extreme duress in something which I admire as a fellow survivor. Her humour, practicality, unique perspectives and willingessness to drive anywhere, anytime makes her an incredible friend.

Thank you to my friend Heather Paul for her wonderful example of assertiveness, professionalism and compassion. Her integrity, responsibility and ideals are carried with her as a badge of honour. I have learned much about myself, friendship and my own goals through my many, many conversations with her.

I would also like to thank the two Kathy's in my life. My friend Kathy is another harbinger from Smiths Falls whose support and understanding during the past few years is that much more meaningful upon completion of her own graduate studies. My step-mother Kathy has provided a wonderful home for the holidays, a keen interest in my studies and a newfound friendship. Thank you both.

None of this would have been possible without the love and encouragement of my father, Bob Phillips. His refusal to define limitations has revealed many roads, some travelled, some yet to be explored. The value he placed on education, knowledge of science and math in addition to a good work ethic has provided an important foundation from which anything and everything can be possible.

If my father provided a foundation, it was not built alone. My mother, Patricia Phillips valued language, words, mysteries and solutions. It is this love of mystery that interests the scientist, but the quest for the solution that provides the driving force. As

someone who befriended all who knew her, I thank my mother for the woman that she was and the woman that I am today. I would like to dedicate this thesis to the memory of my mother, whom I believe would have been proud of the journey.

INTRODUCTION

I. FOLLICULAR, OOCYTE, AND EARLY EMBRYO DEVELOPMENT

Follicular development

Mammalian ovaries contain thousands of primordial follicles which represent the lifetime supply of female gametes (Fig. 1). Primordial follicles consist of a single layer of flattened pre-granulosa cells which surround the *primordial oocyte* which is arrested in prophase of meiosis I (Fig. 2). Primordial follicles develop during the late stages of gestation and are then progressively recruited to enter a growth phase by an unknown signal (Eppig et al., 1996; Wandji et al., 1997). Once recruited, the activated *primary preantral follicle* and oocyte undergo many changes including growth, resumption of meiosis, and differentiation of the follicular somatic cells (Qu et al., 2000). Once primary follicles have been recruited, their growth and development is regulated by two major reproductive hormones produced by the anterior pituitary- follicle stimulating hormone (FSH) and luteinizing hormone (LH) which stimulate differentiation and growth of the follicular granulosa cells and theca cells (Wandji et al., 1997; Eppig et al., 1998).

Oocytes within preantral follicles undergo a greater than 30-fold increase in volume which is correlated with increased protein content (Schultz and Wassarman, 1977), as essential resources required for maturation, fertilization and embryo development are synthesized and accumulated by the oocyte (Bleil and Wassarman, 1980). FSH is required for follicular growth and formation of the antral cavity (Eppig et al., 1996). Oocytes in early antral follicles are competent to resume meiosis and undergo

Figure 1. Ovarian Cycle. *A. Schematic of the mammalian ovary with developing follicles.* 1. Primordial follicle. 2. Primary follicle. 3. Preantral follicle 4. Antral follicle. 5. Ovulation. 6. Cumulus-oocyte-complex. 7. Corpus luteum. *B. Antral follicle.* GV-oocyte enclosed by zona pellucida and granulosa cells (cumulus cells). Follicle contains prominant antral cavity, surrounded by granulosa and theca cells.

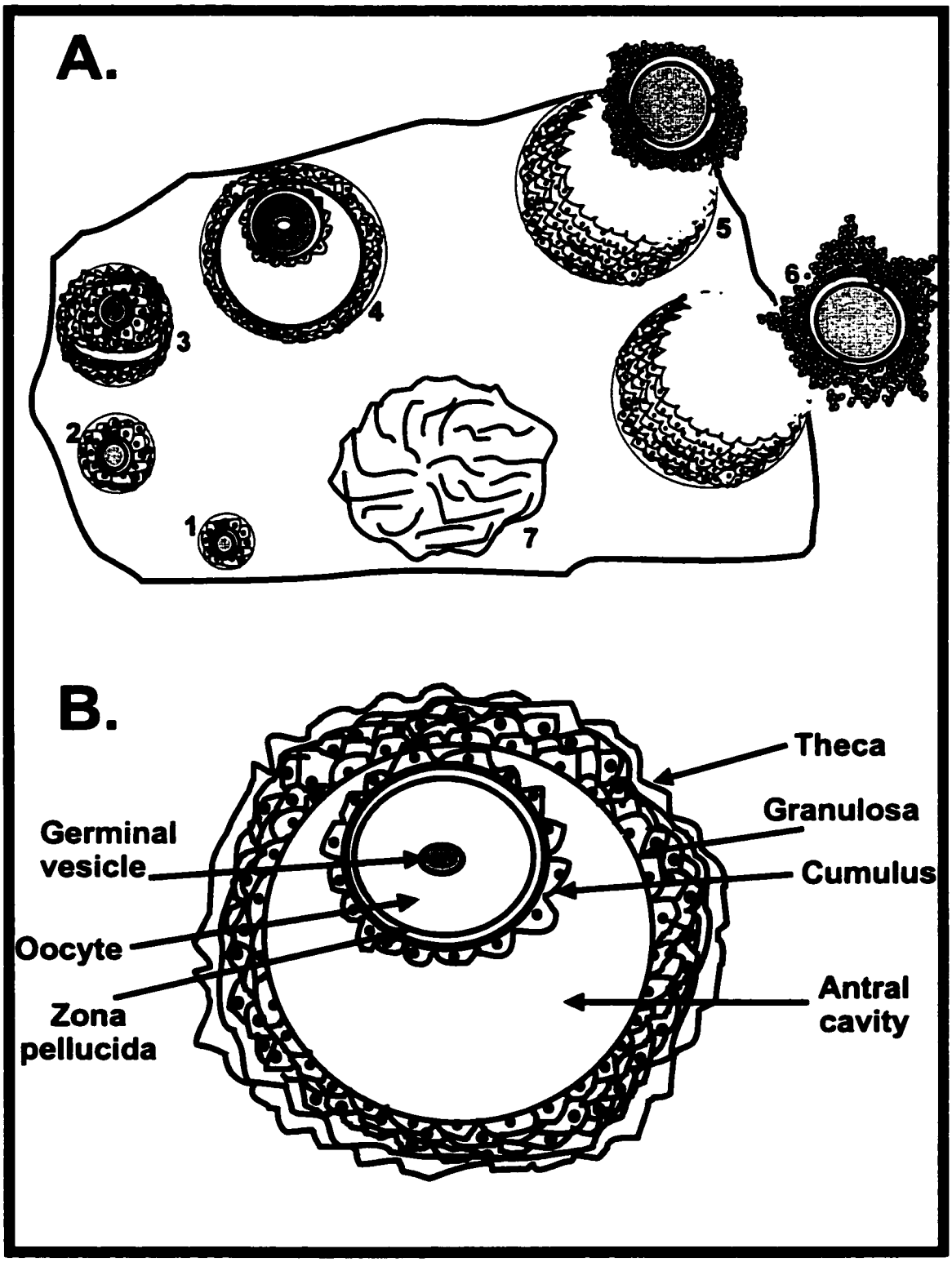
A.
1
2
3
4
5
6
7
B.
Theca
Granulosa
Germinal vesicle
Cumulus
Oocyte
Zona pellucida
Antral cavity

Figure 2. Images of mouse oocytes. **GV** (germinal vesicle) and **MI** (metaphase I) oocytes were obtained from PMSG primed (48 h prior to collection) CF-1 female mice. GV oocytes were maintained in dbcAMP until fixation. Some GV oocytes were cultured for 18 h with 50 μg/ml cycloheximide to produce oocytes arrested in MI. **MII** egg and cumulus-oocyte-complex (**COC**) were collected from superovulated (PMSG/hCG) female CF-1 mice. GV-germinal vesicle, MI-metaphase I, MII-metaphase II, PB-polar body, E-egg, C-cumulus. Scale bars represent 50 μm.

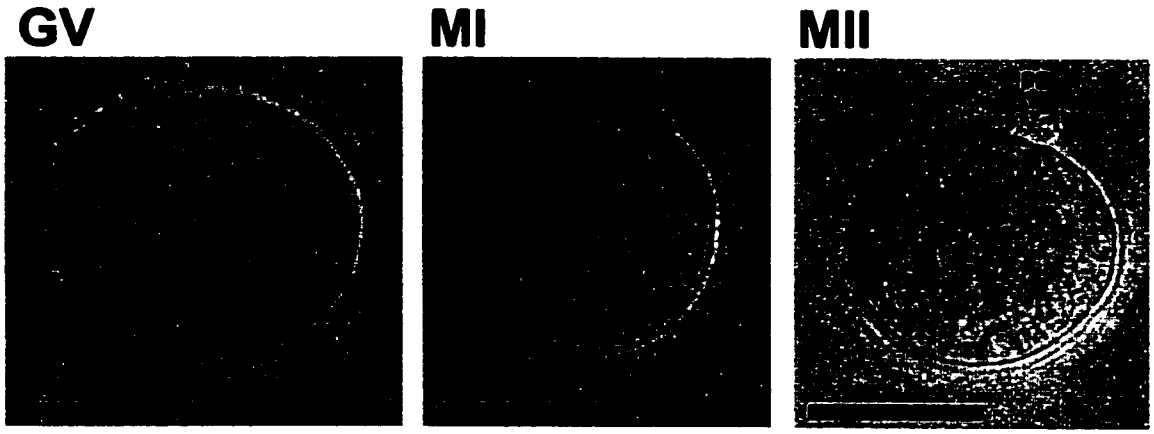
GV
MI
MII

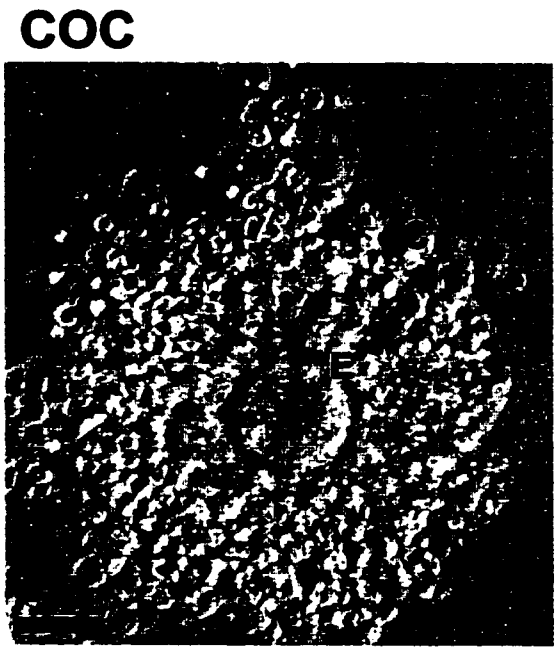
COC

germinal vesicle breakdown (GVBD; disappearance of the prophase I nuclear envelope and nucleoli), chromosome condensation and progression into metaphase I (MI; Fig. 2). In most mammalian species, GVBD and progression to metaphase II (MII) normally occurs following the preovulatory surge of gonadotropins (Eppig et al., 1996). Prior to ovulation, gonadotropins stimulate cumulus cells to produce and secrete hyaluronic acid which causes the cumulus cells to become loosely aggregated around the oocyte within a mucus-like matrix. This process is called 'mucification' or 'cumulus expansion' (Eppig, 1979).

Preimplantation embryo development

The fallopian tube, or oviduct (Fig. 3), is a muscular tube into which the ovulated egg is deposited (Fig. 2). It is the site of fertilization (Fig. 4) as well as the environment for early embryogenesis. This period of embryo development within the oviduct is part of *preimplantation embryo development* and involves a series of reductive cleavages producing 2-cell, 4-cell, 8-cell and 16-cell embryos (Fig. 3, 4). Each daughter cell is called a *blastomere* and is totipotent. At the 8-16-cell stage, depending on the species, the embryo undergoes compaction to form a *morula*. The morula stage is characterized by increased intercellular connections between adjacent blastomeres (Winkel et al., 1990). The morula undergoes cavitation and forms a fluid-filled cavity called a *blastocoel*. The embryo, now a *blastocyst*, has a differentiated *trophectoderm* (TE) layer (epithelial cells) which will form extra-embryonic structures and an *inner cell mass* (ICM) which will form the fetus (Fig. 3, 4; MacPhee et al., 2000). The blastocyst implants in the uterus, with fetal development completed within a species-specific gestation period.

Figure 3. Preimplantation development. The female mammalian reproductive tract is composed of the **ovary**, **oviduct** or **fallopian tube**, and the **uterus**. The unfertilized egg, arrested in MII, is ovulated from the **follicle** into the oviduct. The oviduct is divided into three major segments; *fimbriae*, *ampulla* and the *isthmus*. The fimbriae are specialized to capture the ovulated egg into the oviduct. The ampulla is the site of fertilization. The isthmus of the oviduct is the site of preimplantation development and is quite alkaline compared to the pH of follicular or uterine fluid. Following fertilization, the 1-cell embryo undergoes a series of reductive cleavages (2-cell, 4-cell, 8-cell), followed by compaction to form a morula. By the morula (mor) stage, the embryo begins to enter the uterus. The morula cavitates, forming a fluid-filled cavity surrounded by trophectoderm (TE) cells. The blastocyst (blast) hatches out of the zona pellucida and implants in the wall of the uterus. The trophectoderm will form extra-embryonic tissues such as the placenta while the inner cell mass (ICM) will develop into the fetus.

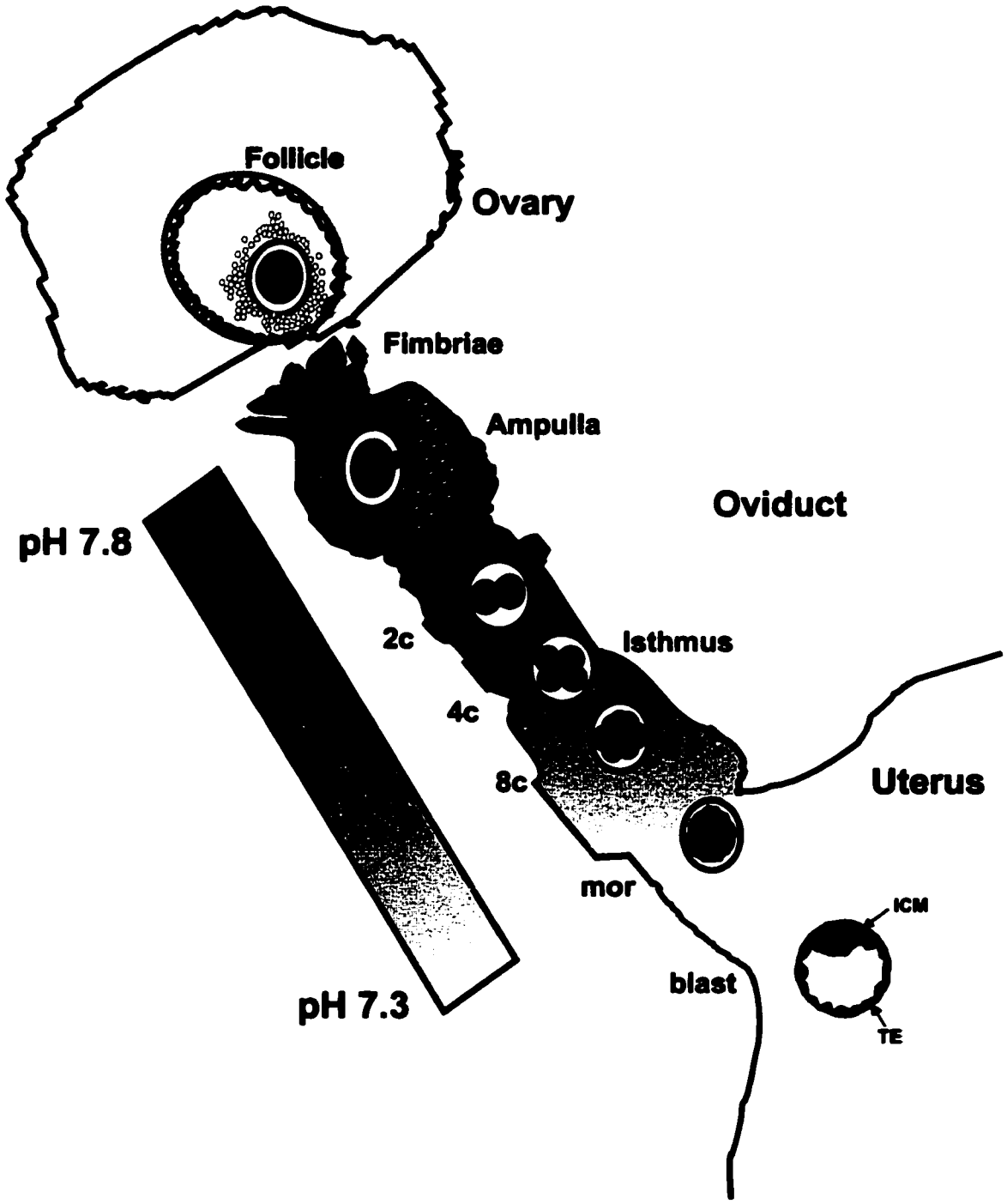
Follicle
Ovary
Fimbriae
Ampulla
Oviduct
pH 7.8
2c
Isthmus
4c
8c
Uterus
mor
ICM
blast
TE
pH 7.3

Figure 4. Images of mouse preimplantation embryos. Embryos derived from matings of CF-1 females x BDF males, removed from oviducts as 1-cell embryos and then cultured for up to 4 days. Shown: 1-cell (1c), 2-cell (2c), 4-cell (4c), 8-cell (8c), morula and blastocyst-stage embryos. PN-pronucleus, N-nucleus, PB-polar body, ICM-inner cell mass, TE-trophectoderm. Scale bar represents 50 μm.

1c

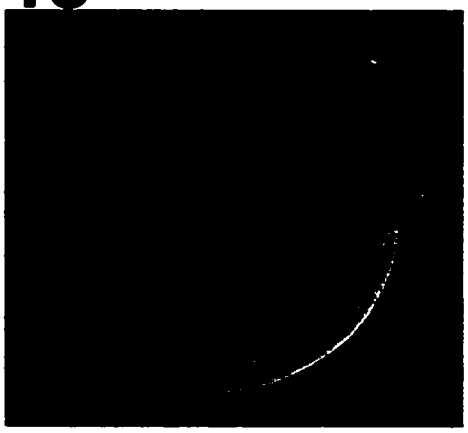

2c

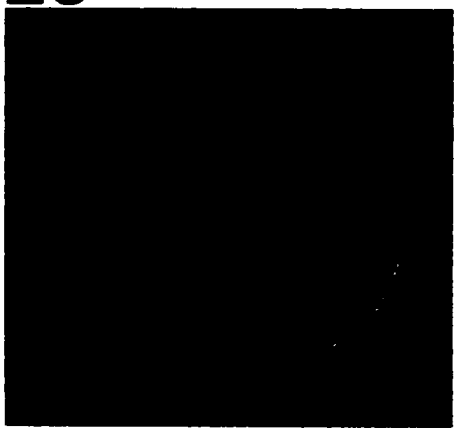

4c

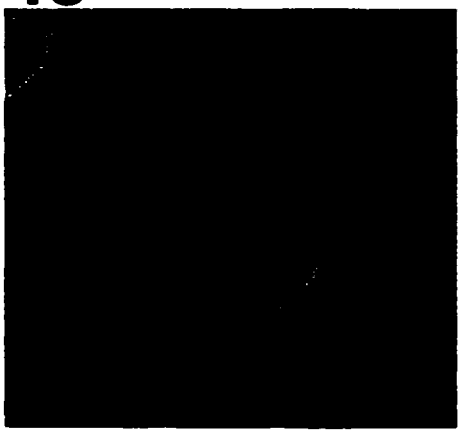

8c

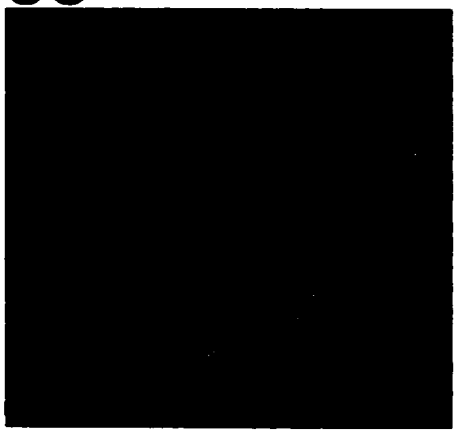

morula

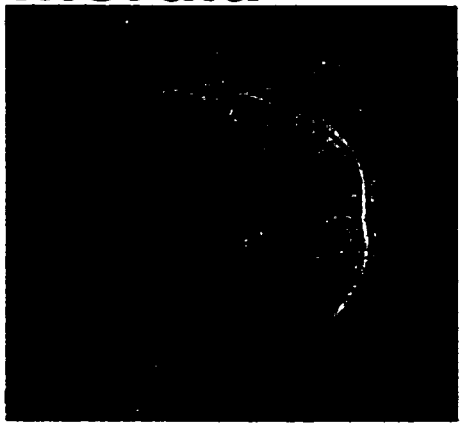

blastocyst

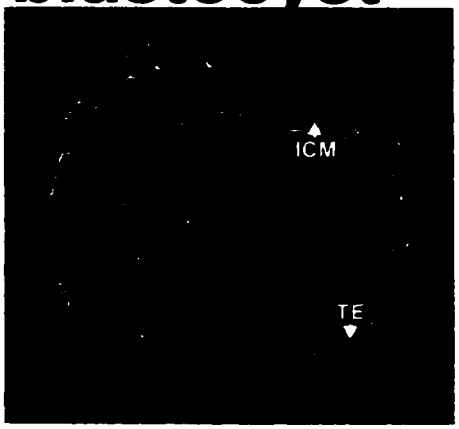

Mammalian oviduct: environment for preimplantation embryo development

The oviduct is divided into three regions: fimbriae, ampulla and isthmus (Fig. 3). The fimbriae are characterized by finger-like projections with highly ciliated epithelial cells. The ampulla is the site of fertilization, while the isthmus may be important in the transport of sperm, eggs and the developing embryo (Crow et al., 1994). Oviductal fluid is a mixture of constituents from plasma and some oviduct-specific proteins (Leese, 1988). Early studies examining tubal fluid formation (Brunton and Brinster, 1971; Brunton, 1972) demonstrated that rabbit ampullae exhibit net Cl^- secretion (into the lumen) with Na^+ flux equivalent in both directions. Oviduct lumen K^+, HCO_3^- (Borland, 1977; 1980), Cl^- and Na^+ levels are significantly higher than plasma, although osmolarity is essentially the same (Dickens and Leese, 1994; Collins and Baltz, 1999).

The electrolyte composition of oviductal fluid is important to maintain osmolarity and pH. It has been observed that tubal fluid pH is much higher than plasma (pH 7.5-8.0; Fig. 3), as measured in several species. Maas et al (1977) measured oviduct pH in rhesus monkey and found that during the follicular phase pH was 7.1 -7.3 while at ovulation pH increased to 7.5 to 7.8, remaining high through the luteal phase. During the follicular phase HCO_3^- was 35 mM, rising to 90 mM during ovulation (Maas et al., 1977). pH of rabbit oviducts was about 7.8-7.9 (Maas et al., 1984), while rat ampullar fluid, 10 h post-hCG, ranged from pH 8.0 to 8.2 (Ben Yosef et al., 1996). High HCO_3^- and K^+ levels in the oviduct have been proposed to aid in the dispersal of the cumulus mass and to help regulate sperm motility and embryo metabolism (Boatman, 1997).

II. OOCYTE MATURATION

Acquisition of meiotic competence

Following oogenesis, oocytes are arrested in prophase I of meiosis and are characterized by a nucleus or *germinal vesicle* (GV; Fig 2). The oocyte must undergo many processes during follicular development to acquire the ability or competence to undergo GVBD and progress through MI to produce a mature MII egg (meiotic competence). Immature oocytes from primordial or primary follicles are meiotically incompetent and are unable to complete GVBD (Grondahl et al., 2000). Meiotic competence requires both nuclear and cytoplasmic maturation of the oocyte. Nuclear maturation involves the ability to reinitiate and complete the first meiosis, including GVBD and progression to MII (Eppig et al., 1996; Hegele-Hartung et al., 1999). Nuclear maturation can be divided into two steps; first, the oocyte becomes competent to undergo GVBD and to assemble an MI spindle with condensed chromosomes; later, the oocyte acquires the ability to progress further to MII. During oocyte growth, oocytes accumulate inactive pools of cell cycle regulatory molecules whose subsequent activation is important for the resumption of meiosis and progression to MII. Meiotically incompetent oocytes may lack some of these cell cycle regulators and are thus unable to reinitiate meiosis or complete MI (de Vantery et al., 1997).

Cytoplasmic maturation includes the processes that prepare the oocyte for fertilization, activation and preimplantation development such as synthesis and secretion of the zona pellucida and the acquisition of sensitivity of intracellular Ca^{2+} release to inositol trisphosphate (IP_3; Eppig et al., 1996). The potential of the ovulated egg to become fertilized and develop normally is dependent not only on meiotic/chromosomal

events but also on the quality and maturity of the ooplasm and plasma membrane. Thus, nuclear maturation is required for the production of a mature MII egg, while cytoplasmic maturation is essential for fertilization and development of the new embryo (Hegele-Hartung et al., 1999).

M-phase promoting factor (MPF)

Meiotic progression is controlled by MPF (M-phase promoting factor) which is comprised of cyclin B1/B2 and a serine-threonine kinase - $p34^{cdc2}$ protein kinase (cdk2 or cdc2; Fig. 5). MPF has cyclical activity which peaks at metaphase (Taieb et al., 1997). Meiotic competence is acquired at the end of the period of oocyte growth and requires a pool of accumulated pre-MPF (inactive cdc2 kinase and cyclin B). De novo translation of cdc2 kinase mRNA is triggered during oocyte growth and inactive cdc2 protein is accumulated in the oocyte. Exit from prophase I is accompanied by an increase in MPF activity and GVBD. Activation of MPF occurs in several steps. First, cyclin B (regulatory protein) is complexed with inactive cdc2 kinase to form pre-MPF. Cyclin B, synthesized during oocyte growth, is not available for cdc2 kinase complexing in incompetent oocytes, suggesting that cyclin B is compartmentalized or requires post-translational modifications prior to complexing. cdc2 kinase, once complexed with cyclin B, is phosphorylated on Thr-14 and Tyr-15 by wee-1 and/or Myt-1 protein kinase, which maintain pre-MPF in an inactive state. Dephosphorylation of these residues by cdc25 phosphatase is required prior to activation of cdc2 kinase activity. Finally, cdc2 kinase is phosphorylated by CAK (cdc2 activating kinase) on Thr-161 which fully activates MPF. Thus, the acquisition of meiotic competence and activation of MPF at GVBD can be

Figure 5. Activation of MPF at GVBD. Oocyte growth during meiotic maturation is accompanied by synthesis and accumulation of cyclin B and inactive cdc2 kinase molecules. Activation of MPF occurs in several steps. First, cyclin B is complexed with inactive cdc2 kinase to form pre-MPF. cdc2 kinase, once complexed with cyclin B, is phosphorylated on Thr-14 and Tyr-15 by wee-1 and/or Myt-1 protein kinase, which maintain pre-MPF in an inactive state. Dephosphorylation of these residues by cdc25 phosphatase is required prior to activation of cdc2 kinase activity. Finally, cdc2 kinase is phosphorylated by CAK (cdc2 activating kinase) on Thr-161 which fully activates MPF (de Vantery et al, 1997).

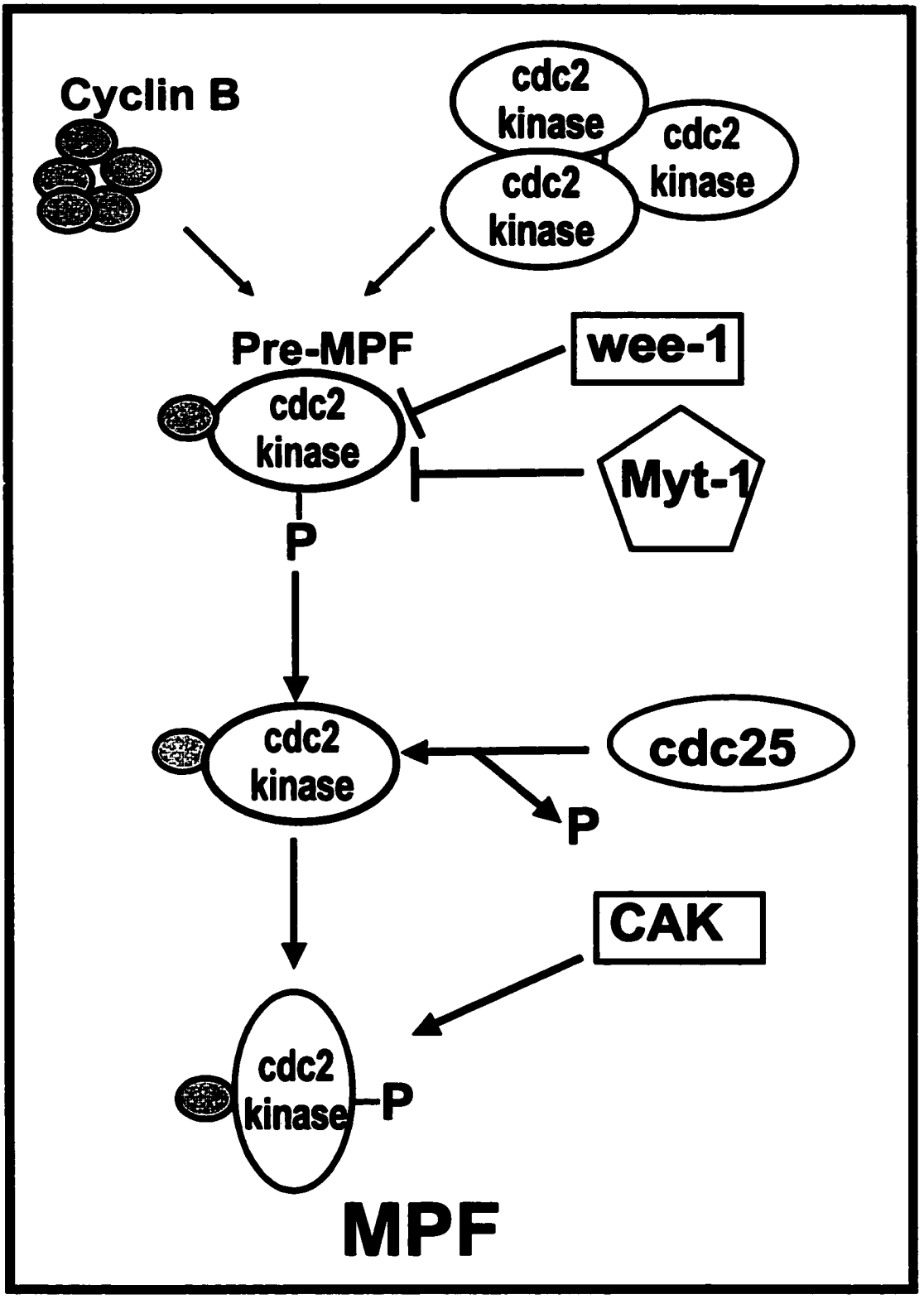
Cyclin B
cdc2 kinase
cdc2 kinase
cdc2 kinase
Pre-MPF
cdc2 kinase
wee-1
Myt-1
P
cdc2 kinase
cdc25
P
CAK
cdc2 kinase
P
MPF

regulated at several levels; translation of cyclin B and cdc2 kinase, inhibitory phosphorylation by wee-1/Myt-1, dephosphorylation by cdc25 phosphatase and activation by CAK (de Vantery et al., 1997).

In maturing mouse oocytes, cdc2 kinase activity gradually increases, reaching maximal activity at MI. Although GVBD *in vitro* does not appear to require protein synthesis, treatment of mouse oocytes with protein synthesis inhibitors results in lower activation of cdc2 kinase activity (~20-30% maximal activity) at MI. As newly synthesized cyclin B is immediately complexed with cdc2 kinase, this suggests that de novo cyclin B synthesis is required for full cdc2 kinase activation during meiotic maturation (Taieb et al., 1997).

MPF activation may also be regulated by cyclin B phosphorylation. In *Xenopus* oocytes, cyclin B may be phosphorylated coincident with the appearance of cdc2 kinase activity. Purified MPF phosphorylates cyclin B2 in vitro, suggesting that cdc2 kinase phosphorylates cyclin B in vivo. Other candidates include mitogen-activated protein kinase (MAPK) or its upstream activator mos (MAPKKK). cdc2 kinase activity, cdc2 kinase-cyclin B complex stability and cyclin destruction are independent of cyclin B phosphorylation. It has been suggested that phosphorylation of cyclin B may be involved in targeting cyclin B1 complexes to subcellular locations, such as the nucleus (Taieb et al., 1997).

At the MI - MII transition, MPF activity decreases. In *Xenopus* oocytes, this loss of MPF activity results from the destruction of up to 80% of cyclin B2. Cyclin B is normally degraded at the onset of mitotic anaphase by a ubiquitin-dependent proteolytic system. Coincident with cyclin B destruction, cyclin B1 and B2 synthesis is stimulated

three- to fourfold. The subsequent reactivation of MPF is probably due to the accumulation of new cyclins. At this transition, MPF does not decrease to the basal level of the prophase state, but rather reaches a minimum of about 25% of its maximal activity. This can be explained by a period when both cyclin B synthesis and destruction overlap (Taieb et al., 1997).

Using mutant (LT/Sv) mouse oocytes that arrest in MI rather than progressing to MII, it has been shown that decreased cyclin B degradation can produce MI arrest (Hampl and Eppig, 1995). As inactivation of $p34^{cdc2}$ kinase is normally coupled to the degradation of cyclin, the reduction of cyclin destruction, together with persistent cyclin synthesis, sustains active $p34^{cdc2}$ kinase in these mutant mice. This is consistent with regulation of MI-MII progression by cyclin degradation and synthesis. Partial degradation of cyclin B, together with sustained cyclin B synthesis, leaves a substantial cyclin B pool to reactivate $p34^{cdc2}$ kinase for entry into MII (Hampl and Eppig, 1995).

One purpose for the immediate reactivation of MPF during this MI-MII transition is the suppression of S-phase. With an additional round of DNA synthesis diploid eggs would be produced with triploid embryos resulting from fertilization. Instead, suppression of S-phase followed by polar body emission results in the production of haploid eggs. Low levels of cyclin B can trigger exit from metaphase and entry into S-phase and hence, cyclin B is maintained at unusually high levels during the MI-MII transition (Gross et al., 2000). Thus, upon MPF reactivation there is the immediate formation of the MII spindle, without reformation of a nuclear envelope, chromosome decondensation or DNA replication (Taieb et al., 1997).

The transient decrease in MPF activity at the MI/MII border corresponds

temporally to the emission of the first polar body. This meiotic cytokinesis differs from normal mitotic cleavages as the nuclear material, but not cytoplasm, is divided equally between the two daughter cells. The unequal division of cytoplasm is important as the unfertilized mouse egg will not undergo much transcription or translation until embryonic genome activation at the 2-cell stage. The unfertilized egg will therefore rely on stored maternal transcripts and proteins to undergo resumption of the cell cycle, fertilization and DNA synthesis (Taieb et al., 1997).

Cytostatic factor (CSF)

Near the end of meiosis, the mature egg remains arrested in MII until fertilization or parthenogenetic egg activation (cell cycle resumption in the absence of sperm; see below), with chromosomes condensed and aligned on the MII spindle (Jones et al., 1995b). During MII arrest in mouse eggs, cyclin B is continually synthesized and degraded, with cyclin B degradation dependent on the presence of intact microtubules (Kubiak et al., 1993; Winston et al., 1995a). Sustained cyclin B synthesis allows the prolonged maintenance of MPF activity, which supports MII arrest and the persistence of the MII spindle (Taieb et al., 1997).

In MII oocytes, an additional factor - cytostatic factor (CSF) - helps maintain MII arrest (Kubiak et al., 1993). CSF activity was originally demonstrated by microinjection of MII cytoplasm into one blastomere of a 2-cell frog embryo, which induced metaphase arrest of the injected blastomere (Masui and Markert, 1971). Similarly, fusion studies using mouse MII eggs and mitotic 1-cell embryos demonstrated the presence of CSF activity in mouse eggs (Kubiak et al., 1993). Many proteins have CSF activity,

including mos, MAPK, cdk2 and $p90^{RSK}$ (Taieb et al., 1997; Bhatt and Ferrell, 1999; Gross et al., 2000).

MAPK are serine/threonine kinases that become activated in mitogen-activated and transformed cells (Fig. 6). MAPK targets include the 90 kDa ribosomal S6 kinase ($p90^{RSK}$) and specific transcription factors (Verlhac et al., 1994). The MAPK pathway has been well examined in *Xenopus* oocytes during oocyte maturation. Frog oocyte maturation is stimulated by progesterone which causes a decrease in intraoocyte cAMP followed by protein synthesis, required for GVBD in this species. One key protein synthesized during this period is the mos oncoprotein. Mos activates the MAPK cascade by phosphorylating MEK1 at Ser-218 and Ser-222. MEK1 is a dual specificity kinase that activates p42 MAPK (ERK1) and p44 MAPK (ERK2) by phosphorylating threonine and tyrosine residues. Phosphorylation of MAPK is associated with a marked increase in its kinase activity. Mos protein accumulates in the oocyte followed by abrupt activation of MEK1, p42 MAPK and the M phase regulators xPlkk1, Plx1, cdc25 and cdc2. Mos antisense oligonucleotides inhibit mos accumulation and progesterone-induced oocyte maturation, suggesting that mos accumulation is essential for oocyte maturation in *Xenopus*. Microinjection of purified mos protein has been shown to induce cdc2 activation and GVBD indicating that mos is sufficient to trigger GVBD. Microinjection of mos into cleaving blastomeres results in metaphase arrest, indicating that mos has CSF activity (Ferrell, 1999).

Although the MAPK cascade is generally depicted as a linear chain of phosphorylation-dependent events (mos→MEK1→ERK1/2) there is also regulation of the cascade by positive feedback. Microinjection of active MEK1 or ERK1 into frog

Figure 6. Oocyte maturation. *A. Schematic of MPF and MAPK activation during oocyte maturation.* MPF is activated by the complexing of cdc2 kinase with presynthesized cyclin B1 and B2. MAPK activation requires mos synthesis, followed by activation via MEK. *B. Time-course of MPF activity and MAPK activity during oocyte maturation.* MPF and MAPK are both inactive in the GV oocyte. MPF becomes activated after a very brief lag period following GVBD. The oocyte is now in metaphase I (MI). MAPK is activated slowly following GVBD, becoming fully active 7-9 h later in the MI oocyte. There is a transient decrease in MPF activity between at the end of meiosis I, coincident with the emission of the first polar body (PB1). MPF is reactivated and the egg is arrested in metaphase II (MII). MAPK activity does not decrease between metaphase I and II.

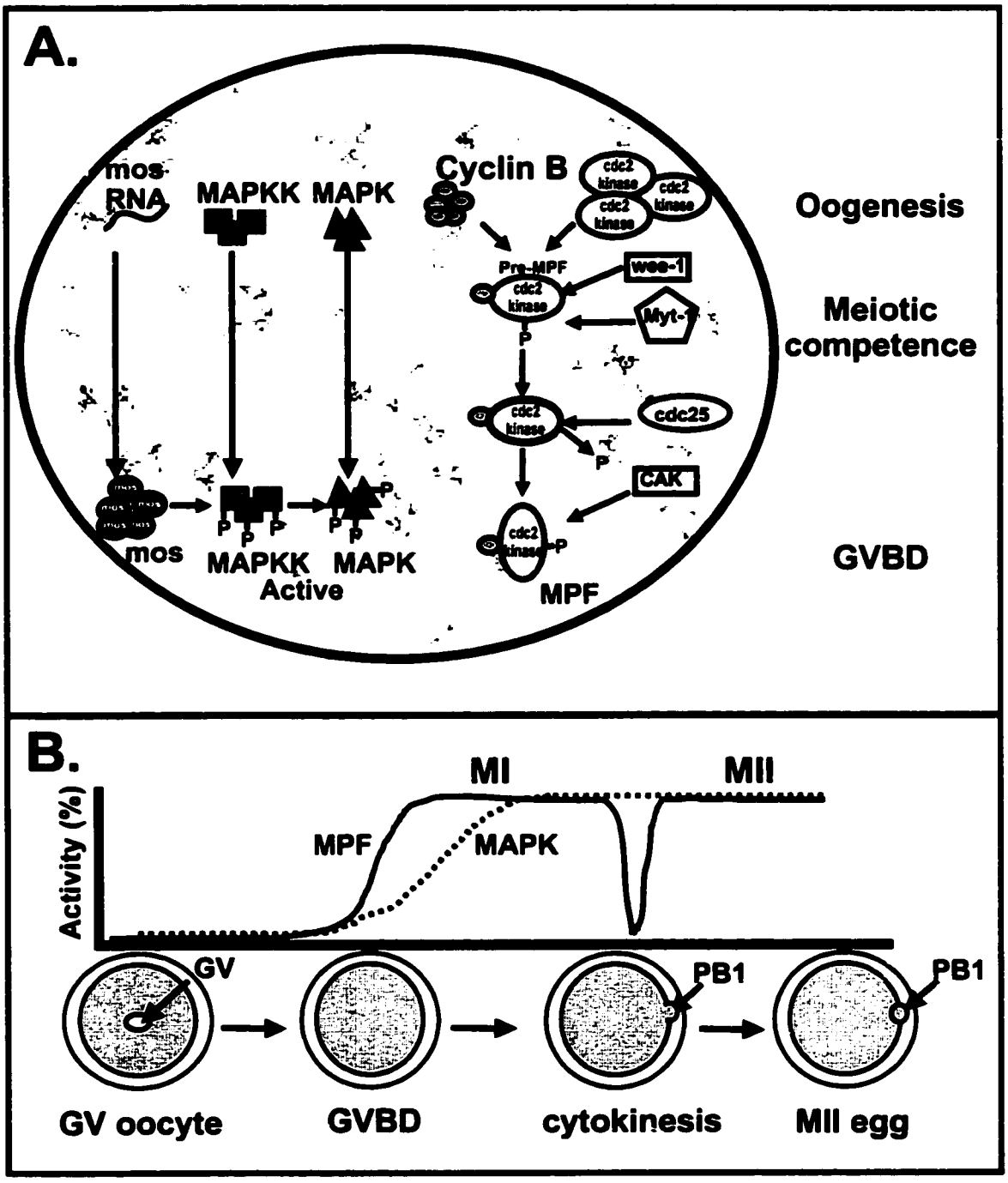
A.
mos RNA
MAPKK
MAPK
Cyclin B
cdc2 kinase
cdc2 kinase
cdc2 kinase
Oogenesis
Pre-MPF
cdc2 kinase
wee-1
Myt-1
P
Meiotic competence
cdc2 kinase
cdc25
P
CAK
cdc2 kinase
P
GVBD
mos
MAPKK Active
MAPK
MPF
B.
MI
MII
Activity (%)
MPF
MAPK
GV
PB1
PB1
GV oocyte
GVBD
cytokinesis
MII egg

oocytes induces the accumulation of mos protein. ERK1 stimulates mos mRNA polyadenylation and mos translation. ERK1 inhibits mos destruction, in part by phosphorylation of mos at Ser-3, which occurs in vitro. Because of this positive feedback, it is possible that the progesterone signal initiating *Xenopus* oocyte maturation targets mos or causes a small change in the activity of MEK1 or ERK1 that may lead to the accumulation of mos and activation of the entire signaling cascade (Ferrell, 1999).

The MAPK cascade is activated by different pathways in somatic cells and in later embryo development. Binding of mitogens, such as insulin or growth factors, to their receptors results in the activation of Ras, a membrane associated GTP-binding protein. Ras dissociates from GDP and binds GTP. Raf-1 protein, a cytosolic Ser/Thr kinase is activated by transport to the membrane and subsequent interaction with Ras-GTP. The translocation of Raf-1 to the membrane is thought to involve 14-3-3 protein which may transfer or anchor Raf-1 to the membrane. Following Raf-1 activation 14-3-3 protein dissociates. The activated Raf-1 phosphorylates serine residues of MAPKK (e.g. MEK1) resulting in activation of MAPKK, which in turn activates MAPK as described (Haraguchi et al., 1998). MAPKK can also be activated by MEKK1 and Tpl-2. The Raf-1 dependent pathway is conserved from yeast to vertebrates, while the mos pathway has been shown only in oocytes (Verlhac et al., 1996).

Both the ERK1 and ERK2 forms of MAPK are present in mouse oocytes. MAPK activity develops slowly following GVBD, remains active throughout meiotic maturation and in MII eggs (Verlhac et al., 1994). The protein synthesis inhibitor puromycin inhibits the activation of MAPK during oocyte maturation, but does not affect the increase in MPF activity following GVBD. This suggests that MPF activity is not sufficient to

activate MAPK activity in mouse oocytes and that MAPK activation is dependent on protein synthesis (Verlhac et al., 1993). Raf-1 is present in immature mouse oocytes but in an inactive form. As Raf-1 does not become activated until late in meiotic maturation (MII) this suggests that mos activation of MAPK is independent of the Ras/Raf-1 pathway at GVBD. This is consistent with the fact that the synthesis of Ras, which lies upstream of Raf-1, is not required for meiosis in mouse oocytes, but is required for progression to the 2-cell stage. Raf-1 is, however, activated in MII arrested eggs such that Raf-1 may play a role later in fertilization (Verlhac et al., 1996).

The kinetics of MPF and MAPK activity are different at GVBD. MPF becomes activated coincident with GVBD, whereas MAPK activation is delayed until about 2 h following GVBD in the mouse (Verlhac et al., 1994). Unlike in *Xenopus* oocytes, in mouse oocytes mos and the MAPK pathway are not required for GVBD, MPF activation or progression from MI to MII, since these occur normally in $mos^{-/-}$ mice. However, mos is required for MII arrest (Oh et al., 1998).

A MAPK target, the protein kinase $p90^{RSK}$, is a downstream mediator of CSF arrest. Constitutively active $p90^{RSK}$ maintains CSF arrest in the absence of an active MAPK pathway in frog oocytes (Gross et al., 1999). Depletion of $p90^{RSK}$ from frog oocytes removed CSF activity, which could be restored by replacement of $p90^{RSK}$. This is consistent with identification of $p90^{RSK}$ as a component of CSF (Bhatt and Ferrell, 1999). MAPK phosphorylates $p90^{RSK}$ in *Xenopus* oocytes and in mitotic cells on multiple Ser/Thr residues. Phosphorylation of $p90^{RSK}$ by MAPK also increases $p90^{RSK}$ autophosphorylation. Targets of $p90^{RSK}$ include histone H3 kinase, c-Fos, c-Jun and Nur77. Mouse oocyte $p90^{RSK}$ (Rsk1 and Rsk2) is phosphorylated and activated in vitro

and in vivo by ERK1/2 (Palmer et al., 1998).

Activation of $p90^{RSK}$ requires two phosphorylation events - a MAPK-independent pathway, resulting in partial activation, and a MAPK-dependent pathway, which results in full activation. $p90^{RSK}$ is partially activated shortly after GVBD in mouse oocytes independent of MAPK, followed by MAPK-dependent-$p90^{RSK}$ activation, yielding full activity. The timing of the initial activation of $p90^{RSK}$ is consistent with regulation by $p34^{cdc2}$ kinase (Kalab et al., 1996). However, the sequence of mouse $p90^{RSK}$ does not contain consensus sequences for phosphorylation by $p34^{cdc2}$ kinase. Thus, it is possible that an intermediary kinase, controlled by $p34^{cdc2}$ kinase, mediates the initial activation of $p90^{RSK}$ (Kalab et al., 1996). The loss of $p90^{RSK}$ activity following egg activation is most likely due to the concomitant loss of MAPK activity (Verlhac et al., 1994; Kalab et al., 1996). Thus, the MAPK pathway, including upstream regulators (mos and MEK1/2) in addition to downstream targets ($p90^{RSK}$), is an essential component of CSF activity (Taieb et al., 1997; Gross et al., 2000).

Parthenogenetic activation in the absence of CSF

As discussed, mos and the MAPK pathway including $p90^{RSK}$ are essential for the maintenance of the MII arrest. This is evident in oocytes from $mos^{-/-}$ mice. In $mos^{-/-}$ oocytes, GVBD and MPF activation occur normally. Progression to MI and extrusion of the first polar body also occur with no developmental delays. However, in the absence of mos, MAPK and other pathways downstream of mos are not activated following GVBD, and these $mos^{-/-}$ oocytes do not arrest at MII but become parthenogenetically activated (Colledge et al., 1994; Hashimoto et al., 1994).

$mos^{-/-}$ parthenogenotes display several phenotypes that have been separated into three classes (Fig. 7). Class I includes parthenogenotes with up to two polar bodies, such that the oocyte and polar bodies are similar to normal unfertilized eggs or 1-cell embryos (Hirao and Eppig, 1997). Class II oocytes exhibit atypical divisions, fragmentation and include oocytes with extremely large polar bodies (Choi et al., 1996), or oocytes that have undergone fragmentation. This suggests atypical cytokinesis has occurred in either MI or MII, thereby producing extremely large polar bodies and unequally-sized blastomeres (Choi et al., 1996; Hirao and Eppig, 1997). Class III oocytes resemble normal 2-cell embryos, with each blastomere containing a visible nucleus. Some $mos^{-/-}$ oocytes do form a pronucleus right after MI (Araki et al., 1996) and may divide symmetrically to produce a 2-cell embryo, although this phenotype composes only a small percentage of $mos^{-/-}$ parthenogenotes in vivo (Hirao and Eppig, 1997).

Developmental fates of these $mos^{-/-}$ parthenogenotes vary between classes. Class I parthenogenotes most likely become activated during MII and produce either a second polar body or a pronucleus. Many oocytes, however, do not produce a pronucleus even following extrusion of the second polar body (Hirao and Eppig, 1997). These oocytes most likely progress to a third metaphase (MIII) instead of interphase following emission of the second polar body. The majority of these parthenogenetically activated $mos^{-/-}$ oocytes progress to MIII, which persists for at least 10 h. MIII is not a true metaphase as the spindle formed is monopolar rather than bipolar. This metaphase III arrest is not due to CSF activity (mos is absent), but probably because the metaphase spindle is monopolar and not functional (Verlhac et al., 1996).

Following in vitro culture, about 30% of the $mos^{-/-}$ oocytes cleaved to the 2-cell

Figure 7. Parthenogenetic classes of mouse mos$^{-/-}$oocytes. Observations that mos$^{-/-}$ oocytes exhibited a parthenogenetic phenotype led to the establishment of three parthenogenetic classes by Hirao and Eppig (1997). Class I includes parthenogenotes with pronuclei and/or two polar bodies. Class II parthenogenotes exhibit atypical divisions and include oocytes with extremely large polar bodies, or oocytes that have undergone fragmentation. Class III parthenogenotes resemble normal 2-cell embryos, with each blastomere containing a visible nucleus (Hirao and Eppig, 1997).

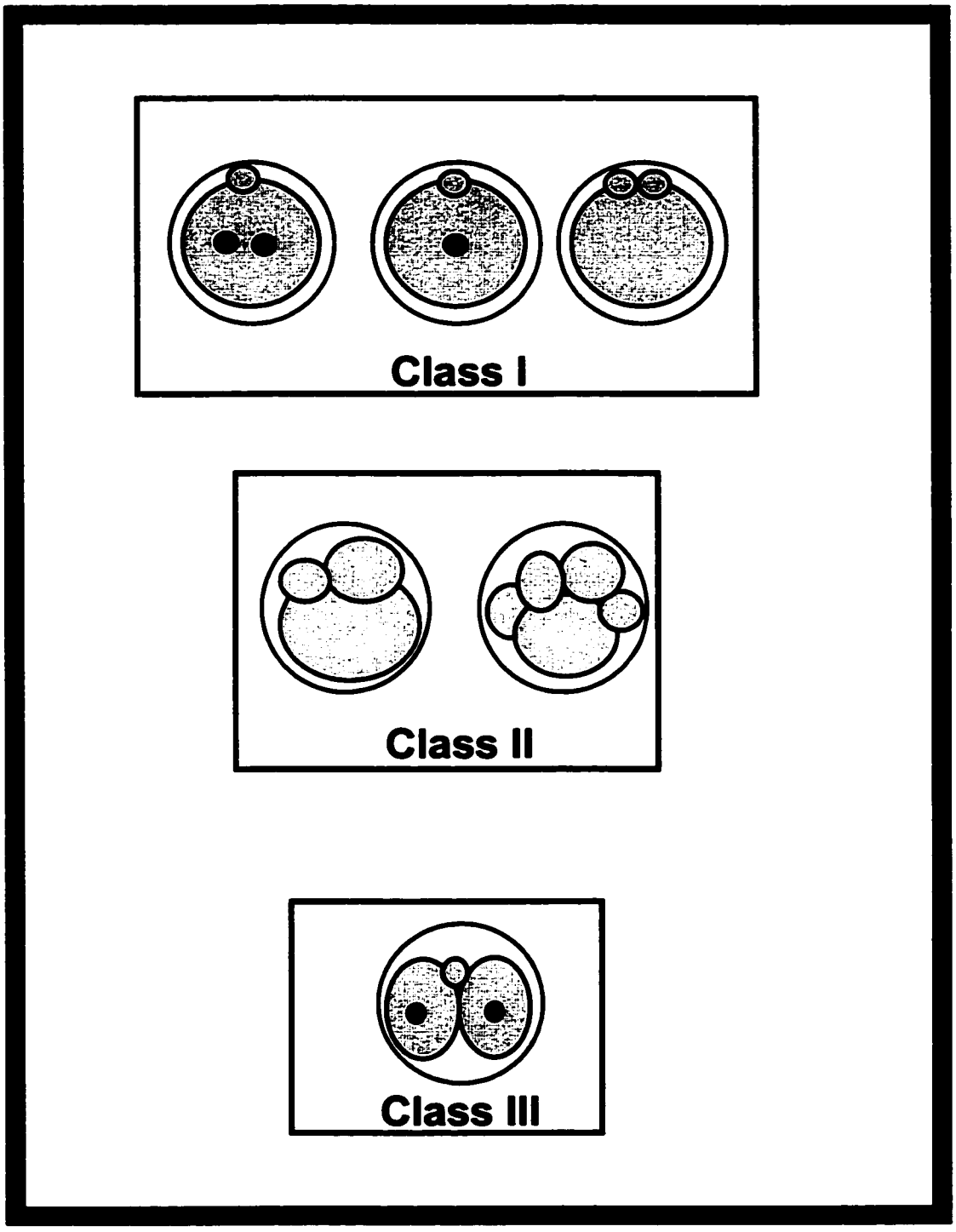
Class I
Class II
Class III

stage, with each blastomere containing a nucleus. The developmental potential of these $mos^{-/-}$ embryos in vivo and in vitro was generally limited to early cleavage stages (4-cell stage; Colledge et al., 1994). Class III parthenogenotes exhibit normal morphology and some (~15%) may develop to the blastocyst stage following in vitro culture. Class I and II parthenogenotes, however, develop poorly with only about 5% blastocyst development (Hirao and Eppig, 1997). Spontaneous parthenogenetic activation of $mos^{-/-}$ oocytes clearly demonstrates the role of mos in the maintenance of MII arrest. The different phenotypes exhibited by these $mos^{-/-}$ oocytes reflect the atypical organization of the cytoskeleton and spindle due to the absence of mos (Verlhac et al., 1996).

Interdependence of CSF and MPF

The MAPK pathway, and hence, CSF, may also be involved in the suppression of S-phase between MI and MII. In somatic cells, The specific ubiquitin protein ligase that targets cyclin B for destruction in mitosis is the anaphase-promoting complex (APC). Changes in the abundance of cyclin B have been correlated with changes of the phosphorylation state of the APC regulatory kinase cdc27. MAPK activity appears to maintain MII arrest by inhibition of the APC. Ordinarily, only a portion of cyclin B is targeted for destruction by APC during exit from MI. In *Xenopus* oocytes, MAPK acting via $p90^{RSK}$ promotes phosphorylation of the cdc27 component of the APC, thereby inhibiting the APC-mediated degradation of cyclins. Treatment of *Xenopus* GV oocytes with the MAPKK (MEK1/2) inhibitor U0126 prevents phosphorylation of cdc27 resulting in the formation of a nucleus following MI and progression into an inappropriate S-phase. Entry into interphase, characterized by the appearance of the

nucleus, results from increased degradation of cyclin B by the APC in the absence of MAPK activity. U0126-treated GV oocytes can be prevented from forming an interphase nucleus if they are injected with active $p90^{RSK}$. This suggests that the APC is under control of the MAPK pathway. (Gross et al., 2000).

MAPK upregulates MPF by stimulation of cyclin B synthesis (Fig. 8). The mRNA cap-binding protein eIF-4E, a subunit of the initiation factor eIF-4F, is usually rate-limiting in protein synthesis as it is complexed to the protein PHAS-1. This inhibitory PHAS-1:eIF-4E complex is observed when MAPK activity is low. When MAPK is active, MAPK phosphorylates PHAS-1 causing it to dissociate from eIF-4E, thereby rendering eIF-4E available to initiate translation (Moos et al., 1996). MAPK may also phosphorylate eIF-4E. In mouse oocytes MAPK and $p90^{RSK}$ are activated together with eIF-4E phosphorylation. Thus, MAPK regulation of MPF involves regulation of cyclin B availability, either through eIF-4E to stimulate cyclin B synthesis (Moos et al., 1996) or via $p90^{RSK}$ to inhibit cyclin B degradation (Gross et al., 2000).

MAPK may more directly regulate $p34^{cdc2}$ kinase activity. In *Xenopus* oocytes, as discussed, $p34^{cdc2}$ /cyclin B complexes exist as preformed MPF, maintained in an inactive form by phosphorylation on Thr-14, Tyr-15 and Thr-161 residues of $p34^{cdc2}$ kinase. Activation of MPF requires dephosphorylation of these residues, which appears to be catalyzed by the phosphatase cdc25. Conversely, inhibition of the kinases which phosphorylate these residues will also activate MPF. One such inhibitory kinase is wee-1 which phosphorylates $p34^{cdc2}$ kinase only on Tyr-15, but not Thr-14. This suggests that a separate kinase also regulates MPF activity. The candidate for this second kinase is Myt-1, which is a membrane-associated wee-1 homologue that can phosphorylate $p34^{cdc2}$

Figure 8. Interdependence of CSF and MPF pathways. The MAPK cascade is activated in somatic cells by binding of mitogens to their receptors resulting in the activation of Ras-GDP. Ras dissociates from GDP and binds GTP. Raf-1 protein is activated by transport to the membrane, thought to involve 14-3-3 protein, and subsequent interaction with Ras-GTP. The activated Raf-1 phosphorylates serine residues of MEK which in turn activates MAPK (Haraguchi et al, 1998). In contrast, in oocytes MAPK is activated via the mos→MEK pathway. MAPK phosphatases, MKP1 and PAC1, dephosphorylate MAPK, thereby resulting in its inactivation. MAPK acting via $p90^{RSK}$ has been shown to cause phosphorylation of the cdc27 component of the APC, thereby inhibiting the APC-mediated degradation of cyclins (Gross et al, 2000). MAPK has been shown to upregulate MPF by stimulation of cyclin B synthesis. Active MAPK phosphorylates PHAS-1 causing it to dissociate from eIF-4E, thereby rendering eIF-4E available to initiate translation. MAPK may also phosphorylate eIF-4E. In mouse oocytes MAPK and $p90^{RSK}$ are activated together with eIF-4E phosphorylation. (Moos et al, 1996). MAPK may also more directly regulate $p34^{cdc2}$ kinase activity. Myt-1 is a target of MAPK-activated $p90^{RSK}$ which phosphorylates the C-terminal regulatory domain of Myt-1 and downregulates the inhibitory activity of Myt-1 on $p34^{cdc2}$ kinase/cyclin B complexes in vitro (Palmer et al, 1998). In *Xenopus* oocytes, the N-terminal domain of cdc25 can be phosphorylated by the polo-like kinase, Plx1. Plx1, which may be regulated by MAPK, has been shown to activate cdc25 in vitro (Gavin et al, 1999).

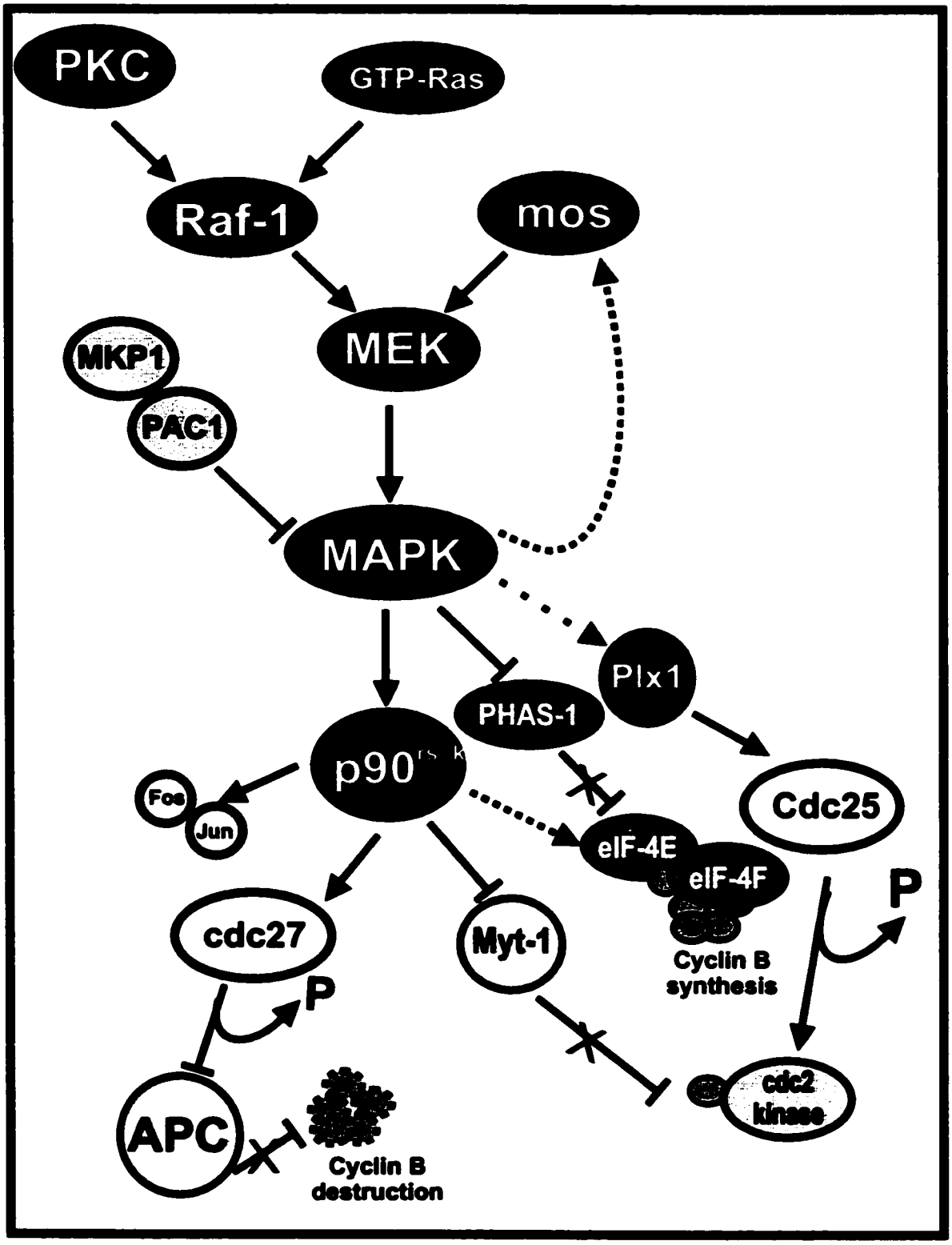
PKC
GTP-Ras
Raf-1
mos
MEK
MKP1
PAC1
MAPK
Plx1
PHAS-1
p90
Fos
Jun
Cdc25
eIF-4E
eIF-4F
P
cdc27
Myt-1
Cyclin B
synthesis
P
cdc2
kinase
APC
Cyclin B
destruction

kinase on both Tyr-15 and Thr-14. Myt-1 may become phosphorylated during *Xenopus* oocyte maturation and $p90^{RSK}$ is associated with Myt-1 in mature oocytes. While cdc25 activity increases during mitosis (increased dephosphorylation of these inhibitory residues), wee-1 and Myt-1 activity decreases (decreased phosphorylation of these residues) resulting in a decrease in MPF activity. Myt-1 is a target of MAPK-activated $p90^{RSK}$ which phosphorylates the C-terminal regulatory domain of Myt-1 and downregulates the inhibitory activity of Myt-1 on $p34^{cdc2}$ kinase/cyclin B complexes in vitro (Palmer et al., 1998).

In *Xenopus* oocytes, the N-terminal domain of cdc25 can be phosphorylated by the polo-like kinase, Plx1. Plx1 phosphorylation can activate cdc25 in vitro, suggesting that Plx1 may be one of the triggering kinases responsible for the phosphorylation and activation of cdc25 at the onset of M-phase (Gavin et al., 1999). Plx1 may also be activated by a MAPK-dependent pathway. In mos-injected *Xenopus* oocytes MAPK ($p42^{mpk1}$) activation is followed by the partial phosphorylation and activation of Plx1. The MAPK-dependent phosphorylation of Plx1 is inhibited by cycloheximide indicating that protein synthesis is required (Gavin et al., 1999). Thus, MAPK-dependent activation of Plx1 in *Xenopus* may be important for MPF activation at the onset of M-phase.

Control of meiotic maturation

Two main hypotheses have been proposed to explain the regulation of mammalian oocyte maturation. The first proposed that termination or reduction in intercellular coupling between the oocyte and cumulus cells, which would result from the withdrawal of cumulus cell cytoplasmic processes, ends oocyte maturation inhibition by physically

interrupting the flow of a meiosis-inhibiting factor to the oocyte. The model also proposed that cAMP, originating in the granulosa/cumulus cells, enters the oocyte via gap junctions and regulates maturation. The loss of the cytoplasmic processes and associated gap junctions would prevent the transfer of cAMP, and intraoocyte cAMP levels would thereby decrease due to an oocyte cAMP phosphodiesterase. The decrease of intracellular cAMP below a critical level would somehow trigger resumption of meiosis. The second hypothesis suggested that a quantitative or qualitative change in the signal communicated from the cumulus cells to the oocyte, but not a termination of the intercellular coupling between the cells, triggers oocyte maturation. This was based upon the observation that follicular fluid contains a putative low-molecular-weight polypeptide inhibitor called 'oocyte maturation inhibitor' (OMI) that reversibly inhibits maturation of cumulus cell-enclosed oocytes, but does not inhibit maturation of denuded oocytes. It has been proposed that the inhibitor's action is terminated by action of gonadotropins on the granulosa cells (Eppig, 1982; Schultz et al., 1983a).

The first hypothesis was studied by examining the degree of cumulus expansion in mouse oocytes retrieved at various times following hCG. GVBD occurs within about 3 h following hCG, which preceded cumulus expansion and mucification. Retraction of the cytoplasmic processes did not occur until about 9 h following hCG. Intercellular coupling between cumulus cells and oocytes was also measured at various times following hCG. Intercellular coupling was determined by measuring uptake of [^{3}H]uridine and [^{3}H]choline in cumulus-intact oocyte complexes and denuded oocytes. Both cumulus cells and oocytes could take up these radiolabelled compounds. Increased uptake by cumulus-oocyte complexes would indicate that oocytes were coupled to

cumulus cells via gap junctions. Indeed, oocytes, denuded of cumulus cells subsequent to radioactive uptake, exhibited significantly higher uptake compared to oocytes denuded of cumulus cells prior to radioactive uptake. This suggests that compounds similar in size to cAMP could be transferred between the oocyte and its cumulus mass. However, intercellular coupling decreased significantly approximately 3-4 h post-hCG (following the onset of GVBD). Thus, uncoupling of the cumulus processes from the oocyte, both physically and electrochemically, cannot be the normal physiological trigger of GVBD as this uncoupling occurs several hours following GVBD (Eppig, 1982).

Mammalian oocytes in antral follicles spontaneously resume meiosis in culture if released from their follicles. Meiotic arrest is maintained, however, if the oocytes are handled in the presence of permeable analogues of cAMP or inhibitors of cyclic nucleotide phosphodiesterase (PDE). These observations led to the proposal that cAMP is involved in the regulation of meiotic maturation and arrest in mammalian oocytes via the activity of a cAMP-dependent protein kinase (PKA; Fig. 9). This model proposed that a phosphoprotein (XP), a substrate of PKA, maintains meiotic arrest. A decrease in PKA activity, caused by a decrease in intracellular cAMP concentration would, due to phosphoprotein phosphatase activity, result in a net dephosphorylation of XP. The dephosphorylated protein, X, would then promote resumption of meiosis (Bornslaeger et al., 1986). A decrease in mouse oocyte cAMP does occur prior to maturation, both in vivo and in vitro, during the time when oocytes become committed to resume meiosis (Schultz et al., 1983b). In addition, specific oocyte phosphoproteins are dephosphorylated during this period. This model has been supported by the evidence that a microinjected inhibitor of PKA (PKI) induces GVBD, even under conditions which

Figure 9. Model for role of cAMP in oocyte maturation. *Adapted from Schultz et al, 1983b.* A. Meiotic arrest is maintained by a phosphoprotein XP, the active form of the protein. High intra-oocyte levels of cAMP activate a cAMP-dependent protein kinase (PKA) which phosphorylates protein X. B. Oocyte cAMP levels decrease resulting in inactive PKA, enabling phosphatases (PP) to dephosphorylate XP, thereby producing X, the inactive form of the protein which leads to GVBD. Low oocyte cAMP levels are maintained by robust phosphodiesterase (PDE) activity which hydrolyzes cAMP to 5'AMP.

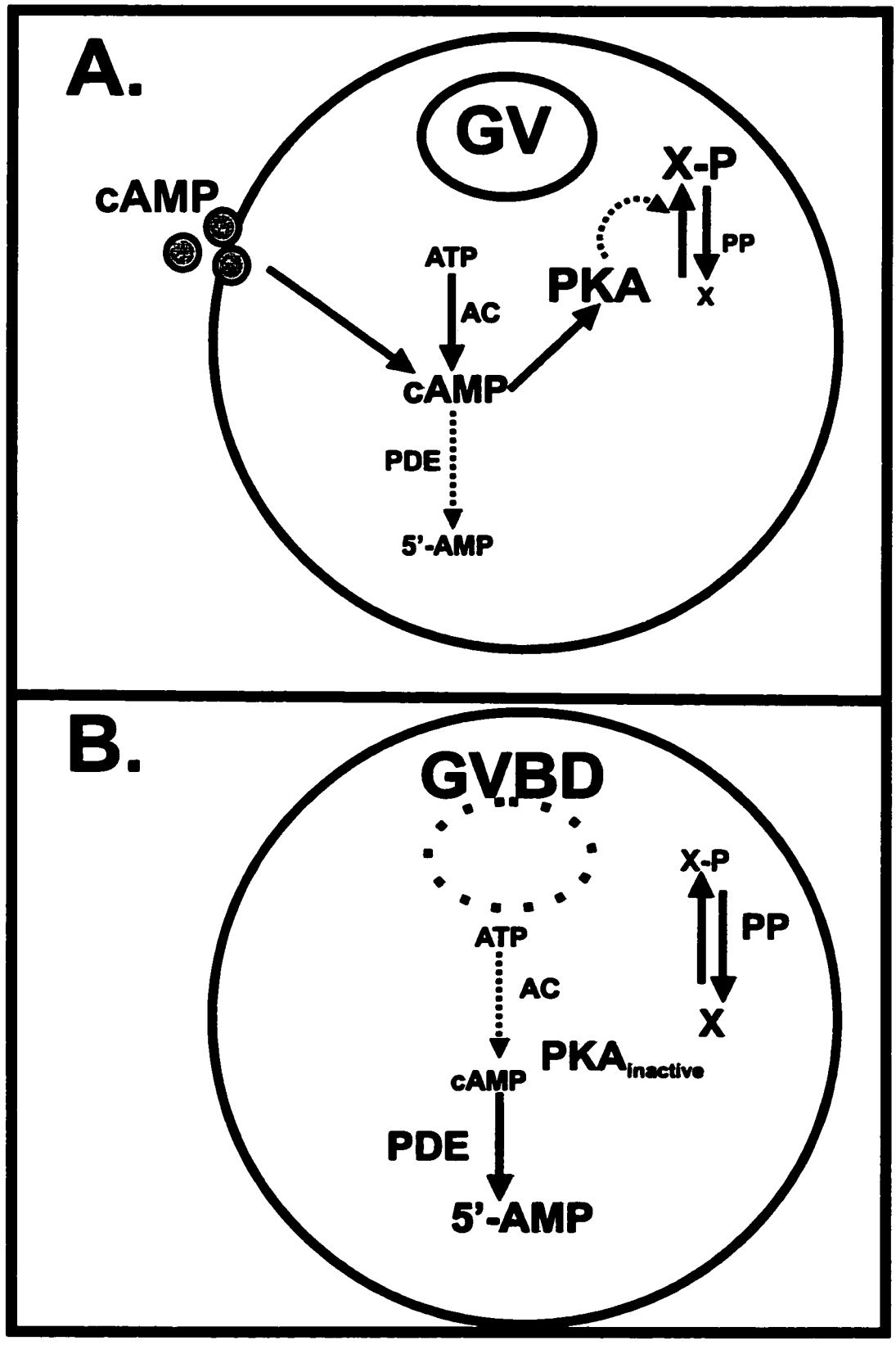
A.
GV
cAMP
X-P
PP
X
ATP
AC
PKA
cAMP
PDE
5'-AMP
B.
GVBD
X-P
PP
X
ATP
AC
PKA inactive
cAMP
PDE
5'-AMP

elevate oocyte cAMP levels and would normally inhibit meiotic resumption (Bornslaeger et al., 1986). Thus, these results seems to favour the second hypothesis which proposes that a change in the signal (cAMP) communicated from the follicle cells or follicular fluid triggers oocyte maturation.

III. FERTILIZATION

Sperm-capacitation, acrosome reaction, zona binding and penetration

Capacitation encompasses a series of changes to the spermatozoa to render it capable of undergoing the *acrosome reaction* (see below) and fertilization (Yanagamachi, 1988). Capacitation is correlated with changes in sperm plasma membrane fluidity, intracellular ion concentrations, metabolism, and motility. HCO_3^-, and a macromolecule such as albumin, are required for capacitation. Capacitation can be achieved in vitro in a balanced salt solution containing these components and a metabolic energy source. Albumin is believed to be responsible for the removal of cholesterol from the sperm plasma membrane, and may account for the changes in membrane fluidity (Visconti et al., 1995a). HCO_3^- appears to stimulate intracellular cAMP production without accompanying changes in pH_i (Visconti et al., 1995b). This is consistent with a recent report demonstrating that HCO_3^- directly activates the sperm-specific soluble adenylate cyclase (sAC) which thus increases intracellular cAMP (Chen et al., 2000).

The acrosome is a membrane-bound cap-like structure covering the anterior portion of the sperm nucleus. Functionally, the acrosome reaction serves to release hydrolytic enzymes to aid in the enzymatic dissolution of the zona pellucida to enable penetration through the zona. The acrosome reaction involves multiple fusion events

between the outer acrosomal membrane and the overlying plasma membrane, which enables the contents of the acrosome to escape though the fenestrated membranes (Yanagamachi, 1988).

Following capacitation, sperm must bind to the surface of the zona pellucida (Fig. 10). Sperm-egg binding in the mouse is mediated by zona glycoproteins ZP1, ZP2 and ZP3. These zona proteins are encoded by single copy genes, expressed by the oocyte during oogenesis and folliculogenesis. Zona pellucidae from $ZP1^{-/-}$ oocytes are structurally abnormal suggesting that ZP1 is an important structural component (Evans, 2000). ZP3 is the primary sperm receptor, which binds to sperm prior to the acrosome reaction. ZP2 is the secondary sperm receptor, which binds to the sperm following the acrosome reaction. ZP3 has both sperm-receptor and acrosome reaction-inducing activities (Yanigamachi, 1988). Following fertilization, both ZP2 and ZP3 are modified such that ZP3f can no longer bind or acrosome react sperm and ZP2f cannot interact with acrosome-reacted sperm. These modifications to ZP2 and ZP3 constitute the ZP block to polyspermy and represent an early event of egg activation (Xu et al., 1994).

Penetration through the zona pellucida is achieved by vigorous sperm tail movement (mechanical) and enzymatic digestion of the zona pellucida. Upon penetration of the zona, the sperm head crosses the perivitelline space, becomes attached to the vitellus and is gradually incorporated into it (Yanagamachi, 1988). Initial contact between sperm and egg is followed by adhesion to the egg plasma membrane. The egg plasma membrane, like the zona pellucida, also expresses sperm receptors which are members of the integrin family (Bronson et al., 1999; Zhu et al., 2000). Sperm surface ligands thought to be involved in sperm-egg interactions are members of the ADAM (a disintegrin and

Figure 10. Mouse in vitro fertilization. An egg from a CF-1 female mouse is fertilized in vitro by sperm (sp) from a CD-1 male. The visible sperm are bound to the zona pellucida (zp). Scale bar represents 50 μm.

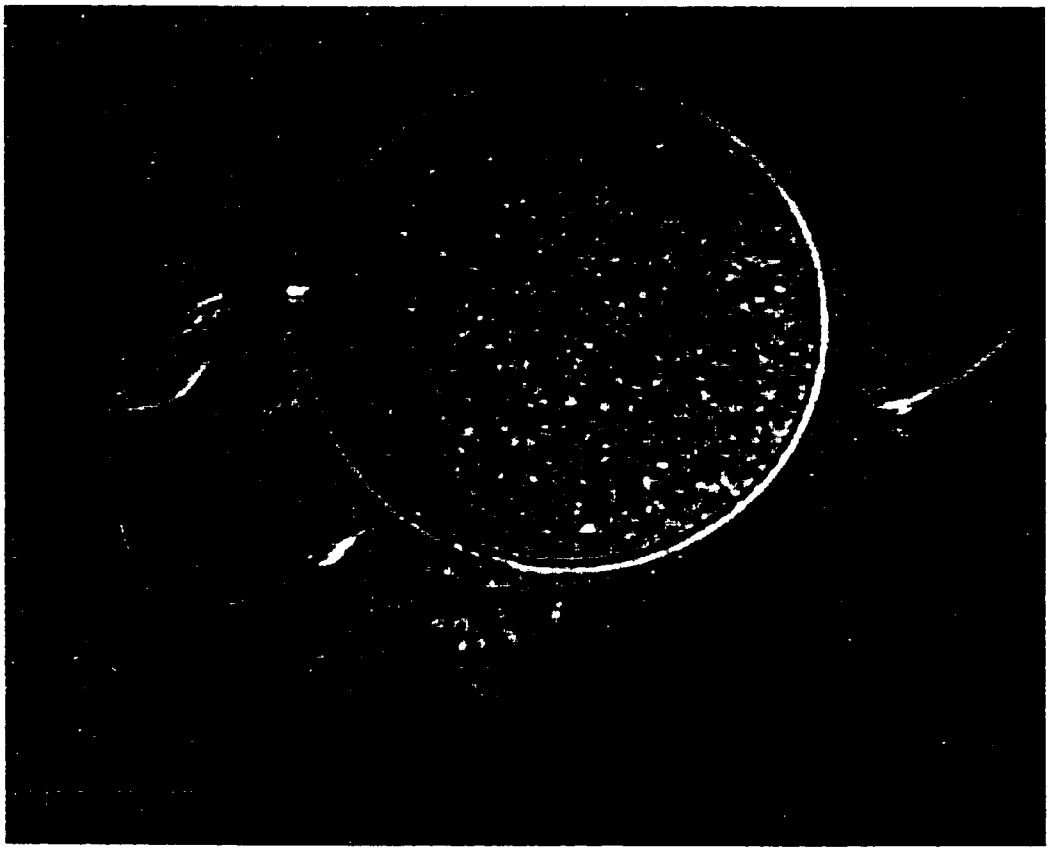

metalloprotease) family (Bigler et al., 2000). Five members of the ADAM family have been identified in mouse testis; fertilin α, fertilin β (PH-30; Moore et al., 1993), cyritestin, ADAM 4 and ADAM 5 (Yuan et al., 1997). Fertilin β and cryitestin are the two leading candidate ligands that have been proposed to mediate sperm-egg membrane binding and possibly fusion in the mouse (Shamsadin et al., 1999; Bigler et al., 2000).

Production of Ca^{2+}_i transients

Fertilization in all species studied to date is accompanied by a large, transient increase in intracellular Ca^{2+} (Ca^{2+}_i) in the egg (Fig. 11). In many animals, including mammals, this is followed by a series of repetitive Ca^{2+} transients lasting for several hours (Kline and Kline, 1992). In the mouse, the initial increase in Ca^{2+}_i is observed about 20-30 sec post-sperm attachment and spreads like a wave across the egg (Fig. 11B; Xu et al., 1994). In the hamster, Ca^{2+}_i increases from about 0.1 μM, prior to fertilization to 0.3 μM following sperm binding (Miyazaki, 1991). The ability to sustain repetitive Ca^{2+} transients for several hours is found only in mature oocytes, while immature oocytes exhibit only a brief period of Ca^{2+} transients with lower amplitudes upon activation (Jones et al., 1995a).

Ca^{2+}_i transients are dependent on the release of Ca^{2+} from Ca^{2+}_i stores (endoplasmic reticulum, ER; Xu et al., 1994). Net influx of extracellular Ca^{2+} is required for the continuation of the transients, as the frequency of the transients is dependent on external Ca^{2+} (Cheek et al., 1993; Igarashi et al., 1997). Intracellular stores are refilled primarily by Ca^{2+}_i uptake mediated by ER Ca^{2+}ATPase (Igarashi et al., 1997). Underlying

Figure 11. Ca^{2+}-dependent events at fertilization. A. At fertilization there is an increase in $Ca^{2+}{}_i$, however the mechanism by which this occurs is under some debate. One theory (illustrated here) suggests that sperm bind to receptors on the zona pellucida (ZP2 and ZP3), thereby activating a G-protein (Miyazaki et al., 1990; Jaffe, 1990; Cheek et al., 1993). GTP is hydrolyzed to GDP resulting in the activation of phospholipase C (PLC) and hydrolysis of phosphoinositol (PIP_2) into inositol trisphosphate (IP_3) and diacylglycerol (DAG). IP_3 mediates Ca^{2+} release from intracellular stores (ER, mitochondria) via IP_3 receptors. Following a Ca^{2+} wave or transient, Ca^{2+} uptake back into intracellular stores is mediated by Ca^{2+}-ATPase. Some Ca^{2+} is removed from the egg by Na^{+}/ Ca^{2+} exchanger or Ca^{2+}-ATPase. The increase in $Ca^{2+}{}_i$ results in cortical granule (CG) exocytosis which leads to the zona block to polyspermy. *B. Calcium wave.* Sperm binding triggers localized release of Ca^{2+} from intracellular stores resulting in Ca^{2+}-induced-Ca^{2+}-release (CICR).

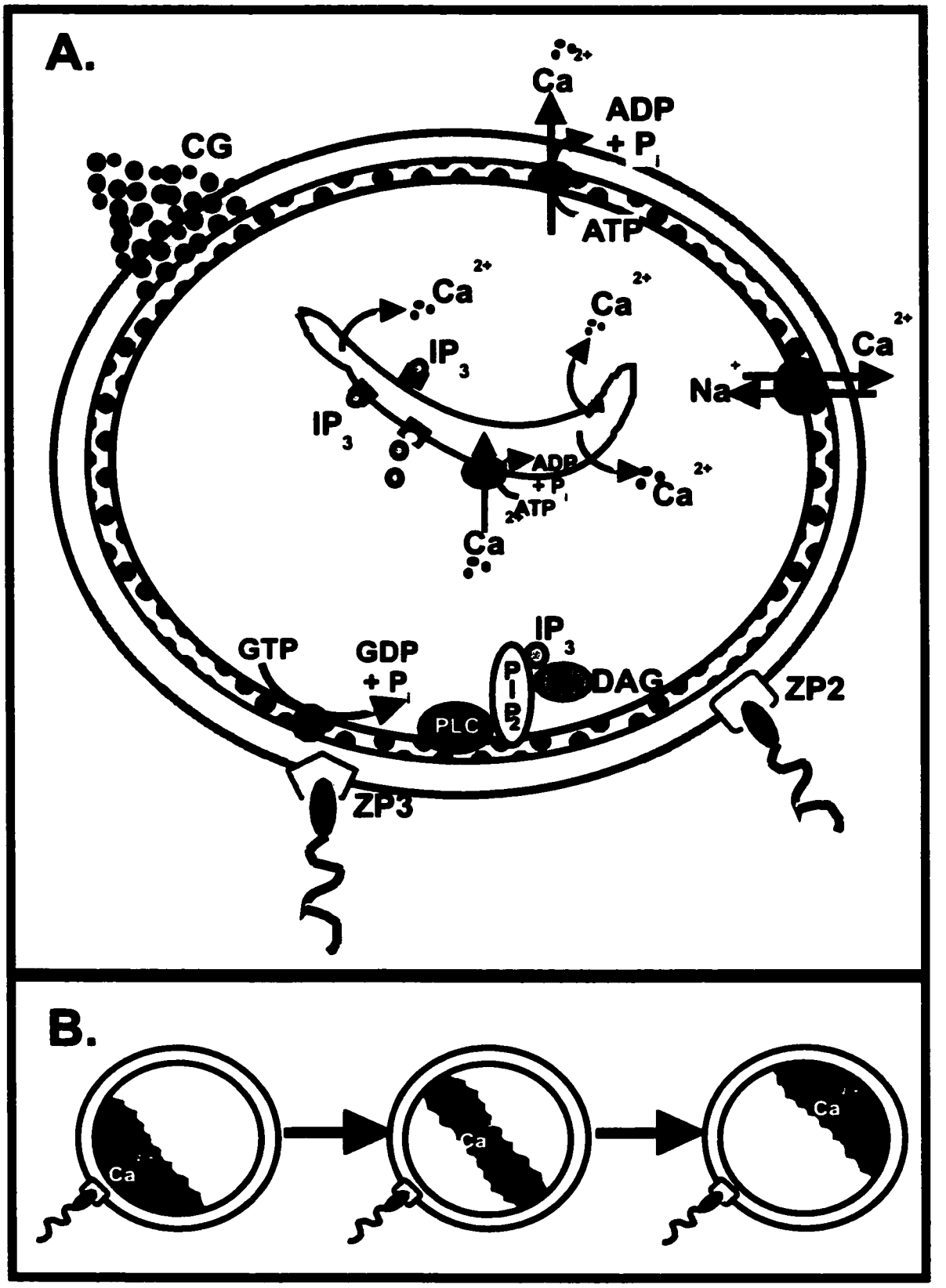
A.
Ca 2+
ADP + P i
CG
ATP
Ca 2+
Ca 2+
IP 3
Ca 2+
Na +
IP 3
ADP + P i
ATP
Ca 2+
Ca 2+
GTP
GDP + P i
IP 3
PIP 2
DAG
ZP2
PLC
ZP3
B.
Ca 2+
Ca 2+
Ca 2+

each Ca^{2+}_i transient is the continuous influx of Ca^{2+} through plasma membrane channels. This continuous influx of Ca^{2+} sets the frequency of Ca^{2+}_i transients, establishing the rate of refilling Ca^{2+}_i stores such that subsequent transients can be initiated (McGuinness et al., 1996).

Release of Ca^{2+} from intracellular stores is mediated by at least two pathways, IP_3-induced-Ca^{2+} release (IICR) and Ca^{2+}-induced-Ca^{2+} release (CICR), mediated by the ryandodine receptor/channel (RyR; Chini et al., 1998). Both receptors are located on intracellular Ca^{2+} stores (e.g. ER) and induce Ca^{2+}_i release upon agonist binding. The RyR can be activated by the endogenous nucleotide 5'-cyclic diphosphoribose (cADPR), however, the mechanism of activation of the RyR by cADPR is poorly understood (Chini et al., 1998). cADPR promotes Ca^{2+}_i release in sea urchin egg homogenates and microsomes (Galione and White, 1994). In addition to the IP_3 and RyR pathways, sea urchin egg Ca^{2+}_i release at fertilization may be mediated by yet another pathway activated by nicotinate-adenine dinucleotide phosphate (NAADP; Chini et al., 1998). IICR mediates Ca^{2+}_i transients and waves in mammalian eggs such as mouse and hamster (Miyazaki et al., 1992; Kline and Kline, 1994; Jones et al., 1995a).

Initiation of Ca^{2+}_i transients

How the sperm induces Ca^{2+} transients is unknown. However, there are two major hypotheses. One hypothesis suggests that a sperm-associated molecule may interact with a receptor coupled to a GTP binding protein or G-protein in the oocyte membrane to activate phospholipase C (PLC). PLC hydrolysis of PIP2 to produce Ca^{2+}_i release agonist IP_3 would result in Ca^{2+}_i release and the production of Ca^{2+} transients (Miyazaki, 1990;

Jaffe, 1990; Cheek et al., 1993). While G-protein activation in hamster oocytes does induce a series of Ca^{2+} transients, GDP-β–S (G-protein antagonist) injection does not inhibit sperm incorporation and poorly inhibits the production of Ca^{2+}_i transients (Cheek et al., 1993). This suggests that a G-protein may not be involved at fertilization (Swann and Whitaker, 1990). The timing of the initial Ca^{2+}_i transient also appears to preclude transmembrane receptor-mediation of Ca^{2+}_i release as egg-sperm membrane fusion occurs prior to the increase in Ca^{2+}_i (McCulloh and Chambers, 1992). If a transmembrane receptor coupled to an Ca^{2+}_i releasing-signalling pathway were involved, the initial Ca^{2+}_i transient would be expected to occur upon sperm binding to the putative receptor, not upon membrane fusion (Macháty et al., 2000).

The second hypothesis suggests that sperm-egg fusion results in a soluble sperm factor being released into the oocyte (Dale et al., 1985; Swann, 1990). This soluble sperm factor would be expected to act at or upstream of Ca^{2+} channel-coupled receptors regulating Ca^{2+}_i release from Ca^{2+}_i stores (mainly ER). As discussed, the main receptors regulating Ca^{2+}_i release are the IP_3R and the RyR (Tesarik, 1998). Direct evidence for a soluble sperm factor was shown by microinjecting soluble components from sperm into sea urchin and ascidian oocytes (Dale et al., 1999). The success of intracytoplasmic sperm injection (ICSI) seems to confirm this hypothesis, as injection of a sperm directly into the oocyte leads to normal embryogenesis in the absence of any normal sperm-egg membrane interaction (Tesarik et al., 1994). The identity of the soluble sperm factor is controversial. Perhaps the most conservative but reasonable hypothesis suggests that there are multiple sperm factors and possibly a membrane-bound component that initiates

Ca^{2+}_i release at fertilization. Multiple sperm factors would explain the growing number of Ca^{2+}_i release pathways identified and could include Ca^{2+}, IP_3, cGMP, ryanodine, cADPR, NAADP or PLCγ. Any of these molecules, or factor(s) that stimulate these pathways, could be the soluble sperm factor (Dale et al., 1999).

Cell cycle-dependence of Ca^{2+}_i transients

While the initiation of Ca^{2+}_i transients appears to be triggered by soluble sperm factor(s), the duration of Ca^{2+}_i transients may be dependent on the cell cycle. The ability of sperm to trigger Ca^{2+}_i transients is dependent on the stage of maturation of the egg as MII oocytes (12-14 h post-maturation) but not immature MI oocytes (10 h post-maturation) produce Ca^{2+}_i transients in response to insemination. However, MI oocytes that failed to progress to metaphase II (extrusion of the first polar body) by 14 h post-maturation were able to produce repetitive Ca^{2+}_i transients. This suggests that the egg's ability to generate continuous Ca^{2+}_i transients develops late in maturation between MI and MII (12-14 h post-maturation; Jones et al., 1995a; Cheung et al., 2000). Ca^{2+}_i transients, once initiated, last a number of hours, during which time the second polar body is emitted. The amplitude of the transients decreases shortly before pronuclear formation and ceases when pronuclei become visible. Ca^{2+}_i transients have been observed for up to 18 h in fertilized eggs maintained in metaphase arrest by microtubule depolymerizer colcemid (Kubiak et al., 1993; Jones et al., 1995b). Thus, Ca^{2+}_i transients appear to be regulated by the cell cycle.

Since Ca^{2+}_i transients cease at pronuclear formation and can be sustained

indefinitely if MII arrest is maintained experimentally after egg activation (Jones et al., 1995b), this suggests that Ca^{2+}_i transients may be specific to the portion of metaphase II starting at egg activation and ending with nuclear envelope reformation (PN formation). Metaphase in general is characterized by the activity of $p34^{cdc2}$ kinase/cyclin B. In ascidian oocytes, MPF $p34^{cdc2}$ kinase/cyclin B activity appears to be required for Ca^{2+}_i transients. Sperm trigger two series of Ca^{2+}_i transients in MI arrested ascidian oocytes, one of which triggers exit from MI arrest and the other terminates when the egg exits MII. Each series of Ca^{2+}_i transients is correlated with high MPF activity. The appearance of Ca^{2+}_i transients correlates with elevated MPF activity which is low during the extrusion of the first polar body, becoming increased at fertilization. The second phase of Ca^{2+}_i transients can be prevented by addition of roscovitine, an inhibitor of $p34^{cdc2}$ kinase/cyclin B suggesting that $p34^{cdc2}$ kinase/cyclin B controls Ca^{2+}_i transients in ascidian oocytes. There was no evidence, however, to suggest that $p34^{cdc2}$ kinase/cyclin B triggered the initial Ca^{2+}_i transient (Levasseur and McDougall, 2000). Ca^{2+}_i transients following fertilization in the mouse have also been demonstrated to be roscovitine-sensitive (Deng and Shen, 2000). Thus, $p34^{cdc2}$ kinase/cyclin B may be required to sustain Ca^{2+}_i transients.

Nuclei transferred from 1- and 2-cell embryos to MII eggs cause the release of Ca^{2+}_i that is sufficient to cause parthenogenetic activation. Ca^{2+}_i release and subsequent parthenogenetic activation were only observed following nuclear envelope breakdown (NEBD). This suggests that Ca^{2+}_i-releasing ability is associated with the nucleus. A possible mechanism for the initiation of Ca^{2+}_i transients may be that the soluble sperm factor(s) causes the release of Ca^{2+}_i and then associates with the nucleus. Alternatively, a

soluble sperm factor may initiate Ca^{2+}_i transients while another nuclear factor subsequently sustains the Ca^{2+}_i transients. After nuclear transfer and subsequent NEBD, the putative nucleus-associated factor is released and stimulates Ca^{2+}_i transients and parthenogenetic activation. Several proteins are localized in the nucleus during interphase and become cytoplasmic after NEBD and thus may be candidates for this Ca^{2+}_i transient-inducing nuclear factor. These proteins include cdc25 and $p34^{cdc2}$/cyclin B. This model would suggest that Ca^{2+}_i transients could be reinitiated during NEBD of the first mitotic cell cycle prior to cleavage to the 2-cell stage (Kono et al., 1995). There are reports that Ca^{2+}_i transients have been observed during this period in mouse (Tombes et al., 1992), *Xenopus* (Kubota et al., 1993), and sea urchin embryos (Poenie et al., 1985; Whitaker and Patel, 1990). Thus, the presence of Ca^{2+}_i transients during NEBD of embryonic mitosis is consistent with Ca^{2+}-releasing activity associated with a nucleus factor which becomes cytoplasmic following NEBD (Kono et al., 1995). That a nucleus-associated protein may have Ca^{2+}_i-releasing activity is consistent with the cessation of Ca^{2+}_i transients upon formation of pronuclei and presumably, sequestration of the nuclear factor within the pronuclei (Jones et al., 1995b).

Cortical granule exocytosis

Cortical granules are small, spherical, membrane-limited organelles containing hydrolytic enzymes and saccharide components located beneath the plasma membrane of mature unfertilized eggs. The release of cortical granules, just following sperm-egg fusion, alters the physical and chemical characteristics of the zona pellucida causing the zona to become refractory to further sperm penetration. This is called the *cortical granule*

reaction (Yanagamachi, 1988). Cortical granule exocytosis occurs 2.5-5 min after sperm attachment to zona-free hamster eggs and 5-15 min after sperm attachment to zona-free mouse eggs (Kline and Stewart-Savage, 1994). Cortical granule exocytosis is one of the most Ca^{2+}-sensitive events of egg activation. Cortical granule exocytosis occurs over a narrow threshold range of injected free Ca^{2+} concentration (between 0.5 and 1 μM) whereas later events, such as cell cycle resumption are not observed below 2.5 μM injected free Ca^{2+} (Xu et al., 1994). Activators of the protein kinase C (PKC) pathway, such as phorbol esters and DAG, have been shown to induce cortical granule exocytosis, suggesting that PKC may mediate cortical granule exocytosis (Ducibella and LeFevre, 1997).

Egg plasma membrane block

The egg plasma membrane also has the ability to reject excess sperm. This block to polyspermy has been called the *vitelline block* or *egg plasma membrane block* (Yanagamachi, 1988). In the sea urchin egg, the egg plasma membrane becomes refractory to excess sperm within a few seconds after attachment of the first sperm to the membrane. The fast block to polyspermy is electrical in nature (Payan et al., 1981). The depolarization of the membrane follows sperm attachment and serves two functions: 1) it permits entry of the fertilizing sperm and 2) it blocks entry of supernumerary sperm (Chambers and McCulloh, 1990; Jaffe, 1990). In *Xenopus,* the fertilization potential is caused by Ca^{2+}-sensitive Cl^- channels (Grandin and Charbonneau, 1991a).

In hamster and human oocytes the fertilization-induced hyperpolarization is Ca^{2+}

dependent (Gianaroli et al., 1994). The increase in Ca^{2+}_i activates a Ca^{2+}-dependent K^+ current resulting in membrane hyperpolarization (Cherr and Ducibella, 1990; Miyazaki et al., 1992). The first hyperpolarization occurs as the sperm fuses with the egg, in contrast to the depolarization seen in sea urchin eggs that accompanies sperm binding (Cherr and Ducibella, 1990). In the mouse, the plasma membrane block occurs too slowly to be electrophysiological in nature and seems to involve a permanent change of the egg surface (Tatone et al., 1994). Thus, although the plasma membrane block differs between species, its presence functions to exclude supernumerary sperm.

Changes in intracellular pH (pH_i)

Fertilization in the sea urchin is accompanied by a large increase (~0.3 pH units) in intracellular pH (pH_i; Johnson et al., 1976). This observation triggered much interest in the study of pH_i changes at fertilization to determine whether cytoplasmic alkalinization was yet another universal event at fertilization, in addition to the increase in Ca^{2+}_i. *Xenopus* and some marine invertebrates also exhibit changes in pH_i upon egg maturation or fertilization, although not to the same extent as the sea urchin egg (Epel, 1988).

pH_i of the unfertilized sea urchin egg is low (pH_i~6.8) and becomes subsequently increased 1 to 4 min following fertilization to pH_i 7.2-7.3 (Johnson et al., 1976; Shen and Steinhardt, 1978). This fertilization-induced increase in pH_i results from the Na^+-dependent efflux of H^+ (Johnson et al., 1976; Payan et al., 1981). As H^+ efflux was shown to require external Na^+ (Chambers, 1976) and was sensitive to the Na^+/H^+ antiporter inhibitor amiloride (Johnson et al., 1976; Shen and Steinhardt, 1979), this

suggested that the increase in pH_i at fertilization in the sea urchin was mediated by an amiloride-sensitive Na^+/H^+ antiporter with a stoichiometry of 1:1 (Johnson et al., 1976; Girard et al., 1982; Payan et al., 1983).

Na^+/H^+ antiporter activity is present in the unfertilized egg. At fertilization, the Na^+/H^+ antiporter is activated resulting in the increased efflux of H^+ thereby causing cytoplasmic alkalinization (Payan et al., 1983). This suggested that the pH_i set-point, or threshold below which Na^+/H^+ antiporter activity is increased, was shifted in the alkaline direction at fertilization. Activation of the Na^+/H^+ antiporter at fertilization most likely involved phosphorylation following a signal transduction pathway, such as PKC (Epel, 1988; Jiang et al., 1990).

To investigate the PKC pathway, phorbol esters and DAG analogs have both been used to activate the PKC pathway in the absence of fertilization in the sea urchin egg. Both of these agents activated Na^+/H^+ exchanger in the absence of fertilization resulting in Na^+-dependent H^+ efflux. This suggested that PKC may regulate Na^+/H^+ antiporter activity (Swann and Whitaker, 1985). However, Na^+/H^+ antiporter activity can also be activated by Ca^{2+}-calmodulin-dependent kinase (CaMKII). An inhibitor of CaMKII, W-7, was shown to inhibit the fertilization-induced increase in pH_i, suggesting that the fertilization-dependent cytoplasmic alkalinization may be mediated by both CaMKII and PKC-activation of Na^+/H^+ antiporter (Shen, 1989; Shen and Buck, 1990).

The increase in pH_i in the sea urchin egg is an important component of fertilization. In the absence of sperm, egg activation results from simply raising pH_i by the addition of ammonia or other organic amines. As exposure to weak bases (ammonia, procaine, nicotine) alkalinizes the cytoplasm independent of external Na^+, this suggests

that parthenogenetic activation by these agents is independent of Na^+-coupled H^+ efflux (Johnson et al., 1976; Boron et al., 1978; Winkler and Grainger, 1978).

While many processes triggered by fertilization are dependent on the increase in Ca^{2+}_i, protein synthesis can be triggered by alkalinization of the cytoplasm by ammonia or other weak bases (Winkler and Grainger, 1978). The increased pH_i seems to be the major immediate cause of increased protein synthesis (Swann and Whitaker, 1985; Lau et al., 1986). The rate of protein synthesis is increased by 5-30 fold beginning 5 min after fertilization and can be manipulated by changing pH_i. Lowering pH_i decreases the rate of protein synthesis while increasing pH_i causes an increase in the rate of protein synthesis. This is consistent with regulation of protein synthesis by cytoplasmic alkalinization (Grainger et al., 1979; Winkler, 1982; Dubé et al., 1985).

Other fertilization-associated processes shown to be pH_i-sensitive include development of new K^+ conductance (Shen and Steinhardt, 1980), the post-fertilization organization of actin bundles in microvilli and the microfilamentous contractile ring responsible for the formation of cleavage furrow (Dubé et al., 1985; Epel, 1988), DNA synthesis (Lopo and Vacquier, 1977; Whitaker and Steinhardt, 1981; Lau et al., 1986) and the post-fertilization respiratory burst (Heinecke and Shapiro, 1990). Thus, the fertilization-dependent activation of Na^+/H^+ antiporter activity resulting in cytoplasmic alkalinization in the sea urchin egg mediates many metabolic and ionic events in the newly fertilized egg.

pH_i changes in other species

Fertilization in *Xenopus* is accompanied by a biphasic change in pH_i. First a

transient acidification followed by a permanent increase in pH_i of about 0.3 pH units. A gradual increase in pH_i occurs 5-10 min following egg activation, raising pH_i from 7.4 to 7.7. This increase in pH_i is permanent and is sustained through at least 10 cleavage cycles, with small cell-cycle-dependent pH_i oscillations (Webb and Nuccitelli, 1981). Similar to sea urchin eggs, *Xenopus* eggs can be parthenogenetically activated by weak bases, suggesting a role for cytoplasmic alkalinization in egg activation. However, unlike the sea urchin egg, weak base activation releases membrane-bound $Ca^{2+}{}_i$ (Grandin and Charbonneau, 1991a; Grandin and Charbonneau, 1991b).

The mechanism of cytoplasmic alkalinization in *Xenopus* eggs at fertilization is not well understood. No efflux of H^+ appears to occur during cytoplasmic alkalization and it is independent of external Na^+, either of which would preclude Na^+/H^+ antiporter activity. Intracellular sequestration of H^+ has been proposed to increase cytoplasmic pH_i which is consistent with the low permeability to ions exhibited by the fertilized *Xenopus* egg and the lack of effect of external pH on pH_i (Webb and Nuccitelli, 1981). $Ca^{2+}{}_i$ may regulate the increase in pH_i at fertilization. Inhibition of $Ca^{2+}{}_i$ transients at fertilization by BAPTA or EGTA, two potent chelators of $Ca^{2+}{}_i$, delayed the activation-associated increase in pH_i, suggesting that the increase in pH_i is a consequence of the $Ca^{2+}{}_i$ wave and transients (Grandin and Charbonneau, 1992).

Xenopus oocyte maturation is also accompanied by an increase in pH_i (~0.3 pH unit) by a mechanism that does involve loss of H^+ (Cicirelli et al., 1983) and is independent of the membrane potential (Lee and Steinhardt, 1981). Na^+ influx steadily increases during maturation, beginning almost immediately after progesterone exposure, followed by an increase in passive Ca^{2+} influx. This suggests that Na^+/H^+ antiporter may

indeed regulate the increase in pH_i observed during oocyte maturation in *Xenopus* (Cicirelli et al., 1983). At GVBD, oocytes undergo an increase in pH_i in response to progesterone. GVBD, as discussed, can be prevented by agents which increase or maintain high levels of intraoocyte cAMP (e.g. forskolin, methylxanthines). These same compounds also prevent upregulation of Na^+/H^+ antiporter activity during meiotic maturation (Rezai and Wasserman, 1994). This may indicate that low cAMP is required for Na^+/H^+ antiporter upregulation or that upregulation is dependent on resumption of meiosis. Na^+/H^+ antiporter activity upregulation results from microinjection of mos, indicating that a mos-dependent mechanism may regulate Na^+/H^+ antiporter (Rezai et al., 1994). Another report suggested that Raf-1 activation, independent of mos and MAPKK, regulated the upregulation of Na^+/H^+ antiporter activity during oocyte maturation. High levels of cAMP were able to prevent the increase in pH_i but were unable to block the Raf-1-induced increase in pH_i. Thus, Na^+/H^+ antiporter activity is upregulated during meiotic maturation of *Xenopus* oocytes by a mechanism involving Raf-1 and perhaps by a second pathway which is dependent on mos (Kang et al., 1998).

An increase in pH_i is an important feature of fertilization for *Urechis caupo*. *Urechis* eggs are fertilized as primary oocytes and thus GVBD is not initiated until after fertilization. The acid release is required for egg activation and begins 10 sec after fertilization, increasing the pH_i by 0.25-0.3 pH units. The increase in pH_i occurs prior to GVBD and is necessary for this event (Paul, 1975; Gould and Stephano, 1993). The identity of the exchangers that mediate this acid efflux is not yet clear, but there is substantial Na^+ uptake at fertilization, suggesting that some H^+ release may be mediated via Na^+/H^+ antiporter (Gould and Holland, 1984).

Molluscan oocytes are also fertilized at prophase I. Meiotic resumption appears dependent on both Ca^{2+} influx and an increase in pH_i. *Barnea*, a bivalve mollusc, undergoes a 0.2 pH unit increase in pH_i; however, artificially raising pH_i alone is ineffective to trigger maturation. Artificially lowering oocyte pH_i by the addition of weak acids does prevent GVBD, indicating some role of increased pH_i at maturation (Brassard et al., 1988; Freeman and Ridgway, 1993). In *Spisula* (surf clam) oocytes, also fertilized in prophase I, an increase in pH_i appears necessary for GVBD. This acid release is Na^+-dependent and is mediated by Na^+/H^+ antiporter activity, as in the sea urchin (Dubé et al., 1985; Dubé, 1988; Dubé and Eckberg, 1997). Parthenogenetic activation also results in acid release, suggesting that this is a feature of egg activation (Suprenant, 1989).

Patella vulgata (limpet) oocytes are fertilized at metaphase of MI. Meiosis reinitiation proceeds in two steps and is regulated by ionic factors. The first step, which leads to GVBD, includes chromosome condensation and the formation of an MI spindle and involves an increase in pH_i. The second step involves the release of the oocyte from the MI block and is dependent on an increase in $Ca^{2+}{}_i$. MPF is necessarily important in this reinitiation as it promotes GVBD, nuclear envelope disruption and chromosome condensation. Simply raising pH_i by about 0.6 units can induce GVBD and the reinitiation of meiosis up to MI (Guerrier et al., 1986; Néant and Guerrier, 1988). During activation, the rate of the acidification of the external medium is proportional to the rate of GVBD indicating a correlation between pH_i and maturation (Guerrier et al., 1986). Voltage-gated Na^+ channels activated by sperm mediate the fertilization potential and H^+ release is also voltage-sensitive (Néant and Guerrier, 1988).

The increase in pH_i has been a well documented feature of fertilization in the sea

urchin for almost a century (Loeb, 1906; 1913), however, pH_i had not been examined during mammalian fertilization. As some events at fertilization are apparently universal, such as the increase in Ca^{2+}_i, changes in pH_i may be a feature of mammalian fertilization as well. There was some evidence to suggest that mammalian (mouse) eggs can be activated by a permeant weak base, methylamine, in a dose-dependent manner (Dyban and Noniashvili, 1990), which would support this idea. However, it was also possible that methylamine exposure induced a transient Ca^{2+}_i increase, rather than having its effect via pH_i. As upregulation of pH_i regulatory transporters at egg activation appears to be a widespread phenomenon, clearly this is an avenue of investigation which requires further study in a mammalian model.

Egg activation

The activation of the egg, defined here as resumption of the cell cycle and progression into interphase, is initiated by the destruction of MPF, and thus cessation of MII arrest (Fig. 12). As discussed above, CSF is essential for the maintenance of metaphase II arrest in mice. Loss of CSF activity does not occur until several hours following the loss of MPF activity in interphase at the time of pronuclear formation. The deactivation of MPF and CSF at fertilization occur after the initial increase in Ca^{2+}_i and involve CaMKII. In mouse oocytes, the respective time-courses of MPF and CSF deactivation are similar whether the egg is activated by a series of Ca^{2+}_i transients (fertilization) or a single Ca^{2+}_i transient (as in some methods of parthenogenetic activation, see below; Zernicka-Goetz et al., 1995). As discussed above, the destruction

Figure 12. Egg activation. *A. Schematic of MPF and MAPK activation during egg activation.* The increase in $Ca^{2+}{}_i$ caused by sperm binding activates the ubiquitination pathway, thereby increasing cyclin B1/2 destruction. Loss of cyclin B1/2 leads to inactivation of MPF. The $Ca^{2+}{}_i$ threshold for cyclin destruction is lower than the threshold for mos destruction. MAPK activity is lost very slowly resulting from a loss of mos protein (Vincent et al., 1992). *B. Time-course of MPF activity and MAPK activity during egg activation* (Verlhac et al, 1994; Moos et al, 1995). MPF and MAPK are both active in the MII egg. MPF becomes inactivated soon after sperm (sp) binding. The egg exits metaphase II and extrudes the second polar body (PB2). MAPK is inactivated very slowly following egg activation, becoming significantly lower at the time of pronuclear (PN) development (interphase). A male (large) and female (small) pronucleus forms. MAPK is fully inactive 7-9 h following activation.

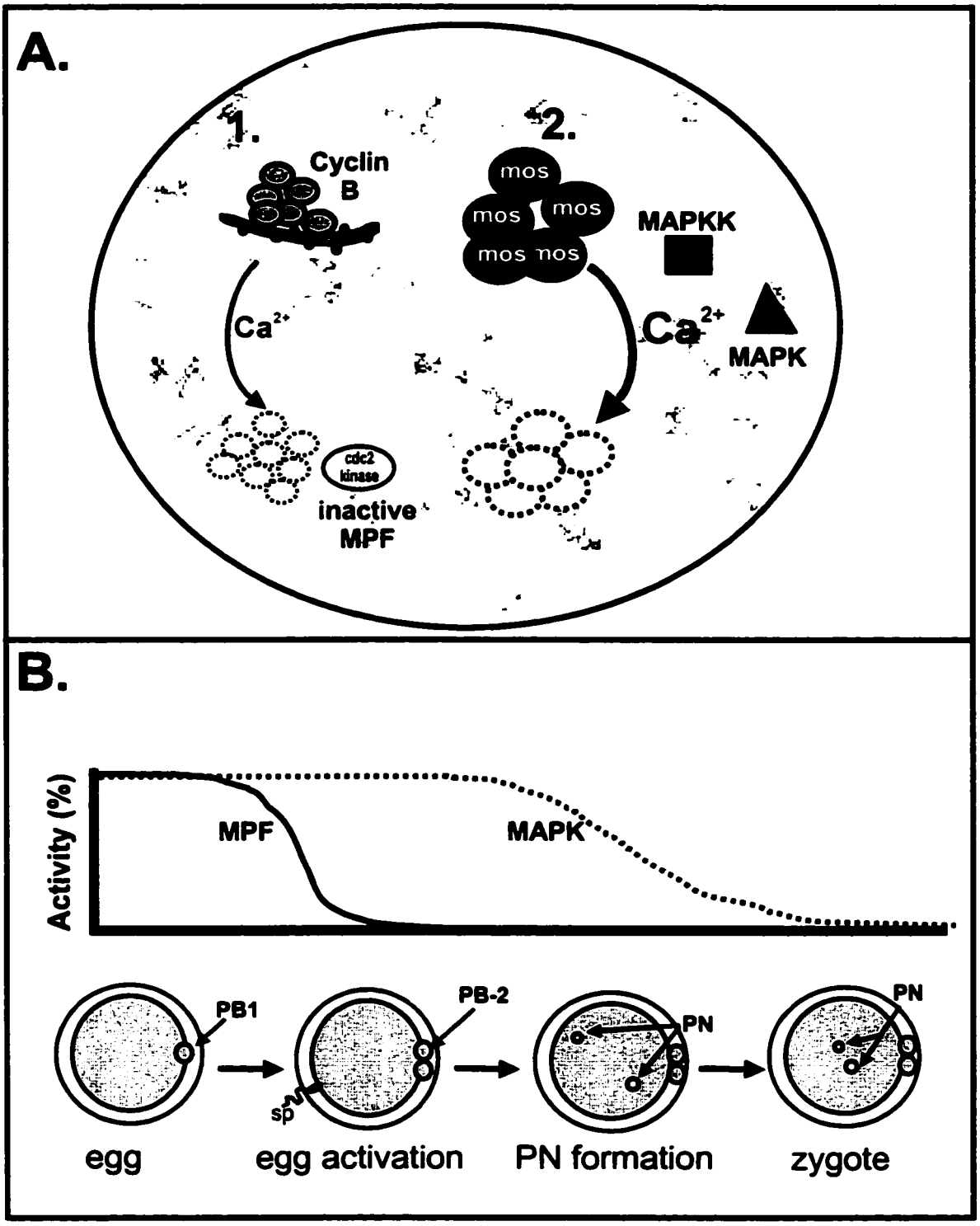
A.
1.
Cyclin B
2.
mos
mos
mos
mos
MAPKK
Ca2+
Ca2+
MAPK
cdc2 kinase
inactive MPF
B.
Activity (%)
MPF
MAPK
PB1
PB-2
sp
PN
PN
egg
egg activation
PN formation
zygote

of cyclin B, and thus the loss of MPF activity, requires an intact mitotic spindle. Thus, agents which disrupt microtubules, such as demecolcine or nocadozole, prevent cyclin degradation and cell cycle resumption (Winston and Maro, 1995b). Ca^{2+} transients play an important role in the initiation of cell cycle resumption, as increased Ca^{2+}_i results in destruction of cyclin B and mos via CaMKII activation of the ubiquitination pathway (Lorca et al., 1991) and the Ca^{2+}-dependent cysteine protease calpain, respectively (Watanabe et al., 1989). The different rates of MPF and CSF inactivation (Fig. 12) may be dependent on their respective sensitivities to Ca^{2+}_i, since cyclin B destruction occurs at much lower Ca^{2+}_i than mos destruction (Vincent et al., 1992; Taieb et al., 1997).

Once activated, the egg undergoes a second unequal cleavage, producing the second polar body (Fig. 4) between 1 and 3 h post-insemination. Following cytokinesis, the egg is haploid and the remaining chromosomes will form the female pronucleus. The first polar body typically degenerates during the first cell cycle, although in 60-70% of mouse embryos, it cleaves prior to degeneration (Howlett and Bolton, 1985). Polar body emission is accompanied by an accumulation of actin in the region of the second polar body, as the cytoplasm 'dimples' just prior to emission (Gallicano et al., 1997).

Formation of male and female pronuclei

Following insemination, the emission of the second polar body signals the completion of meiosis and entry into interphase. In mitotic cell cycles, the formation of the nuclear envelope occurs immediately upon entry into interphase. However, pronuclear formation following fertilization is delayed by 2-4 h after second polar body formation (Fig. 13; Smith and Johnson, 1986). The pronuclei form at opposite poles of the egg; the

Figure 13. Timing of events at fertilization and first cell cycle in the mouse. *Adapted from Howlett and Bolton, 1985.* The egg becomes activated upon loss of MPF activity followed by emission of the second polar body (PB2) and entrance into G1 (1.5-3 h post-insemination). The larger male pronucleus forms distal to PB2 (4-7 h). The smaller female pronucleus forms proximal to PB2 (6-8 h). Pronuclei migrate to centre of egg (8-10 h). The embryo enters S-phase around 13 h post-insemination at which time DNA replication will occur. The embryo then enters metaphase around 18 h post-insemination followed by nuclear envelope breakdown, cleavage to form a 2-cell embryo, and nuclear reformation (G2).

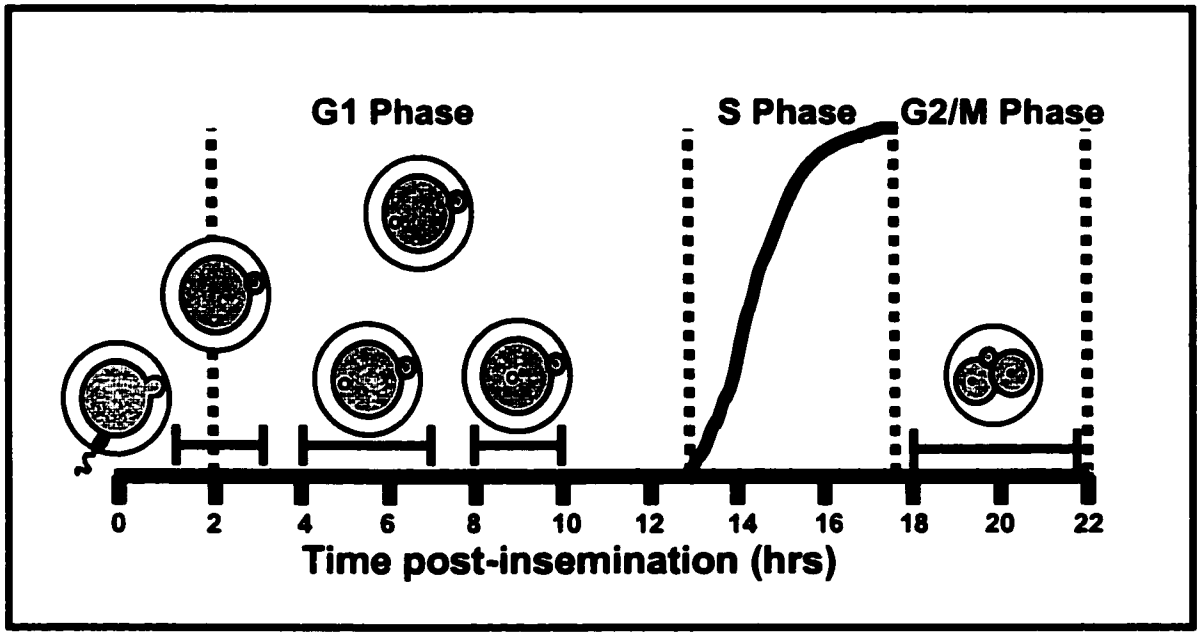
G1 Phase
S Phase
G2/M Phase
0
2
4
6
8
10
12
14
16
18
20
22
Time post-insemination (hrs)

much larger male pronucleus at the point of the sperm entry and the smaller female pronucleus near the second polar body. The male pronucleus forms between 4 and 8 h post-insemination while the female pronucleus forms between 5 and 9.5 h (Fig. 13). Both pronuclei migrate to the centre of the egg by 8-10 h post-insemination (Howlett and Bolton, 1985). The migration of the pronuclei towards the centre of the egg is mediated by the cytoskeleton, requiring both microfilaments and microtubules (Yanagamachi, 1988).

How the formation of pronuclei is regulated is not well known, but MAPK activity is implicated. MAPK becomes activated during meiotic maturation and remains high in the unfertilized egg (Fig. 6). Just as MAPK is activated slowly during GVBD, MAPK is deactivated (dephosphorylated) with a very slow time-course after egg activation. MAP kinase is still fully active until about 2 h following the emission of the second polar body, becoming significantly lower around the time of the formation of pronuclei and becoming fully inactive 7-9 h following fertilization (Verlhac et al., 1994). This loss of MAPK activity appears to be essential for the formation of the pronuclear envelope, as experimental manipulations which maintain active MAPK prevent pronuclei formation (Moos et al., 1996). Okadaic acid (OA), a specific inhibitor of phosphatase I and 2A, prevents pronuclear envelope formation when added to eggs during activation. OA treatment of fertilized mouse oocytes activates both histone H1 (MPF substrate) kinase and MAPK activities (Schwartz and Schultz, 1991). Both H1 kinase (MPF) and MAPK phosphorylate nuclear lamins (nuclear envelope component) in other cells (Peter et al., 1992), and OA treatment of fertilized oocytes also results in hyperphosphorylation of nuclear lamins (Schwartz and Schultz, 1991) which are present on the surface of the

male and female pronuclei (Yanagamachi, 1988). This suggests that MPF and/or MAPK are involved in the regulation of nuclear envelope assembly. In addition, expression of a constitutively active MAPKK, MEKE, in mouse oocytes prevented the fertilization-induced decrease in MAPK activity and also prevented development of pronuclei. MPF activity does decrease normally, however, and emission of the second polar body occurs. This indicates that MAPK, the only known target of MEKE, may regulate pronuclear envelope assembly/disassembly in mouse oocytes independent of MPF (Moos et al., 1996).

IV. PARTHENOGENETIC ACTIVATION

Parthenogenesis is the activation of unfertilized eggs in the absence of sperm. Egg activation can include early events characteristic of fertilization (Ca^{2+}-dependent changes to the zona pellucida and cortical granule exocytosis) as well as cell cycle resumption (end of metaphase arrest). Parthenogenetic activation (cell cycle resumption) can be achieved by inhibition of cyclin B synthesis or by the destruction of cyclin B; both of which decrease MPF activity. Thus, agents that inhibit protein synthesis (cycloheximide) or raise $Ca^{2+}{}_i$ and trigger the Ca^{2+}-dependent cyclin degradation pathway (ethanol, Sr^{2+}, A23187) induce parthenogenetic egg activation by causing a decrease in cyclin B, and therefore a decrease in MPF activity (Moos et al., 1996). Parthenogenetic egg activation may be followed by polar body extrusion in which haploid parthenogenotes are generated. Conversely some eggs may retain both sets of telophase chromosomes to generate two female pronuclei and thus form diploid parthenogenotes. Artificially activated mouse oocytes will develop with variable success to just post-implantation, but

have little subsequent developmental potential due to deficiencies of placental development arising from the lack of paternal chromosomes (Johnson et al., 1990).

Some parthenogenetic agents trigger the release of Ca^{2+}_i by affecting the properties of the plasma membrane, thereby releasing bound Ca^{2+}_i. These include electrical pulse, cold shock, heat shock, acid Tyrode's solution, hyaluronidase and pronase (Kaufman, 1978). Aged eggs can be activated by exposure to room temperature and are more easily activated than freshly ovulated eggs, as MPF is lower and therefore more readily decreased to a level which permits exit from metaphase (Stice et al., 1994).

Ca^{2+} releasing agents

A23187 is a Ca^{2+} ionophore which causes egg activation by increasing Ca^{2+}_i concentration and thereby stimulating cyclin B destruction via a specific Ca^{2+}_i -activated ubiquitination pathway. The destruction of cyclin B is followed by a decrease in MAPK activity with similar time-courses for deactivation as in fertilized eggs. Activation results in only a monotonic increase in Ca^{2+}_i (single transient), rather than multiple, repetitive Ca^{2+}_i transients, but this is sufficient for ZP2-ZP2f conversion and cortical granule exocytosis (Moos et al., 1996). The combination of A23187 and Ca^{2+}-free solution may act synergistically to activate eggs by increasing intracellular Ca^{2+} and inhibiting protein synthesis, as Ca^{2+} and Mg^{2+}-free medium markedly inhibits protein synthesis (Bos-Mikich et al., 1995). IP_3 microinjection can parthenogenetically activate both hamster and mouse eggs by inducing release of Ca^{2+}_i. IP_3 causes only partial egg activation, as the cortical granule reaction and zona modifications are induced without resulting in cell cycle resumption or the recruitment of maternal mRNAs (Winston et al., 1991; Tatone et

al., 1994; Xu et al., 1996). Microinjection of a single bolus of IP_3 induces a single Ca^{2+}_i transient, whereas fertilization produces a repetitive train of Ca^{2+}_i transients. Fertilization-induced repetitive Ca^{2+}_i transients also "reset" the basal Ca^{2+}_i concentration between transients to a higher level. This is not observed following IP_3 injection. Instead, following production of a single Ca^{2+}_i transient, Ca^{2+}_i returns to basal levels (Miyazaki et al., 1992). This suggests that the establishment of a higher basal concentration of Ca^{2+}_i is required for resumption of the cell cycle and recruitment of maternal mRNAs (Xu et al., 1996). Indeed, a higher Ca^{2+}_i threshold for these 'later events' of egg activation was shown using step-wise increments of the Ca^{2+} chelator BAPTA. Cortical granule exocytosis occurs between 0.5 and 1 μM injected free Ca^{2+}_i, while recruitment of maternal mRNA is only partially stimulated at 2.5 μM, with the threshold for cell cycle resumption well above 2.5 μM free Ca^{2+}_i (Xu et al., 1996).

Eggs exposed to a brief pulse of ethanol (5-8%) are parthenogenetically activated by an increase in Ca^{2+}_i (Fig. 14A). The majority of activated eggs develop a single pronucleus following second polar body extrusion. With optimal activation protocols, high proportions of single pronuclear haploids develop to the blastocyst stage. Maximum rates of activation can be achieved following exposure to a 7% solution of ethanol in PBS (phosphate-buffered saline) for 3-4.5 min (Kaufman, 1982). Activation is accompanied by a monotonic increase in Ca^{2+}_i, extrusion of the second polar body and formation of pronuclei (Kono et al., 1995). Parthenogenetic egg activation by ethanol results in the exocytosis of cortical granules and the changes to the plasma membrane to prevent polyspermy (Tatone et al., 1994). MPF and MAPK activities are deactivated with time-

Figure 14. Parthenogenetically activated eggs. A. Eggs exposed to 7% ethanol (EtOH) for 5 min, followed by standard KSOM culture. This activated egg is shown 7 h post-activation. B. Eggs exposed to 10 mM SrCl for 2 h followed by standard KSOM culture. This activated egg is shown 9 h post-activation. C. Eggs exposed to 50 μg/ml cycloheximide (protein synthesis inhibitor) for 2 h followed by standard KSOM culture for 9 h. D. Egg exposed to 50 μM U0126 (MEK inhibitor) for 9 h. Scale bar represents 50 μm. PN-pronucleus, PB-polar body.

A. EtOH

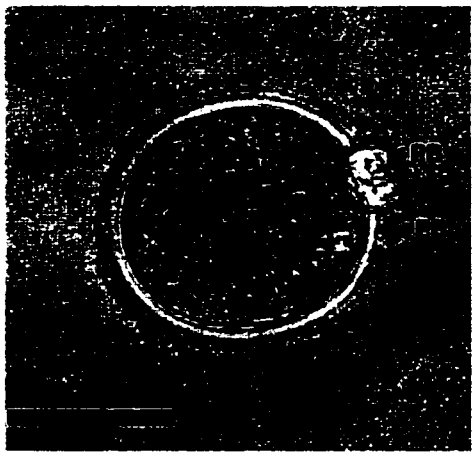

B. Sr^{2+}

C. cyclo.

D. U0126

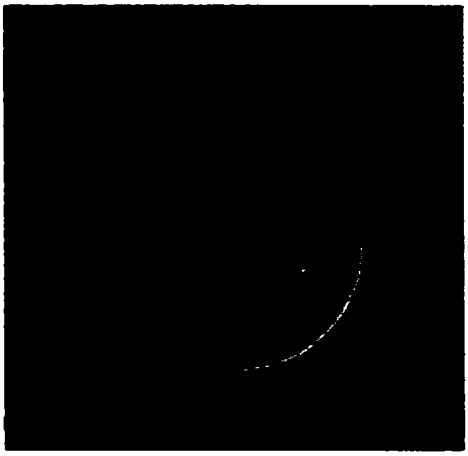

courses similar to fertilized eggs. Decreased MAPK activity occurs coincident with pronuclear formation (Kalab et al., 1996; Verlhac et al., 1996).

Mammalian oocytes, including hamster, mouse and rat can be parthenogenetically activated by Sr^{2+} or Ba^{2+}. Activation rates following microinjection of 0.2 mM $SrCl_2$ or $BaCl_2$ were not significantly different from microinjection of $CaCl_2$. The ability of Sr^{2+} and Ba^{2+} to parthenogenetically activate eggs was assumed to reflect their comparative binding affinities to Ca^{2+}-sensitive stores (Fulton and Whittingham, 1978).

Sr^{2+} can also parthenogenetically activate eggs when introduced externally (Fig. 14B). Almost total cortical granule exocytosis follows exposure to Sr^{2+}, and egg activation by Sr^{2+} produced nuclear development indistinguishable from activation by sperm, producing cell cycle resumption and extrusion of the second polar body within 75 min of Sr^{2+} exposure with low rates of aneuploidy (Fraser, 1987). Sr^{2+} exposure produces repetitive Ca^{2+}_i transients and thus Sr^{2+}-induced activation most closely mimics the normal repetitive calcium transients seen at fertilization. As discussed, most parthenogenetic agents, such as ethanol and Ca^{2+}_i ionophores, produce only a single Ca^{2+}_i transient. Sr^{2+} activation is therefore considered to most closely resemble the natural activation seen with sperm. When Sr^{2+} activated eggs were treated with cytochalasin D to suppress the emission of the second polar body, thereby producing a diploid egg, over 80% of activated eggs developed to the blastocyst stage. Of these diploid parthenogenotes, about 44% implanted following transfer to pseudo-pregnant mothers (Bos-Mikich et al., 1993).

Sr^{2+} induces repetitive Ca^{2+}_i transients that, while similar to fertilization-induced Ca^{2+}_i transients, exhibit delayed onset with slightly lower spiking amplitudes (Cheek et al., 1993). Sr^{2+} appears to induce Ca^{2+}_i transients in cells such as rat hepatocytes by

binding to the stimulatory Ca^{2+}_i site of the IP_3R (Hajnóczky and Thomas, 1997). Studies on frog skeletal muscle suggest that the relative affinity of the internal Ca^{2+}_i releasing store appears to be $Ba^{2+} > Sr^{2+} > Ca^{2+}$ (Cognard and Raymond, 1985), although Ba^{2+} does not support fertilization as effectively as Sr^{2+} (Fraser, 1987). Thus, Sr^{2+} is an effective parthenogenetic agent, producing high rates of activation while closely mimicking the natural repetitive Ca^{2+}_i transients produced by sperm via the IP_3-mediated Ca^{2+} release pathway.

Protein synthesis inhibitors

Treatment of mouse eggs with protein synthesis inhibitors such as cycloheximide or puromycin result in parthenogenetic egg activation (Fig. 14C). Activation is induced with concentrations of cycloheximide that inhibit protein synthesis by more than 70%. Pronuclear formation occurs when protein synthesis is almost totally inhibited. Cycloheximide-activated eggs are capable of development to the blastocyst stage (Siracusa et al., 1978), although eggs exposed to continuous cycloheximide treatment do not progress further than the pronuclear stage due to the requirement for protein synthesis in DNA replication. Thus, activated eggs must be removed from cycloheximide to allow further development. Within 5 h of cycloheximide treatment, cyclin B1 and histone H1 (MPF substrate) kinase activity decrease to levels similar to fertilized eggs. The time-course of the decrease in histone H1 kinase (MPF) activity is slower than in fertilized eggs (i.e. activated by sperm). However, the decrease in MAPK activity occurs within a time frame similar to that in fertilized eggs (7-10 h). Cycloheximide treatment does not induce the post-fertilization, Ca^{2+}-dependent conversion of ZP2 to $ZP2_f$, suggesting that

cycloheximide does not cause changes in Ca^{2+}_i. Indeed, Fura-2 measurements of Ca^{2+}_i in cycloheximide-activated eggs have confirmed that no change in Ca^{2+}_i or Ca^{2+}_i transients accompany cycloheximide-induced egg activation. Instead, Ca^{2+}_i remains at the basal level characteristic of unfertilized eggs even though polar body emission and pronuclear formation occur (Moos et al., 1996).

Activation by weak bases

As discussed, weak bases such as ammonia or the local anaesthetic procaine, results in parthenogenetic activation of sea urchin (Lopo and Vacquier, 1977), *Xenopus* (Grandin and Charbonneau, 1991), and some marine invertebrate eggs. In these species, an increase in pH_i is a characteristic event of meiotic maturation or fertilization. There is one report which suggests that mouse eggs can be activated by application of methylamine, a weak base, in a dose-dependent manner (Dyban and Noniashvili, 1990). However, an increase in Ca^{2+}_i or inhibition of protein synthesis caused by methylamine can not be excluded as the underlying cause for activation rather than increased pH_i.

V. PREIMPLANTATION DEVELOPMENT

First cell cycle

Early development in embryos of most species is controlled by the maternal genome with the sequential activation and utilization of components synthesized and stored during oocyte maturation. In the mouse embryo, this period of maternal control extends from ovulation to the early 2-cell stage (18-22 h; Bolton et al., 1984). In the mouse, the use of in vitro fertilization (IVF) enables the production of a population of

embryos with a high degree of developmental homogeneity- one of the many advantages of IVF. Following formation of the pronuclei, the embryo enters S-phase and begins DNA replication (Fig. 13). S phase in mouse embryos lasts about 7 h, with DNA replication commencing between 10 and 12 h post-insemination. Both pronuclei appear to enter S phase at the same time. IVF-produced mouse embryos cleave fairly synchronously beginning about 18 h post-insemination, in contrast to in vivo produced embryos which are more asynchronous, presumably due to variation in the timing of sperm-egg interaction in vivo. Cytokinesis or cleavage to the 2-cell stage occurs in most mouse embryos within about 3 h (Howlett and Bolton, 1985).

Zygotic gene activation (ZGA)

During meiotic maturation, ovulation, fertilization and formation of pronuclei, the egg is supported by maternal mRNA and proteins. In the mouse, maternally-derived proteins and maternal genes are sufficient to direct only the first cell cycle (Bolton et al., 1984), although in other species, such as *Xenopus*, maternally-derived products control several cell cycles (Taieb et al., 1997). Thus, the newly-fertilized egg is transcriptionally inactive with no new mRNA synthesis required to complete fertilization. Zygotic gene activation (ZGA), the transition from reliance on stored maternal mRNA to transcription of the embryonic genome, is absolutely essential for continued development (Bellier et al., 1997). In the mouse, maternal mRNAs, as well as rRNA and tRNA, are progressively degraded during oocyte maturation. ZGA is necessary in order to replace transcripts common to both the oocyte and early embryo, as well as to create new transcripts that are unique to the developing embryo (Schultz and Worrad, 1995).

The transition from maternal to embryonic control was found to occur during the 2-cell stage in the mouse. In mice, ZGA is independent of cytokinesis or DNA synthesis and involves a two step process. A minor ZGA phase is initiated at the late 1-cell stage (G2 phase) and is the first α-amanitin- (inhibitor of transcription by RNA polymerase II) sensitive event (Bolton et al., 1984). This minor ZGA is accompanied by the synthesis of a restricted set of proteins at the early 2-cell stage (G1/S phase) and includes the 70 kDa heat-shock proteins (Bensaude et al., 1983), the transcription-requiring complexes (TRCs; Conover et al., 1991), the U2afbp-rs splicing factor (Latham et al., 1995) and the translation initiation factor eIF-4C (Davis et al., 1996). At the late 2-cell stage (G2 phase) there is a second α-amanitin-sensitive event, the major ZGA, which includes a sharp increase in transcription and an increase in translational activity. ZGA, including the translation of proteins directed by the new embryonic genome, is essential for continued development (Bolton et al., 1984; Bellier et al., 1997).

Cleavage and compaction

Preimplantation development following formation of pronuclei, cleavage and ZGA continues with the embryo blastomeres cleaving, relatively synchronously, to 4-cells, 8-cells and 16-cells (Fig. 4). Unlike somatic mitotic cycles, these mitotic cycles involve reductive cleavages, such that each daughter cell or new blastomere is half the volume of the original parent cell. At the 8-16 cell stage (depending on species), a phenomenon known as "compaction" occurs. Compaction in mouse embryos occurs at the 8-cell stage, at which time embryo changes from a loose collection of blastomeres to a

tightly packed cluster of cells called a morula. Compaction represents the first evidence of cell polarity as microfilaments (Johnson and Maro, 1984), microtubules (Ducibella et al., 1977; Houliston et al., 1987, Houliston and Maro, 1989), mitochondria (Ducibella et al., 1977; Batten et al., 1987), endosomes (Fleming et al., 1986) and clatherin vesicles (Maro et al., 1985) become unequally distributed. In addition to the polarization of cytoskeletal proteins, compaction also involves the formation of gap junctions and apical tight junctions (Ducibella et al., 1975). There is polarization of the outer surface as well as the inner collection of cells, with an accumulation of microvilli over the apical region (Johnson and Maro, 1984; Maro et al., 1985). The polarization results in two distinct populations of cells, large outer cells and small inner cells. (Ohsugi et al., 1993).

Compaction in the mouse embryo is mediated by the cell adhesion molecule E-cadherin (also known as uvomorulin; Vestweber et al., 1987). The distribution of E-cadherin is fairly uniform in early cleavage stages, with increased concentration between blastomeres of mouse 4-cell embryos (Shirayoshi et al., 1983; Johnson et al., 1986). Other molecules involved in compaction include α-catenin and β-catenin, which link E-cadherin to the actin cytoskeleton thereby promoting interblasomere adhesion (Pauken and Capco, 1999).

PKC has been implicated in compaction of mouse embryos as PKC activators stimulate premature compaction of 2-cell, 4-cell and 8-cell embryos and sphingosine, a PKC inhibitor, inhibits compaction (Winkel et al., 1990). PKC becomes colocalized with cell adhesion molecules E-cadherin and β-catenin during compaction suggesting that PKC may regulate cell-cell adhesion (Bloom et al., 1989; Pauken and Capco, 1999).

Blastocyst formation

Following compaction, the embryo undergoes "cavitation" resulting in the formation of the characteristic "blastocoel" (fluid-filled cavity), and thus becomes a blastocyst (Fig. 4). The blastocyst features a trophectoderm layer of epithelial cells which encloses the blastocoel and the inner cell mass (ICM). The trophectoderm arises *de novo* from the previously unspecialized blastomeres which were on the outside of the compacted morula and is the part of the embryo that initiates uterine contact and implantation (MacPhee et al., 2000). The trophectoderm also gives rise to extra-embryonic membranes while the ICM consists of pluripotent cells which develop into the embryo and eventually the fetus (Brison and Schultz, 1998).

Fluid transport into the blastocoel is mediated by the net uptake of Na^+ and Cl^-, energized by the basolateral Na^+,K^+-ATPase located in the trophectoderm layer. In the mouse, apical Na^+ entry is mediated by Na^+/H^+ antiporter activity and possibly an amiloride-sensitive Na^+ channel (Manejwala et al., 1989). Cl^- transport into the blastocoel may be mediated by apical Cl^- channels, with efflux mediated by HCO_3^-/Cl^- exchanger (Zhao et al., 1997). This transport is driven by the activity of Na^+,K^+-ATPase, present in all stages of preimplantation embryo development (Watson et al., 1990). Total Na^+,K^+-ATPase increases about twofold during preimplantation development particularly following morula development, at which time Na^+,K^+-ATPase is targeted to basolateral membranes (Van Winkle and Campione, 1991).

VI. pH_i REGULATION

pH_i affects many cellular processes including membrane transport, ion conductances, gap junctions and intracellular communication and therefore must be regulated within a narrow range for cell survival. Most mammalian cells maintain a pH_i of about 7.2, which is maintained by pH_i regulatory transporters (Fig. 15). Natural biological membranes display a greater permeability to H^+ than to any other ion (Putnam, 1988). pH_i regulation is necessary to maintain pH_i within a narrow range by mediating the electrochemically-driven movement of acid/base equivalents across the membrane. Metabolism contributes to intracellular acid load by the intracellular production of CO_2 and its conversion to carbonic acid as well as the metabolic production of other weak acids (e.g. lactate). Maintenance of pH_i is carried out by a number of different mechanisms, most involving transmembrane ion transporters. In addition to pH regulation, these transporters often function in the maintenance of ionic gradients, electrolyte balance and cell volume (Fliegel and Frohlich, 1993).

Membrane transporters are synthesized in the ER and move through the Golgi to the plasma membrane. Some pH_i regulatory transporters are functional before exit from the ER which suggests that the activity of some transporters may regulate the milieu of the ER lumen. Membrane proteins are targeted to the ER membrane by signal sequences composed of the first transmembrane segment in the mature protein in many transporters. These signal sequences may then be removed in the ER as seen with Na^+/Ca^{2+} and Na^+/H^+ exchangers which undergo cotranslational cleavage of these N-terminal signal sequences in the ER (Reithmeier, 1994).

In order for a transmembrane protein to function as a pH_i regulatory transporter,

Figure 15. pH_i regulation. A. Major pH_i regulatory transporters. *Acidosis*. Na^+-dependent HCO_3^-/Cl^- exchanger, Na^+/H^+ antiporter and Na^+ -HCO_3^- cotransporter (stoichiometry varies). *Alkalosis*. Na^+-HCO_3^- cotransporter and HCO_3^-/Cl^- exchanger. B. Dependence on pH_i for activities of three pH_i regulatory transporter (Na^+/H^+ antiporter, Na^+, HCO_3^-/Cl^- exchanger and HCO_3^-/Cl^- exchanger). Na^+/H^+ antiporter has high activity at low pH_i and functions to regulate intracellular acidosis. HCO_3^-/Cl^- exchanger has high activity at high pH_i and functions to mediate alkalosis. Na^+, HCO_3^-/Cl^- exchanger regulates intracellular acidosis but is active primarily at resting pH_i.

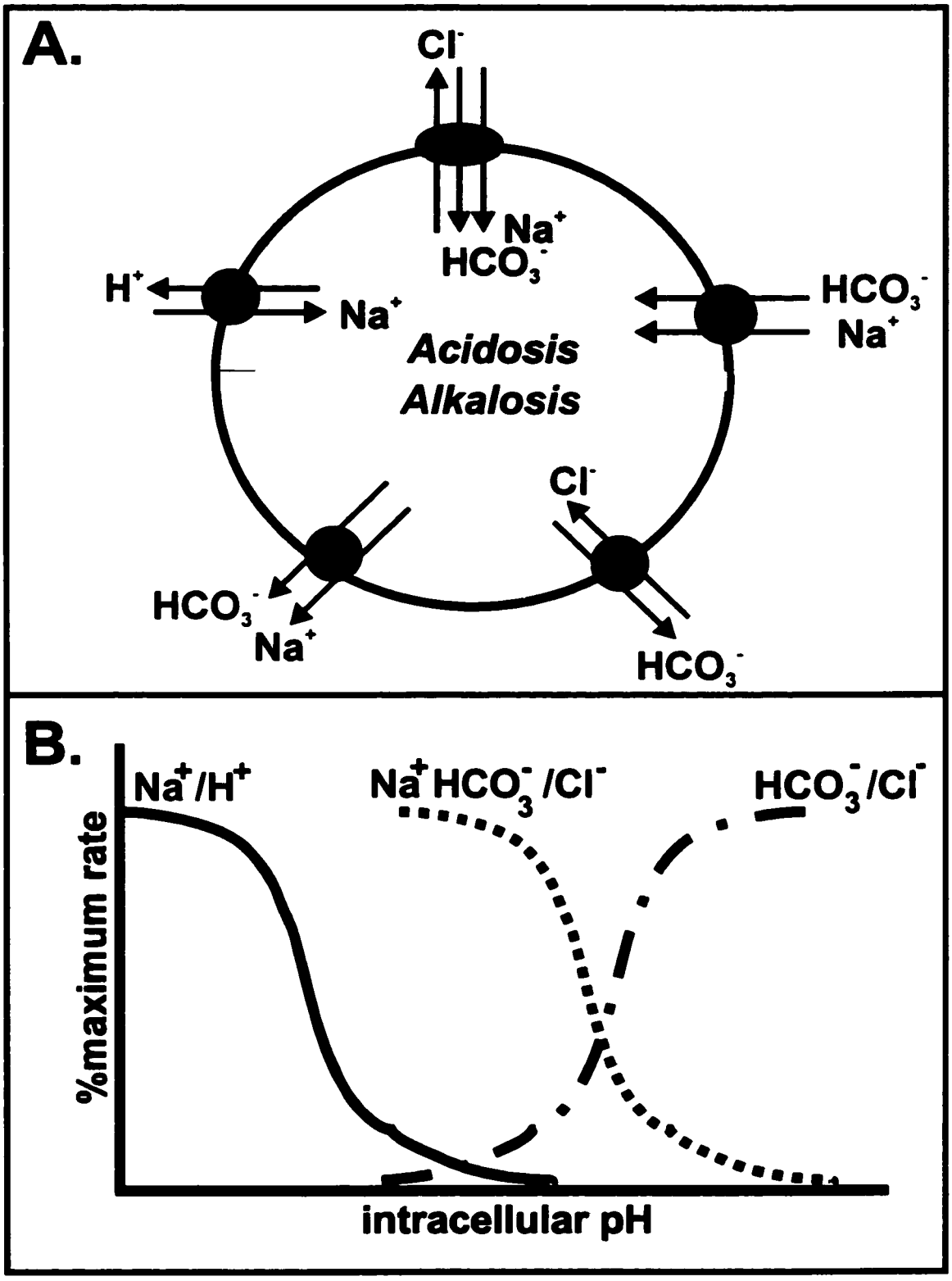
A.
Cl-
Na+
HCO3-
H+
Na+
HCO3-
Na+
Acidosis
Alkalosis
Cl-
HCO3-
Na+
HCO3-
B.
Na+/H+
Na+HCO3-/Cl-
HCO3-/Cl-
%maximum rate
intracellular pH

the protein must consume energy to translocate acid/base equivalents across the membrane. This transport may be active transport that requires ATP (e.g. H^+-ATPase) or secondary active transport that is driven by the electrochemical gradient of a co- or counter-transported ion (e.g. Na^+/H^+ antiporter or HCO_3^-/Cl^- exchanger). Transport of acid/base equivalents may occur across a wide range of pH_i (AE1- HCO_3^-/Cl^- exchanger isoform) or may demonstrate a steep pH_i dependence with high transport rates only within a specific pH_i range (NHE1- Na^+/H^+ antiporter isoform). Transporters which exhibit pH_i dependent kinetics are activated at a threshold pH_i called the "pH_i set-point". pH_i transporters that alleviate intracellular acidosis, for example, are activated only when pH_i falls below the set-point. When pH_i is returned to steady-state and is at or above the pH_i set-point, the activity of the transporter becomes negligible. At least two major pH_i regulatory transporter families exist; Na^+/H^+ antiporters and HCO_3^--dependent transporters which include Na^+/HCO_3^- cotransporters, K^+/HCO_3^- cotransporters, Na^+-HCO_3^-/Cl^- exchangers and HCO_3^-/Cl^- exchangers. While Na^+/H^+ antiporters primarily regulate perturbations in the acid range, some HCO_3^--dependent transporters regulate alkalosis (HCO_3^-/Cl^- exchangers), some regulate acidosis (Na^+- HCO_3^-/Cl^- exchangers) and some regulate both acidosis or alkalosis depending on their expression in a particular tissue, the ion gradients present, membrane potential and the resulting stoichiometry of exchange (Na^+/HCO_3^- cotransporters, K^+/HCO_3^- cotransporters). In addition to the alleviation of perturbations in acid-base balance many pH_i transporters also regulate cell volume and intracellular ion concentration (Boron, 1986; Romero et al., 1997).

Na^+/H^+ antiporter

The Na^+/H^+ antiporter mediates the electroneutral exchange of extracellular Na^+ for intracellular H^+ to increase pH_i. Na^+/H^+ antiporters are encoded by members of the NHE gene family (NHE1-6; Orlowski and Grinstein, 1997). NHE1 expression is ubiquitous. In epithelial cells, it is generally localized to the basolateral membrane (Coupaye-Gerard et al., 1996). NHE2 has been detected in intestine (Dujeda et al., 1996), kidney (Soleimani et al., 1994; Sun et al., 1997; Bookstein et al., 1997) and apical membranes of epithelial cells (Counillon and Pouyssegur, 2000). NHE3 is highly expressed in the kidney (proximal tubule, thin and thick limbs of the loop of Henle; Soleimani et al., 1994) and intestine (jejunum, ileum, colon and rectum; Dujeda et al., 1996) where it is specifically targeted to the apical membrane (Noel et al., 1996; Hoogerwerf et al., 1996). NHE4 mRNA has been detected in the stomach, intestine, kidney and hippocampus (Bookstein et al., 1997). NHE5 has been detected predominantly in brain, but also in testis, spleen and skeletal muscle (Klanke et al., 1995). NHE6 has a wide tissue distribution and is also expressed in mitochondria (Counillon and Pouyssegur, 2000).

NHE1 knockout mice have no apparent defects in acid-base homeostatic balance or in their kidney or intestine function. Instead, these mice exhibit defects in brain function, as the brain is highly sensitive to changes in pH_i (Cox et al., 1997; Bell et al., 1999). NHE2 knockout mice exhibit no detectable changes in intestine function, though the gastric mucosa is modified resulting in deficient acid secretion in the stomach. NHE3 knockout mice exhibit a decrease in blood pressure, and are mildly acidotic. As NHE3 is important for intestinal and kidney sodium absorption, these knockout experiments

demonstrate that NHE3 mediates the majority of such absorption in the kidney and intestine (Schultheis et al., 1998; Counillon and Pouyssegur, 2000).

Structure

Na^+/H^+ antiporters are integral membrane proteins with a hydrophobic N-terminal region that spans the membrane 10-12 times. The central region of the transmembrane domain (226-281, human NHE1) is quite hydrophobic but contains several negatively charged residues. The C-terminus, however, is hydrophilic and is localized in the cytoplasm for NHE1. Part of the C-terminus in the NHE3 isoform may be exposed extracellularly as is the glycosylated loop between the transmembrane segments 1 and 2 in NHE1 and 2. The transmembrane domain exhibits between 45-65% amino acid sequence identity between isoforms with only 25-35% identity for the cytoplasmic domains (Counillon and Pouyssegur, 2000). The membrane-spanning regions M6 and M7 are highly conserved with 95% identity, suggesting that this region participates in transport of Na^+ and H^+ (Orlowski and Grinstein, 1997).

Na^+/H^+ antiporter isoforms range in length between 717-835 amino acids. Less is known about the tertiary or quaternary structure of the antiporters, although evidence suggests they exist in the membrane as homodimers (Fliegel et al., 1993; Fafournoux et al., 1994; Orlowski and Grinstein, 1997). Dimerization appears to occur selectively between two identical isoforms because coexpression of NHE1 and NHE3 does not produce heterodimers (Counillon and Pouyssegur, 2000). The monomeric protein is glycosylated, with a molecular mass of 110 kDa. Human NHE1 has three consensus sites for glycosylation while NHE3 and NHE4 have between three and five, depending on the

species (Fliegel and Frohlich, 1993; Counillon and Pouyssegur, 2000).

Inhibitors

At physiological pH_i, amiloride exists primarily as a protonated (95%) monovalent cation and acts as a competitive inhibitor of Na^+ transport by NHE1 (K_i 1-100μM; Aronson et al., 1982; Benos et al., 1982). Inhibition of the antiporter by amiloride is immediate in onset and is rapidly reversed upon removal of amiloride (Grinstein and Foskett, 1990). Inhibition of NHE by amiloride derivatives, cimetidine, and HOE694 is reduced by high external Na^+, suggesting that these compounds bind near the external Na^+ transport site (Aronson, 1985; Counillon et al., 1993; Orlowski and Grinstein, 1997). While amiloride is widely used as an inhibitor of Na^+/H^+ antiporter activity, other compounds have been developed which have 10-100-fold higher K_i values for NHE1 than amiloride itself. These inhibitors are alkyl-5-*N*-substituted derivatives of amiloride such as 5-*N*-dimethyl amiloride or 5-*N*-ethyl isopropyl amiloride (EIPA). While highly specific for NHE1, these amiloride derivatives interact poorly with other isoforms, which are often referred to as 'amiloride-resistant' Na^+/H^+ antiporters (Vigne et al., 1984; L'Allemain et al., 1984). Other compounds which inhibit Na^+/H^+ antiporter activity include cimetidine, clonidine and harmaline (Yu et al., 1993; Ramamoorthy et al., 1991). The NHE isoforms vary in their sensitivity to amiloride and amiloride derivatives, generally following the order NHE1 > NHE2 >> NHE3 > NHE4 (Orlowski, 1993; Bookstein et al., 1996; Counillon et al., 1993; Orlowski and Kandasamy, 1996). Inhibitors of NHE all possess either an imidazoline (amiloride) or guanidinium

(HOE694) moiety and are thus, structurally similar (Orlowski and Grinstein, 1997).

Transport Models

Under physiological conditions the antiporter mediates the electroneutral exchange of one extracellular Na^+ for one intracellular H^+. For NHE1-3 isoforms, the binding site for extracellular Na^+ cannot be distinguished from the Na^+ transport site and the saturation of transport can be described by Michaelis-Menten kinetics, such that the rate of Na^+/H^+ exchange demonstrates a hyperbolic dependence on the external Na^+ concentration. Similar transport kinetics have been observed for NHE1-3. Thus, the simplest transport model suggests that Na^+ binds to a unique external site and is then translocated. In contrast to NHE1-3, NHE4 exhibits a sigmoidal dependence on external Na^+, although the functional significance of this is unknown. For most isoforms, K_m for external Na^+ is about 3 times below the physiological extracellular Na^+ concentration, which suggests that Na^+/H^+ antiporter activity operates close to saturation with respect to external Na^+ and that modest variations in external Na^+ have no effect on the transport rate of the antiporter (Orlowski and Grinstein, 1997; Counillon and Pouyssegur, 2000). The external cation site, which normally binds Na^+, can also transport H^+ and Li^+, indicating that this site is not exclusively selective for Na^+ (Paris and Pouyssegur, 1983; Aronson et al., 1982).

Regulation by pH

The activity of Na^+/H^+ antiporter is determined by the pH_i set-point. When the pH_i falls below the pH set-point, the modifier or sensor becomes protonated, thereby

enhancing the rate of transport. Similarly, deprotonation of this site at pH_i above the set-point lowers the rate of transport, resulting in only basal activity at resting pH_i (Grinstein et al., 1990). Activation of NHE1-3 is extremely sensitive to low pH_i. At physiological pH_i, NHE1 and 2 are essentially inactive but become rapidly activated when pH decreases below the set-point of the exchanger (Paris and Pouyssegur, 1983; Aronson et al., 1982). NHE3 exhibits a lower affinity for intracellular H^+ and is therefore active at resting pH_i (Wakabayashi et al., 1995).

NHE1-3 transport is allosterically affected by proton binding to a cytoplasmic sensor which modifies the sensor's affinity for additional proton binding. Activation of Na^+/H^+ antiporter results from an increased affinity of the antiporter for intracellular H^+ at this allosteric modifier site. The proton sensor is believed to be distinct from the Na^+/H^+ transport sites (Aronson et al., 1982). The construction of deletion mutants containing different portions of either the Na^+/H^+ antiporter cytoplasmic domain or transmembrane domain was used to map the location of the proton sensor and functional transport domain. Deletion of the complete cytoplasmic domain preserved 25% of the transport activity indicating that the N-terminal transmembrane domain is sufficient for both insertion of the antiporter into the plasma membrane and for amiloride-sensitive ion transport. Deletion of the cytoplasmic domain shifted the sensitivity of Na^+/H^+ antiporter activity to intracellular H^+ to an acidic range such that the truncated antiporter was inactive above pH_i 6.6. However, the pH_i dependence of the antiporter was still preserved indicating that the H^+ modifier site is located within the N-terminal transmembrane domain. As the cytoplasmic domain controlled the pH_i sensitivity of the antiporter, this suggests that the C-terminal cytoplasmic domain regulates the set-point value

(Wakabayashi et al., 1992).

The Na^+/H^+ antiporter proton sensor may be a single or cluster of histidine residues. In *Escherichia coli (E. coli)* His-226 is involved in the pH_i sensitivity of NhaA (NhaA and NhaB are two *E. coli* Na^+/H^+ antiporter isoforms). None of the eight histidines in NhaA are required for Na^+/H^+ transport, as shown by site-directed mutagenesis. However, substitution of His-226 with either positively or negatively charged amino acids revealed charge-dependent shifts in pH_i sensitivity. This suggests that at position 226 of NhaA, charge and/or H^+ binding affect the pH sensitivity of Na^+/H^+ antiporter (Rimon et al., 1995).

Na^+/H^+ antiporter activity is also affected by external pH (pH_o). In the pH_o range 6.0-8.5, external H^+ interacts with Na^+/H^+ antiporter at a single site with a pK_a 7.3-7.5. This site is the external transport site, where H^+, Na^+, Li^+, NH_4^+ and amiloride all compete for binding. The sequence of binding affinities for the external transport site of the renal Na^+/H^+ antiporter is H^+>> amiloride >> $Li^+ > NH_4^+ \geq Na^+ >> K^+$, Rb^+, Cs^+, choline. This suggests that low pH_o would inhibit Na^+/H^+ exchange, as the antiporter possesses a greater affinity for external H^+ than external Na^+. Inhibition of Na^+ uptake by low pH_o has been shown in renal microvillus membrane vesicles. Additionally, Na^+/Na^+ exchange was also inhibited by low pH_o, suggesting that external H^+ competes for the external Na^+ transport site, thereby inhibiting exchange (Aronson et al., 1982).

Regulation of pH_i set-point

Na^+/H^+ antiporter activity is driven by chemical gradients for Na^+ and H^+ and does not directly consume metabolic energy. However, ATP is required for optimal Na^+/H^+

antiporter activity. ATP depletion decreases activity of NHE1-3 by reducing the affinity of the antiporter for intracellular H^+ (Orlowski and Grinstein, 1997). The set-point of the antiporter can be shifted down by ATP-depletion but shifted up by growth factors or osmotic cell shrinkage (Grinstein et al., 1990). ATP depletion has been proposed to trigger dephosphorylation of NHE1 at critical sites, followed by conformational changes that segregate spatially and functionally, the cytoplasmic domain from the proton sensor (Wakabayashi et al., 1992).

Regulation of NHE transporters is mediated by a wide variety of pathways and signals including tyrosine kinases, Ser/Thr kinases PKC and PKA, increases in $Ca^{2+}{}_i$, changes in cell volume (Fleigel and Frohlich, 1993) and p160 ROCK, a Rho effector associated with the assembly of stress fibers and focal adhesions (Sahai et al., 1998). Consensus sequences for PKA, PKC, CaMKII (Kemp and Pearson, 1990), MAPK and $p34^{cdc2}$ kinase are present in both the N-terminal and C-terminal regions of the Na^+/H^+ antiporter (Pelech and Sanghera, 1992). NHE2-4 contain CaMKII phosphorylation sites while NHE2, 3 and βNHE (a cAMP-dependent isoform found in trout erythrocytes) contain sites for PKA and PKC phosphorylation. NHE1 is phosphorylated following growth factor, phorbol ester or phosphatase inhibitor treatment (Sardet et al., 1990; Sardet et al., 1991) while NHE3 is phosphorylated following elevation of intracellular cAMP (Orlowski and Grinstein, 1997). Thus, phosphorylation of the Na^+/H^+ antiporter may increase the affinity of the transporter for intracellular H^+. One model suggests that the cytoplasmic tail cooperates with the central pH_i sensor to decrease the pH_i set-point. These intracellular signals are transduced by the cytoplasmic tail resulting in Na^+/H^+

antiporter activation and intracellular alkalinization (Wakabayashi et al., 1992; Bertrand et al., 1994).

NHE activity is activated by heteromeric, small GTP-binding proteins (GTPases $G_{\alpha q}$, $G_{\alpha 12}$, $G_{\alpha 13}$). $G_{\alpha q}$ activates Na^+/H^+ antiporter activity through a PKC-dependent pathway (Dhanasekaran et al., 1994). Constitutively active $G_{\alpha 13}$, shown to stimulate the Jun kinase and JNK cascades, activates NHE1 through a Cdc42- and MEK1-dependent mechanism. Two members of the Rho subfamily of GTPases, Rac1 and cdc42 may regulate MEK1, though probably not directly. $G_{\alpha 13}$ also stimulates NHE1 through a RhoA-dependent pathway that is independent of MEK1. These findings indicate a new target for Rho-like proteins: the regulation of Na^+/H^+ antiporter and pH_i (Hooley et al., 1996).

MAPK may regulate Na^+/H^+ antiporter activity. Treatment with phorbol esters and AVP activates both MAPK and Na^+/H^+ antiporter in human platelets with a similar time-frame and concentration dependence (Aharonovitz and Granot, 1996). p45 MAPK activation of Na^+/H^+ antiporter activity in *Xenopus* oocytes occurs through the p39mos, Raf-1 kinase pathway (Rezai et al., 1994). In addition, long term expression of c-Ras stimulates Na^+/H^+ antiporter activity in fibroblasts (Kaplan and Boron, 1994). AVP stimulates the phosphorylation and activation of p42/44 MAPK and Na^+/H^+ antiporter activity through a signal transduction pathway that is independent of PKC. MAPK activation is proposed to be indirect and may involve phosphorylation of a regulatory protein. Interaction between Na^+/H^+ antiporter and a regulatory protein could induce the exchanger to undergo a conformational change, thereby altering transport kinetics and pH_i sensitivity (Aharonovitz and Granot, 1996).

Inhibition of p42/44 MAPK by expression of a dominant negative form of p44 MAPK, expression of the MAPK phosphatase MKP-1, or by inhibition of MEK1 by PD098059, reduced NHE1 activation by 50-60% (Bianchini et al., 1997). p42/p44 MAPK, signaling through $p90^{RSK}$ phosphorylates NHE1 Ser-703 in vitro. Ser-703 is a major site for serum activation. Thus, the MEK1-ERK1/2-$p90^{RSK}$ pathway is involved in serum-stimulated phosphorylation of NHE1 (Takahashi et al., 1999).

Although Na^+/H^+ antiporter is phosphorylated by many different stimuli, direct phosphorylation alone does not appear to regulate the transporter as deletion of the distal cytoplasmic tail containing Ser-703 and other major phosphorylation sites did not completely abolish growth factor activation of Na^+/H^+ antiporter activity. The residual activation (~50%) was sensitive to the MEK inhibitor PD098059, suggesting that other molecules activated by the MAPK pathway, such as $p90^{RSK}$, may regulate Na^+/H^+ antiporter activity (Bianchini et al., 1997). Thus, regulation of Na^+/H^+ antiporter activity may involve multiple signaling pathways which phosphorylate regulatory accessory proteins, such as Hsp70 (heat shock protein 70; Silva et al., 1995) and CHP (calcineurin B homolog protein; Lin et al., 1996; Counillon and Pouyssegur, 2000), that interact with the Na^+/H^+ antiporter, thereby causing changes in activity (Orlowski and Grinstein, 1997; Counillon and Pouyssegur, 2000).

Summary

Na^+/H^+ antiporter activity is important for pH_i regulation, ion homeostasis, and cell volume regulation. It has nearly ubiquitous expression. Na^+/H^+ antiporter activity is regulated by many signaling pathways including PKA, PKC, MAPK and many more. The

upregulation of Na^+/H^+ antiporter activity at fertilization in the sea urchin and oocyte maturation in *Xenopus* are major developmental events, resulting in increased pH_i regulation throughout subsequent embryogenesis. Whether upregulation of Na^+/H^+ antiporter activity at fertilization is restricted to these few species is unknown.

HCO_3^-/Cl^- exchanger

HCO_3^-/Cl^- exchangers, or "anion exchangers", mediate the electroneutral exchange of extracellular Cl^- for intracellular HCO_3^- which decreases pH_i and thereby alleviates intracellular alkalosis (Alper, 1994). HCO_3^-/Cl^- exchangers are inhibited by disulfonic stilbene derivatives such as DIDS and SITS (Boron, 1986). HCO_3^-/Cl^- exchangers function in concert with other transport systems to regulate pH_i, cell volume and Cl^-_i (Alper, 1991). HCO_3^-/Cl^- exchangers are encoded by members of the AE (anion exchanger) gene family, of which there are three members: AE1, AE2 and AE3 (Alper, 1994). All of these AE genes have been cloned in mouse (Alper, 1991). AE1 expression appears to be restricted to erythrocytes (Kopito and Lodish, 1985), a truncated from of the polypeptide in the kidney (Kudrycki and Shull, 1989; Brosius et al., 1989) and an AE1-like protein in cardiac myocytes (Puceat et al., 1995). AE2 is largely thought to be a housekeeping gene, with ubiquitous expression at least at the level of mRNA (Alper et al., 1988; Kudrycki et al., 1990; Jiang et al., 1994) while AE3 is found in excitable tissues, brain (Kudrycki et al., 1990; Kopito et al., 1989; Yannoukakos et al., 1994), heart (Yannoukakos et al., 1994; Linn et al., 1992), and retina (Sterling and Casey, 1999). AE-3 exists as at least two alternate transcripts, one in the neurons and glia in the brain (Kudrycki et al., 1990; Kopito et al., 1989; Yannoukakos et al., 1994) as well as in the

stomach and heart, and a second shorter transcript restricted to the heart (Yannoukakos et al., 1994).

A major function of non-erythrocyte HCO_3^-/Cl^- exchangers is the regulation of pH_i in the alkaline range. A graded stimulation of exchanger activity occurs as pH_i increases above the pH_i set-point, so that large increases in pH_i are vigorously opposed. As pH_i returns to the set-point value HCO_3^-/Cl^- exchange activity falls to zero (Nord et al., 1988; Olsnes et al., 1986; Kurtz and Golchini, 1987; Lee et al., 1991).

AE1 has several sub-isoforms; AE1e is found in erythroid cells (Kopito and Lodish, 1985) and two isoforms are found in the kidney; AE1k1 and AE1k2 (Kudrycki and Shull, 1989; Brosius et al., 1989; Kudrycki and Shull, 1993; Kollert-Jons et al., 1993; Wang et al., 1996). In the kidney, AE1 encodes a polypeptide otherwise identical to AE1e but lacking 79 amino acid residues at the extreme N-terminus. AE1 gene is expressed as an abundant ~100 kDa integral plasma membrane glycoprotein (AE1e) in erythrocytes where it mediates the dual function of HCO_3^-/Cl^- exchanger and cytoskeleton anchor (Lee et al., 1991). AE1- deficient cattle and mice are mildly acidotic, and this acidosis becomes more severe during exertion or dietary acid load. In addition to acidosis, these animals also suffer from chronic hemolytic anemia resulting from premature erythrocyte destruction due to the loss of AE1 as a structural component (see below; Jarolim et al., 1998; Van Winkle, 1999).

It is speculated that AE2 and AE3 have arisen from a common gene which had earlier diverged from AE1. Thus, AE2 and AE3 share more structural and functional homology compared to AE1. A number of sub-isoforms of AE2 have been described for the rat, mouse and human; AE2a is widely distributed, AE2b is expressed primarily in the

stomach and AE2c1 and AE2c2 seem to be expressed exclusively in the stomach. There are two isoforms of AE3, AE3b is expressed in brain while AE3c is expressed in heart (see above; Yannoukakos et al., 1994; Wang et al., 1996; Van Winkle, 1999). Size variations in AE2 mRNA seems to be due to differences at the 5' ends and may be related to the use of alternative promoters that encode protein variants which differ in their N-terminal sequences. This is consistent with earlier studies which revealed multiple mRNAs for each of the three AE genes (Wang et al., 1996).

AE2 expression in the tissues specialized for transport such as the kidney or GI tract reflects the importance of base regulation in these systems. AE2 can be expressed apically or basolaterally in epithelial cells found in the ileum, stomach, colon and kidney (Dudeja et al., 1999). In the stomach, AE2 is expressed at high levels on the basolateral membrane of gastric parietal cells where it presumably mediates HCO_3^-/Cl^- exchanger activity during acid secretion across the apical membrane. In small intestine, AE2 is localized on the apical membranes of both villus and crypt enterocytes in ileum, consistent with a role in both NaCl absorption and HCO_3^- secretion (Wang et al., 1996).

Heart and retina both contain an extensive network of electrically coupled cells with gap junctional conductances that are extremely sensitive to changes in pH_i. A small change in pH_i (0.2-0.3 unit decrease) results in 50% decrease in junctional conductance in the retina and 30-80% decrease in junctional conductance in the heart, with gap junctions composed of connexin 45 being the most severely affected (Sterling and Casey, 1999). The regulation of pH_i in these tissues is performed by AE3, found in excitable tissues such as brain, heart, and retina (Sterling and Casey, 1999).

Structure

AE1 is an integral membrane protein with two structural domains, each with independent functions. The N-terminal cytoplasmic domain attaches the spectrin-actin cytoskeleton to the plasma membrane via its binding interactions with ankyrin, protein 4.1 and 4.2, while the C-terminal transmembrane domain mediates a HCO_3^-/Cl^- exchanger that increases by 5-fold the total CO_2 carrying capacity of blood (Alper, 1991). This C-terminal domain is composed of 14 transmembrane α-helices with intervening intracellular and extracellular loops of varying sizes (Van Winkle, 1999).

Human erythrocytes roughly contain 10^6 AE1 proteins assembled into 4×10^5 intramembrane particles comprised primarily of dimers as well as a smaller number of higher oligomers. AE1 exists as a dimer in the membrane such that the presence of two binding sites allows ankyrin to interact with four AE1 proteins simultaneously as AE1 (dimer) is present at a 4-5 fold higher concentration than ankyrin (Michaely and Bennett, 1995a). Ankyrin interacts not only with AE1, but also with AE2 and AE3, voltage-gated Na^+ channels, 205 kDa brain glycoprotein, α subunit of Na^+ K^+- ATPase in kidney, 85 kDa GTP binding glycoprotein and 116 kDa CD44-like protein in endothelial cells (Luna and Hitt, 1992). Mutations or reductions in ankyrin which disrupt the linkage with AE1 decouple the structural support of the spectrin skeleton from the membrane and result in hemolytic spherocytosis and anemia (Michaely and Bennett, 1995b).

AE2 and AE3 share little sequence similarity to AE1 at the N-terminal domain, which is significantly longer (~320 amino acids) in AE2/3 compared to AE1 (~60 amino acids). The N-terminal domain, as described for AE1, is associated with specific protein

molecules in the membrane, cytoskeleton and cytosol, whereas the C-terminal domain forms the pathway for anion transport (Zhang et al., 1996; Van Winkle, 1999). The C-terminal domain, however, shares about 80% identity between AE1 and AE2/3 and is therefore far more conserved than the N-terminal domain. The transmembrane domains of AE2 and AE3, consisting of about 530 C-terminal amino acids, are sufficient to mediate anion exchange, as was demonstrated by the removal of the N-terminus resulting in normal transport function mediated by the remaining intact C-terminal portion. This suggests that the N-terminus is not directly involved in transport. However, this does not preclude a regulatory role as the N-terminus appears to coordinate anion transport with cellular metabolism and structure (Lee et al., 1991).

The polypeptide products of AE2 and AE3 genes are proposed to act as major membrane anchors for the spectrin/ankyrin/actin cytoskeleton, analogous to band 3 (Zhang et al., 1996). There is much debate as to whether AE2 and AE3 participate in the spectrin/ankyrin binding of the cytoskeleton. No significant binding has been observed between ANK1 (erythrocyte-specific isoform of ankyrin) and either AE2 or AE3 (Ding et al., 1991). In contrast, it has been suggested that AE3 binds ankyrin in Muller cells such that ankyrin association would contribute to polarized distribution of AE3 (Kobayashi et al., 1994).

Inhibitors

One important characteristic of all three AE isoforms is their sensitivity to disulfonic stilbenes. These agents (e.g. DIDS, SITS) can reversibly block the exchanger by competing with extracellular anions for the external binding site (non-covalent

binding) or can irreversibly block the exchanger by covalently binding to conserved lysine residues (Sekler et al., 1995a). DIDS inhibits AE1, expressed in erythrocytes, with a K_i of 0.04 μM (Fudner et al., 1978). Stilbene sensitivities for AE2 range from 142 μM (IC_{50} for H_2DIDS) in transfected HEK293 cells (Lee et al., 1991), 1-10 μM (K_i for DIDS) in K562 cells (Law et al., 1983; Demuth et al., 1986), and 4 μM (K_i for stilbene disulfonate compound DNDS) in reconstituted proteoliposomes (Sekler et al., 1995a). AE3 in HEK293 cells has an IC_{50} for DIDS of 0.42 μM (Lee et al., 1991). The difference in affinity for DIDS between AE isoforms suggests differences in the stilbene disulfonate binding sites between AE1, 2 and 3. Alternatively the difference in the DIDS affinity may arise from different densities of the exchangers in various expression systems or the complex nature of covalent and noncovalent binding of DIDS (Sekler et al., 1995a).

Stilbenes act by binding to lysines in a conserved, lysine-rich portion of AE proteins (Alper et al., 1991). Modification of the lysine-rich site by stilbene disulfonate and other lysine- specific reagents inhibits transport activity. However, site directed mutagenesis of this stilbene disulfonate covalent binding site fails to alter the ion affinity or the rate of ion transport. This suggests that this lysine-rich site is not directly involved in the transport process (Sekler et al., 1995b). At higher concentrations and over extended incubations DIDS binds covalently to one of two highly conserved lysines (539 or 542 on human AE1) irreversibly blocking the transporter. Both of these lysines are conserved in AE2 and AE3 from all species studied, which is consistent with observation of irreversible inhibition of nonerythroid anion exchange by stilbene isothiocyanates (Lee et al., 1991).

Transport models

AE1 activity (HCO_3^-/Cl^- exchange) is relatively unresponsive to changes in pH_i (Lee et al., 1991; Sterling and Casey, 1999). AE1 displays a broad pH vs activity profile for Cl^-/monovalent anion exchange. This has an important physiological basis as the erythrocyte is exposed to both CO_2 and acid-generating tissue and thus, anion exchange must remain constant under both alkaline and acid conditions (Zhang et al., 1996). AE1 can, however, be titrated by pH_i to function either as a monovalent anion exchanger or a divalent anion/proton cotransporter. Protonation of a site (pKa ~6) on AE1 simultaneously inhibits monovalent anion exchange and activates the transport of divalent anions (Lee et al., 1991). The transport of the divalent anions such as sulfate occurs at a much slower rate (100-1000 times slower) than Cl^-. Sulfate transport is steeply pH_i-dependent which may indicate a requirement for cotransport of a proton and sulfate which preserves the monovalent nature of transport (Sekler et al., 1995a).

Anion translocation can be explained by a 'ping-pong' kinetic model in which anion translocation in one direction is temporally distinct from, but dependent upon anion translocation in the opposing direction. This tight substrate coupling ensures that the flow of one substrate is driven by the electrochemical potential of the other, thus HCO_3^- /Cl^- exchangers can be used by cells to establish Cl^- gradients at the expense of pH_i. It has been proposed that protonation of the key AE1 carboxyl groups alters the net charge in the binding pocket, thereby neutralizing the extra charge on the bound sulfate and hence facilitating carrier reorientation. This suggests that steric as well as electrostatic interactions at this position contribute to sulfate transport (Sekler et al., 1995b).

Regulation by pH_i

AE2 and AE3 are regulated by changes in pH_i. HCO_3^-/Cl^- exchanger activity in cells, for example renal mesangial cells (Boyarsky et al., 1988ab), gastric parietal cells (Wenzl and Machen, 1989) and Vero cells (Olsnes et al., 1986; Olsnes et al., 1987), is very dependent on pH_i. Inhibition of HCO_3^-/Cl^- exchange occurs as pH_i is decreased below 7.0-7.1 (Lee et al., 1991). Alkaline pH_i activates AE2 in HEK293 cells with the pH_i set-point well above the range of resting pH_i, such that AE2 activation was measurable only during Cl^- restoration. This would seem to indicate that AE2 in these cells does not contribute to the maintenance of resting pH_i (Lee et al., 1991). AE2 transfection produced HCO_3^-/Cl^- exchange with pH_i sensitivity dependent on the transfected cell type. AE2 activity, overexpressed in Sf9 cells, was insensitive to changes in pH_i up to pH_i 7.5 (He et al., 1993), whereas mouse AE2, overexpressed in Xenopus oocytes, exhibited the full range of activity when pH_i and pH_o were changed simultaneously (Humphreys et al., 1994). The pH_i set-point of AE2 overexpressed in *Xenopus* oocytes was (7.1-7.2) and consistent with a role for AE2 in the regulation of resting pH_i (Jiang et al., 1994). The variable set-points obtained following AE2 overexpression suggest that transfection of AE2 does not result in the same pH_i dependence as native expression. Nonerythroid cells, which express endogenous AE2 and/or AE3, exhibit a steep pH_i dependence with pH_i set-points within the range of resting pH_i. This suggests that AE2 and AE3 contribute not only to cellular defense against intracellular alkaline loads, but also in some tissues to the maintenance of resting pH_i (Alper, 1994; Ganz et al., 1989) and Cl^- (Vaughn-Jones, 1986).

The transmembrane domains of AE1 and AE2 are 65% identical in amino acid

sequence while overlapping regions of N-terminal cytoplasmic domain are only 33% identical. This would seem to suggest a role for the N-terminal domain in the regulation of exchanger. However, the model for the Na^+/H^+ antiporter suggests that the regulatory pH sensor of NHE1 appears to be in cytoplasmic loop within the transmembrane domain with a modulatory region in the cytoplasmic domain (Wakabayashi et al., 1992). Thus, the HCO_3^-/Cl^- exchanger pH_i sensor may be similarly localized to one of the cytoplasmic loops within the transmembrane domain. To investigate the location of the pH_i sensor, Zhang and colleagues constructed chimeric and truncated AE exchangers in *Xenopus* oocytes and measured Cl^- transport across wide range of pH_o. Wild-type (WT) AE2 exhibited a steep pH_i dependence with maximal activity at alkaline pH_o. Substitution of the AE2 membrane domain with the AE1 membrane domain produced AE activity similar to WT-AE1 with a broad pH dependence. In contrast, substitution of the cytoplasmic domain of AE2 by AE1 produced a steep pH versus activity curve, similar to WT AE2. This suggests that a pH sensor resides within the transmembrane region of AE2. Similar experiments showed that the N-terminal cytoplasmic region contains a modifier site, located between amino acids 100 and 510, that is required to enhance the H^+ sensitivity of the AE2 proton sensor (Zhang et al., 1996). The transport capacity of the HCO_3^-/Cl^- exchanger seems to be dependent on the C-terminal transmembrane domain, as truncated mutants of each isoform (AE1; Grinstein et al., 1978; AE2; Lindsey et al., 1990; AE3; Kopito et al., 1989) lacking the N-terminus still possess active HCO_3^-/Cl^- transport. This would suggest that the N-terminal and C-terminal domains are functionally independent. However, as the chimeric construct experiments have shown, the N-terminus may play a role in modifying the pH_i sensitivity of the exchanger (Zhang

et al., 1996). Preliminary evidence had also suggested that a proton sensor resides within the N-terminal cytoplasmic domain. A cluster of four histidine residues, located within the extreme N-terminus of the cytoplasmic domain, may be present in pH_i sensitive exchangers AE2 and AE3 but absent from AE1 (Sekler et al., 1996). Unfortunately, this study, which identified the histidine cluster as well as an interaction between the N-terminal and C-terminal domains which regulated exchanger activity in response to changes in pH_i, has since been retracted (Cell. 1997. 90:6). The N-terminal regions of AE2a, AE2b and AE3b do contain clusters of histidine and glutamine residues (Van Winkle, 1999). There is, however, some supporting evidence from the literature that may indicate a role for histidine as a pH_i sensor. Histidine is the only naturally occurring amino acid with a side chain pK_a near neutral (pK_a in solution = 6.0; Sekler et al., 1996). Histidine residues participate in coupling pH to the activity of the bacterial Na^+/H^+ antiporter (Rimon et al., 1995), a voltage-dependent mitochondria pore (Petronilli et al., 1994), and the external pH sensor of inward rectifier K^+ channels (Coulter et al., 1995).

Another amino acid, a conserved glutamate residue, predicted to be located near the cytoplasmic interface of transmembrane helix 8 (Tang et al., 1998), may play a key role in ion selectivity, pH_i dependence and kinetics of anion transport. This glutamate residue is conserved in all AE isoforms (mouse AE1-Glu-699; AE2-Glu-1007; AE3 Glu-998, human AE1 Glu 681) sequenced to date (Sekler et al., 1995b). Chemical mutagenesis of human AE1 Glu-681 abolishes the pH dependence of sulfate transport and eliminated H^+ flux normally associated with sulfate transport. These studies led to the hypothesis that Glu-681 acts as a switch such that protonation of Glu-681 can switch AE1 between monovalent and divalent anion transport (Jennings and Smith, 1992; Sekler et

al., 1995b).

Regulation of pH_i set-point

AE2 and AE3 HCO_3^-/Cl^- exchangers are activated by elevated pH_i and inactivated by lowered pH_i. Each cell type displays a characteristic profile of maximal activity, hormone responsiveness and pH_i set-point (Alper et al., 1991). The pH_i set-point can be a major locus of regulation by hormones and growth factors which can stimulate the hydrolysis of phospholipids and other signaling factors (e.g. cAMP, Ca^{2+}; Moolenaar et al., 1983; Frelin et al., 1983; Vigne et al., 1984; Paris and Pouyssegur, 1984). In mesangial cells; arginine vasopressin (AVP) activates Na^+/H^+ antiporter, Na^+-dependent HCO_3^-/Cl^- exchanger and HCO_3^-/Cl^- exchanger in parallel by shifting the pH_i set-point of each of these exchangers in concert (Ganz et al., 1989). Similarly, AVP and phorbol esters activate Na^+/H^+ antiporter activity in A7r5 (rat aortic smooth muscle cell line) cells. AVP mobilizes $Ca^{2+}{}_i$ stores in A7r5 cells. AVP may also stimulate hydrolysis of PIP2 to produce DAG as the effects of AVP on pH_i in A7r5 cells can be mimicked by phorbol esters. This suggests that AVP regulation of pH_i may be transduced by PKC (Vigne et al., 1988). HCO_3^-/Cl^- exchanger activity in other cell types may also be regulated by a $Ca^{2+}{}_i$-dependent pathway such as PKC. In an osteoblast cell line extracellular Ca^{2+} entry activates HCO_3^-/Cl^- exchanger activity (Green et al., 1990). Serum, which contains growth factors, strongly activates Cl^-/Cl^- self exchange and HCO_3^-/Cl^- exchange while inhibiting Na^+-dependent HCO_3^-/Cl^- exchange. Both effects appear to be mediated by PKC (Tonnessen et al., 1990).

In other cell types, a cAMP-dependent pathway regulates HCO_3^-/Cl^- exchanger

activity. cAMP either stimulates (Schuster and Stokes, 1987) or inhibits anion exchange (Vigne et al., 1988). The unique N-terminus of AE2a contains a potential phosphorylation site for PKA at Ser-10 (Wang et al., 1996). This site is not present in AE2b, suggesting that transport activity of AE2a but not AE2b may be regulated in a cAMP-dependent manner (Van Winkle, 1999). Increasing intracellular cAMP levels in A7r5 cells using β-adrenergic receptor agonist isoproterenol, 8-Br-cAMP or forskolin inhibits HCO_3^-/Cl^- exchanger activity (Vigne et al., 1988). cAMP is reported to inhibit NaCl uptake across *Necturus* gallbladder epithelium due to inhibition of Na^+/H^+ antiporter (Reuss and Petersen, 1985) and HCO_3^-/Cl^- exchanger (Reuss, 1987). Thus, increased production of HCO_3^- could lead to stimulation of a cAMP-dependent pathway, through activation of the sAC, which could regulate HCO_3^-/Cl^- exchanger activity (Chen et al., 2000).

Purinergic receptor activation activates HCO_3^-/Cl^- exchanger activity in cardiac cells (Puceat et al., 1991), osteoclasts (Yu and Ferrier, 1995) and probably in neurons (De Souza et al., 1995). Exogenous ATP addition induces activation of tyrosine kinases Src and Fyn resulting in association of both Fyn and FAK (focal adhesion kinase) with AE1. The model for purinergic activation of AE1 exchange suggests that ATP induced phosphorylation of FAK provides a docking site for Fyn through SH2 and SH3 domains. FAK then recruits Fyn where it phosphorylates AE1 (Puceat et al., 1995; 1998).

It is unknown whether changes in HCO_3^-/Cl^- exchanger activity result from direct phosphorylation of the exchanger or involve the phosphorylation of a regulatory molecule. AE isoforms contain consensus sequences for casein kinase II (CKII), PKA,

PKC and protein tyrosine kinase (Yannoukakos et al., 1994). This suggests that phosphorylation of the exchanger by a protein kinase could regulate HCO_3^-/Cl^- exchanger activity, although this has yet to be shown directly (Alper et al., 1991; 1994).

Summary

HCO_3^-/Cl^- exchanger activity is essential for the regulation of pH_i against intracellular alkalosis in mammalian cells. HCO_3^-/Cl^- exchanger activity exhibits characteristic stilbene sensitivity and dependence on both Cl^- and HCO_3^- (Alper, 1991). AE1 is important as a cytoskeleton anchor as well as for HCO_3^-/Cl^- exchanger (Lee et al., 1991). AE2 and AE3 exhibit a steep pH_i dependence, such that HCO_3^-/Cl^- exchange becomes activated above a pH_i threshold or set-point. Below the pH_i set-point, the exchange is inactive. Endogenously expressed AE2 and AE3 may contribute to the maintenance of resting pH_i and Cl^- homeostasis (Alper et al., 1991; 1994). The pH_i set-point may be regulated by protein kinase phosphorylation with numerous different signaling pathways implicated.

Na^+- HCO_3^-/Cl^- exchanger

The Na^+- HCO_3^-/Cl^- exchanger is believed to alleviate intracellular acidosis, is Na^+-dependent, DIDS-sensitive and imports HCO_3^- in exchange for Na^+ and Cl^- thereby increasing pH_i. Na^+- HCO_3^-/Cl^- transporter regulates pH_i in invertebrate cells and activity has been demonstrated in the basolateral membrane of the *Necturus* proximal tubule (Boron, 1986). Recently, Romero et al (2000) have cloned and characterized a Na^+- HCO_3^-/Cl^- transporter- NDAE1- from *Drosophila*. When expressed in *Xenopus* oocytes,

this membrane protein mediates the transport of Cl^-, Na^+, H^+ and HCO_3^- but is not strictly dependent on HCO_3^- (Romero et al., 2000). NDAE1 mediates Na^+- HCO_3^-/Cl^- exchanger activity characterized in neurons (Russell and Boron, 1976; Thomas, 1977; Schwiening and Boron, 1994), kidney (Guggino et al., 1983; Ganz et al., 1989), and fibroblasts (Kaplan and Boron, 1994; Romero et al., 2000).

A Na^+- HCO_3^-/Cl^- transporter has been cloned from human brain- NDCBE1. NDCBE1 encodes 1044 amino acids, is 34% identical to mammalian AE2 and 47% identical to NDAE1. NDCBE1 is expressed in the brain and testis, with weaker expression in the kidney and ovary. NDCBE1 expressed in *Xenopus* oocytes is electroneutral, HCO_3^--dependent and DIDS-sensitive (Grichtchenko et al., 2000). A Na^+- HCO_3^-/Cl^- transporter has also been cloned from the insulin-secreting cell line MIN6 cDNA library and has been designated NCBE. The NCBE protein consists of 1088 amino acids having 74, 72, and 55% amino acid identity to the human skeletal muscle, rat smooth muscle, and human kidney Na^+- HCO_3^- cotransporter, respectively. NCBE protein expressed in *Xenopus* oocytes and HEK293 cells transports extracellular Na^+ and HCO_3^- into cells in exchange for intracellular Cl^- and H^+, thus raising the pH_i (Wang et al, 2000).

VII. pH_i REGULATION IN MAMMALIAN PREIMPLANTATION EMBRYOS

Na^+/H^+ antiporter

Although upregulation of Na^+/H^+ antiporter activity at fertilization in the sea urchin and *Xenopus* is a major event at fertilization, detection of Na^+/H^+ antiporter activity in mammalian embryos has not been consistent. Hamster 2-cell embryos are able to successfully develop to the blastocyst stage when cultured at acidic external pH,

however, blastocyst development is significantly reduced in the presence of EIPA (an amiloride derivative; Lane et al., 1998). This suggests that mammalian embryos possess transporters capable of alleviating intracellular acidosis, thereby enabling development even at acidic pH. Na^+/H^+ antiporter activity has been demonstrated in hamster (Lane et al., 1998) and Quackenbush strain mouse 2-cell embryos (Gibb et al., 1997), but was not originally detected in mouse CF-1 strain 2-cell embryos (Baltz et al., 1991a; Baltz et al., 1990). In hamster and in Quackenbush 2-cell embryos, the Na^+/H^+ antiporter was involved in the recovery from induced intracellular acidosis (Gibb et al., 1997; Lane et al., 1998). In CF-1 mouse embryos, however, recovery to baseline pH_i after intracellular acidification did not occur (Baltz et al., 1990). Further investigation of Na^+/H^+ antiporter activity in several mouse strains has revealed Na^+/H^+ antiporter activity that is appropriately Na^+-dependent and inhibited by amiloride. The level of Na^+/H^+ antiporter activity, however, varies considerably among different strains of mice, being very low in CF-1 strain embryos, and high in Balb/c embryos (Steeves, C.L., Lane, M., Bavister, B.D., Phillips, K.P., and Baltz, J.M., unpublished).

NHE-1 mRNA expression has been demonstrated in mouse eggs and in all stages of mouse embryo development, and immunohistochemistry of mouse blastocysts has shown NHE-1 protein localization to the blastocoel membrane (Barr et al., 1998). NHE-3, whose mRNA has only been detected in unfertilized mouse eggs, immunolocalizes to the outer surface of the blastocyst (Barr et al., 1998). Thus, pH_i is regulated by Na^+/H^+ antiporter in hamster embryos (Lane et al., 1998), and to varying extent in mouse embryos, depending on the strain of mouse (Gibb et al., 1997;Steeves, C.L., Lane, M., Bavister, B.D., Phillips, K.P., and Baltz, J.M., unpublished).

HCO_3^-/Cl^- exchanger

Regulation against alkalosis has been well-examined in mouse (Baltz et al., 1991b; Zhao et al., 1995; Zhao and Baltz, 1996; Zhao et al., 1997) and hamster (Lane et al., 1999b) preimplantation embryos from the mid-1-cell stage onwards. HCO_3^-/Cl^- exchanger activity was first described in mouse 2-cell embryos, and was shown to mediate recovery from induced intracellular alkalosis. Recovery was shown to be HCO_3^- and Cl^--dependent and was inhibited by DIDS (Baltz et al., 1991b). HCO_3^-/Cl^- exchanger activity is highest at the 1-cell (zygote) and 2-cell stages and decreases by the morula and blastocyst stages when the embryo enters the uterus (Zhao and Baltz, 1996). HCO_3^-/Cl^- exchanger activity is required for maintenance of normal pH_i in the embryo and for recovery from intracellular alkalosis, and embryo development will not occur in the absence of functional exchangers when external pH is near that of oviductal fluid (Zhao et al., 1995). The pH_i set-points for HCO_3^-/Cl^- exchanger activity in mouse embryos were 7.20, 7.20, 7.16 and 7.07 for 1-cell, 2-cell, morula and blastocyst, respectively (Zhao et al., 1995). HCO_3^-/Cl^- exchanger activity in preimplantation mouse embryos displayed characteristic inhibition by DIDS, with IC_{50} of 4, 17 and 22 μM at 1-cell, 2-cell and blastocyst stages, respectively (Zhao and Baltz, 1996).

Resting pH_i of 2-cell mouse embryos cultured under alkaline conditions (0.8% CO_2 ~pH 7.8) in the presence of DIDS (i.e. no functional HCO_3^-/Cl^- exchanger activity) rose to pH_i 7.57 which was much higher than the pH_i of 7.24 in embryos cultured under the same conditions without DIDS (Zhao et al., 1995). Resting 2-cell embryo pH_i was also higher when embryos were cultured under standard culture conditions (5% CO_2 ~pH 7.35) in the presence of DIDS (pH_i 7.29) compared to embryos cultured in the absence of DIDS (7.10; Zhao et al., 1995).

Using RT-PCR, AE mRNA expression was determined in mouse preimplantation embryos. AE1 mRNA was not detected in any embryo stage, while AE2 mRNA was expressed throughout embryo development, with the greatest amount at the 1-cell stage and blastocyst. AE3 was present from the 2-cell stage through to blastocyst stage and only weakly detected in a minority of 1-cell embryo samples. Thus, AE2 is both maternally and embryonically derived as it is present in the 1-cell embryo, whereas AE3 would seem to be a product of the embryonic genome only as it appears only after ZGA at the 2-cell stage (Zhao et al., 1995).

At the blastocyst stage, where there is little exchanger activity detectable in the outer (apical) trophectoderm, AE2 protein is localized to the inner (basolateral) membrane (Zhao et al., 1997), where it may function in Cl^- and fluid transport to the blastocoel cavity (Brison and Leese, 1993; Zhao et al., 1997).

Since mammalian fertilization and early embryo development occurs within the alkaline environment of the oviduct, expression and function of HCO_3^-/Cl^- exchangers is vital for preimplantation embryo development. How HCO_3^-/Cl^- exchanger activity is regulated in the unfertilized mammalian egg remained to be determined.

VIII. OBJECTIVE AND SPECIFIC AIMS

Mammalian gametes and embryos are highly sensitive such that even small deviations in pH, osmolarity or other characteristics of their environment prove detrimental to successful fertilization, development and implantation. Mammalian preimplantation embryos exhibit robust pH_i regulation, particularly against alkalosis, mediated by HCO_3^-/Cl^- exchangers (Zhao et al., 1995; Zhao and Baltz, 1996; Zhao et al., 1997; Lane et al., 1998). pH_i is an important mediator of events at fertilization in the sea

urchin, *Xenopus* and many marine invertebrates, and an increase in pH_i is a characteristic feature of oocyte maturation or egg activation, depending on the species. As very few studies had examined pH_i regulation in the unfertilized mammalian egg, the focus of this project was to determine how the unfertilized egg regulates pH_i against alkalosis and whether changes in pH_i or the activity of pH_i regulatory transporters are a conserved feature of fertilization.

OBJECTIVE: The objective of this project is to study pH_i regulation in the unfertilized mouse egg and early zygote to determine whether changes in pH_i or pH_i regulation accompany egg activation in the mammal.

Specific Aim #1: *Determine whether a pH_i change accompanies mouse meiotic maturation or egg activation.*

An increase in pH_i is an important feature of egg activation in the sea urchin (Johnson et al., 1976), egg maturation and fertilization in *Xenopus* (Webb and Nuccitelli, 1981), and meiotic maturation and fertilization in several marine invertebrates. A preliminary report of pH_i of unfertilized mouse eggs had indicated it was about 7.2 (House, 1994), within the range of mammalian somatic cells and at a level which should be permissive for cellular metabolism and DNA synthesis (Roos and Boron, 1981), in contrast to the low pH_i of unfertilized sea urchin eggs (~6.8; Johnson et al., 1976). This is also about the same as pH_i measured for cleavage stage mouse embryos (Zhao et al., 1995). *Thus, I hypothesize that an increase in pH_i is not a feature of mammalian egg activation.*

Specific Aim #2: *Determine how unfertilized mouse eggs regulate pH_i against intracellular alkalosis*

HCO_3^-/Cl^- exchanger activity is the principal mechanism employed by mammalian cells to alleviate intracellular alkalosis (Alper, 1991). HCO_3^-/Cl^- exchanger activity is the major pH_i-regulatory mechanism in mouse embryos and is present throughout embryo development, with highest activity found at the 1-cell and 2-cell stages. AE2 mRNA is expressed throughout mouse preimplantation embryo development, particularly at the 1- to 2-cell stage. If mammalian fertilization shares similar features with the sea urchin and *Xenopus*, egg activation may be accompanied by the net upregulation of pH_i regulatory transporters, such that unfertilized eggs have very low pH_i regulatory capacity. As Na^+/H^+ antiporter and HCO_3^-/Cl^- exchanger regulate pH_i in opposite directions (alkaline versus acid, respectively), upregulation of both transporters could result in no net change in pH_i but a greatly increased capacity to control pH_i.

Physiologically, ovulation of an unfertilized egg into an alkaline oviduct with low HCO_3^-/Cl^- exchanger activity is difficult to understand. However, the microenvironment of the cumulus mass may afford the egg protection as it has been shown to persist until about 20 h post-fertilization (Roblero et, 1989). Alternatively, a pH_i increase induced by the alkaline oviductal environment could contribute to optimal development. *I hypothesize that HCO_3^-/Cl^- exchanger activity contributes to pH_i regulation in the unfertilized mouse egg, but that pH_i regulation becomes greatly enhanced as a consequence of fertilization.*

Specific Aim #3: *Determine the mechanism of upregulation of HCO_3^-/Cl^- exchanger activity following egg activation*

As discussed, HCO_3^-/Cl^- exchanger activity is regulated by several intracellular signaling pathways and may involve phosphorylation of the exchanger or a regulatory protein (Alper, 1991; Alper, 1994). AE isoforms possess consensus sequences for casein kinase II (CKII), PKA, PKC and protein tyrosine kinase (Yannoukakos et al., 1994), which supports regulation by different protein kinase pathways, dependent on the tissue type and the isoform expressed. Candidate pathways that may upregulate of HCO_3^-/Cl^- exchanger activity at fertilization include PKC, PKA, Ca^{2+} and cell-cycle dependent kinases. cAMP and PKA are involved in the maintenance of GV arrest in mouse oocytes (Schultz et al., 1983b). Changes in intraoocyte cAMP could provide the necessary trigger for upregulation of HCO_3^-/Cl^- exchanger activity. Similarly, an increase in Ca^{2+}_i is a major event at fertilization, which leads to the activation of many Ca^{2+}-dependent pathways including PKC, Ca^{2+}/calmodulin and others. Thus, a Ca^{2+}-dependent pathway may regulate HCO_3^-/Cl^- exchanger activity. Finally, as egg activation involves the resumption of the cell cycle following a prolonged metaphase arrest, upregulation of HCO_3^-/Cl^- exchanger could be cell cycle dependent and may involve one of the many cell-cycle regulatory molecules active in eggs such as cdc2 kinase or the MAPK pathway. *As HCO_3^-/Cl^- exchanger activity has been shown to be modulated by protein kinase activity in mammalian cells (Moolenaar et al., 1983; Frelin et al., 1983; Vigne et al., 1984; Paris and Pouyssegur, 1984; Ganz et al., 1989), I hypothesize that enhanced HCO_3^-/Cl^- exchanger activity following fertilization may be regulated by one of the signaling pathways central to fertilization.*

MATERIALS AND METHODS

I. CHEMICALS AND SOLUTIONS

Chemicals

All components of media (embryo culture or cell culture grade) as well as amiloride, brefeldin A, cytochalasin D, cycloheximide, demecolcine, digitonin, hyaluronidase, pregnant mare's serum gonadotropin (PMSG), human chorionic gonadotropin (hCG), formaldehyde, Triton X-100, EGTA (ethylene glycol-bis[β-aminoethyl ether]-N,N,N',N',-teraacetic acid), 3-isobutyl-1-methylxanthine (IBMX), dibutyrl adenosine 3-5-cyclic monophosphate (dbcAMP), forskolin, phorbol 12-myristate 13-acetate (PMA), D-erythro-sphingosine, mineral oil, okadaic acid (OA) and nigericin were obtained from Sigma (St. Louis, MO). DIDS, H_2DIDS, valinomycin, A23187 (4-Bromo-A23187), SNARF-1-AM (carboxyseminaphthorhodafluor-1-acetoxymethyl ester), MQAE (N-(6-methoxyquinolyl)acetoethyl ester), Fura-2-AM (5-oxazolecarboxylic acid, 2-(6-(bis(2-((acetyloxy)methoxy)-2-oxoethyl)amino)-5-(2-(2-(bis(2-((acetyloxy)methoxy)-2-oxoethyl)amino)-5methylphenoxy)ethoxy)-2-bensofuranyl)-, (acetyloxy)methyl ester) and rhodamine phalloidin were obtained from Molecular Probes (Eugene, OR). N-[2-((p-Bromocinnamyl)amino)ethyl]-5-isoquinolinesulfonamide, HCl (H-89), phorbol-12,13-didecanoate (PDD) and U0126 were obtained from Calbiochem (La Jolla, CA). Absolute ethanol was obtained from Corby Distilleries Ltd, (Corbyville, ON) and methanol from AnaLar (BDH; Toronto, ON). Solvents used for stock solutions for chemicals were as follows: cycloheximide, dbcAMP: water; cytochalasin D, demecolcine, nigericin: ethanol; brefeldin A: methanol;

valinomycin, H-89, PMA, PDD, sphingosine, forskolin, IBMX, A23187, rhodamine phalloidin, BAPTA-AM, DIDS, H_2DIDS, Fura-2-AM, OA, U0126 and SNARF-1-AM: DMSO. Stock concentrations were as indicated below. All stock solutions were stored at -20°C.

List of pharmaceutical agents

A23187: Ca^{2+} ionophore

amiloride (AMIL): Na^+/H^+ antiporter inhibitor

BAPTA-AM: Ca^{2+} chelator

brefeldin A: disrupts Golgi apparatus

cycloheximide: protein synthesis inhibitor

cytochalasin D: disrupts F-actin filaments

dbcAMP (dibutyrl cAMP): membrane permeant cAMP analogue

demecolcine (deme): microtubule depolymerizer; maintains metaphase arrest

DIDS: anion exchange inhibitor; inhibits Cl^- channels; HCO_3^-/Cl^- exchanger

digitonin: used to permeabilize cell membrane

ethanol: used to parthenogenetically activate eggs

forskolin: adenylate cyclase inhibitor

Fura-2-AM: Ca^{2+}-sensitive fluorophore

H-89: PKA inhibitor

H_2DIDS: anion exchange inhibitor, not fluorescent under UV illumination

hCG (human chorionic gonadotropin): used to trigger ovulation in mice

hyaluronidase: enzyme used to disperse cumulus cells

IBMX (3-isobutyl-1-methylxanthine): phosphodiesterase inhibitor

KSOM: standard mouse embryo culture medium

MQAE: halide (Cl^-)-sensitive fluorophore

nigericin: H^+/K^+ exchanger; used for pH_i calibration

OA (okadaic acid): protein phosphatase (PP1 and PP2A) inhibitor

PDD (phorbol-12,13-didecanoate): phorbol ester

PMA (phorbol 12-myristate 13-acetate): phorbol ester

PMSG (pregnant mares' serum gondadotropin): used to stimulate follicle development

rhodamine phalloidin: fluorophore used to detect F-actin

SNARF-1-AM: pH-sensitive fluorophore

sphingosine: PKC inhibitor

Sr^{2+}: divalent cation used to parthenogenetically activate eggs

U0126: MEK1/2 inhibitor

valinomycin: K^+ ionophore; used for pH_i calibration

Solutions

A. Egg/embryo handling media and culture media

KSOM (K^+ supplemented Simplex Optimized Medium) embryo culture medium (Lawitts and Biggers, 1993) contains (in mM except as noted) 95 NaCl, 2.5 KCl, 0.35 KH_2PO_4, 0.2 $MgSO_4$, 10 sodium lactate, 0.2 glucose, 0.2 sodium pyruvate, 25 $NaHCO_3$, 1.7 $CaCl_2$, 1.0 glutamine, 0.01 tetrasodium EDTA, 0.03 streptomycin SO_4, 0.16 K penicillin G and 1.0 mg/ml bovine serum albumin (BSA) (all from Sigma, embryo culture tested or tissue culture tested grades), and is equilibrated with 5% CO_2/air (pH

7.35). Hepes-KSOM medium, wherein 21 mM of the $NaHCO_3$ in KSOM is replaced by equimolar Hepes (pH adjusted with NaOH to 7.4 at 37°C) was used for obtaining and handling the embryos.

B. Media for sperm capacitation and in vitro fertilization (IVF)

A modified KSOM was used for sperm capacitation and in vitro fertilization (IVF) in which glucose was increased to 5.56 mM and 30 mg/ml fatty acid free-BSA was used in place of BSA (Summers et al., 1995).

C. PBS and 7% ethanol-PBS

Phosphate-buffered saline (PBS), pH 7.2, (Hogan et al., 1986) contained (in mM) 137 NaCl, 2.7 KCl, 8.1 Na_2HPO_4, 1.5 KH_2PO_4. Absolute ethyl alcohol was used as a 7% (v/v) solution in PBS for parthenogenetic activation (Hogan et al., 1986).

D. Media for Sr^{2+}-mediated parthenogenetic activation of eggs

Ca^{2+}-free KSOM was prepared identically to KSOM (see above) but 1.7 mM $CaCl_2$ was omitted. 10 mM $SrCl_2$ (prepared as 1 M stock and stored at 4°C) was added just prior to Sr^{2+}-induced egg activation, described below.

E. Media for pH_i measurements

Media used for pH_i measurements were based on KSOM mouse embryo culture medium (Lawitts and Biggers, 1993). Modified KSOM contained (in mM) 104 NaCl, 2.5 KCl, 0.35 KH_2PO_4, 0.2 $MgSO_4$, 1 Na^+ lactate, 0.2 glucose, 0.2 Na^+ pyruvate, 25

$NaHCO_3$, 1.7 $CaCl_2$, 1 glutamine, 0.01 tetrasodium EDTA, 0.03 streptomycin SO_4 and 0.16 K penicillin G. Media were equilibrated with 5% CO_2/air except where noted. Modified Hepes-KSOM, used for egg/embryo handling and to produce HCO_3^--free solutions, was produced by replacing 21 mM (of 25 mM) $NaHCO_3$ (modified KSOM recipe above) with equimolar Hepes (pH adjusted to 7.4 with NaOH or KOH, as appropriate). For Cl^- free solutions, all Cl^- salts were replaced with corresponding gluconate or SO_4^- salts. For Na^+-free (< 1 mM) solutions, NaCl was replaced with equimolar choline Cl^-, and Na^+ pyruvate, Na^+ lactate and $NaHCO_3$ were replaced by K^+ pyruvate, lactic acid and choline HCO_3^-, respectively. Hepes-KSOM was modified to produce HCO_3^--free medium by replacing $NaHCO_3$ with equimolar NaCl. NH_4^+-KSOM contained 35 mM NH_4Cl with either 12 mM or 25 mM $NaHCO_3$ (as specified) and NaCl reduced accordingly. $0Cl^-$ NH_4^+-KSOM was produced by replacement of NH_4Cl by equimolar NH_4SO_4 and all other Cl^- salts replaced with corresponding gluconate salts. pH_i calibration solutions used for nigericin/high K^+ calibration of pH_i (see below) contained (in mM): 25 NaCl, 100 KCl, 20.8 Hepes and 75 sucrose (pH adjusted to 6.9, 7.3, 7.6 and 7.9 with NaOH; Thomas et al., 1979).

II. ANIMALS, AND GAMETE AND EMBRYO MANIPULATIONS

Animals

Oocytes were collected from superovulated (see below) female CF1 mice (age 5-6 weeks). Superovulated females were housed singly with stud BDF males (age 8-30 weeks) overnight for the production of embryos. For IVF, sperm were obtained from

male CD-1 mice (age 12-15 weeks). Mice were obtained from Charles River, Canada. All experimental protocols involving animals were approved by the Animal Care Committee of the Ottawa Hospital-Civic Site.

Superovulation

Pregnant mare's serum gonadotropin (PMSG), also called equine chorionic gonadotropin (eCG), was used to mimic follicle-stimulating hormone (FSH) for the production of supernumerary follicles. Human chorionic gonadotropin (hCG) was used to mimic luteinizing hormone (LH) to induce oocyte maturation and ovulation. Animals (both males and females) were maintained on a 12 h light (7:00 am-7:00 pm): 12 h dark cycle (7:00 pm-7:00 am). 5 IU PMSG was injected intraperitoneally (i.p.) at 4:00 pm and 5 IU hCG was injected i.p. 47.5 h later at 3:30 pm. Ovulation was estimated to occur between 10 and 13 h following hCG injection (1:30-4:30 am) and was confirmed by egg collection during this time period. Endogenous LH is released in response to PMSG 15-20 h after the midpoint of the second dark period following injection of PMSG (5:00-10:00 pm). As hCG administration (at 3:30 pm) preceded the release of endogenous LH, egg/embryo yield could be maximized with ovulation and fertilization more precisely timed (Hogan et al., 1986).

Egg and zygote collection

To obtain zygotes, females were housed with BDF males, as described above, immediately following administration of hCG. Unfertilized eggs (Fig. 2-MII) were collected 13.5-16 h post-hCG while zygotes (Fig. 4-1c) were collected either 15-17 h

('am-zygotes') or 20-24 h post-hCG, as specified. Cumulus masses (Fig. 2) were released into 300 μg/ml hyaluronidase in Hepes-KSOM for 6-8 min until the eggs/zygotes could be removed from cumulus cells. Eggs were then used immediately for pH_i measurements, used for IVF, or cultured, as specified. Zygotes were used immediately for pH_i measurements or cultured, as specified.

Germinal vesicle (GV) oocyte collection

Female mice were primed with PMSG 45-47 h prior to collection of GV oocytes. At the time of collection, ovaries were removed and mechanically homogenized using a razor blade. Homogenized tissue was transferred to Hepes-KSOM containing 300 μM dbcAMP to prevent GVBD (Cho et al., 1974). GV oocytes were easily identified by the presence of an intact germinal vesicle and no polar body (Fig. 2-GV). GV oocytes were continuously maintained in medium containing dbcAMP (unless otherwise stated) prior to pH_i measurements.

Microdrop culture

Embryos were cultured according to standard techniques. Briefly, droplets of culture media (~ 50 μl) were placed in 35 mm tissue culture dishes (Falcon #3001, Fisher, Pittsburgh, PA) and overlaid with KSOM-washed mineral oil. Culture media and oil were preequilibrated in an incubator with 5% CO_2/air at 37°C and 100% humidity overnight prior to preparation of culture dishes. Embryos were placed into the drops using a mouth-operated flame-drawn glass pipette, and the dishes returned to the

incubator. This technique routinely produces 80-100% blastocysts from the culture of in vivo-produced 1-cell mouse embryos (CF1♀ x BDF♂) by 120 h post-hCG in our laboratory (Fig. 4).

Sperm collection and in vitro fertilization (IVF)

CD-1 males were killed by cervical dislocation. Neat epididymal fluid containing sperm was removed from vas deferens and cauda epididymides and placed into Eppendorf tubes containing 1 ml modified KSOM (5.56 mM glucose, 30 mg/ml fatty-acid free BSA). Sperm were allowed to swim up into the medium and capacitate for 1 h at 37°C, 5% CO_2. Unmated female CF-1 mice were killed by cervical dislocation 13.5 h post-hCG, oviducts removed and cumulus masses released into Hepes-KSOM. Each cumulus mass was transferred to a separate 25 µl microdrop of modified KSOM (see above) under preequilibrated oil (37°C, 5% CO_2). At 14.5 h post-hCG, 500 µl of sperm suspension from each Eppendorf tube was removed and all were combined in a separate clean tube. 75 µl of this medium, containing motile, capacitated sperm, was added to each microdrop containing cumulus masses for a final concentration of approximately 1 million sperm/ml. Eggs and sperm were then co-incubated for 1 h. At 15.5 h post-hCG, eggs were washed free of remaining cumulus cells and unbound sperm (Fig. 10) by pipetting eggs sequentially through at least three microdrops of KSOM under oil. Eggs were then cultured for 1 to 26 h as described above.

Parthenogenetic activation

A. Ethanol: Unfertilized eggs were collected and denuded of cumulus cells as described

above. Eggs were then washed in Hepes-KSOM and transferred to 7% ethanol in PBS at room temperature for 5 min. Following the exposure to ethanol, eggs were washed in Hepes-KSOM and then transferred to pre-equilibrated (37°C, 5% CO_2) microdrops of KSOM under oil (Fig. 14A). Control eggs were exposed to PBS without ethanol for 5 min and otherwise treated identically.

B. Sr^{2+}: Unfertilized eggs were collected and denuded of cumulus cells, as described above. Eggs were then washed in Hepes-KSOM and transferred to 10 mM $SrCl_2$ in Ca^{2+}-free KSOM and cultured for 2 h (37°C, 5% CO_2). Eggs were then transferred to pre-equilibrated (37°C, 5% CO_2) microdrops of KSOM (Fig. 14B).

C. Cycloheximide: Unfertilized eggs were collected and denuded of cumulus cells, as described above. Eggs were washed in Hepes-KSOM and transferred to 50 μg/ml cycloheximide in KSOM and cultured for 2 h (37°C, 5% CO_2). Eggs were then transferred to pre-equilibrated (37°C, 5% CO_2) microdrops of KSOM (Fig. 14C).

Fertilization and egg activation assessment

Oocyte and embryo morphology and development were assessed using a Nikon dissecting microscope Generally, fertilization was confirmed by various morphological indices such as the appearance of pronuclei, emission of the second polar body, and slightly granular, dark cytoplasm, all of which were used to assess successful fertilization or egg activation when possible. AM-zygotes (15-17 h post-hCG) were scored as

fertilized if at least 1 pronucleus, 1 polar body, and darker cytoplasm could be detected. Zygotes (20-24 h post-hCG) were assessed as fertilized if 2 pronuclei could be detected (Fig. 4-1c). Eggs fertilized in vitro (IVF) were sampled at various time points following sperm-egg incubation from the pool of eggs fertilized each day. Fertilization could be confirmed in some eggs as early as 3-4 h post-sperm egg incubation by the appearance of 2 pronuclei, although these embryos made up a small percentage of the total pool. Pronuclei were clearly visible in most fertilized eggs starting from 4.5 h post-sperm egg incubation. Parthenogenotes with clearly visible pronuclei (either one or two) were considered activated (Fig. 14).

III. FLUORESCENT IMAGING

The development of ion-sensitive fluorophores has been invaluable for the measurement of concentrations of inorganic ions (e.g. Ca^{2+}, H^{+}, Cl^{-}) inside intact, living cells. The fluorescent properties of ion-sensitive fluorophores are affected by the relevant ion, usually by ion binding. The effect of ion binding can be either to decrease (or increase) fluorescence intensity, or instead to shift the spectrum of the fluorescence. By quantitative measurement of the fluorescence arising from these fluorophores, it is possible to determine either the absolute ion concentration or relative changes in ion concentration (Baltz and Phillips, 1999).

Fluorescence is the result of a three-step process which occurs in certain molecules (generally polyaromatic hydrocarbons or heterocycles) called fluorophores (Fig. 16). Fluorescence begins with excitation illumination (which in practice is usually

Figure 16. Principles of fluorescence. *Adapted from Haugland, 1996.* Molecules of the fluorophore exist at ground state (S_0). Upon excitation illumination (EX), energy is absorbed (①), increasing the energy state (S'_1). The molecules exist in this excited state during which time some absorbed energy is lost as heat or light or by collisional quenching (②), dropping to energy state S_1. The remaining absorbed energy is released as fluorescence emission (③), returning the energy state back to ground (S_0). Because energy is lost during the excited state, the amount of energy absorbed is always greater than that emitted. Thus, EM is always less than EX, such that fluorescence has a longer wavelength than the excitation illumination (Haugland, 1996).

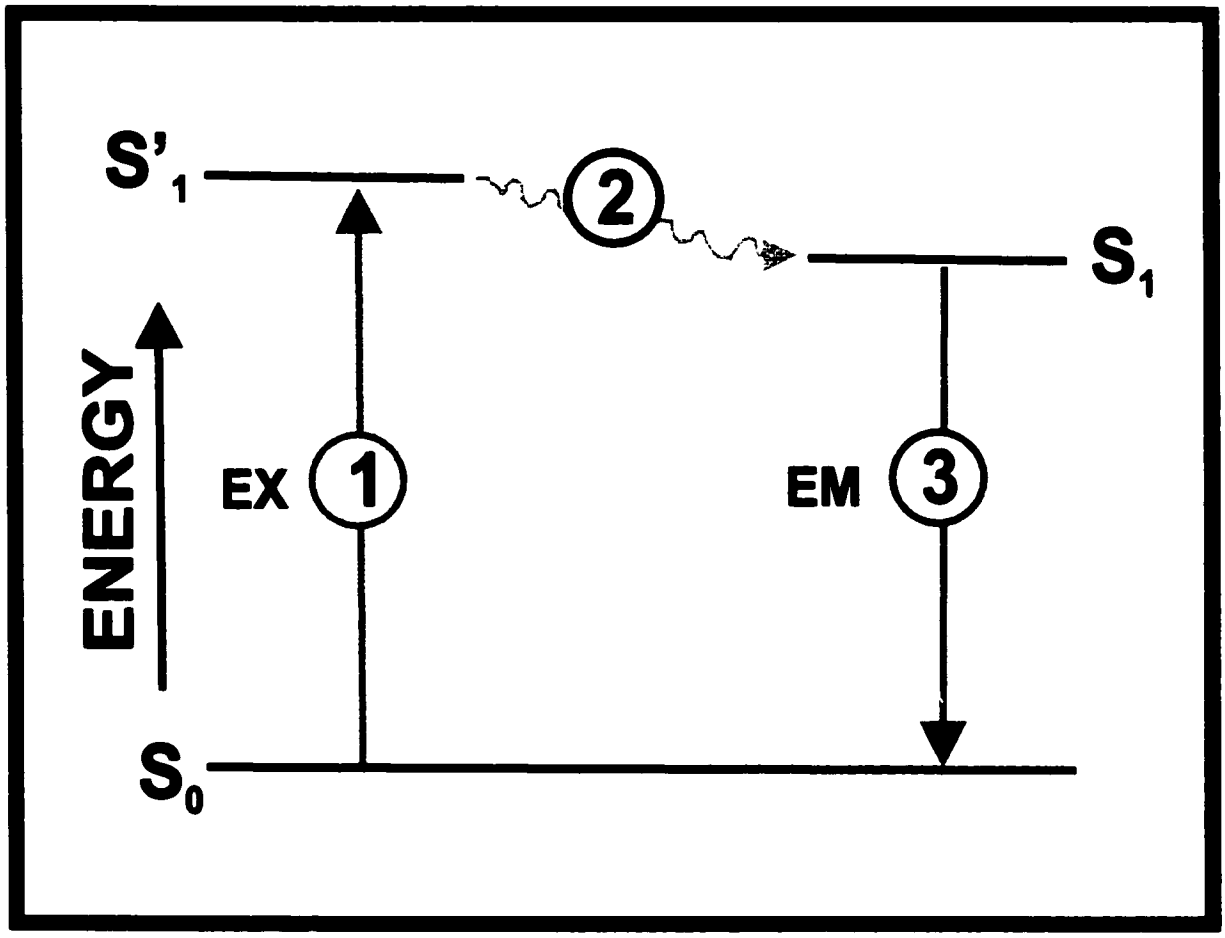
S'1
2
S1
ENERGY
EX
1
EM
3
S0

provided by an incandescent lamp or laser) which is absorbed by the fluorophore. Absorption of excitation photons drives the fluorophore to a higher energy state ($S_0 \rightarrow S_1'$). This excited state of the fluorophore exists very briefly (1-10 nsec) during which time some of the absorbed energy is dissipated usually as heat or by direct energy transfer to other molecules. This results in a transition to a longer-lived excited state (S_1) which is termed the meta-stable state. The fluorophore persists in the meta-stable state for a relatively long period, thus producing a population of fluorophores in which a significant proportion resides in S_1. Finally, the fluorophore drops back to the ground state (S_0), resulting in emission of a photon. The energy of the emitted photons is always less than the energy of the photons originally absorbed because of energy lost during transition to the second excited state ($S_1' \rightarrow S_1$). Thus, emission fluorescence has a longer wavelength, correlating to the lower energy emitted. Fluorophores can be excited and will emit repeatedly until the fluorophore is irreversibly damaged during the excited state (photobleaching; Haugland, 1996).

Fluorescent indicators that show an excitation or emission spectral shift upon ion binding are particularly valuable for intracellular ion measurements (Fig. 17A). For these probes, fluorescence at different wavelengths is affected differently by ion binding, while in contrast, changes in fluorophore concentration, pathlength (ie. cell thickness), or other non-specific effects will have equal effects at all wavelengths. The advantage of such fluorophores is that the ratio of fluorescence intensities at two chosen wavelengths with different dependencies on ion concentration is almost independent of other parameters such as fluorophore concentration, cell geometry, or excitation intensity. Such fluorophores which exhibit a spectral shift upon interacting with an ion are termed

Figure 17. Ratiometric fluorescence imaging. *Adapted from Haugland, 1996.* A. The advantage of ratiometric fluorophores is that the ratio of fluoroscence intensities at two chosen wavelengths with different dependencies on ion concentration is almost independent of other parameters such as fluorophore concentration, cell geometry, or excitation intensity (Haugland, 1996). For example, an ion-selective fluorophore may produce an intensity increase in response to ion binding (λ1). Alternatively, the ion-selective fluorophore may be quenched (intensity decreased; λ3). Finally, fluorescence measured at an isosbestic point (λ2) is independent of ion concentration. Thus, either λ1/λ3 or λ1/λ2 fluorescence intensity ratios will correct for some artifactual variations such as photobleaching or fluorophore leakage from cells. *B. AM loading.* Several fluorophores are available as acetoxymethyl (AM) ester derivatives. Shown is a Ca^{2+} - sensitive fluorophore- Fura-2-AM. In the AM form, the fluorophore is membrane permeable, but is not sensitive to its target ion (Ca^{2+}). Once inside the cell, the AM group is cleaved by intracellular esterases producing acetic acid and formaldehyde. The cleaved form of the fluorophore (Fura-2) is membrane impermeant but sensitive to Ca^{2+} ions (Haugland, 1996).

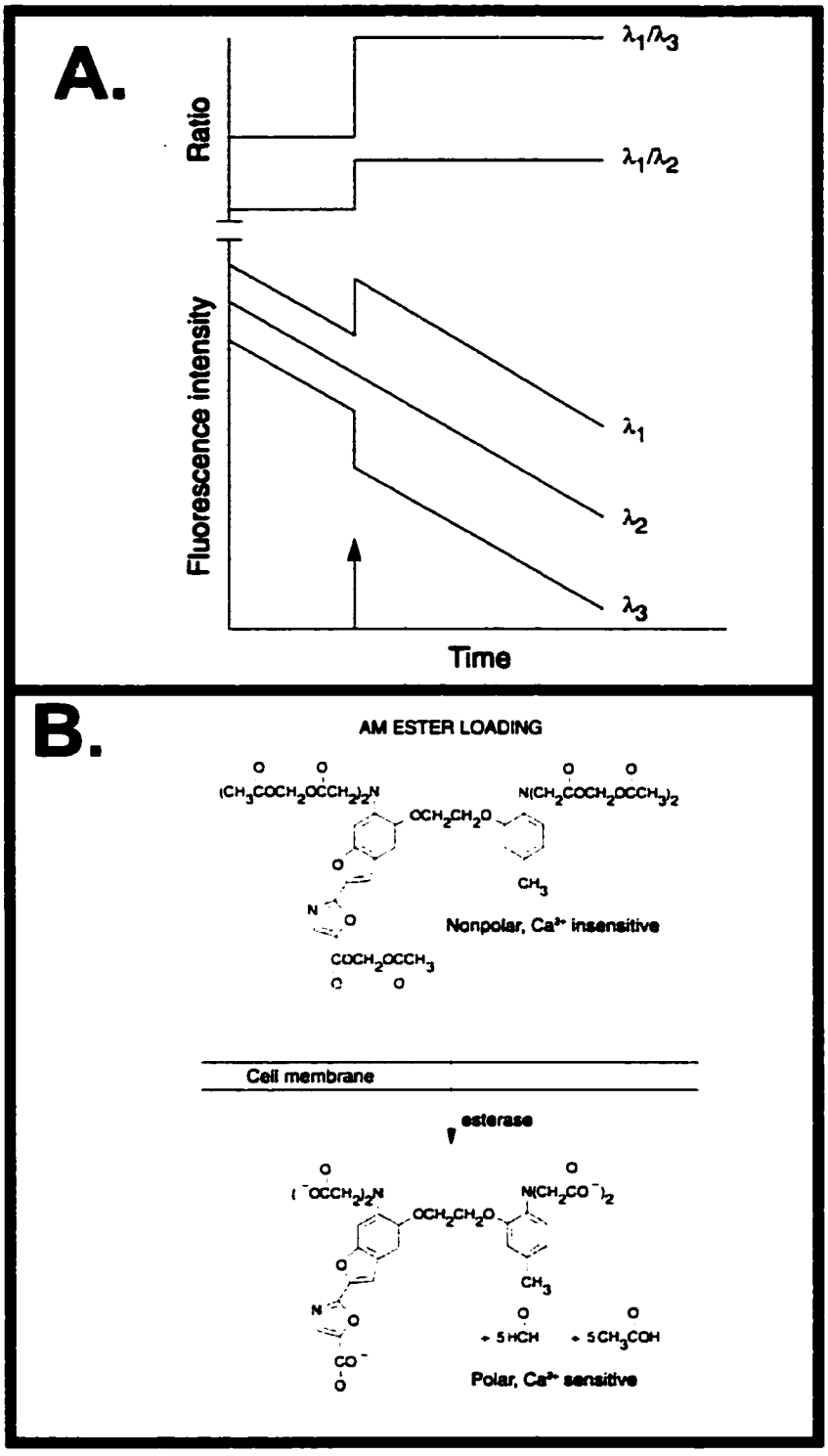
A.
Ratio
λ1/λ3
λ1/λ2
Fluorescence intensity
λ1
λ2
λ3
Time
B.
AM ESTER LOADING
Nonpolar, Ca2+ insensitive
Cell membrane
esterase
+ 5 HCH
+ 5 CH3COH
Polar, Ca2+ sensitive

"ratiometric" fluorophores (Baltz and Phillips, 1999). For example, an ion-selective fluorophore may produce an intensity increase in response to ion binding (λ1). Alternatively, the ion-selective fluorophore may be quenched (intensity decreased; λ3). Finally, fluorescence measured at the isosbestic point (λ2) is independent of ion concentration. Thus, either λ1/ λ3 or λ1/λ2 fluorescence intensity ratios will correct for some artifactual variations such as photobleaching or fluorophore leakage from cells. SNARF-1-AM (Fig. 18), is a ratiometric, pH-sensitive fluorophore, which is calibrated using λ1/λ2 fluorescence intensity ratio (640 nm- pH sensitive, intensity increases upon increases in pH (λ1); 600 nm -isosbestic point, pH insensitive, intensity independent of pH-λ2; Haugland, 1996).

The carboxylate groups of indicators for Ca^{2+} (e.g. Fura-2-AM; Fig. 19) and other cations and the phenolic hydroxyl groups of pH indicators (SNARF-1-AM) are derivatized as acetoxymethyl or acetate esters, respectively, rendering the indicator membrane permeable and non-fluorescent (Fig. 17B). Once inside the cell, these AM-derivatives are hydrolyzed by intracellular esterases, releasing the ion-sensitive, polyanionic fluorescent indicator. Potential problems with AM loading include the production of potentially toxic byproducts (formaldehyde and acetic acid) as well as compartmentalization in various intracellular organelles, since AM-derivatized probes may become compartmentalized in any membrane-bound structure within the cell (Haugland, 1996).

Cl^--sensitive fluorophores, unlike the fluorescent indicators described above, do not bind Cl^-. Instead, fluorescence is quenched by Cl^- in a non-radiative transfer of

Figure 18. SNARF-1 fluorescence. A. SNARF-1-AM, a pH_i sensitive fluorophore, was used to measure egg and embryo pH_i. SNARF-1 flurorescence is excited at 535 nm and emission detected at two wavelengths; 640 nm (pH_i sensitive) and 600 nm (pH_i insensitive). Ratiometric analysis (I_{640}/I_{600}) is calibrated to pH_i, where *I* represents intensity at the wavelength indicated by the subscript. B. *Adapted from Haugland, 1996.* Fluorescence emission spectrum for SNARF-1, excited at 534 nm. Fluorescence emission is maximal around 640 nm and increases with increased pH. The isosbestic point or emission wavelength independent of pH_i is 600 nm. This isosbestic emission wavelength is used in ratiometric imaging (Haugland, 1996). C. An example of a SNARF-1 calibration curve (example shown is from Sr^{2+} activated eggs; see text for details).

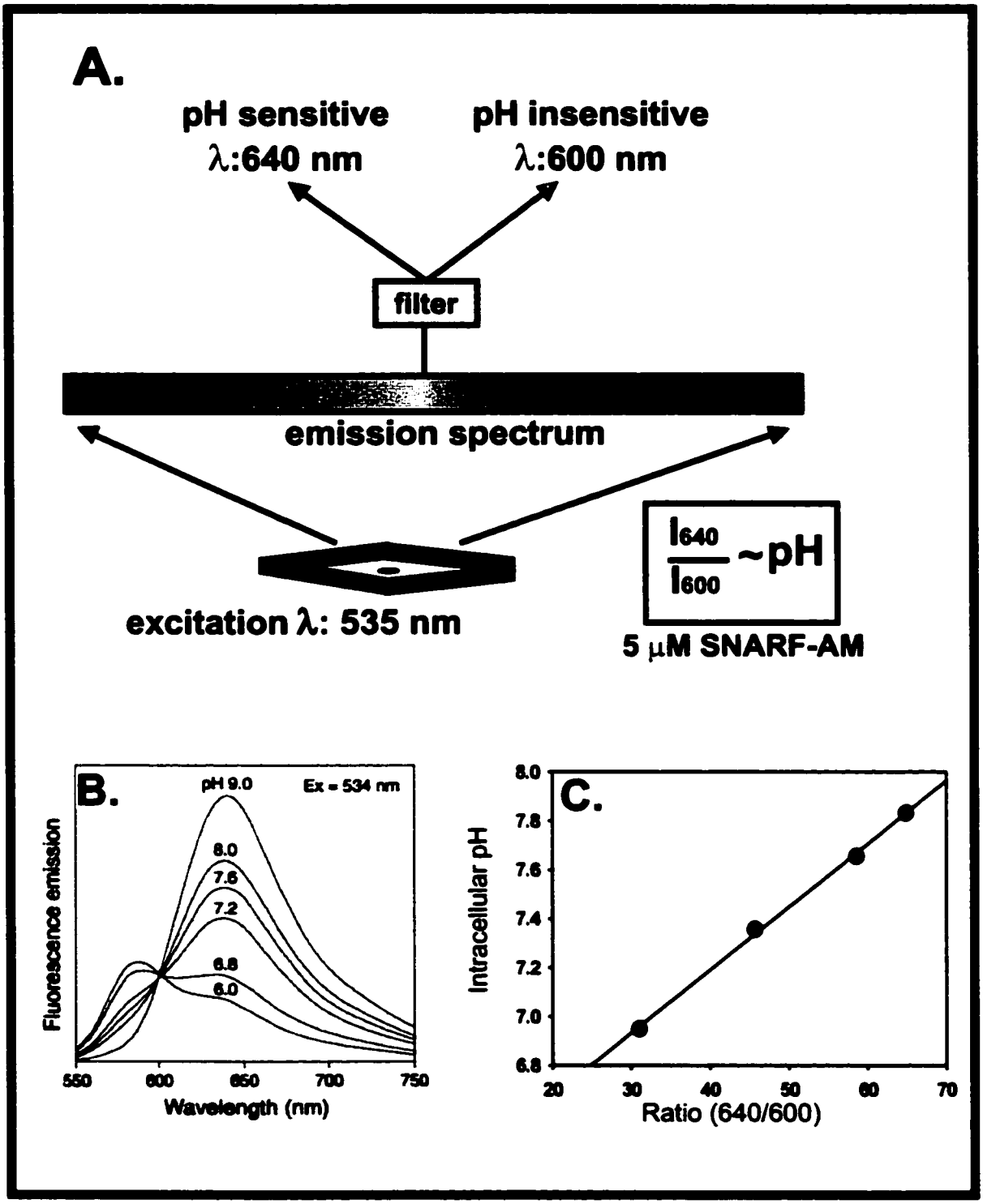
A.
pH sensitive
λ:640 nm
pH insensitive
λ:600 nm
filter
emission spectrum
excitation λ: 535 nm
I640/I600 ~pH
5 μM SNARF-AM
B.
pH 9.0
Ex = 534 nm
8.0
7.6
7.2
6.8
6.0
Fluorescence emission
550
600
650
700
750
Wavelength (nm)
C.
Intracellular pH
8.0
7.8
7.6
7.4
7.2
7.0
6.8
20
30
40
50
60
70
Ratio (640/600)

Figure 19. Fura-2 fluorescence. A. Fura-2-AM, a Ca^{2+}_i-sensitive fluorophore is used to measure Ca^{2+}_i in activated eggs. Fura-2 is excited at two wavelengths, with the corresponding emission intensities detected at 510 nm. The first excitation wavelength (350 nm) is Ca^{2+}_i-sensitive while the second wavelength (380 nm) is Ca^{2+}_i -insensitive. The ratio I_{350}/I_{380} is calibrated to Ca^{2+}_i. B. *Adapted from Haugland, 1996.* Fluorescence excitation spectrum for Fura-2, emission detected at 510 nm. Fluorescence intensity increases with increased Ca^{2+}_i concentration and is maximal at excitation 350 nm. The isosbestic point is approximately 360-370 nm, wherein Fura-2 fluorescence is independent of Ca^{2+}_i (Haugland, 1996).

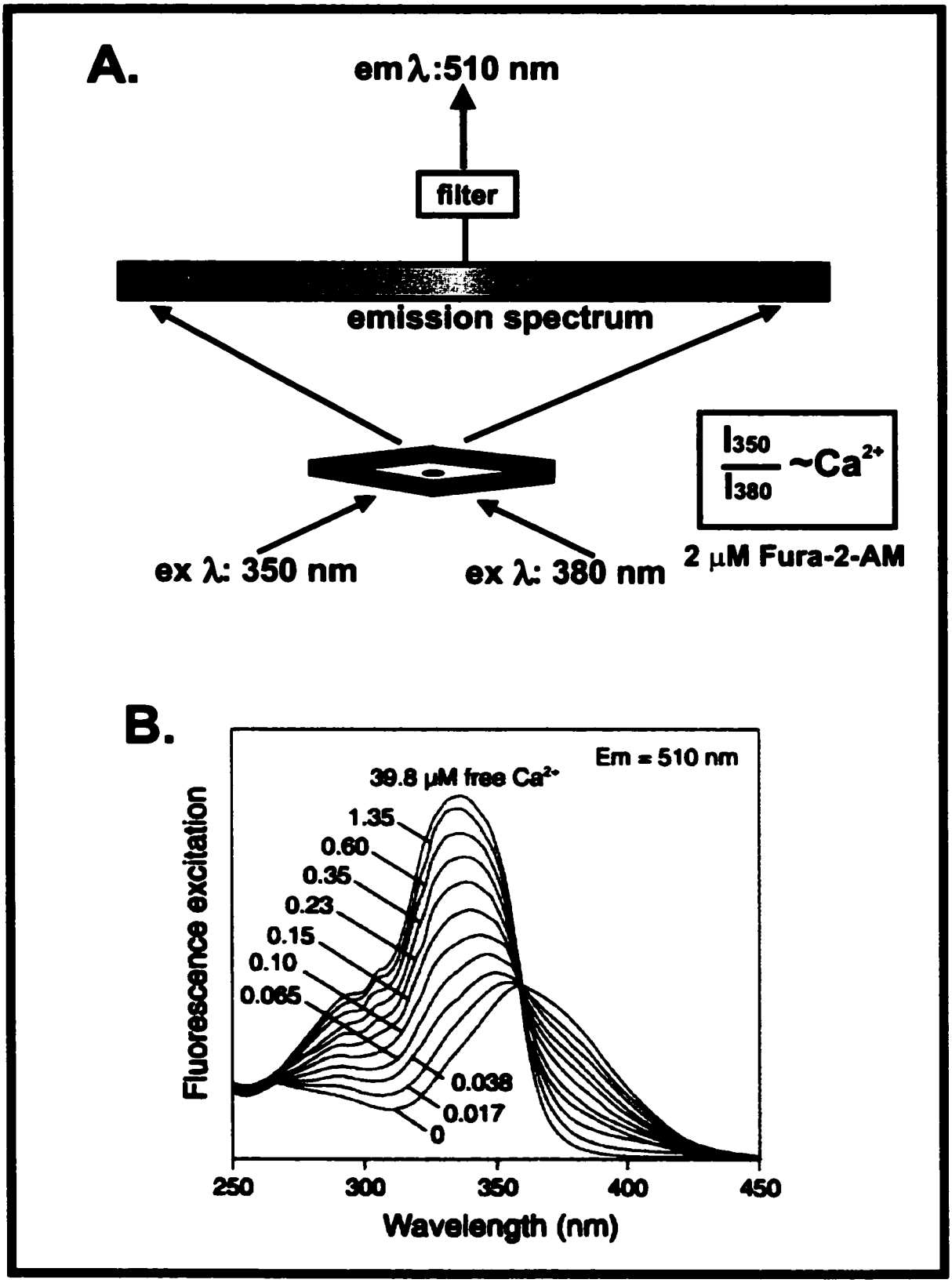
A.
emλ:510 nm
filter
emission spectrum
$\frac{I_{350}}{I_{380}} \sim Ca^{2+}$
2 μM Fura-2-AM
ex λ: 350 nm
ex λ: 380 nm
B.
Em = 510 nm
39.8 μM free Ca2+
1.35
0.60
0.35
0.23
0.15
0.10
0.065
0.038
0.017
0
Fluorescence excitation
250
300
350
400
450
Wavelength (nm)

energy between the fluorophore in its excited state and the Cl^- ion. Thus, as Cl^- concentration increases, fluorescence decreases and vice versa. Because these indicators, such as MQAE (Fig. 20), are Cl^--sensitive due to quenching, these indicators are not ratiometric and only exhibit a change in fluorescence intensity in the presence of Cl^- but no spectral shift. Cl^--sensitive indicators are not currently available in an AM form and thus higher loading concentrations are required as loading relies on diffusion across the plasma membrane of the relatively non-permeant fluorophore, or a process such as pinocytosis (Baltz and Phillips, 1999).

Loading eggs and embryos with intracellular fluorescent ion probes

A. SNARF-1: Eggs/embryos were transferred to Hepes-KSOM containing 5.0 μM SNARF-1-AM and incubated at 37°C for a period of 30 min (House, 1994; Zhao et al., 1995). SNARF-1-loaded eggs/embryos were washed with Hepes-KSOM. The excitation wavelength used for SNARF-1 was 565 nm with emission detected at two wavelengths- 640 nm and 600 nm, as described (Fig. 18).

B. Fura-2: Eggs or zygotes were transferred to Hepes-KSOM containing 2.0 μM Fura-2-AM and incubated at 37°C for a period of 30 min. Fura-2-loaded eggs or zygotes were then washed with Hepes-KSOM. Dual excitation wavelengths were used - 380 nm and 350 nm with emission detected at 510 nm (Fig. 19; Haugland, 1996; Séguin et al., 1997).

C. MQAE: Eggs or zygotes were transferred to Hepes-KSOM containing 20 mM MQAE

Figure 20. MQAE fluorescence. A. MQAE, a Cl^--sensitive fluorophore, is used to detect changes in Cl^-_i in eggs and zygotes. As MQAE is not available in AM form, much higher external concentrations are required for sufficient fluorophore loading, which is accomplished through passive diffusion of MQAE across the membrane. Fluorescence is excited at 365 nm and emission is detected at 460 nm. Fluorescence intensitity is inversely proportional to Cl^-_i, as MQAE is quenched by increasing Cl^-_i. B. *Adapted from Haugland, 1996.* Fluorescence emission spectrum for MQAE, excited at 350 nm. Fluorescence intensity decreases with increased Cl^-_i concentration with maximal emission detected at wavelength 450-460 nm (Haugland, 1996).

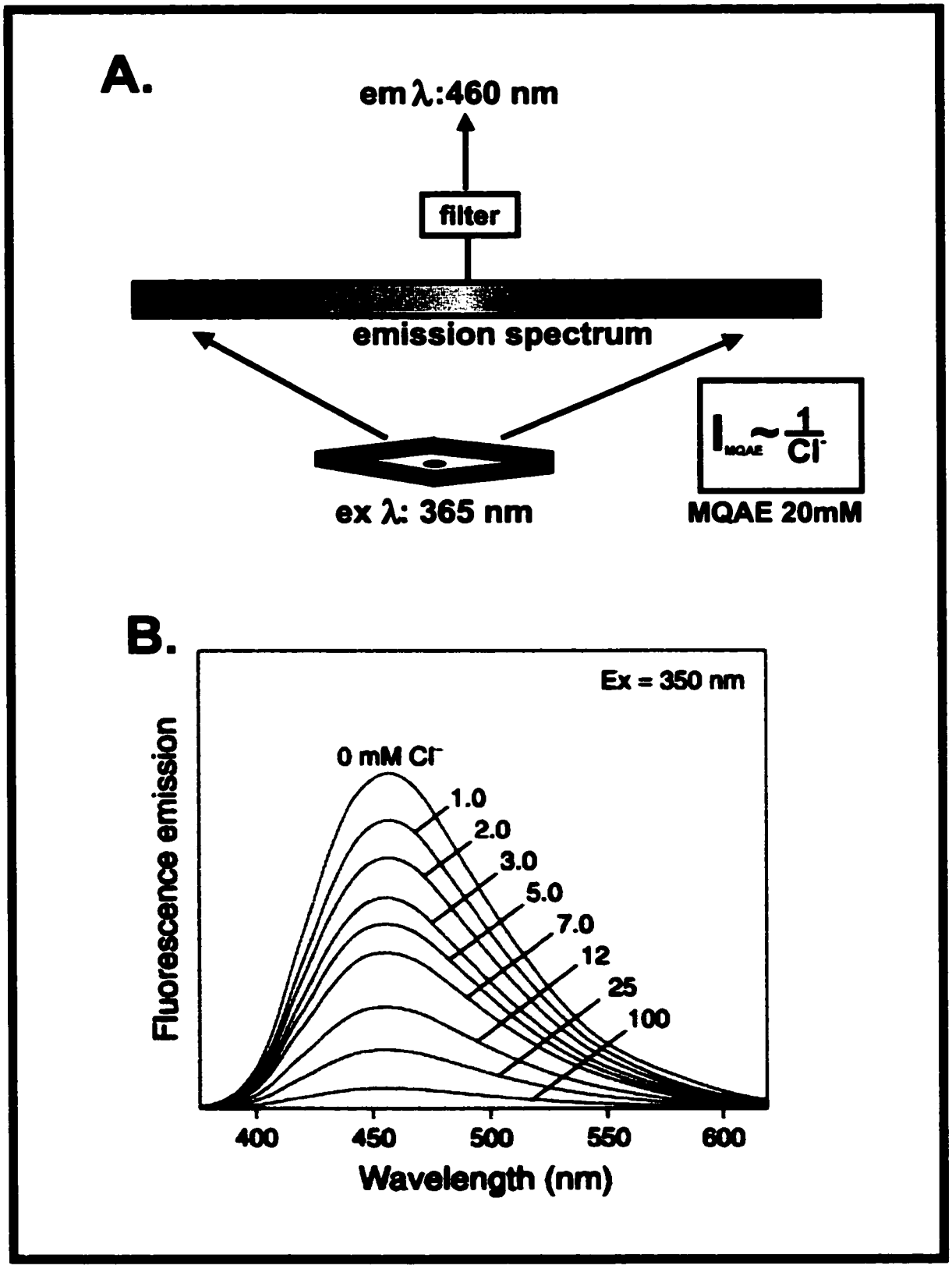
A.
em λ:460 nm
filter
emission spectrum
ex λ: 365 nm
$I_{MQAE} \sim \frac{1}{Cl^-}$
MQAE 20mM
B.
Ex = 350 nm
0 mM Cl⁻
1.0
2.0
3.0
5.0
7.0
12
25
100
Fluorescence emission
400
450
500
550
600
Wavelength (nm)

and incubated at 37°C for a period of 30 min (Haugland, 1996; Zhao et al., 1997). MQAE-loaded eggs or zygotes were washed with Hepes-KSOM. The excitation wavelength used for MQAE was 365 nm with emission detected at 460 nm (Fig. 20).

Intracellular pH, Ca^{2+} and Cl^- measurements

The methods used in pH_i measurements (Fig. 18) have been described in detail previously (Baltz et al., 1990; Zhao et al., 1995). Briefly, each experiment consisted of a group of 5-15 randomly chosen eggs/embryos with pH_i (or $Ca^{2+}{}_i$ or $Cl^-{}_i$ concentration) measured simultaneously. Eggs/embryos were maintained at 37°C (± 0.5°C) in a temperature-controlled chamber (Biophysica, Baltimore, MD) that was modified to allow solution changes and control of the atmosphere. Fluorescence was excited by a Xenon arc lamp (Litemore, USA) with excitation wavelengths specific for each fluorophore as described above. Fluoresence was detected using an intensified CCD (charge-coupled device) camera with output to an image storage and quantification system (Inovision, Durham, NC). Intensified CCD cameras are useful for fluorescent image detection as they are capable of detecting very low light levels and have a linear response to intensity. The advantage of quantitative fluorescent imaging (compared to other methods of fluorescence detection such as photomultiplier tube-based detectors) is that spatial information is retained, and a large number of cells (eggs/embryos) can be imaged at once, thereby increasing the speed of data collection. The disadvantages include increased costs and typically higher emission intensities required (and hence higher fluorophore concentrations and/or excitation intensities) needed for imaging (Baltz and Phillips, 1999).

Intracellular pH calibration (SNARF-1)

Emission ratio (I_{640}/I_{600}) was calibrated to pH using calibration solutions containing 10 μg/ml nigericin and 5 μg/ml valinomycin with 100 mM K^+. The presence of nigericin, a K^+/H^+ exchanger, results in the equilibration of both K^+ and H^+ across the cell membrane. Thus, when $[K^+]_i=[K^+]_o$ ("i" and "o" represent intracellular and extracellular, respectively) pH_i will have the same value of the external medium. To collapse the K^+ gradient, external solutions with high K^+ concentrations (100 mM) that approximate the intracellular K^+ concentration were used. The K^+-selective ionophore valinomycin was included to ensure the K^+ gradient was completely collapsed (Thomas et al., 1979; Baltz et al., 1990). Four different pH calibration solutions were used for each calibration (approximately 6.9, 7.3, 7.6, 7.9). pH_i was essentially linearly related to ratio in this range. Calibration curves were indistinguishable for GV oocytes, unfertilized eggs and zygotes (Fig. 18C).

Intracellular Ca^{2+} measurements (Fura-2)

For intracellular Ca^{2+} measurements, Fura-2-loaded eggs and zygotes were excited using dual excitation wavelengths of 380 nm and 350 nm with emission intensity measured at 510 nm (Fig. 19; Phillips and Baltz, 1999). Intracellular Ca^{2+} was calibrated according to the methods of Grynkiewicz et al. (1985). Basically, measurements of the fluorescent intensitites (I) and ratios (R) in the presence of fully-saturating levels of Ca^{2+} (R_{max}) and in nominally Ca^{2+}-free conditions (R_{min}) were obtained using Ca^{2+}-free KSOM (2 mM EGTA and 5 μM A23187) and saturated Ca^{2+} KSOM (100 μM Ca^{2+} and 5 μM

A23187). EGTA is a Ca^{2+} chelator while A23187 is a Ca^{2+} ionophore. The Ca^{2+} equilibrium binding equation formulated in terms of fluorescence is used to determine the concentration of Ca^{2+}_i such that $[Ca^{2+}_i] = K_d \beta (R-R_{min})/R_{max}-R)$ and $R = I_{350}/I_{380}$. K_d is the dissociation constant for Ca^{2+}. It is common practice to assume, rather than measure, a value for K_d. The K_d value for Fura-2 commonly used is 0.224 μM, which was determined at 37°C in a buffer solution and appears in the report of the original synthesis of Fura-2 (Grynkiewicz et al., 1985). β is the intensity in Ca^{2+}-free conditions divided by the intensity in saturating Ca^{2+}, both taken at the excitation wavelength which least excites the Ca^{2+} bound form (380 nm; Baltz and Phillips, 1999).

Intracellular Cl^- measurements (MQAE)

For intracellular Cl^- measurements, MQAE-loaded eggs and zygotes were excited at 365 nm and emission intensity measured at 460 nm (Fig. 20). Since Cl^- quenches MQAE fluorescence, emission intensity decreases with increasing Cl^- concentration (Verkman 1990). MQAE intensity was normalized to the average baseline intensity (points 2 through 7- total of 5 min). During measurements, eggs or zygotes were maintained at 37°C.

Steady-state pH_i measurements of eggs/embryos in culture

Once loaded with the dye, eggs/embryos were transferred to drops of KSOM under mineral oil in culture dishes (pre-equilibrated at 37°C, 5% CO_2) and maintained at 5% CO_2, 37°C for 30 min. Covered culture dishes were then removed from the

incubator and the pH_i measured immediately. For measurements in nominally HCO_3^--free Hepes-KSOM, SNARF-1-loaded eggs/embryos were transferred to pre-equilibrated (37°C/ air) drops of HCO_3^--free Hepes-KSOM under mineral oil for 30 min with pH_i measured immediately thereafter.

pH_i measurements during parthenogenetic activation with ethanol

To measure pH_i during parthenogenetic activation, eggs were placed in a temperature-controlled chamber in BSA-free, low lactate Hepes-KSOM. The solution was then changed to the experimental medium (i.e. KSOM or HCO_3^--free Hepes-KSOM) for 10-15 min to establish a baseline pH_i. The eggs were then activated by 7% ethanol in PBS for 5 min at room temperature, after which the chamber was flushed with the experimental medium (i.e. KSOM or HCO_3^--free Hepes-KSOM). Exposure to PBS alone, without ethanol, for 5 min at room temperature was used as a control.

Cl^- removal assay for HCO_3^-/Cl^- exchange activity

One method to detect HCO_3^-/Cl^- exchanger activity is to abruptly expose cells to a Cl^--free solution (Fig. 21A). The removal of external Cl^- causes the HCO_3^-/Cl^- exchanger to run in reverse as the Cl^- gradient is reversed and intracellular Cl^- exits the cell via the exchanger. This results in the influx of external HCO_3^- which increases pH_i. Thus, HCO_3^-/Cl^- exchanger activity is revealed as an intracellular alkalinization upon external Cl^- removal (Nord et al., 1988; Boyarski et al., 1988b).

HCO_3^-/Cl^- exchanger activity can also be detected by measuring changes in Cl^-_i upon Cl^- removal. Intracellular alkalinization upon Cl^- removal is accompanied by Cl^-

Figure 21. Assays for HCO_3^-/Cl^- exchanger activity. A. *Cl^- removal assay.* Depicted is the HCO_3^-/Cl^- exchanger (right) shown operating in reverse after external Cl^- has been removed with HCO_3^- influx coupled to Cl^- efflux, both of which are inhibited by anion exchange inhibitor DIDS. Using the Cl^- removal assay, HCO_3^-/Cl^- exchanger activity can be detected as an intracellular alkalinization (top left) which results from HCO_3^- influx, or as a decrease in intracelllular Cl^- (bottom left). B. *Recovery from intracellular alkalosis.* Intracellular alkalosis can be induced by exposure to a NH_4Cl-containing solution. Upon introduction of NH_4Cl, NH_3 (a weak base) rapidly enters the egg/embryo resulting in a very rapid intracellular alkalinization. This is followed by the slower entry of NH_4^+ (weak acid) which is characterized by slight recovery (acidification) of pH_i. A regulated recovery of pH_i back to approximately resting pH_i can be mediated by HCO_3^-/Cl^- exchanger activity. HCO_3^-/Cl^- exchanger (right) is depicted in its physiological orientation, corresponding to high external Cl^- resulting in Cl^- influx coupled to HCO_3^- efflux. The export of HCO_3^- lowers pH_i. Recovery from alkalosis via HCO_3^-/Cl^- exchanger should be Cl^--dependent and inhibitable by DIDS.

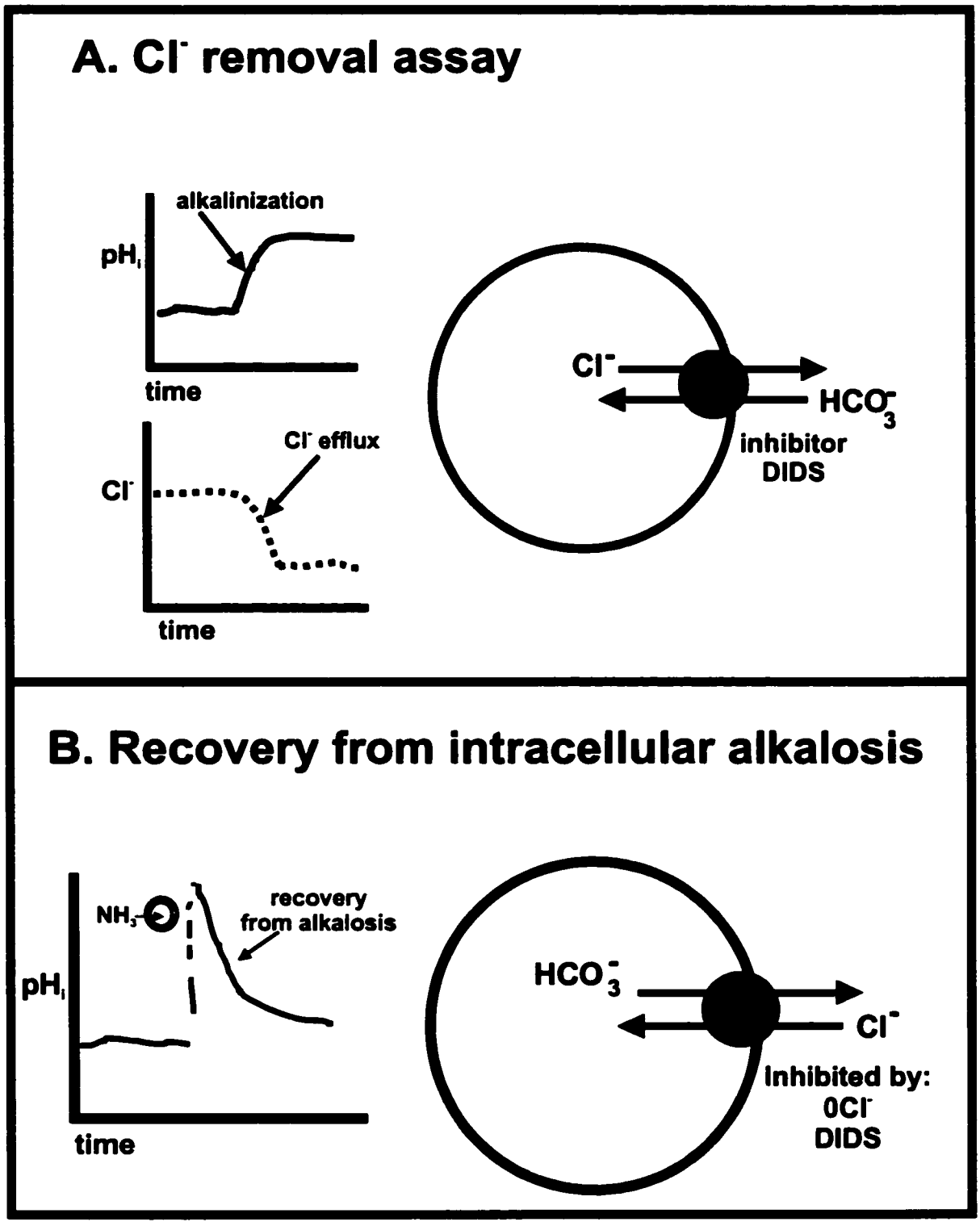
A. Cl- removal assay
alkalinization
pHi
time
Cl- efflux
Cl-
time
Cl-
HCO3-
inhibitor
DIDS
B. Recovery from intracellular alkalosis
NH3
recovery
from alkalosis
pHi
time
HCO3-
Cl-
Inhibited by:
0Cl-
DIDS

efflux. Cl^- efflux is mediated by several Cl^- pathways including Cl^- channels and the HCO_3^-/Cl^- exchanger. Thus, Cl^- efflux upon Cl^- removal can also be used as to reveal HCO_3^-/Cl^- exchanger activity, although results must be interpreted with caution because of the presence of other Cl^- pathways (Olsnes et al., 1986; Vigne et al., 1988).

The Cl^- removal assay was used to assess HCO_3^-/Cl^- exchanger activity in eggs and embryos. Once loaded with the appropriate fluorophore (SNARF-1 or MQAE), eggs/zygotes were placed in a temperature-controlled chamber in BSA-free, low lactate Hepes-KSOM. The solution was then changed to BSA-free, low lactate, KSOM for 10 min to establish a baseline. The solution was then changed to Cl^--free, low lactate KSOM for 20 min. The initial rate of intracellular alkalinization or change in MQAE intensity was determined using linear regression on the pH_i or MQAE intensity measurements obtained within the first 5 min following Cl^- removal (SigmaPlot, Jandel Scientific, San Rafael, CA).

To ensure that the brief period in Cl^- free medium was not detrimental to embryos, embryos were exposed to a mock Cl^- removal with embryos maintained in watchglasses in a volume of 1 ml. In vivo-produced zygotes (CF1 x BDF) were denuded of cumulus cells and incubated in KSOM for 12 min, followed by 20 min in $0Cl^-$ KSOM at CO_2/37°C. This was followed by standard culture in KSOM with development assessed.

Recovery from induced alkaline load

Another method to detect HCO_3^-/Cl^- exchanger activity involves the induction of intracellular alkalosis using a permeant weak base such as NH_3 (Fig. 21B). A recovery from the increase in pH_i back to steady-state pH_i can be mediated by HCO_3^-/Cl^- exchange.

The dependence of the recovery on HCO_3^-/Cl^- exchange can be revealed using an inhibitor such as DIDS or by the effect of the absence of external Cl^- on any recovery mediated by HCO_3^-/Cl^- exchange (Nord et al., 1988).

Once loaded with SNARF-1, eggs/zygotes were transferred to the chamber containing Hepes-KSOM. The solution was immediately changed to Cl^--free, low-lactate KSOM for 20 min to produce an initial intracellular alkalinization (see above). This was followed by 35 mM NH_4Cl, 12 mM HCO_3^- KSOM for 20 min to further alkalinize the eggs/embryos. This 'step-wise' approach to produce an intracellular alkalinization was important for two reasons. First, unloading the eggs/embryos of Cl^-_i upon Cl^- removal would maximize the inward gradient for Cl^-, and thus, maximize the rate of HCO_3^-/Cl^- exchanger activity upon exposure of NH_4Cl-KSOM. Secondly, exposure to NH_4Cl-KSOM alone did not always produce sufficient intracellular alkalinization which would have made detection of any HCO_3^-/Cl^- exchanger activity present difficult.

To determine whether recovery of pH_i from induced alkalosis was mediated by HCO_3^-/Cl^- exchanger activity, intracellular alkalosis was induced by NH_4Cl-KSOM containing 500 μM DIDS. Similarly, to determine whether the recovery from alkalosis was Cl^--dependent, intracellular alkalosis was induced by $0Cl^-$-NH_4^+-KSOM. Inhibition of recovery of pH_i following either condition would be consistent with the presence of HCO_3^-/Cl^- exchanger activity.

The rate of recovery was determined by fitting the recovery by non-linear regression (SigmaPlot) to a single exponential of the form $pH_i = be^{-at}+c$; where *a,b,c* are constants of the fit and *t* represents time from maximal alkalinization upon NH_4Cl-KSOM exposure. The first derivative $(dpH/dt) = pH_i' = -a(pH_i - c)$, was used to calculate the rate of

recovery as a function of pH_i. Calculated recovery rates which were negative were assumed to be zero.

Effect of changes in external pH

Zygotes, fertilized in vivo, were obtained 3-5 h post-fertilization ("am-zygotes") and cultured at either alkaline or acid external pH for 24 h to the 2-cell stage. External pH was varied by either changing the concentration of HCO_3^- in the media (at constant 5% CO_2) or by changing ambient CO_2 (at constant $[HCO_3^-]$=25 mM). External pH was determined under these different conditions (ie.changes to $[HCO_3^-]$ or % CO_2) using the Henderson-Hasselbach equation and confirmed using pH indicators. HCO_3^- concentration was varied to produce changes in external pH such that 10, 25 or 79 mM HCO_3^- at 5% CO_2 corresponded to pH 6.9, 7.3 and 7.8, respectively. Similarly, external pH was altered by changing the ambient CO_2 (ie. 2.5 or 12.5% CO_2 at 25 mM HCO_3^- corresponding to pH 7.6 and 6.9, respectively).

Detection of Ca^{2+}_i transients

A. Ca^{2+}_i transients in eggs fertilized in vitro

Ca^{2+}_i transients were measured in some groups of eggs immediately following sperm-egg incubation. For these, newly-fertilized eggs were loaded with Fura-2 as described above. Fura-2-loaded eggs were then loaded into a temperature controlled chamber and Ca^{2+}_i measured for 20-60 min in KSOM. Ca^{2+}_i was calibrated as described.

B. Suppression of Ca^{2+}_i transients by BAPTA-AM

Immediately following IVF, newly-fertilized eggs were cultured in KSOM in the presence of 20 μM BAPTA-AM (or DMSO vehicle) for 30 min. Eggs were washed free of BAPTA-AM and cultured for 7-9 h whereupon zygotes (with 2 pronuclei) were removed for assessment of HCO_3^-/Cl^- exchange using the Cl^- removal assay with SNARF-1. Similarly, in vitro fertilized eggs were incubated with BAPTA-AM (30 min) beginning 2.5, 4.5 or 6.5 h post-IVF, followed by culture and subsequent assessment of HCO_3^-/Cl^- exchange using the Cl^- removal assay 7-9 h post-IVF.

C. Ca^{2+}_i transients in Sr^{2+}-activated eggs

Unfertilized eggs, denuded of cumulus as described, were first loaded with Fura-2-AM and then transferred to a temperature-controlled chamber in Hepes-KSOM. Ca^{2+}_i measurements were obtained in Ca^{2+}-free modified KSOM containing 10 mM $SrCl_2$. For some experiments eggs were exposed briefly (5 min) to the Ca^{2+}-free, Sr^{2+} KSOM which was then replaced by low-lactate, BSA-free KSOM for an additional 25 min.

D. Ca^{2+}_i changes in cycloheximide-activated eggs

Unfertilized eggs, denuded of cumulus as described, were first loaded with Fura-2-AM and then transferred to a temperature-controlled chamber in Hepes-KSOM. Ca^{2+}_i measurements were obtained in low-lactate, BSA-free KSOM containing 50 μg/ml cycloheximide.

IV.RT-PCR

Isolation of mRNA and preparation of cDNA from eggs and zygotes.

For RNA isolation, eggs and zygotes were obtained as described above, and washed eight times through clean microdrops of Hepes-KSOM. The eggs/zygotes were placed in a ninth drop with micrococcal nuclease (0.006 μM units/ml; Sigma) for 15 min at 37°C, which eliminated false positive signals which otherwise arose from mRNA in the wash medium. Since micrococcal nuclease is Ca^{2+}-dependent, it was only active in this step, as subsequent steps were Ca^{2+}-free, and proteins were subsequently removed from the sample. Groups of 30, 10 or 5 eggs/zygotes were then placed into 300 μl of lysis buffer (0.5% SDS in TE buffer with 0.02 μg of *Escherichia coli* rRNA, Sigma). The samples were phenol-extracted (to remove proteins), and the nucleic acids in the aqueous phase were ethanol-precipitated, pelleted, washed with 70% ethanol, dried on a vacuum concentrator (Savant Speed-Vac #SC110), and resuspended in 6 μl DEPC-treated water containing 1 μl/100 μl RNase inhibitor. The mRNA from the eggs/zygotes was then reverse transcribed in 20 μl total volume using the Promega RT Kit with oligo (dT) primer.

Polymerase chain reaction (PCR) detection of anion exchanger mRNA in eggs and zygotes.

To detect cDNAs reverse transcribed from anion exchanger mRNAs in egg and zygotes, 30 cycles of PCR were performed. Primers were designed for AE2 (Oligo 4.1, National Biosciences, Plymouth, MN) and synthesized (Beckman Oligo 1000). Since

these primers were designed to span an intron in the AE2 gene, any contaminating DNA would yield a larger PCR product than mRNA. The source of the mouse anion exchanger cDNA sequences used for AE2 was Alper et al., 1988. The PCR primer sequences were (shown 5' to 3'): AE2 5': GTC AAA AAG GTT CGG ACC AT; AE2 3': TGC CTC TGG ACA GCA GCT AC. The Perkin Elmer Cetus PCR kit with *Taq* DNA polymerase was used with 1 μl egg/embryo cDNA (equivalent to 2.5 eggs/zygotes) in 20 μl total volume. The temperature cycle was 93°C (1 min), 55°C (1 min), and 72°C (3 min; or 13 min at end), controlled by a PTC-100 thermocycler (MJ Research, Watertown, MA). For increased specificity and increased sensitivity in detecting the small amounts of mRNA produced by a few eggs/zygotes, a "semi-nested" PCR protocol was used in which the products of the 30-cycle PCR were diluted 100-fold, and then a second, 20-cycle round of PCR was performed using the same 5' primer, and a 3' primer internal to the first one (AE2 3' internal: CAC TGG CTC TGC CTC ATT AG.). PCR products were visualized using ethidium bromide-stained agarose gels (4%). The predicted product size arising from AE2 mRNA for the semi-nested PCR (5', 3' internal pair) was 210 bp. This 210 bp PCR product has previously been shown, in mouse embryos from the 1-cell through blastocyst stages, to represent mouse AE2. Restriction digests of the PCR product using RSA1 yielded fragments of the exact sizes expected for mouse AE2 (146 and 64 bp) at each stage of embryo development assessed (1-cell, 2-cell, morula, blastocyst; Zhao et al., 1995). In addition, Southern blot analysis using an AE2-specific probe confirmed the identity of the 210 bp product as AE2 (S.L. Alper and J.M. Baltz, unpublished). Thus, the appearance of a 210 bp product is taken here to indicate the presence of AE2 mRNA.

V. PHARMACOLOGICAL MANIPULATIONS PRIOR TO DETECTION OF HCO_3^-/Cl^- EXCHANGER ACTIVITY

Disruption of protein synthesis, Golgi apparatus and cytoskeleton

Immediately following IVF, newly fertilized eggs were cultured in regular KSOM with either 50 μg/ml cycloheximide (inhibits protein synthesis; DeSousa et al., 1993), 5 μg/ml brefeldin A (disrupts Golgi apparatus; Fujiwara et al., 1998; Ivessa et al., 1995), 10 μM cytochalasin D (disrupts actin filaments; Schatten et al., 1989) or 0.1/1.0 μg/ml demecolcine (disrupts microtubules; Gordon et al., 1989; Schatten et al., 1989) for 7-9 h, whereupon zygotes with 2 pronuclei were removed from culture and assayed using the Cl^- removal assay (see above). In all cases the vehicle for the drug was used as a control (eg. control for brefeldin A was regular KSOM + 0.1% methanol).

Inhibition/activation of PKC and PKA

Immediately following IVF, newly fertilized eggs were cultured in regular KSOM with either 10 μM sphingosine (inhibits PKC; Hannun et al., 1986) or 5 μM H-89 (inhibits PKA; Rose-Hellekant and Bavister, 1996) for 7-9 h whereupon zygotes with 2 pronuclei were removed from culture and assayed using the Cl^- removal assay (see above). Sphingosine prevents compaction of 8-cell mouse embryos (Winkel et al., 1990) and thus, efficacy of sphingosine was confirmed here by culturing 6-8-cell mouse embryos with 10 μM sphingosine (vehicle control) and compaction assessed 8 h later.

Unfertilized eggs were cultured in 0.3 mM dbcAMP (stimulates PKA), 0.2 mM IBMX (inhibits phosphodiesterase (PDE), thereby preventing intracellular hydrolysis of

cAMP) and 0.1 mM forskolin (activates adenylate cyclase) for 3-6 h. The net effect of this combination (dbcAMP + IBMX + forskolin) would be to increase intra-oocyte cAMP and thus, upregulate cAMP-dependent pathways such as PKA activation (Schultz et al., 1983b). Following 3-6 h of dbcAMP/ IBMX/forskolin culture, eggs were assessed for HCO_3^-/Cl^- exchanger activity by the Cl^- removal assay. Control eggs were cultured with the vehicles for these agents (water, DMSO, DMSO) and otherwise treated similarly.

Unfertilized eggs were cultured in 100 nM PDD or PMA or 3-6 h. PDD and PMA, both phorbol esters, activate PKC in mouse embryos (Winkel et al., 1990; Ohsugi et al., 1993). Following PDD or PMA culture, eggs were assessed for HCO_3^-/Cl^- exchanger activity by the Cl^- removal assay. Control eggs were cultured with the vehicles for these agents (both DMSO) and otherwise treated similarly.

Metaphase arrest using demecolcine

Unfertilized eggs denuded of cumulus cells were pretreated for 1 h with 1 μg/ml demecolcine (depolymerizes microtubules, maintains metaphase arrest), activated, and continuously cultured with demecolcine. Eggs were either activated using Sr^{2+} (2 h) or were treated with the MEK inhibitor U0126 (8 h; see below). In both cases, pretreatment with demecolcine prevented pronuclear development.

To arrest embryos in the first mitotic metaphase, Sr^{2+}-activated eggs were cultured with demecolcine at 8 h post-activation for an additional 8 h. At this time, vehicle control embryos had undergone cleavage to the 2-cell stage, while demecolcine-

embryos remained at the 1-cell stage in metaphase.

Okadaic acid

Unfertilized eggs, denuded of cumulus cells, were exposed to 2.5 μM okadaic acid (OA), an inhibitor of protein phosphatases PP1A and PP2A, either prior to Sr^{2+} activation, coincident with activation, or at various times following activation. Treatment of fertilized eggs with OA prevents dephosphorylation of MAPK and prevent pronuclear formation (Moos et al., 1995). OA was introduced at t=-15 min, t=0 h, t=1.5 h and t=3 h following Sr^{2+} activation, and remained present thereafter.

In another protocol, Sr^{2+}-activated zygotes, 8 h post-activation, and 2-cell embryos, 24 h post-activation, were cultured with OA for an additional 8 h followed by HCO_3^-/Cl^- exchanger assay. The timing of pronuclear envelope formation/breakdown was determined where stated by visual inspection using a dissection microscope.

MAP kinase kinase (MEK-1 and MEK-2) inhibitor U0126

Unfertilized eggs, denuded of cumulus cells, were cultured with 5, 10 or 50 μM U0126, a specific inhibitor of MEK, for 8-9 h. U0126 is a noncompetive inhibitor of MEK1/2 (Favata et al., 1998) and prevents activation of downstream targets of MEK such as ERK1/2 and $p90^{RSK}$ in *Xenopus* oocytes (Gross et al., 2000). As U0126 was observed to parthenogenetically activate eggs (see Results), the time-course of second polar body emission, pronucleus formation and cleavage were determined. For some experiments, pretreatment with demecolcine followed by culture with both demecolcine

and U0126 (see above) was performed. Control eggs were cultured with U0126 vehicle DMSO and otherwise treated identically.

VI. CONFOCAL IMAGING

To confirm disruption of cytoskeleton, am-zygotes were collected 15-17 h post-hCG and cultured with either 10 μM cytochalasin D or 1.0 μg/ml demecolcine for 2 h at 37°C, 5% CO_2. In each case, paired controls were cultured simultaneously with vehicle as described above. Following culture, zygotes were fixed and stained using the following protocols. *F-actin:* Zygotes were fixed in 3.7% formaldehyde, extracted in 0.2% Triton X-100 (all in PBS) and stained in 6.6 μM rhodamine phalloidin in PBS + 5 mg/ml BSA at 37°C for 30 min. Control zygotes were exposed to the vehicle for rhodamine phalloidin (DMSO) and were otherwise treated similarly. *Microtubules:* Zygotes were denuded of zona pellucidae using 0.75 mg/ml pronase in Hepes-KSOM for 10 min at 37°C, followed by formaldehyde fix and Triton extraction as described. Fixed zygotes were immunolabelled with primary antibody 5A6, anti-mouse-α-tubulin (courtesy of Dr. Dave Brown, University of Ottawa, Ottawa, ON), diluted 1/1000 in PBS + 5 mg/ml BSA. Zygotes were incubated with primary antibody for 45 min at 37°C, washed in PBS and immunolabelled with secondary antibody Cy3™-conjugated affinity purified goat anti-mouse IgG (Jackson ImmunoResearch Laboratories, Inc). Zygotes were incubated with the secondary antibody, diluted 1/100 in PBS + 5 mg/ml BSA, for 45 min at 37°C. Following fixing and staining, zygotes were mounted in PBS:glycerol (1:1) and examined using the confocal microscope within 24 h. For the negative control the

primary antibody was omitted and zygotes were labelled with secondary antibody only.

Confocal images were collected using an Olympus 1X70 inverted microscope (PlanApo oil immersion lens 60x; NA 1.4) equipped with a BioRad MRC-1024 confocal laser scanning unit. The fluorescent excitation was produced by a Krypton-Argon laser. For rhodamine phalloidin and Cy3 fluorescence, the excitation used was 488 + 568 nm with emission at 585 nm. 1-3 μm sections (z-series) were collected for representative zygotes with equatorial sections compared between control and treatment groups.

VII. STATISTICS

For pH_i, $Ca^{2+}{}_i$ and MQAE intensity measurements, each experimental replicate consisted of a pool of 5-15 eggs/embryos. Raw ratio values were averaged and appropriate calibrations performed on these averaged ratio values. For these protocols the mean of the experimental replicates were compared between treatment groups. Standard error of the mean (s.e.m.) was used to represent variation within this pool of experimental replicates.

To determine whether three or more treatment groups were statistically different, ANOVA (analysis of variance) was performed. Bartlett's test for homogeneity of variance was first used to determine whether variances within each treatment group were significantly different from variances within other treatment groups. A parametric ANOVA was then performed unless a significant difference in variance between different treatment groups was found, in which case a non-parametric ANOVA (nANOVA) was performed. If treatment groups were significantly different by the appropriate ANOVA,

post-hoc tests were performed to compare treatment groups. Tukey-Kramer's Multiple Comparisons Test was used for parametric data and Dunn's test was used for non-parametric data.

For two groups of data, an F-test was performed to test for equality of variances prior to selecting a t-test for analysis. Statistical comparisons of two groups of data were made using Student's t-test or Welch's alternate t-test for equal or unequal variances, respectively.

For experiments designed to assess viability or development (ie. embryo culture), development was expressed as a proportion of the total number of embryos cultured in each experimental replicate. Developmental frequencies were expressed as the average proportion for each experimental replicate. For experiments with only two variables (e.g. treatment vs. outcome) statistically significance was calculated using Chi-Square test or Fisher's Exact Test. For experiments with several variables (treatment vs. outcome 1 vs. outcome 2....vs. outcome "n") individual proportions from each experimental replicate were arcsin transformed and analyzed using ANOVA as described above.

Linear regression was used to determine the initial rate of alkalinization upon Cl^- removal and to determine the rate of pH_i change when recovery from acidosis was inhibited. Non-linear regression, using the appropriate exponential curves as specified, was used to determine the rates of recovery from alkalosis and acidosis.

In all cases, $p<0.05$ was considered significant. Descriptive statistics were obtained using SigmaPlot (Jandel Scientific, San Rafael, CA). Throughout, "n" indicates the total number of eggs or embryos. Statistical comparisons were done using InStat (GraphPad Instat, San Diego, CA).

VIII. EGG/EMBRYO IMAGES

GV oocytes, obtained as described, were cultured in 50 μg/ml cycloheximide for 18 h to produce MI-arrested oocytes. Some GV oocytes were cultured in standard KSOM culture for 18 h to produce MII eggs. Ovulated eggs were activated, as described, with 7% ethanol, 50 μg/ml cycloheximide, 10 mM Sr^{2+} or 50 μM U0126 and cultured for 9-10 h. Eggs were fertilized in vitro (CF1 x CD1), as described and cultured for 4 h. 1-cell embryos (CF1 x BDF) were cultured for up to 120 h to produce 4-cell, 8-cell, morula and blastocyst embryos. Eggs and embryos were washed in PBS (4°C) followed by 30 min incubation in 3% paraformaldehyde-PBS on ice. Eggs and embryos were then washed in cold PBS and mounted on slides. Images were obtained using a Zeiss AxioPhot microscope with Phase-contrast optics and Northern Eclipse (Empix Imaging Inc.; Mississauga, ON) image analysis software. Egg and embryo images were obtained using 40x Nikon PlanApo objective. Cumulus mass image was obtained using a 20x Plan objective.

RESULTS

I. FLUOROPHORES

Assessment of intracellular fluorophore sequestration

To show that the majority of the SNARF-1 was localized to the cytoplasm, SNARF-1-loaded oocytes and zygotes were exposed to 20 μM digitonin, which acts specifically to permeabilize the plasma membrane (House, 1994). SNARF-1-loaded oocytes and zygotes were loaded in the chamber in BSA-free Hepes-KSOM and baseline fluorescence intensity was monitored for 10 min followed by digitonin exposure. The mean residual intensity remaining after digitonin exposure was (expressed as percentage of intensity before digitonin addition), GV oocytes: 5% (range: 1-9%; n=10), eggs: 6% (range: 3-15%; n=21) and zygotes: 4% (range: 3-5%; n=13), thereby indicating that the great majority (around 95%) of SNARF-1 is not sequestered nor compartmentalized in mouse GV oocytes, eggs or zygotes.

Effect of fluorophores on oocyte viability

To determine whether the fluorescent probes used here (SNARF-1, MQAE and Fura-2) were cytotoxic, IVF was performed on fluorophore-loaded eggs and the effects of fluorophore-loading and illumination excitation on fertilization and cleavage rates assessed 24 h post-IVF. IVF of SNARF-1-loaded eggs was used to determine the effect of AM hydrolysis alone on cleavage rates. Control eggs were subjected to mock-loading (incubation in Hepes-KSOM for 30 min) and otherwise treated identically to fluorophore-loaded eggs. There was no significant difference between the rate of cleavage to the 2-

cell stage in SNARF-1-loaded eggs (69% of SNARF-1-loaded eggs) versus control eggs (67%; p=0.93, Chi-square test).

To determine whether fluorophore-loading in combination with excitation illumination was detrimental to egg and embryo viability, eggs were loaded with each of the two AM fluorophores used here - SNARF-1 and Fura-2 - and exposed to appropriate excitation illumination followed by IVF. There was no significant difference between the rates of cleavage to the 2-cell stage in eggs loaded with these AM fluorophores versus their respective controls (SNARF-1-loaded eggs: 63%, n=35, N=3; SNARF-1 control: 78%, n=32, N=3, p=0.19; Fura-2-loaded eggs: 43%, n=54, N=5; Fura-2 control 56%, n=45, N=5, p=0.23; Fisher's Exact Test). Thus, exposure to fluorophore and excitation illumination used to measure pH_i and $Ca^{2+}{}_i$ was not inherently toxic, but permitted IVF and continued development to at least the 2-cell stage.

To determine whether MQAE was cytotoxic, eggs were loaded with MQAE and exposed to an excitation wavelength of 365 nm. Following light exposure, MQAE-loaded eggs and controls were immediately used for IVF and assessed 24 h post-IVF. 15% MQAE-loaded eggs cleaved to the 2-cell stage which was significantly different from control eggs (60%; p<0.0001; Fisher's Exact Test). MQAE, without excitation illumination, significantly decreased pronuclear development at 6-8 h post-IVF (6%); control (64%; p<0.0001; Fisher's Exact Test). However, by 24 h post-IVF, 62% of embryos had developed to the 2 pronuclei stage, demonstrating that most MQAE-loaded eggs had been fertilized in vitro, although at a significantly lower rate compared to control (83%; p=0.017; Fisher's Exact Test). Cleavage of these fertilized eggs was also significantly reduced, as only 17% MQAE-loaded eggs cleaved to the 2-cell stage,

compared to control (62%; $p<0.0001$; Fisher's Exact Test).

MQAE has been used successfully to study specific Cl^- transport during blastocoel formation in mouse blastocysts. Blastocysts expand normally in medium containing 20 mM MQAE, indicating low toxicity over the 4-6 h of incubation (Zhao et al., 1997).

The observation that MQAE slowed pronuclear development and inhibited cleavage indicated toxic effects. However, the ability of MQAE-loaded eggs to be fertilized (pronuclei developed, although slowly) and MQAE-loaded blastocysts to expand normally indicated that short-term experiments are possible. Thus, only a limited set of short-term experiments were performed with MQAE. For further details on fluorophore toxicity in eggs and embryos, see Phillips et al., 1998; Baltz and Phillips, 1999.

II. pH_i CHANGES AT EGG ACTIVATION

No pH_i change accompanies parthenogenetic activation

To determine whether a change in pH_i accompanies egg activation, pH_i was measured during parthenogenetic activation by ethanol (Fig. 14A) in SNARF-1 loaded eggs. The rate of parthenogenetic activation using ethanol was first determined in culture. Egg activation following ethanol treatment was 64% (n=250, N=11) which was significantly higher than control eggs exposed to PBS without ethanol (9% activation; n=219, N=11; $p<0.05$; Chi-Square test). As pH_i measurements of ethanol-activated eggs necessitated fluorophore loading prior to ethanol exposure, egg activation was also

assessed in SNARF-1-loaded eggs. In SNARF-1-loaded eggs, ethanol activation was reduced to 45% (n=269, N=14; compared to 64% in eggs without SNARF-1, above) which was significantly higher than control SNARF-1-loaded eggs, exposed to PBS without ethanol (9%, n=215, N=14; $p<0.05$; Chi-Square test). Thus, about half the eggs exposed to ethanol during pH_i measurements would have been activated.

A representative example of pH_i measurements obtained during the course of parthenogenetic activation by ethanol is shown in Figure 22A. Clearly, no change in pH_i is evident in this example following activation. To analyze the data quantitatively, pH_i measurements just prior to ethanol/PBS exposure (baseline measurements in HCO_3^-/CO_2-buffered medium at 37°C, 5% CO_2) were subtracted from pH_i measurements 13 min post-incubation (ΔpH_i; again in HCO_3^-/CO_2-buffered medium at 37°C, 5% CO_2). The mean (± s.e.m.) ΔpH_i resulting from ethanol exposure was 0.06 ± 0.01 (n=85, N=7), while the mean ΔpH_i following exposure to PBS, alone (no ethanol), was identical: 0.06 ± 0.01 (n=71, N=6). Therefore, there was no significant difference between the ΔpH_i resulting from ethanol activation and control exposure to PBS alone (p=0.76, Student's t-test). Because only about half of SNARF-1-loaded eggs were fully activated by ethanol (i.e. developed pronuclei, see above), eggs were analyzed individually for changes in pH_i following ethanol exposure. No pH_i change occurred in individual eggs within an experimental replicate following ethanol exposure (data not shown), which was similar to the analysis for pooled eggs within an experimental replicate described above.

pH_i varies little among GV oocytes, unfertilized eggs, and zygotes

pH_i of GV oocytes, eggs, and zygotes was compared using ratiometric image

Figure 22. No change in pH_i accompanies egg activation in the mouse. *Adapted from Phillips and Baltz, 1996.* A. Example of pH_i during parthenogenetic activation in HCO_3^- /CO_2-buffered medium (37°C, 5% CO_2; ethanol: n=11; PBS: n=12). The mean pH_i (± SD) of SNARF-1-loaded eggs was measured in a HCO_3^-/CO_2-buffered KSOM to establish a baseline pH_i, followed by a PBS solution (± 7% ethanol) for 5 min for parthenogenetic activation, or control PBS exposure (——) followed by KSOM. No pH_i change due to ethanol activation was observed. B. Resting pH_i of GV oocytes, eggs and zygotes measured in CO_2/HCO_3^- buffered KSOM in microdrop cultures. Mean pH_i was 6.96 ± 0.004 (± SEM) for GV- oocytes, 7.00 ± 0.01 for unfertilized eggs, and 7.02 ± 0.01 for zygotes. C. Example of pH_i during parthenogenetic activation in nominally HCO_3^--free, Hepes-KSOM (ethanol: n=8, PBS: n=6). pH_i measurements (± SD) of SNARF-1-loaded eggs were obtained in HCO_3^- -free, Hepes-KSOM to establish a baseline pH_i followed by PBS solution (± 7% ethanol) for 5 min (——) followed by Hepes-KSOM. No pH_i change due to ethanol activation was observed. D. Resting pH_i measurements of GV oocytes, eggs and fertilized zygotes measured in nominally HCO_3^- -free, Hepes-KSOM. Mean pH_i in the nominal absence of HCO_3^- was 7.18 ± 0.01 (±s.e.m.) for GV oocytes, 7.18 ± 0.10 for unfertilized eggs and 7.10 ± 0.10 for zygotes. ***n[M](N)*** where ***n*** represents the total number of eggs/zygotes, ***M*** represents number of dishes and ***N*** represents the number of experiments. Groups designated with different letters were statistically significant, Fisher's Exact Chi-square; $p<0.05$.

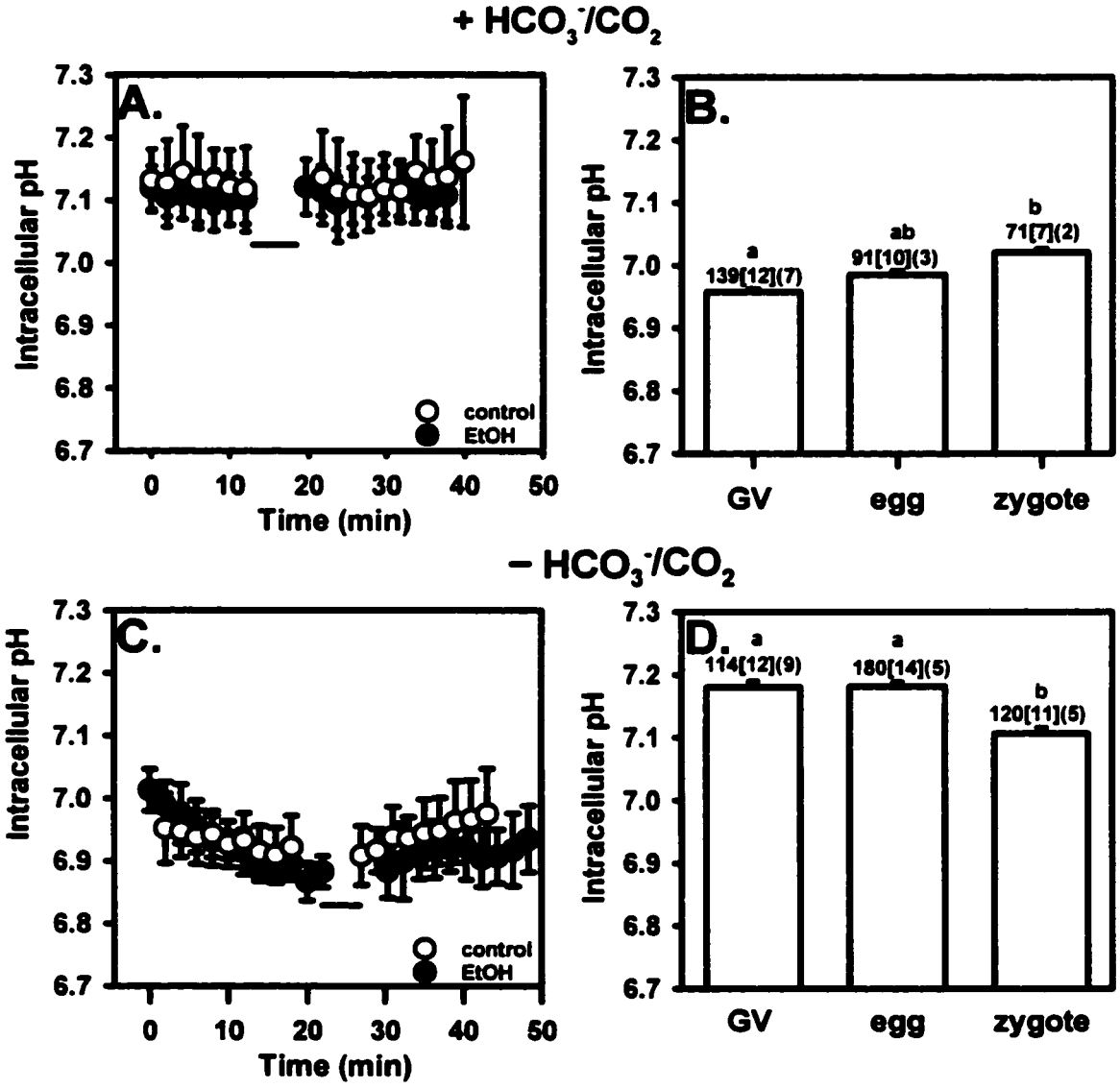
+ HCO3-/CO2
A.
B.
Intracellular pH
7.3
7.2
7.1
7.0
6.9
6.8
6.7
control
EtOH
0
10
20
30
40
50
Time (min)
a
139[12](7)
ab
91[10](3)
b
71[7](2)
GV
egg
zygote
- HCO3-/CO2
C.
D.
a
114[12](9)
a
180[14](5)
b
120[11](5)

analysis of SNARF-1 loaded eggs/zygotes in microdrop cultures under essentially identical conditions (Fig. 22B). The mean pH_i was 6.96 ± 0.004 (± s.e.m.) in GV oocytes (n=139, M=12, N=7), 7.00 ± 0.01 in unfertilized eggs (n=71, M=7, N=2) and 7.02 ± 0.01 in zygotes (n=91, M=10, N=2). There were no significant differences between GV oocytes and eggs nor between eggs and zygotes ($p>0.05$). However, there was a significant difference between GV oocytes and zygotes (ANOVA, Tukey's Multiple Comparisons Test; $p<0.05$). Because pH_i measurements of GV oocytes were made in the presence of dbcAMP, we confirmed that dbcAMP, per se, had no effect on pH_i: removing external dbcAMP caused no change in pH_i (data not shown).

No pH_i change accompanies parthenogenetic activation in HCO_3^--free medium

pH_i during parthenogenetic activation by ethanol was also measured in HCO_3^--free Hepes-KSOM (Fig. 22C). The mean Δ pH_i (± s.e.m.) resulting from exposure to ethanol was 0.10 ± 0.01 (n=47, N=4), as was the mean Δ pH_i following PBS exposure: 0.10 ± 0.02 (n=58, N=4), and thus, there was no significant difference in Δ pH_i between ethanol and PBS exposure (p=0.92, Student's t-test).

pH_i varies little among GV oocytes, unfertilized eggs, and zygotes in HCO_3^--free medium

pH_i of oocytes and zygotes was measured in HCO_3^- -free microdrop cultures (Fig. 22D). This might reveal an activation of any Na^+/H^+ antiporter present in the egg, even if such an increase was normally masked by an opposing increase in HCO_3^-/Cl^- exchanger activity in the presence of HCO_3^- (Ganz et al., 1989). The mean pH_i (± s.e.m.) in the absence of added HCO_3^- or CO_2 was 7.18 ± 0.01 for GV oocytes (n=114, M=12, N=9),

7.18 ± 0.10 for eggs, (n=180, M=14, N=5) and 7.10 ± 0.10 for zygotes (n=120, M=11, N=5). There was no change after GVBD; the mean pH_i of GV oocytes and eggs was identical. The decrease (0.08) between the mean pH_i of eggs and zygotes was statistically significant ($p<0.001$; ANOVA, Tukey's Multiple Comparisons Test).

Summary of initial studies on oocyte pH_i during mammalian fertilization

These initial measurements of oocyte pH_i following fertilization showed that mouse fertilization is not accompanied by a sustained change in pH_i. Measurement of oocyte pH_i during ethanol activation similarly showed that egg activation is not accompanied by transient changes in pH_i. Moreover, the elimination of HCO_3^-/CO_2 in the external medium revealed only a small change in oocyte pH_i at fertilization (0.08 pH units). Thus, mouse fertilization is not accompanied by changes in pH_i, although this does not preclude an upregulation in opposing pH_i regulatory transporters (ie. Na^+/H^+ antiporter and HCO_3^-/Cl^- exchanger), such that no net change in pH_i occurs. HCO_3^-/Cl^- exchanger activity was subsequently measured in mouse eggs to determine whether exchanger activity was upregulated at fertilization.

III. HCO_3^-/Cl^- EXCHANGER ACTIVITY IN UNFERTILIZED EGGS

Effect of external Cl^- removal on pH_i and Cl^-_i in unfertilized eggs and zygotes

HCO_3^-/Cl^- exchanger activity can be detected as an intracellular alkalinization upon removal of external Cl^- (Fig. 21A). Cl^- removal reverses the direction of the HCO_3^-/Cl^- exchanger, if present, which causes an intracellular alkalinization. To confirm that short-term external Cl^- removal (30 min) was not detrimental to embryos, 1-cell embryos

were subjected to external Cl^- removal followed by Cl^- replacement (KSOM) and embryo culture. Following short-term external Cl^- removal, 100% of embryos cleaved to 2-cells within 24 h, with 74% development to morula by 72 h post-hCG, though blastocyst development was low (22%) at 96 h post-hCG (n=38; N=3). Thus, the Cl^- removal protocol used here was not detrimental to embryos for the short-term experiments described herein.

The rates of intracellular alkalinization upon Cl^- removal were measured in unfertilized eggs and zygotes (Fig. 23). The mean initial rate of intracellular alkalinization was about 4-fold lower in eggs (0.013 ± 0.003) than in zygotes 8-12 h post-fertilization (0.052 ± 0.004; $p<0.001$; ANOVA; Tukey-Kramer Multiple Comparisons Test). Furthermore, the maximal pH_i reached after Cl^- removal was generally higher in zygotes (Fig. 23C) than in eggs (Fig. 23B).

HCO_3^-/Cl^- exchanger activity can be inhibited by DIDS. DIDS (500 μM) had no significant effect on the rate of intracellular alkalinization in eggs (0.006 ± 0.002 vs. 0.013 without DIDS; $p>0.05$), but in contrast there was a significant reduction in the alkalinization rate in zygotes in the presence of DIDS (0.001 ± 0.001 vs. 0.052 without DIDS; $p<0.001$; ANOVA, Tukey-Kramer Multiple Comparisons Test among eggs, zygotes (± DIDS) and am-zygotes, see below).

The reversal of HCO_3^-/Cl^- exchanger activity upon Cl^- removal (Fig. 21A) is also accompanied by Cl^- efflux. Cl^- efflux was estimated by the increase in MQAE intensity upon external Cl^- removal (Fig. 24). The mean (± s.e.m.) rate of increase in MQAE intensity upon Cl^- removal was significantly lower in eggs (0.032 ± 0.004 U/min) than

Figure 23. HCO_3^-/Cl^- exchanger activity measured by intracellular alkalinization in eggs and zygotes upon Cl^- removal. *Adapted from Phillips and Baltz, 1999.* A. Initial rates of intracellular alkalinization (mean ± s.e.m.) after external Cl^- removal in eggs and zygotes (8-12 h post-fertilization) in the absence or presence of 500 μM DIDS. Numbers above bars: *n(N)* where *n* represents the total number of eggs/zygotes and *N* represents the number of experiments. B, C. Representative traces of pH_i vs time during removal of external Cl^- (110 mM to 0 mM) for eggs (B) and zygotes (C) in the presence (●) or absence of DIDS (○).

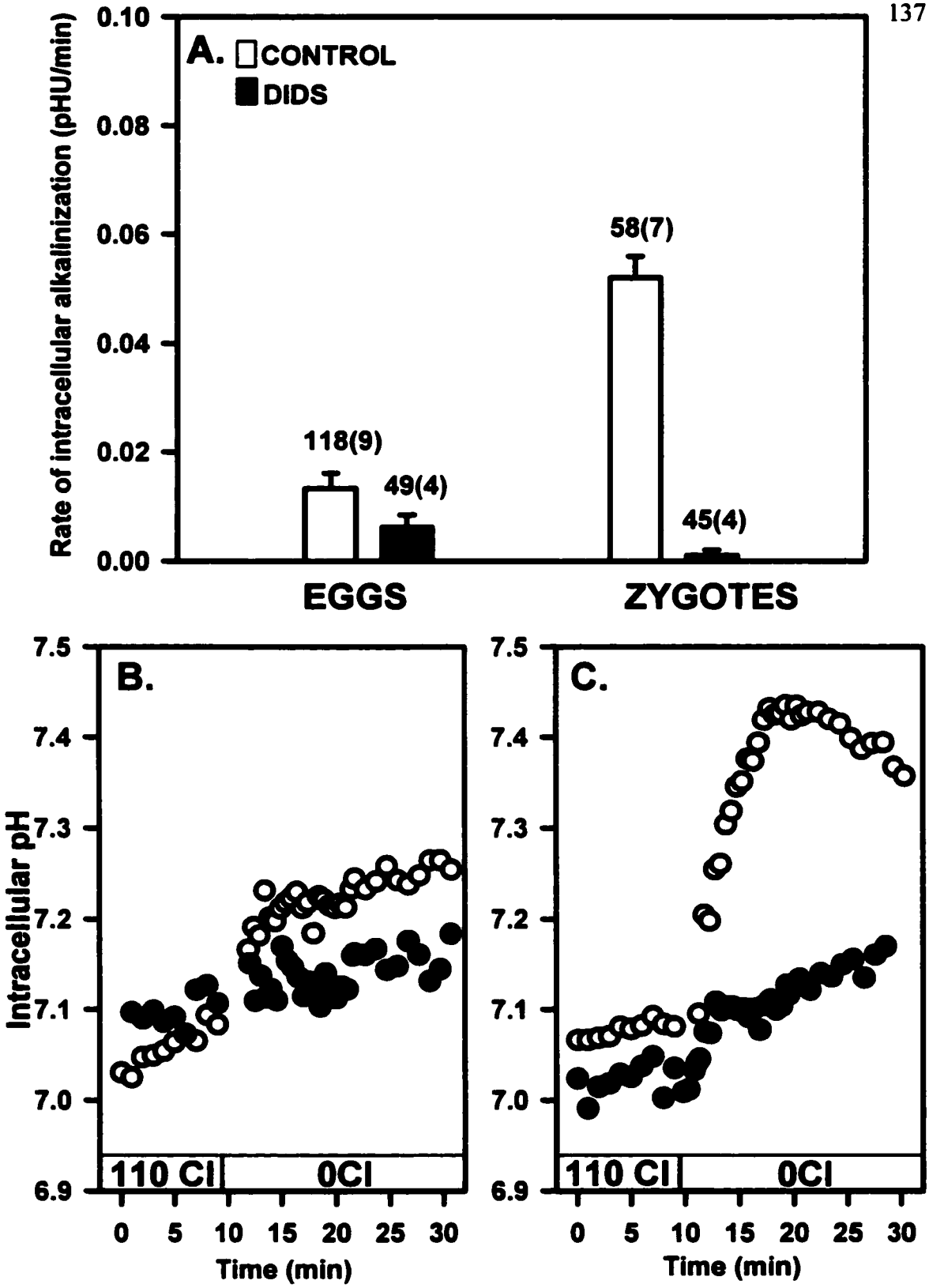
A.
CONTROL
DIDS
Rate of intracellular alkalinization (pHU/min)
0.10
0.08
0.06
0.04
0.02
0.00
118(9)
49(4)
58(7)
45(4)
EGGS
ZYGOTES
B.
C.
Intracellular pH
7.5
7.4
7.3
7.2
7.1
7.0
6.9
110 Cl
0Cl
0
5
10
15
20
25
30
Time (min)

Figure 24. Cl^- efflux upon external Cl^- removal measured by changes in MQAE intensity. *Adapted from Phillips and Baltz, 1999.* Shown is the mean initial rate of change of MQAE intensity upon Cl^- removal (± s.e.m.; open bars) which was significantly lower in unfertilized eggs than zygotes 8-12 h post-fertilization (*: $p<0.05$). 20 μM H_2DIDS (solid bars) greatly reduced the rate of increase in MQAE intensity in both eggs and zygotes. Representative traces of MQAE intensity in eggs (○) and zygotes (●) vs time during Cl^- removal (at 12 min) are shown in the inset. Numbers above bars as in Fig. 23.

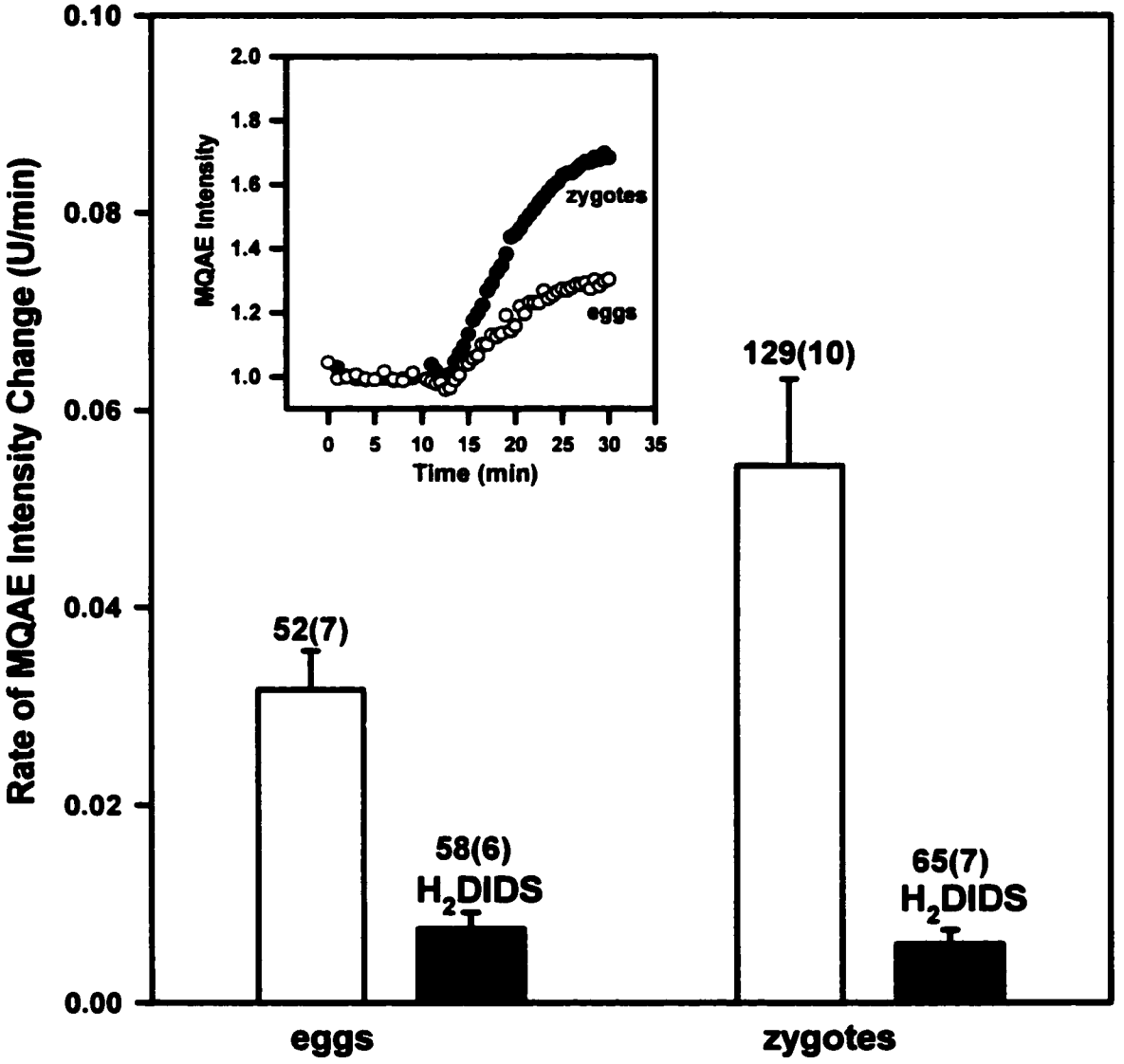
Rate of MQAE Intensity Change (U/min)
0.10
0.08
0.06
0.04
0.02
0.00
MQAE Intensity
2.0
1.8
1.6
1.4
1.2
1.0
zygotes
eggs
0 5 10 15 20 25 30 35
Time (min)
52(7)
58(6)
H2DIDS
129(10)
65(7)
H2DIDS
eggs
zygotes

zygotes (0.054 ± 0.009 U/min; p=0.037; Welch's t-test). The increase in MQAE intensity during Cl^- removal was almost completely inhibited by 20 μM H_2DIDS in both eggs (0.008 ± 0.002 U/min; Welch's t-test) and zygotes (0.006 ± 0.001U/min; Welch's t-test).

Recovery from intracellular alkalosis in unfertilized eggs and zygotes

Intracellular alkalosis can be induced by exposure to NH_4Cl-containing solution (Fig. 21B). Short-term exposure to NH_4Cl is not detrimental to embryo development with 93% 1-cell embryos developing to the morula stage (n=44, N=4), although fewer (48%) developed to the blastocyst stage (Steeves, C.L., Lane, M., Bavister, B., Phillips, K.P., and Baltz, J.M., unpublished). Thus, as long-term embryo development was essentially normal (at least to the morula stage), there should be no deleterious short-term effects associated with exposure to NH_4Cl.

The rate of pH_i recovery from an alkaline load induced by exposure to 35 mM NH_4Cl was compared in eggs and zygotes (Fig. 25). The mean rate of recovery (± s.e.m.), measured at pH_i 7.4, was 0.012 ± 0.004 in unfertilized eggs (Fig. 25A) which was significantly lower than the recovery rate in zygotes (Fig. 25B; 0.054 ± 0.005; $p<0.001$; ANOVA; Tukey-Kramer Multiple Comparisons Test). In the absence of external Cl^- or the presence of DIDS, any HCO_3^-/Cl^- exchanger activity should be inhibited. In the absence of external Cl^-, the mean rate of recovery of pH_i in zygotes was significantly inhibited (0.003 ± 0.003 vs. 0.054 with Cl^-; $p<0.001$; ANOVA) in contrast to the mean rate of recovery of pH_i in eggs which was unaffected by the absence of external Cl^- (0.005 ± 0.003 vs. 0.012 with Cl^-; $p>0.05$; ANOVA; Tukey-Kramer Multiple Comparisons Test). Similarly, the rate of recovery in zygotes was inhibited by the

Figure 25. Recovery from induced alkaline load. *Adapted from Phillips and Baltz, 1999.* The mean rate of recovery (± s.e.m.) from NH_4Cl- induced alkaline load was calculated from exponential fits to recovery data as described in the text for every 0.1 pH unit between 7.1 and 7.6. A. Recovery rates in eggs. B. Recovery rates in zygotes 8-12 h post-fertilization. The dashed line is fit to the linear portion of the data and used to estimate the set-point pH_i (see text). C,D. Representative traces of pH_i showing initial Cl^- unloading (0 Cl^-) and subsequent NH_4^+-induced alkaline loading (NH_4^+) are shown for eggs and zygotes (D) in the presence (○) or absence (●) of external Cl^- during recovery. Numbers in legends as in Fig. 23.

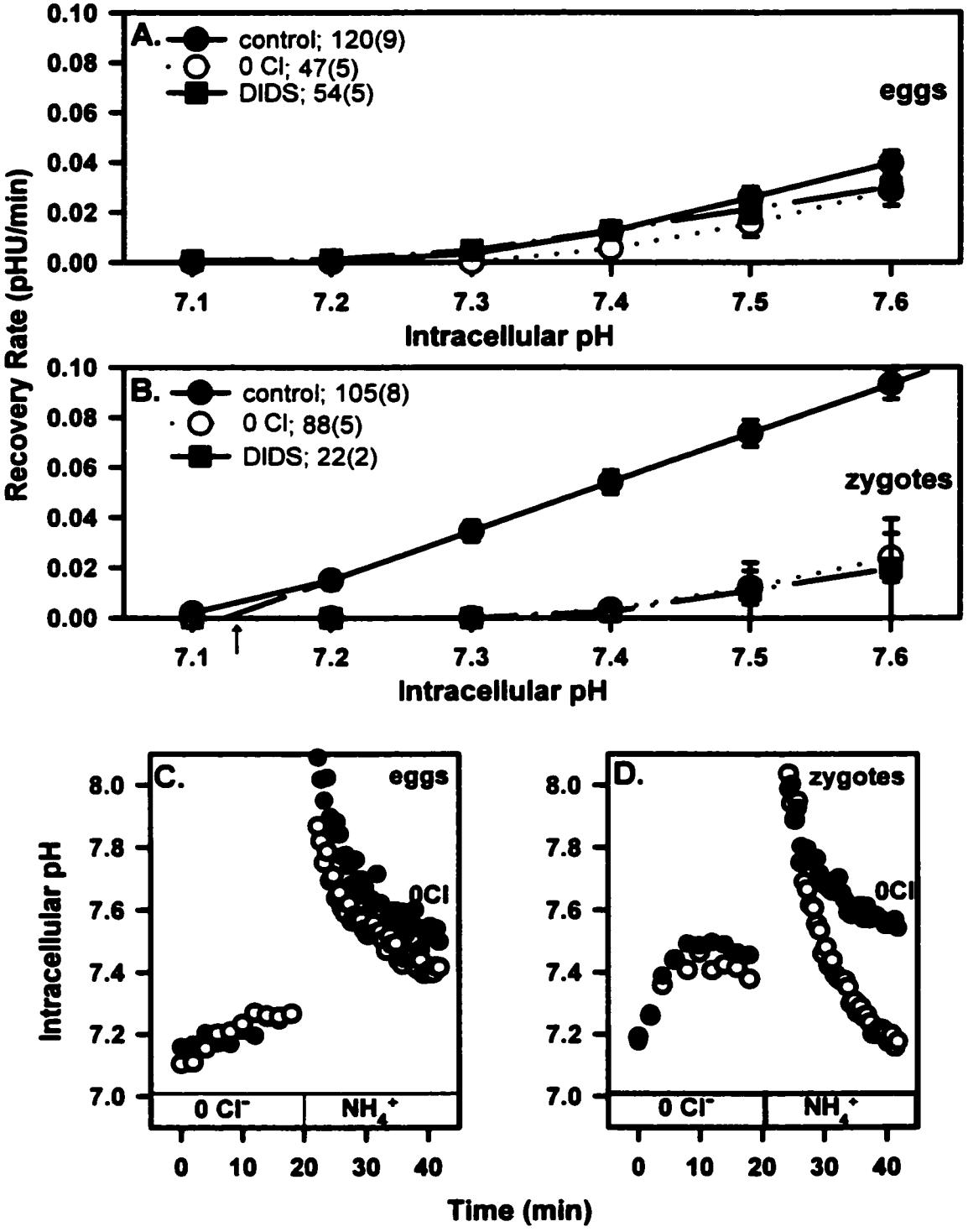
A.
control; 120(9)
0 Cl; 47(5)
DIDS; 54(5)
eggs
Recovery Rate (pHU/min)
0.10
0.08
0.06
0.04
0.02
0.00
7.1
7.2
7.3
7.4
7.5
7.6
Intracellular pH
B.
control; 105(8)
0 Cl; 88(5)
DIDS; 22(2)
zygotes
Intracellular pH
C.
eggs
0Cl
D.
zygotes
0Cl
Intracellular pH
8.0
7.8
7.6
7.4
7.2
7.0
0 Cl⁻
NH4+
0
10
20
30
40
Time (min)

presence of DIDS (0.002 ± 0.002 vs. 0.054 without DIDS; $p<0.001$) whereas DIDS had no significant effect on the rate of recovery in eggs (0.013 ± 0.003 vs. 0.012 without DIDS; $p>0.05$; ANOVA).

In some of the recoveries, amiloride (1 mM) was included to determine whether any Na^+/H^+ antiporter activity present might be slowing recovery by opposing acidification. No effect of amiloride was seen in either eggs or zygotes (data not shown; $p>0.05$; ANOVA; Tukey's Multiple Comparisons Test) and so the data were pooled with control recoveries in the absence of amiloride.

IV. UPREGULATION OF HCO_3^-/Cl^- EXCHANGE AFTER EGG ACTIVATION

Effect of external pH on upregulation of HCO_3^-/Cl^- exchanger activity

HCO_3^-/Cl^- exchanger activity was next measured by the Cl^- removal assay in zygotes fertilized in vivo and collected 3-5 h post-fertilization (15-17 h post-hCG). These 'am-zygotes' were found to have a significantly lower rate of HCO_3^-/Cl^- exchanger activity (0.023 ± 0.007 pHU/min; ± s.e.m.; n=81; N=7) than zygotes collected 8-12 h post-fertilization (20-24 h post-hCG; 0.052 ± 0.004 pHU/min; $p<0.001$; ANOVA; Tukey-Kramer Multiple Comparisons Test) indicating that fertilized eggs within the first few hours after fertilization lacked the robust HCO_3^-/Cl^- exchanger activity exhibited by zygotes 8-12 h following fertilization.

In contrast to am-zygotes, zygotes obtained 8-12 h following fertilization spend a longer period in the oviduct, which is thought to be alkaline. To determine whether differences in external pH could induce increased HCO_3^-/Cl^- exchanger activity, am-zygotes which were collected 3-5 h post-in vivo fertilization (15-17 h post-hCG) were

cultured at either alkaline or acid external pH to the 2-cell stage (Fig. 26). As zygotes collected shortly following fertilization demonstrate sub-maximal rates of HCO_3^-/Cl^- exchanger activity, modifications to culture (i.e. changes to $[HCO_3^-]$ or $\%CO_2$) from this point would reveal any effect of external pH on the upregulation of HCO_3^-/Cl^- exchanger activity. For example, any suppression of upregulation should yield reduced rates of activity in the resulting 2-cell embryos. External pH was varied by either changing the concentration of HCO_3^- in the media (at constant 5% CO_2) or by changing ambient CO_2 (at constant $[HCO_3^-]$=25 mM). External pH was determined under these different conditions (ie. changes to $[HCO_3^-]$ or % CO_2) using the Henderson-Hasselbach equation and confirmed using pH indicators. Thus, in one set of experiments am-zygotes were cultured in varying concentrations of HCO_3^- (ie. 10, 25 or 79 mM, at 5% CO_2 corresponding to pH 6.9, 7.3 and 7.8, respectively) to the 2-cell stage. After 24 h, the 2-cell embryos were removed from culture and HCO_3^-/Cl^- exchanger activity assessed by the Cl^- removal assay as described (pH of media during assay was 7.3 for all groups). There was no significant difference in the mean rates of alkalinization among the alkaline-cultured group (79 mM HCO_3^-), or the acid-cultured group (10 mM HCO_3^-), and the control group (25 mM HCO_3^-; $p>0.05$; Kruskal-Wallis nANOVA Test; Dunn's Multiple Comparisons Test), although there was a significant reduction of HCO_3^-/Cl^- exchanger activity in the alkaline group compared to the acid group ($p<0.05$). Similarly, there was no significant difference in the alkalinization rates when external pH (culture) was altered by changing the ambient CO_2 (ie. 2.5 or 12.5% CO_2; $p>0.05$; Kruskal-Wallis nANOVA Test; Dunn's Multiple Comparisons Test) with standard KSOM (25 mM HCO_3^-) corresponding to pH 7.6 and 6.9, respectively.

Figure 26. Effect of external pH on the development of HCO_3^-/Cl^- exchange. Zygotes fertilized in vivo were obtained 3-5 h post-fertilization and cultured in varying concentrations of HCO_3^- (ie. 10, 25 or 79 mM, at 5% CO_2 corresponding to pH 6.9, 7.3 and 7.8, respectively) for 24 h at which point 2-cell embryos were removed from culture and HCO_3^-/Cl^- exchanger activity assessed by Cl^- removal (standard assay, pH of media 7.3). Similarly, external pH was altered by changing the ambient CO_2 (ie. 2.5 or 12.5% CO_2 at 25 mM HCO_3^- corresponding to pH 7.6 and 6.9, respectively). Different letters indicate statistical significance (Kruskal-Wallis nANOVA Test; Dunn's Multiple Comparisons Test). Numbers above bars as in Fig. 23.

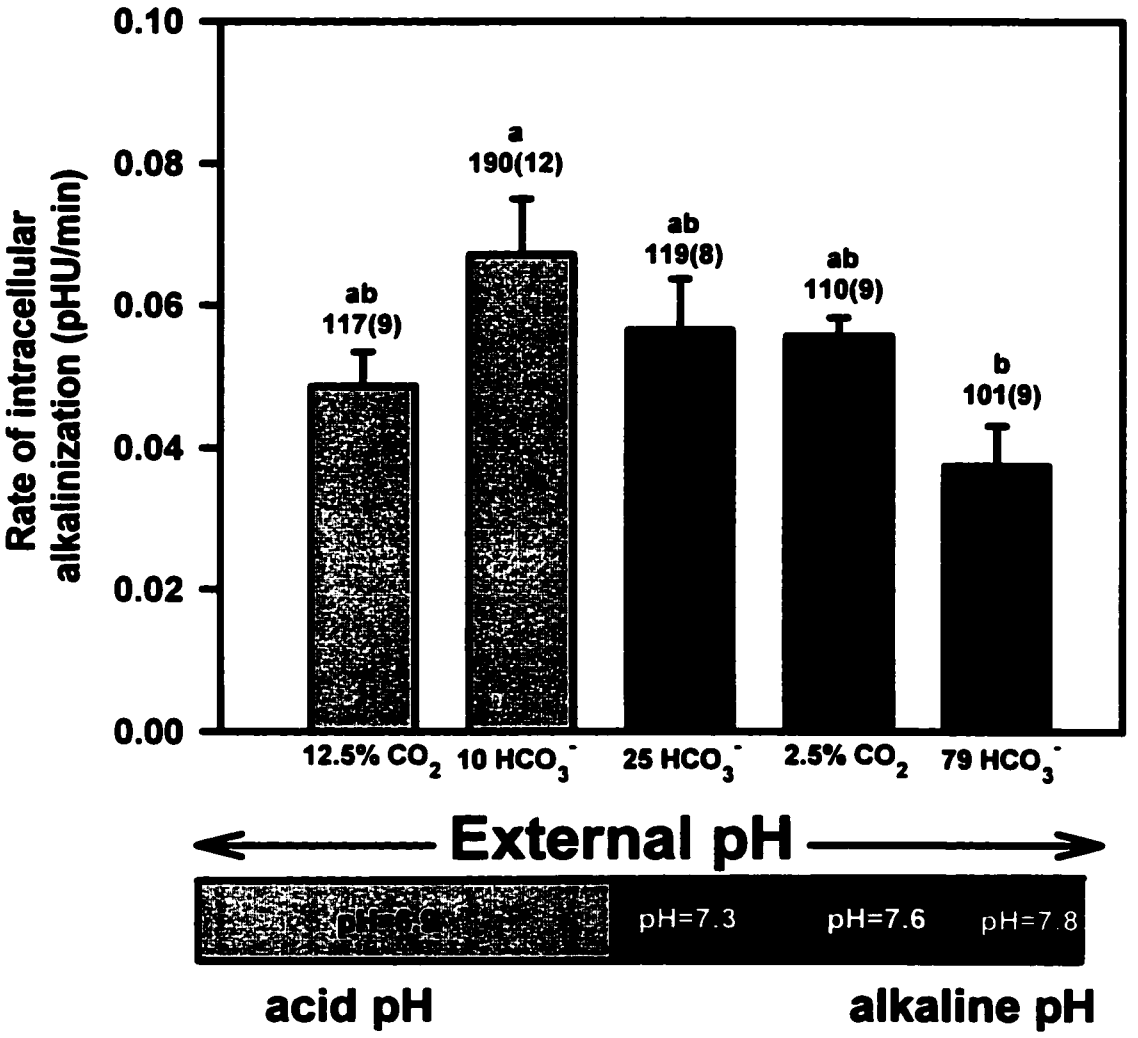
0.10
0.08
0.06
0.04
0.02
0.00
Rate of intracellular alkalinization (pHU/min)
ab
117(9)
a
190(12)
ab
119(8)
ab
110(9)
b
101(9)
12.5% CO2
10 HCO3-
25 HCO3-
2.5% CO2
79 HCO3-
External pH
pH=7.3
pH=7.6
pH=7.8
acid pH
alkaline pH

Timing of appearance of HCO_3^-/Cl^- exchanger activity following fertilization

Zygotes clearly exhibited greater HCO_3^-/Cl^- exchanger activity than unfertilized eggs. This is supported by the higher rates of intracellular alkalinization (Fig. 23) and change in MQAE intensity (Fig. 24) upon Cl^- removal and the faster rate of recovery of pH_i from induced alkalosis in zygotes compared to eggs (Fig. 25). As HCO_3^-/Cl^- exchanger activity increased from 3-5 h post-fertilization (am-zygotes) to 8-12 h post-fertilization (zygotes), HCO_3^-/Cl^- exchanger activity appeared to be gradually upregulated within about 8-12 h of fertilization. However, the use of in vivo fertilized eggs precluded a more precise determination of the timing of appearance of HCO_3^-/Cl^- exchanger activity following egg activation.

As the timing of fertilization in vivo was uncertain, in vitro fertilization (IVF) with a restricted (1 h) sperm-egg incubation was used to more precisely determine the timing of the onset of HCO_3^-/Cl^- exchange activity following fertilization (Fig. 27A). Using this fertilization protocol (1 h sperm-egg incubation) the average incidence of egg activation was 74% (n=460; N=27), assessed by pronuclear development 5-6 h post-sperm-egg incubation. Emission of the second polar body was completed in the majority of eggs between 1-2 h post-sperm-egg incubation with pronuclear development completed between 3-4 h post-sperm-egg incubation (Fig. 27C). Fertilization was also confirmed by measuring Ca^{2+}_i transients in a cohort of Fura-2-loaded eggs, 45 min following sperm-egg incubation (Fig. 27B).

Intracellular alkalinization upon Cl^- removal was used as an index of HCO_3^-/Cl^- exchanger activity. HCO_3^-/Cl^- exchanger activity increased gradually over the first 7-9 h following the end of sperm-egg incubation, reaching maximal activity at about 9 h post-

Figure 27. Development of HCO_3^-/Cl^- exchanger activity after IVF. *Adapted from Phillips and Baltz, 1999.* A. HCO_3^-/Cl^- exchanger activity was measured by the Cl^- removal assay at various times after a 1 h sperm-egg incubation (zygotes) or an identical 1 h incubation without sperm (eggs). Mean rates of intracellular alkalinization (± s.e.m.) upon Cl^- removal are given for IVF eggs cultured for 1 -27 h post-sperm egg incubation (● 16-43 h post-hCG) and for unfertilized eggs (○ 15-23 h post-hCG). The rates in the presence of 500 μM DIDS are also shown for zygotes (■) and eggs (□). B. Example of Ca^{2+}_i transients measured in Fura-2 loaded eggs (n=4), 45 min post-sperm-egg incubation. C. Time-course of emission of the second polar body (PB2) and pronuclear development (PN) following IVF (n=98, N=8). Development is normalized to total number of eggs activated for comparison between different activation protocols. Numbers above points as in Fig. 23.

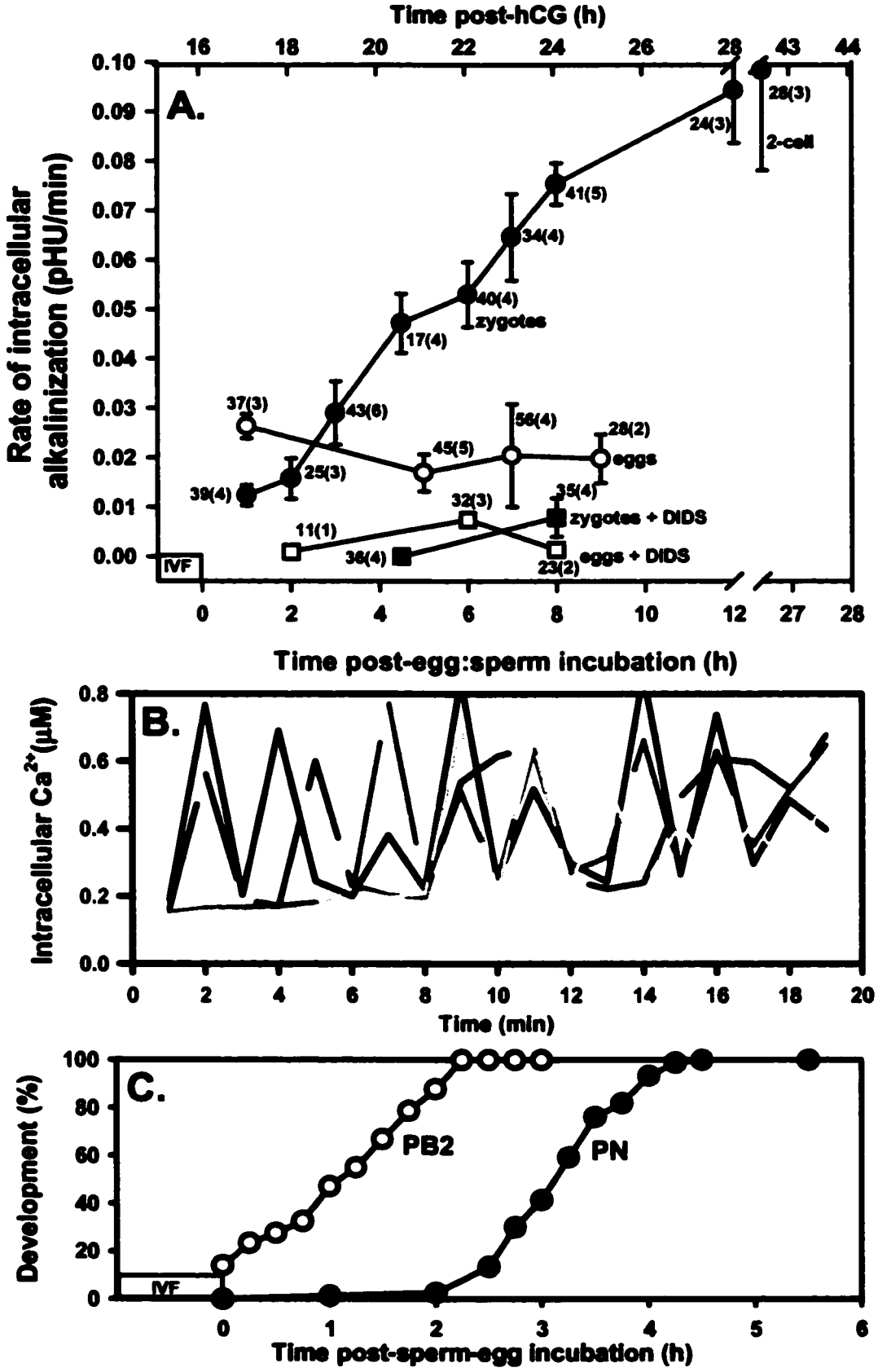
Time post-hCG (h)
16
18
20
22
24
26
28
43
44
A.
Rate of intracellular alkalinization (pHU/min)
0.10
0.09
0.08
0.07
0.06
0.05
0.04
0.03
0.02
0.01
0.00
IVF
28(3)
2-cell
24(3)
41(5)
34(4)
40(4)
zygotes
17(4)
37(3)
43(6)
56(4)
28(2)
eggs
45(5)
25(3)
39(4)
32(3)
35(4)
zygotes + DIDS
11(1)
36(4)
23(2)
eggs + DIDS
0
2
4
6
8
10
12
27
28
Time post-egg:sperm incubation (h)
B.
Intracellular Ca2+ (µM)
0.8
0.6
0.4
0.2
0.0
0
2
4
6
8
10
12
14
16
18
20
Time (min)
C.
Development (%)
100
80
60
40
20
0
PB2
PN
IVF
0
1
2
3
4
5
6
Time post-sperm-egg incubation (h)

fertilization. This rate of activity remained high through to the 2-cell stage, which is consistent with previous measurements showing similar HCO_3^-/Cl^- exchanger activity between zygotes and 2-cell embryos fertilized in vivo (Zhao et al., 1995). In contrast, when unfertilized eggs were maintained under the same in vitro conditions, the very low HCO_3^-/Cl^- exchanger activity did not greatly increase from 5 h post-ovulation (17 h post-hCG or approximately 2 h after the end of sperm-egg incubation would have occurred for eggs undergoing IVF) up to 13 h (25 h post-hCG), by which time fertilized eggs (approximately 10 h after the end of sperm-egg incubation) had developed maximal HCO_3^-/Cl^- exchanger activity.

Upregulation of HCO_3^-/Cl^- exchange activity in ethanol-activated eggs

To determine whether increased HCO_3^-/Cl^- exchanger activity was dependent upon the male genome or other factors introduced by the sperm, eggs were parthenogenetically activated using ethanol (Fig. 14A; Fig. 28A). Egg activation (judged by timing of formation of pronuclei and second polar body) was delayed following ethanol exposure compared with IVF, and thus HCO_3^-/Cl^- exchanger activity was not assessed until 15 h post-ethanol exposure. Alkalinization rates upon Cl^- removal were increased significantly by 15 h post-parthenogenetic activation (0.033 ± 0.006) compared to unactivated controls (0.017 ± 0.005; $p<0.001$; ANOVA, Tukey-Kramer Multiple Comparisons Test). There was a further significant increase in the rate of intracellular alkalinization at 25 h post-activation compared to the rate at 15 h ($p<0.001$; ANOVA; Tukey-Kramer Multiple Comparisons Test), which was consistent with the time-course of HCO_3^-/Cl^- exchanger activity obtained following IVF, allowing for the developmental

Figure 28. Parthenogenetic activation using ethanol. *Adapted from Phillips and Baltz, 1999.* A. Mean rates of intracellular alkalinization (± s.e.m.) upon Cl^- removal are shown for eggs parthenogenetically activated with 7% ethanol/PBS (●) and control eggs (○; exposed only to PBS). B. Example of a single Ca^{2+}_i transient, measured in Fura-2 loaded eggs (n=10), produced upon 5 min exposure to 7% ethanol in PBS (——). Numbers as in Fig. 23.

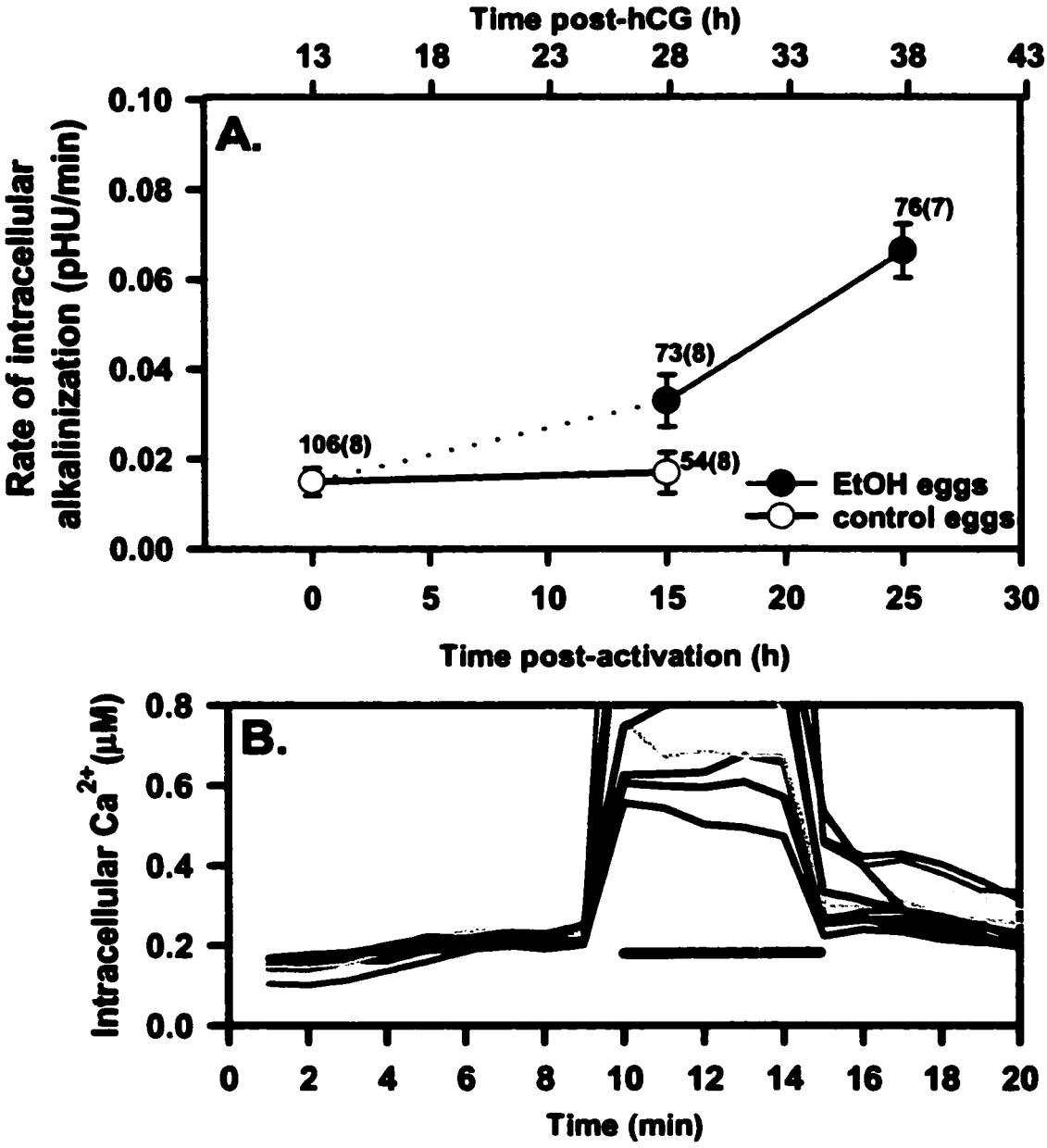
Time post-hCG (h)
13
18
23
28
33
38
43
A.
Rate of intracellular alkalinization (pHU/min)
0.10
0.08
0.06
0.04
0.02
0.00
76(7)
73(8)
106(8)
54(8)
EtOH eggs
control eggs
0
5
10
15
20
25
30
Time post-activation (h)
B.
Intracellular Ca2+ (μM)
0.8
0.6
0.4
0.2
0.0
0
2
4
6
8
10
12
14
16
18
20
Time (min)

delay in parthenogenotes. The rates for unactivated eggs assessed at 15 h did not increase ($p>0.05$; ANOVA) and were consistent with rates obtained for unfertilized eggs not exposed to PBS. Unfertilized eggs could not be assessed at 25 h, as unactivated eggs had degenerated by this time.

HCO_3^-/Cl^- exchanger mRNA in unfertilized eggs

Unfertilized eggs were examined by RT-PCR for expression of AE2 mRNA, shown previously to be the sole known AE isoform expressed in zygotes (Zhao et al., 1995). AE2 was detected in both unfertilized eggs and zygotes (Fig. 29). The comparable intensities of the PCR products obtained from eggs and zygotes, as well as the similarly decreased intensity when only 5 eggs or zygotes instead of 10 or 30 were used for the reverse transcription, indicated that there was qualitatively similar levels of expression in eggs and zygotes. Expression of AE2 mRNA in the unfertilized egg is consistent with the suggestion that AE2 mRNA is a maternally-derived product in the zygote (Zhao et al., 1995).

Effect of inhibition of protein synthesis and protein transport on HCO_3^-/Cl^- exchanger upregulation

To determine whether the time-dependent upregulation of HCO_3^-/Cl^- exchanger activity was dependent on protein synthesis, in vitro fertilized eggs were cultured for 7-9 h in the continuous presence of cycloheximide (50 μg/ml) beginning immediately following removal of sperm (Fig. 30A). At the end of the 7-9 h incubation, HCO_3^-/Cl^- exchanger activity was assessed in zygotes with 2 pronuclei using the Cl^- removal assay. There was no significant difference between the mean rates of alkalinization in control (0.078 ± 0.008 pHU/min) versus cycloheximide-treated zygotes (0.067 ± 0.005 pHU/min

Figure 29. RT-PCR detection of AE2 mRNA expression. *Adapted from Phillips and Baltz, 1999.* Total RNA from 30, 10 or 5 (as marked) eggs or zygotes was reverse transcribed (RT), and 1/20 of the total cDNA from each RT used for PCR. The lane marked B is a sample of the final drop in which zygotes were washed, treated identically to egg/embryo samples (ie. RNA isolation, RT-PCR). Expected size of PCR product is 210 bp, marked at right of gel. Unmarked lane is ϕx174 *Hind* III digest marker (sizes shown on left).


eggs
30 30 10 10 5
B
zygotes
30 30 10 10 5
B
1358
1078
872
603
310
281/271
234
194
AE2
210

Figure 30. Effect of inhibitors of protein synthesis and protein trafficking on the upregulation of intracellular alkalinization upon Cl^- removal. Eggs were fertilized by IVF and then cultured with an inhibitor immediately upon removal from sperm (16 h post-hCG) for 7-8 h. HCO_3^-/Cl^- exchanger activity was measured by alkalinization upon chloride removal at 7-8 h (shown as mean ± s.e.m.). A. 50 μg/ml cycloheximide: protein synthesis inhibitor. B. 5 μg/ml brefeldin A: disrupts Golgi apparatus. C. 10 μM cytochalasin D: disrupts actin filaments. D. 0.1/1.0 μg/ml (pooled data) demecolcine: disrupts microtubules. None of the inhibitors had a significant effect assessed relative to their paired control (vehicle only; Student's t-test). Numbers above bars as in Fig. 23.

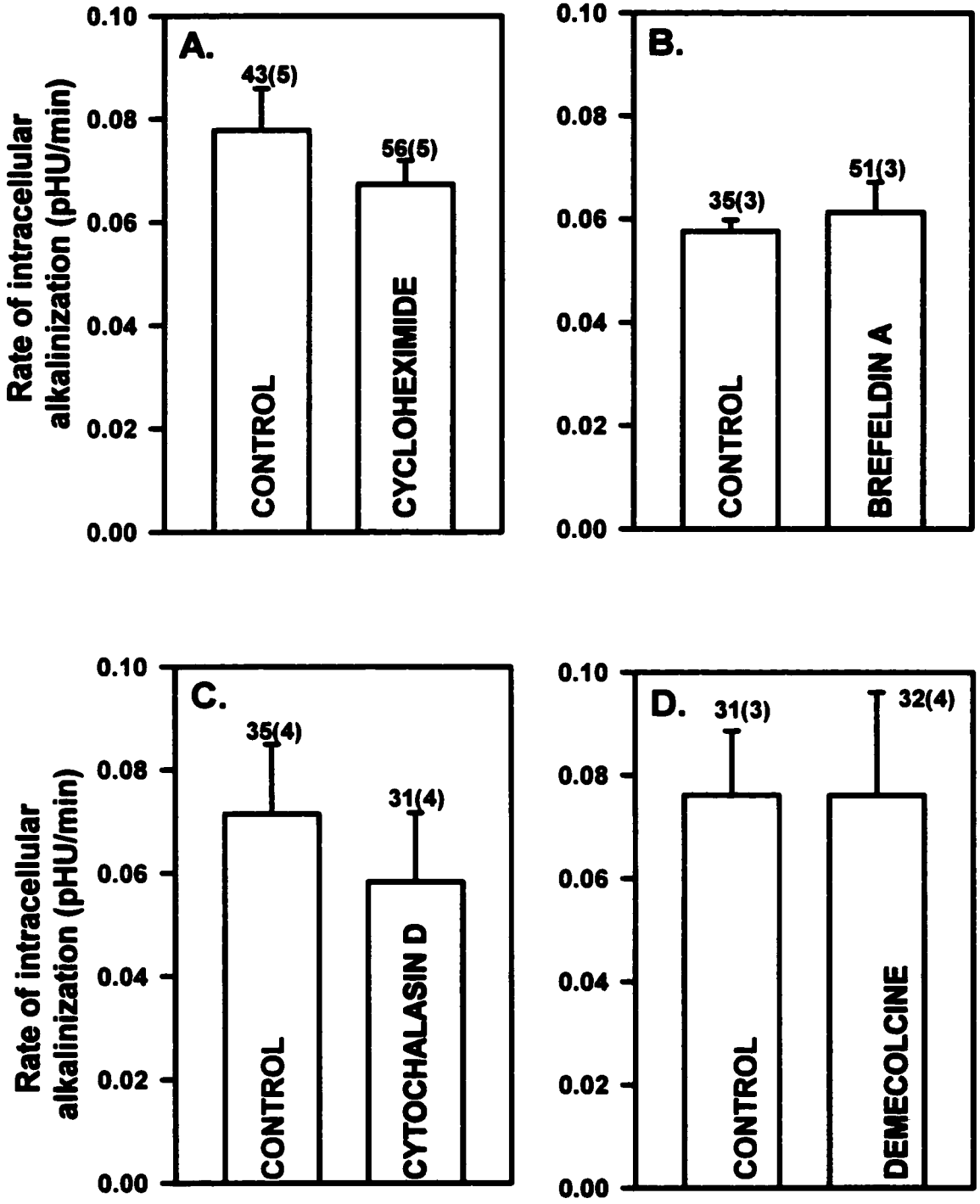
A.
B.
C.
D.
Rate of intracellular alkalinization (pHU/min)
0.10
0.08
0.06
0.04
0.02
0.00
43(5)
56(5)
CONTROL
CYCLOHEXIMIDE
35(3)
51(3)
CONTROL
BREFELDIN A
35(4)
31(4)
CONTROL
CYTOCHALASIN D
31(3)
32(4)
CONTROL
DEMECOLCINE

± s.e.m., p=0.15; Student's t-test).

Drugs targeting the Golgi apparatus (brefeldin A; Fig. 30B), actin filaments (cytochalasin D; Fig. 30C) or microtubules (demecolcine; Fig. 30D) were investigated to determine whether the upregulation of HCO_3^-/Cl^- exchanger activity following fertilization was dependent on intracellular protein transport or an intact cytoskeleton. In each case, the mean rates of alkalinization were not significantly different between the group with the inhibitor and its respective control ($p>0.05$; Student's t-test). Note that for demecolcine two concentrations were tested: 0.1 and 1.0 μg/ml. As the groups were not significantly different ($p=0.11$), the data were pooled. To demonstrate that these agents were effectively targeting the cytoskeleton, confocal microscopy was performed following treatment with either cytochalasin D or demecolcine (Fig. 31). Demecolcine disruption of microtubules was further confirmed by demonstrating that cleavage to the 2-cell stage, a process dependent on intact microtubules (due to the requirement for microtubules in the mitotic spindle), was prevented (0%; n=23; N=2) following demecolcine treatment compared to embryos treated with vehicle (ethanol; 93% cleaved; n=22; N=2).

Role of PKA and PKC in HCO_3^-/Cl^- exchanger upregulation

To determine whether the upregulation of HCO_3^-/Cl^- exchanger activity was dependent on PKA activity, intracellular cAMP ($cAMP_i$) was raised in unfertilized eggs by exposure to 0.1 mM forskolin, 0.3 mM dbcAMP and 0.2 mM IBMX for 3-6 h in culture (Fig. 32A). dbcAMP (0.3 mM) alone sufficiently raises $cAMP_i$ as demonstrated by dbcAMP inhibition of GVBD (Fig. 38B). Other studies have shown, both by direct

Figure 31. Confocal imaging of zygotes following treatments designed to disrupt the cytoskeleton. Representative zygotes collected 19 h post-hCG were cultured with cytochalasin D (10 μM) or demecolcine (1 μg/mL) for 2 h and then fixed and stained for confocal microscopy. In all cases control zygotes were cultured with vehicle only. A-C. Zygotes were stained with 6.6 μM rhodamine phalloidin. A. negative control, no stain. B. control. C. cytochalasin D exposure. D-F. Zygotes immunolabelled with anti-α-tubulin (1/1000 dilution; primary) and Cy3 goat-anti-mouse (1/100 dilution; secondary). D. negative control, secondary antibody exposure only. E. control. F. demecolcine exposure. Differences in relative size resulted from compression during slide preparation. Bar represents 20 μm. PN-pronucleus; pb- polar body, zp- zona pellucida, sp- spindle.

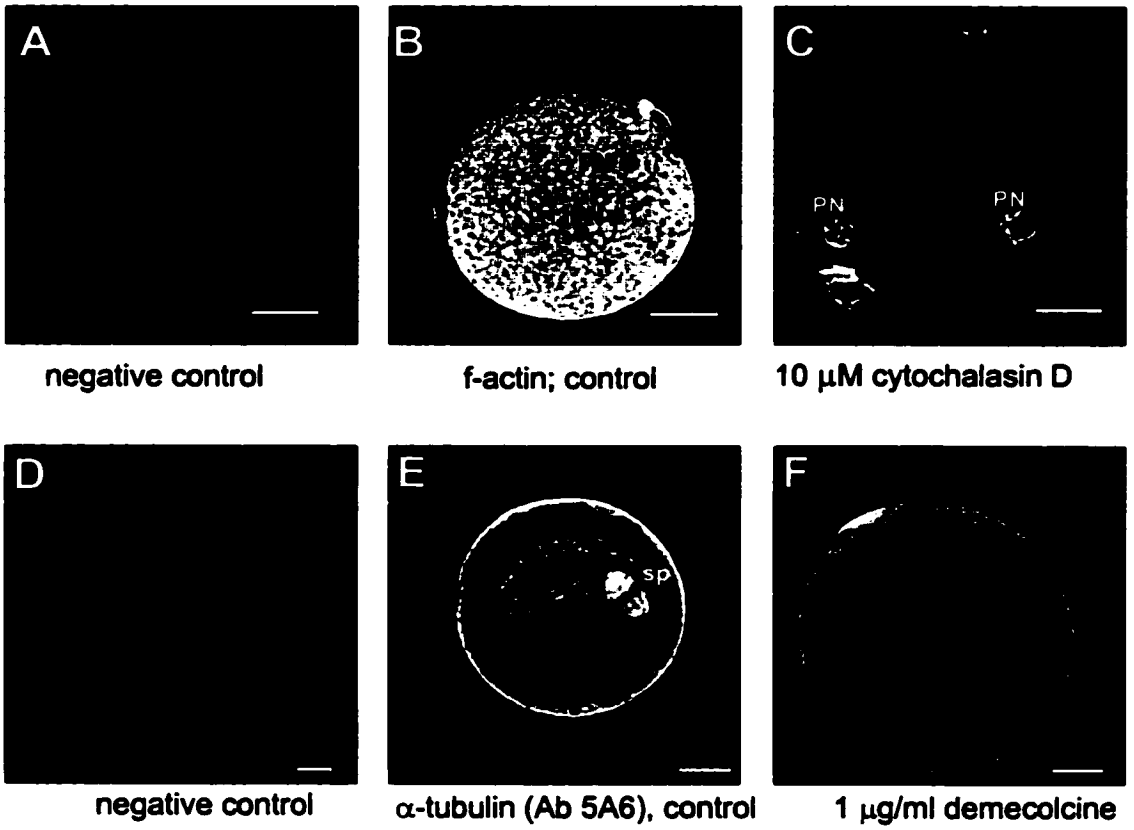

negative control | f-actin; control | 10 μM cytochalasin D

negative control | α-tubulin (Ab 5A6), control | 1 μg/ml demecolcine

Figure 32. HCO_3^-/Cl^- exchanger activity following activation/inhibition of PKA/PKC. PKA. A. Unfertilized eggs were exposed to 0.1 mM forskolin, 0.3 mM dbcAMP and 0.2 mM IBMX ($\uparrow$ cAMP) or vehicle (control) for 3-6 h followed by Cl^- removal assay. B. Immediately following IVF, zygotes were exposed to 5 μM H-89 (PKA inhibitor) for 7-9 h followed by Cl^- removal assay. **PKC**. C. Unfertilized eggs were exposed to 100 nM PDD or PMA (phorbol esters) or vehicle (control) for 3-6 h followed by Cl^- removal assay. D. IVF eggs were exposed to 10 μM sphingosine for 7-9 h followed by Cl^- removal assay. In all cases, there was no significant difference between appropriate control and treatment. Numbers above bars as in Fig. 23.

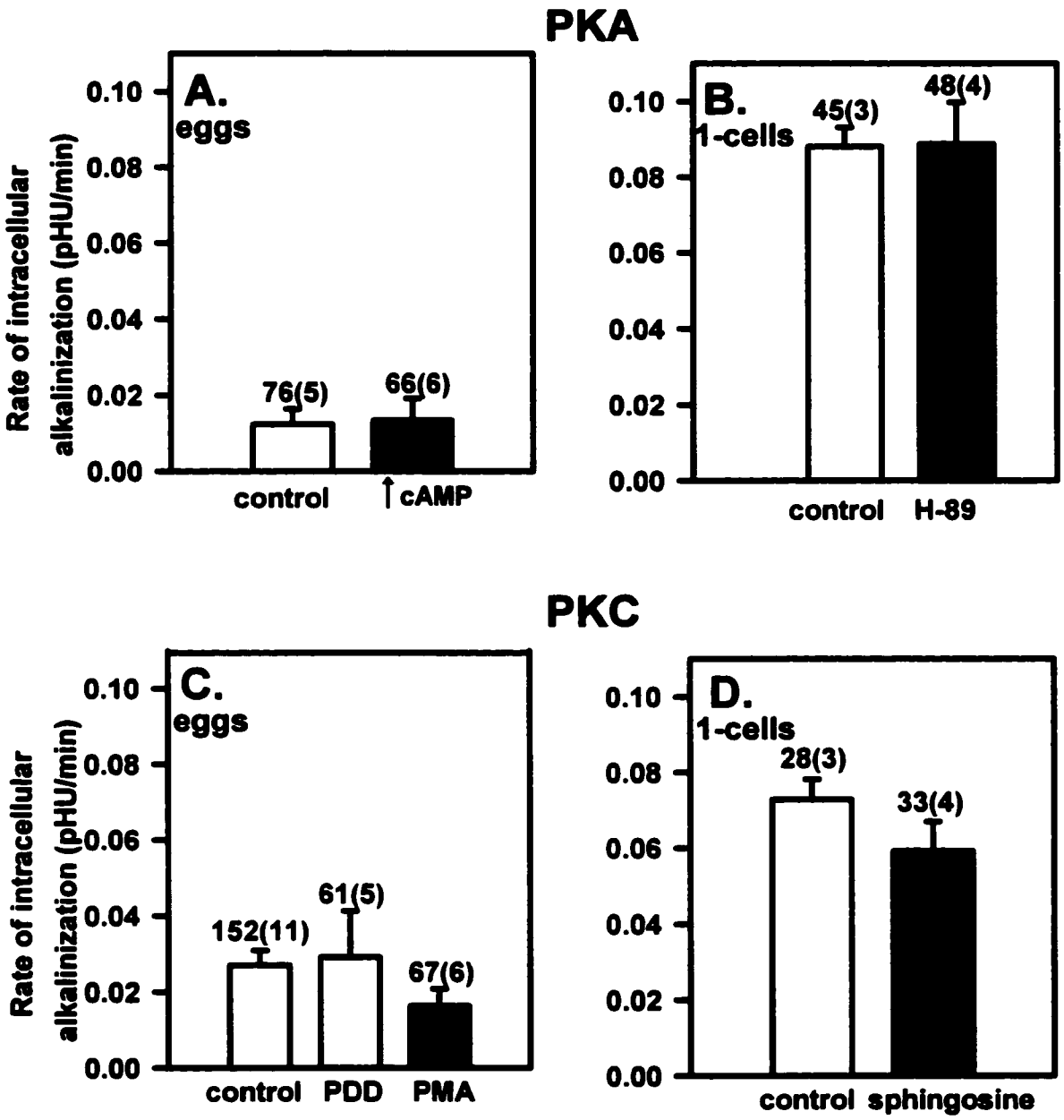
PKA
A.
eggs
Rate of intracellular alkalinization (pHU/min)
0.10
0.08
0.06
0.04
0.02
0.00
76(5)
66(6)
control
cAMP
B.
1-cells
45(3)
48(4)
control
H-89
PKC
C.
eggs
152(11)
61(5)
67(6)
control
PDD
PMA
D.
1-cells
28(3)
33(4)
control
sphingosine

measurements of $cAMP_i$ and by inhibition of GVBD, that similar concentrations of IBMX and forskolin increase $cAMP_i$ (Schultz et al., 1983ab; Bornslaeger et al., 1994; Bornslaeger et al., 1996). HCO_3^-/Cl^- exchange was not stimulated by increased $cAMP_i$ in unfertilized eggs, as the mean rates (s.e.m.) of intracellular alkalinization upon Cl^- removal were not significantly different between eggs in which $cAMP_i$ was increased (0.014 ± 0.006) versus control (0.012 ± 0.009; p=0.26; Student's t-test). To determine whether upregulation of HCO_3^-/Cl^- exchange following IVF was dependent on PKA activation, in vitro fertilized eggs were cultured with H-89 (5 μM; PKA inhibitor), immediately following sperm-egg incubation, for 7-9 h (Fig. 32B). HCO_3^-/Cl^- exchange in zygotes with 2 pronuclei was then assessed using the Cl^- removal assay. There was no significant difference between the mean rates of alkalinization in control (0.090 ± 0.005 pHU/min) and H-89 (0.090 ± 0.011 pHU/min; ± s.e.m., p=0.96; Student's t-test).

A possible role for PKC in HCO_3^-/Cl^- exchanger upregulation was examined by exposing unfertilized eggs to phorbol esters (Fig. 32A). Eggs were cultured with 100 nM PDD or PMA for 3-6 h in culture, followed by the Cl^- removal assay. Similar phorbol ester treatment has been demonstrated to partially upregulate Na^+/H^+ antiporter activity in hamster eggs (Lane et al., 1998). HCO_3^-/Cl^- exchange was, however, not stimulated in unfertilized eggs by phorbol ester treatment, as the rates of intracellular alkalinization were not significantly different between eggs exposed to PDD (0.029 ± 0.012), PMA (0.016 ± 0.005) or control (0.027 ± 0.004 ; p=0.37; ANOVA). To determine whether upregulation of HCO_3^-/Cl^- exchange following IVF was dependent on PKC activation, in vitro fertilized eggs were cultured with sphingosine (10 μM; PKC inhibitor), immediately following sperm-egg incubation, for 7-9 h (Fig. 32D). HCO_3^-/Cl^- exchange was then

assessed in zygotes with 2 pronuclei using the Cl^- removal assay. Sphingosine-treatment had no significant effect on the mean rates of alkalinization upon Cl^- removal (0.059 ± 0.015 pHU/min) compared to vehicle (0.073 ± 0.009 pHU/min; Student's t-test; p=0.28). Sphingosine inhibits compaction in 8-cell embryos by inhibition of PKC activity (Winkel et al., 1990). To confirm that 10 μM sphingosine effectively inhibited PKC activity under our conditions, 8-cell embryos were cultured with 10 μM sphingosine and compaction assessed after 8 h or 24 h. Sphingosine treatment significantly reduced compaction assessed after 8 h (10%; n=24; N=3; vehicle: 100%; n=16; N=3; Fisher's Exact test, $p<0.0001$) and 24 h (sphingosine: 32%, n=62; N=6; vehicle: 98%; n=54; N=6; Fisher's Exact test, $p<0.0001$).

Role of Ca^{2+} transients following fertilization

To determine whether upregulation of HCO_3^-/Cl^- exchange required the Ca^{2+} transients which follow fertilization, newly-fertilized eggs (by IVF) were loaded with the Ca^{2+} chelator BAPTA (Fig. 33). Using the Ca^{2+}-sensitive fluorophore, Fura-2, to measure intracellular Ca^{2+}, robust Ca^{2+} transients were seen in fertilized eggs (Fig. 33C). In fertilized eggs loaded with BAPTA, however, the Ca^{2+} transients were completely suppressed (Fig. 33D). HCO_3^-/Cl^- exchange was assessed in fertilized eggs with or without BAPTA by the Cl^- removal assay at 7-9 h post-sperm-egg incubation (Fig. 33A). Development of HCO_3^-/Cl^- exchange at 7-9 h post-fertilization was significantly inhibited in fertilized eggs which had been loaded with BAPTA immediately after fertilization compared to fertilized eggs exposed to vehicle only (Fig. 33A; p=0.01; Student's t-test). In contrast, loading with BAPTA 6-8 h post-sperm-egg incubation had no significant

Figure 33. Effect of BAPTA-inhibition of early Ca^{2+} transients on HCO_3^-/Cl^- exchanger activity. *Adapted from Phillips and Baltz, 1999.* A. Dependence of HCO_3^-/Cl^- exchanger activity on early Ca^{2+} transients. IVF eggs were exposed to 20 μM BAPTA (●) or vehicle (control, ○) for 30 min at 0, 2.5, 4.5 or 6.5 h post-sperm egg incubation, followed by standard culture and Cl^- removal assay at 7-8 h post-sperm egg incubation. Mean rates of intracellular alkalinization (± s.e.m.) are shown. B. The timing of development of the second polar body (PB2) and pronuclei (PN) were not different when eggs were exposed to BAPTA (●; n=22, N=3) or vehicle (control, ○; n=15, N=2) for 30 min immediately following sperm-egg incubation (1 h). Development is normalized to total number of eggs activated for comparison between different activation protocols. C. D. Example of Ca^{2+}_i transients measured in Fura-2 loaded eggs treated with vehicle (C, n=7) or BAPTA (D, n= 6) immediately following IVF. Numbers above points as in Fig. 23.

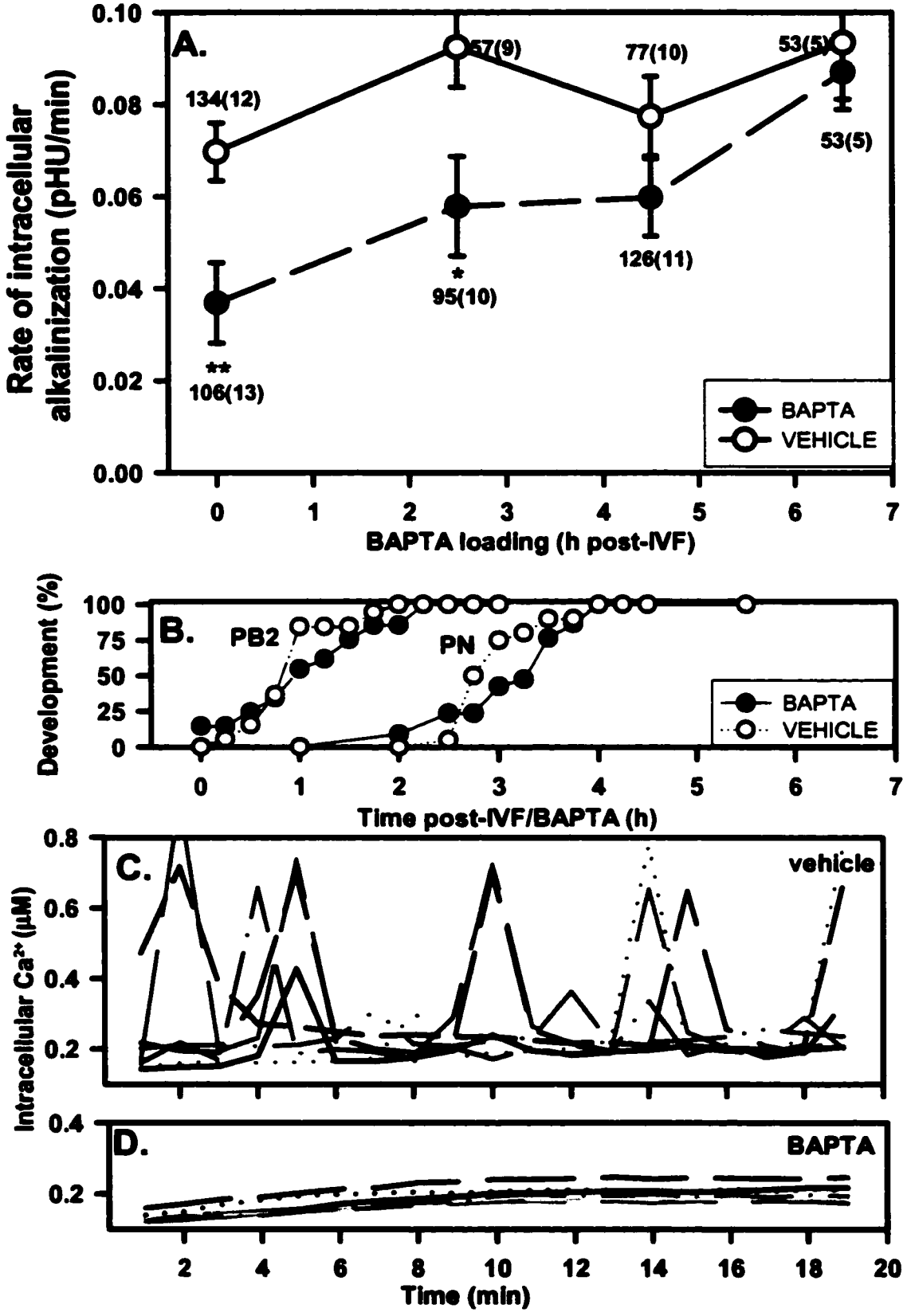
A.
Rate of intracellular alkalinization (pHU/min)
0.10
0.08
0.06
0.04
0.02
0.00
134(12)
57(9)
77(10)
53(5)
53(5)
126(11)
*
95(10)
**
106(13)
BAPTA
VEHICLE
0
1
2
3
4
5
6
7
BAPTA loading (h post-IVF)
B.
Development (%)
100
75
50
25
0
PB2
PN
BAPTA
VEHICLE
Time post-IVF/BAPTA (h)
C.
vehicle
Intracellular Ca2+ (μM)
0.8
0.6
0.4
0.2
D.
BAPTA
0.4
0.2
2
4
6
8
10
12
14
16
18
20
Time (min)

effect on the rate of intracellular alkalinization (p=0.69, Student's t-test) measured soon after BAPTA loading. To ensure that BAPTA exposure was not detrimental to embryo development, emission of the second polar body and pronuclear development was assessed following IVF/BAPTA exposure in BAPTA and vehicle-treated eggs (Fig. 33B). BAPTA exposure immediately following sperm-egg incubation had no effect on the timing of emission of the second polar body or the development of pronuclei. Similarly, the average incidence of egg activation following early BAPTA exposure (t=0 h) was 60% (n=122; N=11), comparable to activation in the vehicle group (65%; n=75; N=7). Since HCO_3^-/Cl^- exchanger measurements were made within 3-4 h of PN development this suggests that the effect of BAPTA seemed to be due to its suppression of Ca^{2+}_i transients and not due to a general deleterious effect on eggs.

Development of HCO_3^-/Cl^- exchanger activity in Sr^{2+}-activated eggs

To further examine the mechanism of upregulation of HCO_3^-/Cl^- exchanger activity, eggs were parthenogenetically activated by exposure to 10 mM $SrCl_2$ (Fig. 14B). As discussed (Introduction), exposure to Sr^{2+} causes Ca^{2+}_i release and exit from metaphase. HCO_3^-/Cl^- exchanger activity was assessed using the Cl^- removal assay at various time points following Sr^{2+} activation (Fig. 34A). In addition, the timing of second polar body extrusion and pronuclear development following Sr^{2+} activation was determined (Fig. 34C). Sr^{2+} exposure resulted in 89% activation (pronuclear development) within 5 h (n=90, N=6). The timing of pronuclear development was similar to that of IVF eggs (Fig. 26C). HCO_3^-/Cl^- exchanger activity developed gradually following Sr^{2+}-activation (Fig. 34A) with the same timing as the development of HCO_3^-/Cl^- exchanger activity following IVF (Fig. 26A). Sr^{2+}-activation produced repetitive Ca^{2+}

Figure 34. Parthenogenetic activation using Sr^{2+}. A.Eggs were activated by 2 h exposure to Sr^{2+} followed by KSOM culture. HCO_3^-/Cl^- exchanger activity was assessed at 3, 4.5, 7 and 9 h following introduction of Sr^{2+}. Level of HCO_3^-/Cl^- exchanger activity (measured by Cl^- removal assay) in eggs represented by dotted line (see Fig. 27A). B. Example of Ca^{2+}_i transients measured in Fura-2 loaded eggs (n=5) exposed to 10 mM Sr^{2+}. C. Time-course of emission of second polar body (PB2; n=65, N=6) and pronuclear development (PN; n=155, N=11). Development is normalized to total number of eggs activated for comparison between different activation protocols. Numbers above points as in Fig. 23.

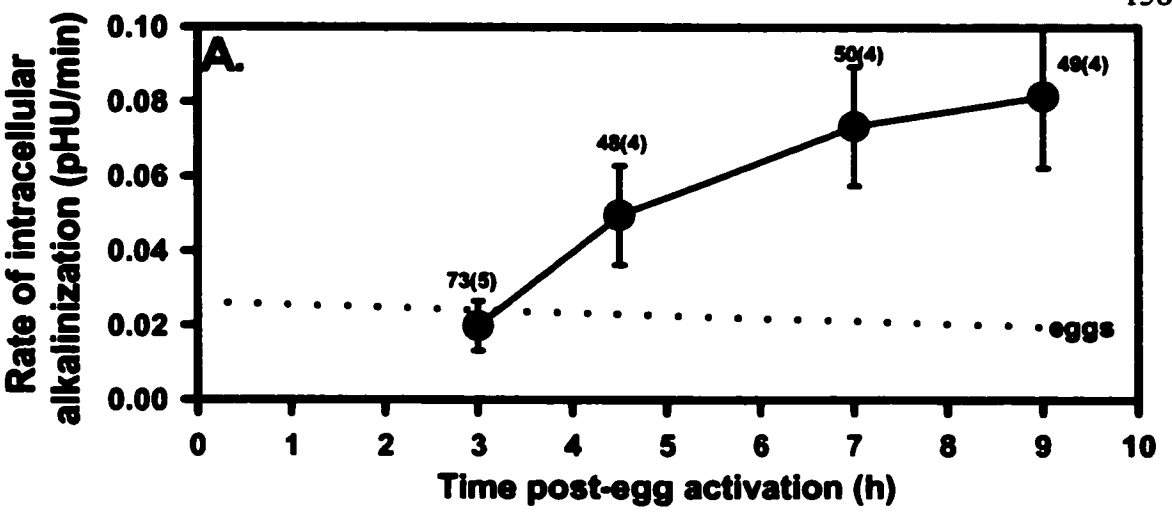
A.
Rate of intracellular alkalinization (pHU/min)
0.10
0.08
0.06
0.04
0.02
0.00
73(5)
48(4)
50(4)
49(4)
eggs
0 1 2 3 4 5 6 7 8 9 10
Time post-egg activation (h)

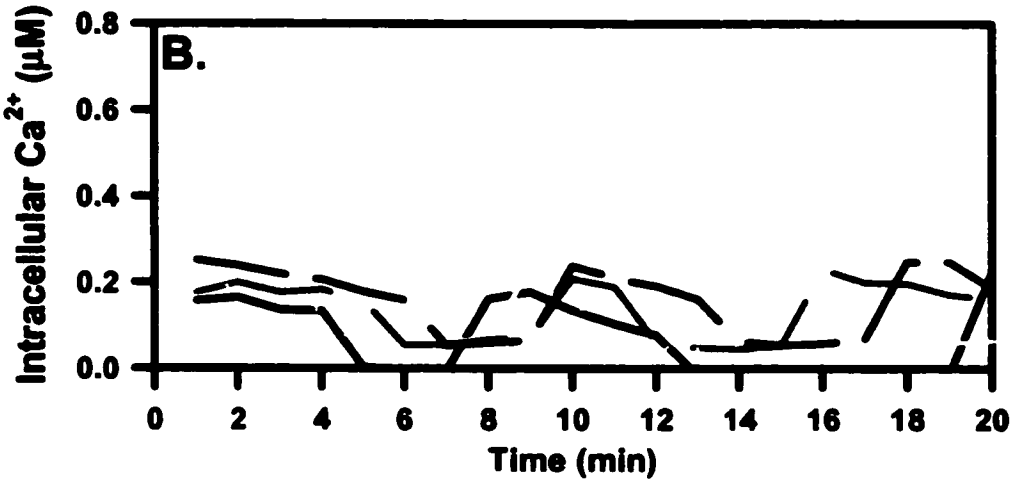
B.
Intracellular Ca^{2+} (μM)
0.8
0.6
0.4
0.2
0.0
0 2 4 6 8 10 12 14 16 18 20
Time (min)

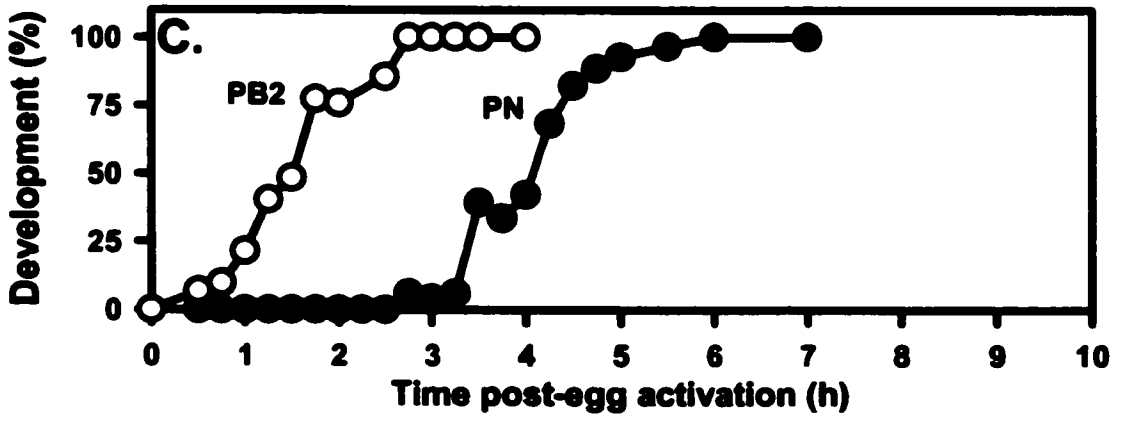
C.
Development (%)
100
75
50
25
0
PB2
PN
0 1 2 3 4 5 6 7 8 9 10
Time post-egg activation (h)

transients similar in frequency to transients produced following IVF (Fig. 26B), although with a much smaller amplitude (Fig. 34B). HCO_3^-/Cl^- exchanger activity in both IVF eggs and $SrCl_2$ activated eggs developed as pronuclei were formed. To determine the developmental potential of Sr^{2+} activation, activated eggs were cultured for up to 120 h. 96% Sr^{2+} activated eggs developed to the 2-cell stage (24 h post activation; n= 90, N=6), 58% developed to morula (72 h post activation; n=60, N=4) and 14% formed blastocysts (120 h post activation n=45, N=3), indicating that almost all eggs were activated and able to at least cleave to the 2-cell stage. Decreased ability to form blastocysts is common for parthenogenotes (Kaufman, 1978; Kaufman, 1982; Johnson et al., 1990).

Upregulation of HCO_3^-/Cl^- exchanger activity following a single Ca^{2+}_i transient

HCO_3^-/Cl^- exchanger activity developed very slowly following ethanol activation (Fig. 28A). Ethanol activation, unlike IVF, is accompanied by only a single, large Ca^{2+}_i transient (Fig. 28B). To determine whether upregulation of HCO_3^-/Cl^- exchanger activity is augmented by the presence of repetitive Ca^{2+}_i transients (IVF- Fig. 27B; Sr^{2+}- Fig. 34B) rather than a single Ca^{2+}_i transient (ethanol- Fig. 28B), Sr^{2+} activation was used. Sr^{2+}-activated eggs produce Ca^{2+}_i transients, and the removal of Sr^{2+} stops these oscillations immediately, enabling manipulation of the duration of these transients. To further define any role of Ca^{2+}_i transients, a 5 min pulse of $SrCl_2$ (10 mM) was applied, which produced only a single, large Ca^{2+}_i transient coincident with Sr^{2+} exposure (Fig. 35B). This brief Sr^{2+} exposure was sufficient to activate eggs in culture (100% activation as determined by pronuclear development and emission of the second polar body, data not shown) within 6 h. These eggs developed HCO_3^-/Cl^- exchanger activity (Fig. 35A), measured 7-9 h

Figure 35. Parthenogenetic activation using Sr^{2+} pulse. To determine whether a single Ca^{2+} transient was sufficient to induce HCO_3^-/Cl^- exchanger activity, eggs were exposed to a brief (5 min) pulse of 10 mM Sr^{2+}. A. Following Sr^{2+} pulse, eggs were cultured for 7-9 h and assessed for HCO_3^-/Cl^- exchanger activity using the Cl^- removal assay. Shown is the mean rate of intracellular alkalinization (± s.e.m.). Level of HCO_3^-/Cl^- exchanger activity (measured by Cl^- removal assay) in eggs represented by dotted line (Fig. 27A) and in Sr^{2+} activated (2 h protocol) eggs at 7-9 h post-activation represented by dashed line (Fig. 34A). B. Example of a single Ca^{2+}_i transient, measured in Fura-2 loaded eggs (n=13), produced following a 5 min exposure to 10 mM Sr^{2+} (——), which was immediately replaced by KSOM. Numbers above bar as in Fig. 23.

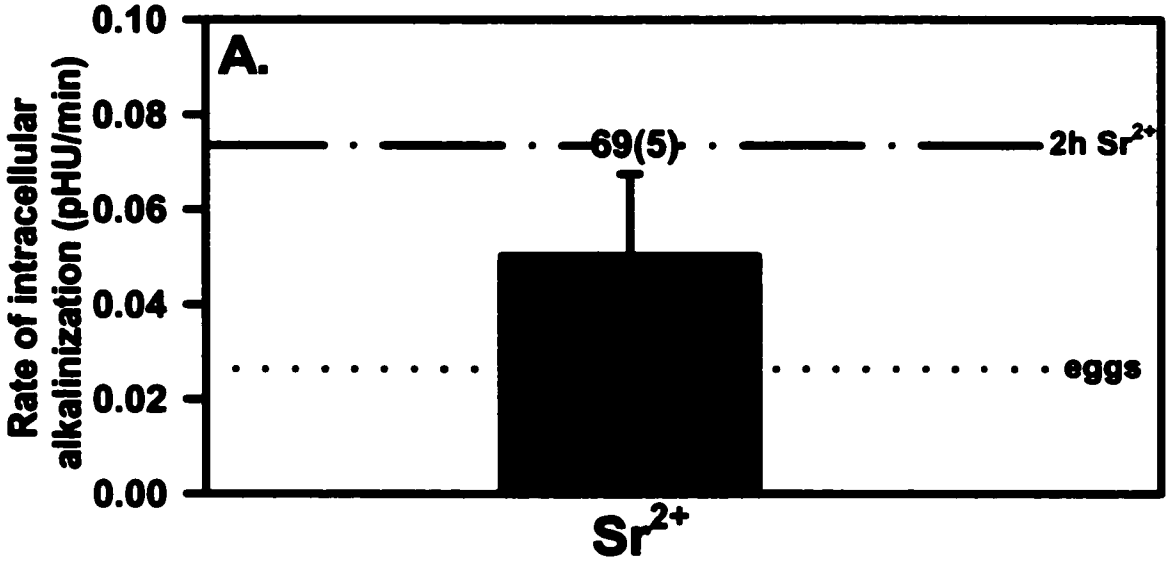
A.
Rate of intracellular alkalinization (pHU/min)
0.10
0.08
0.06
0.04
0.02
0.00
69(5)
2h Sr2+
eggs
Sr2+

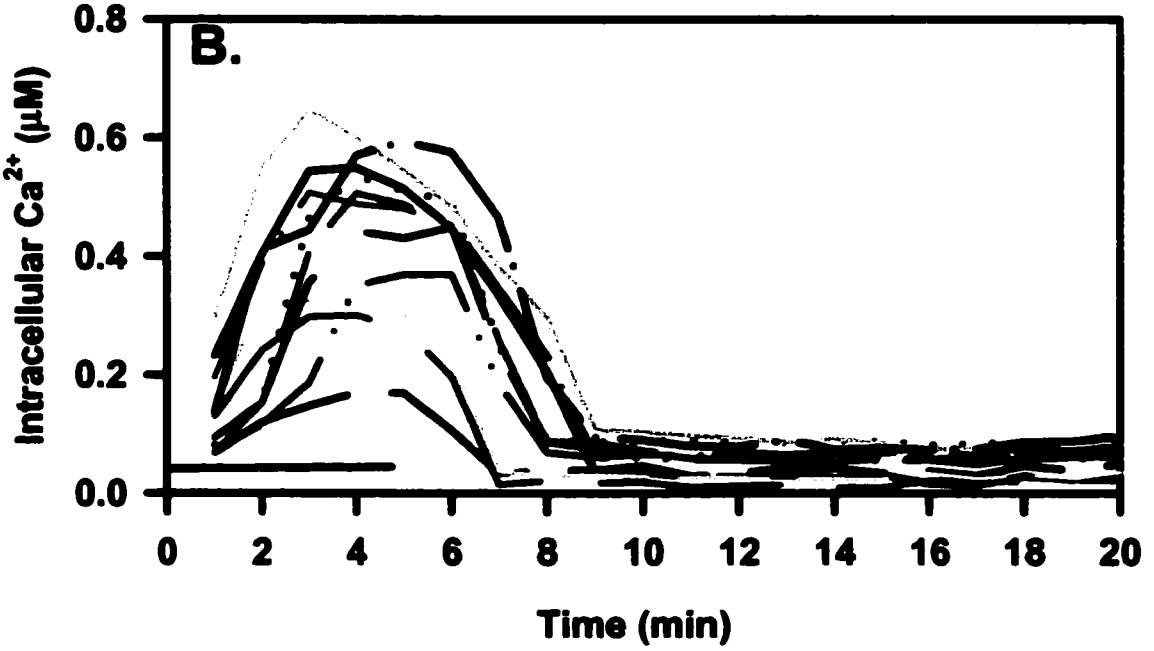
B.
Intracellular Ca2+ (μM)
0.8
0.6
0.4
0.2
0.0
0
2
4
6
8
10
12
14
16
18
20
Time (min)

following a Sr^{2+} pulse and a single Ca^{2+} transient. The mean rate of intracellular alkalinization (± s.e.m.) was 0.050 ± 0.02 pHU/min (n=69; N=5), which was not quite as high as the activity which developed after a 2 h Sr^{2+} exposure.

Development of HCO_3^-/Cl^- exchanger activity in cycloheximide-activated eggs

The results of a 5 min Sr^{2+} exposure indicated that a single Ca^{2+}_i transient was sufficient to induce upregulation of HCO_3^-/Cl^- exchanger activity, consistent with the upregulation by ethanol. I thus wished to determine whether even a single Ca^{2+}_i transient was required for upregulation of HCO_3^-/Cl^- exchanger activity. To investigate this, eggs were activated by exposure to cycloheximide (Fig. 14C), a protein synthesis inhibitor. As discussed (Introduction), cycloheximide can activate eggs by disrupting the normal continuous synthesis of cyclins by the MII-arrested egg. This results in the loss of MPF activity and exit from metaphase. Cycloheximide-induced egg activation occurs without changes in Ca^{2+}_i (Moos et al., 1996).

Eggs were exposed to 50 µg/ml cycloheximide for 2 h, which resulted in 68% activation (n=109, N=8; pronuclear development) with similar timing of pronuclear development (Fig. 36C) compared to IVF (Fig. 27C). Measurements using Fura-2 confirmed that there were no Ca^{2+}_i transients (Fig. 36B). Cycloheximide-activated eggs did, however, develop HCO_3^-/Cl^- exchanger activity (Fig. 36A) with a mean rate of intracellular alkalinization (± s.e.m.) of 0.070 ± 0.009 pHU/min (n=24; N=3) at 7-9 h post-egg activation even in the absence of Ca^{2+}_i transients.

Figure 36. Parthenogenetic activtion using protein synthesis inhibitor cycloheximide. A. HCO_3^-/Cl^- exchanger activity was assessed in eggs activated by 2 h exposure to cycloheximide followed by 7-9 h KSOM culture. Shown is mean rate of intracellular alkalinization (± s.e.m.) upon Cl^- removal. Level of HCO_3^-/Cl^- exchanger activity (measured by Cl^- removal assay) in eggs represented by dotted line (Fig. 27A) and in Sr^{2+} activated eggs represented by dashed line (Fig. 34A). B. Example of $Ca^{2+}{}_i$ measured in Fura-2 loaded eggs (n=11) upon exposure to 50 μg/ml cycloheximide. C. Time-course of pronuclear development following cycloheximide exposure. Development is normalized to total number of eggs activated for comparison between different activation protocols. Numbers as in Fig. 23.

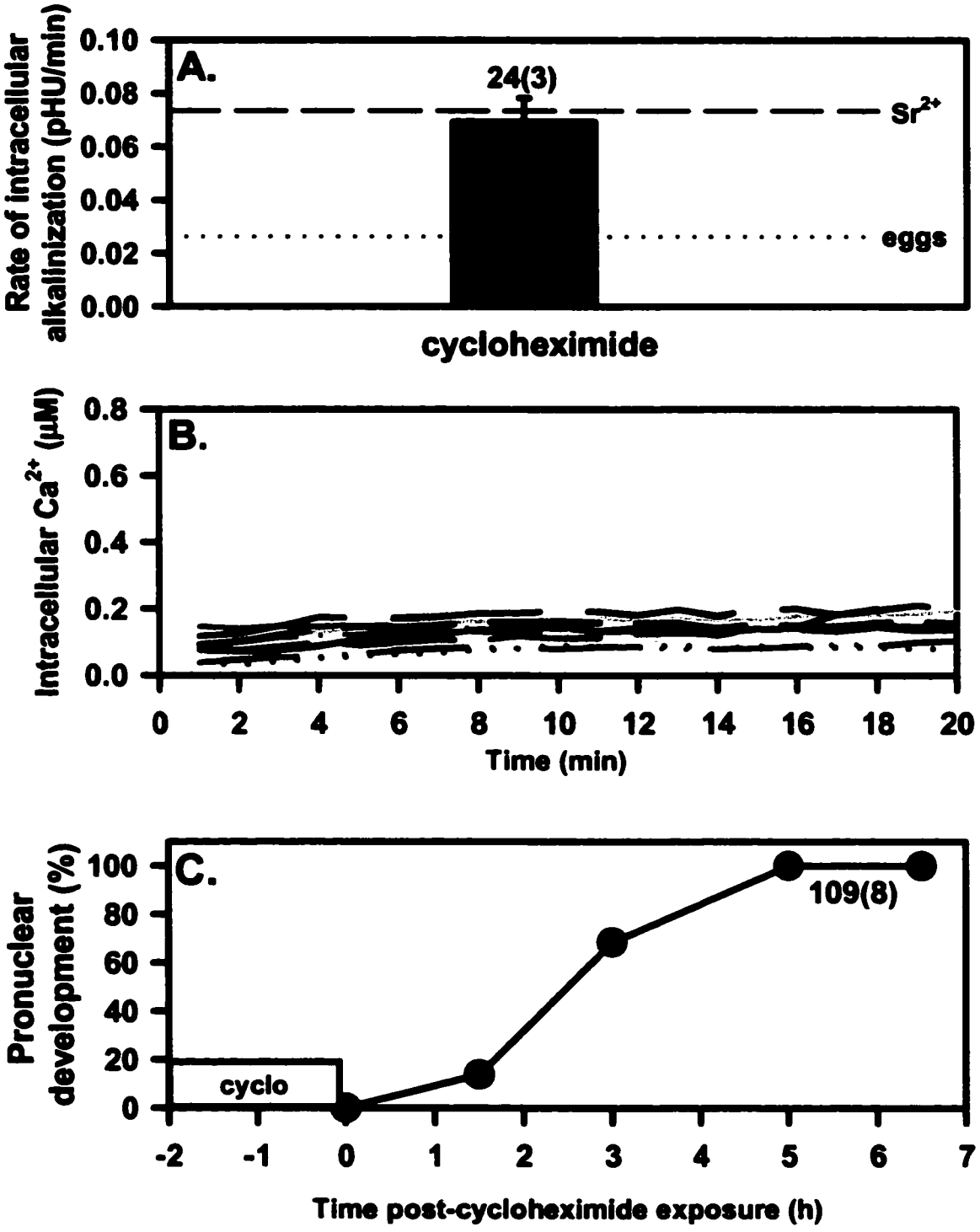
A.
24(3)
Sr^{2+}
eggs
Rate of intracellular alkalinization (pHU/min)
0.10
0.08
0.06
0.04
0.02
0.00
cycloheximide
B.
Intracellular Ca^{2+} (μM)
0.8
0.6
0.4
0.2
0.0
0
2
4
6
8
10
12
14
16
18
20
Time (min)
C.
Pronuclear development (%)
100
80
60
40
20
0
cyclo
109(8)
-2
-1
0
1
2
3
4
5
6
7
Time post-cycloheximide exposure (h)

Low HCO_3^-/Cl^- exchanger activity is not a general feature of metaphase

As unfertilized eggs, arrested in metaphase II, have very low HCO_3^-/Cl^- exchanger activity, it is possible that low HCO_3^-/Cl^- exchanger activity is a feature of any metaphase, at least during early development. HCO_3^-/Cl^- exchanger activity was therefore measured in metaphase at the end of the first cell cycle (first mitosis) - just prior to the first cytokinesis (cleavage to the 2-cell stage). Using the Sr^{2+}-activation protocol, HCO_3^-/Cl^- exchanger activity was measured before, during and after pronuclear envelope breakdown and cleavage. There was no decrease in HCO_3^-/Cl^- exchanger activity associated with this period in the cell cycle (Fig. 37A,B), indicating that once the exchanger is activated it remains active through the metaphase at the end of the first cell cycle.

One difference between MII eggs and metaphase embryos is the duration of metaphase. Unfertilized eggs are arrested in metaphase for at least several hours (by maintenance of high MPF and CSF) while mitotic metaphase is brief and there is no arrest. Thus, any metaphase-induced downregulation may require a longer period in metaphase than occurs between the 1- and 2-cell stages. To test this hypothesis, Sr^{2+}-produced zygotes (12 h post-activation) were cultured in the presence of the microtubule depolymerizing agent demecolcine (1 μg/ml) for 8 h. Demecolcine disrupts microtubules and prevents exit from metaphase, and thus demecolcine treatment arrested zygotes in metaphase at the end of the first cell cycle. Metaphase arrest using demecolcine could be maintained for at least as long as the MII arrest in unfertilized eggs. After 8 h in metaphase arrest, HCO_3^-/Cl^- exchanger activity was measured by the Cl^- removal assay. The extended demecolcine-induced metaphase arrest of Sr^{2+}-activated embryos in first

Figure 37. HCO_3^-/Cl^- exchanger activity during metaphase of first mitotis. To determine whether low HCO_3^-/Cl^- exchanger activity is a feature of mitotic metaphase, exchanger activity was measured throughout metaphase of the first cell cycle. A. Mean rates of intracellular alkalization (± s.e.m.) upon Cl^- removal. B. Timing of nuclear envelope breakdown (NEBD) and cytokinesis (cleavage to 2-cell stage; n=60, N=3). C. As eggs are arrested in metaphase II for several hours, the effects of a prolonged metaphase arrest were examined in Sr^{2+}-derived 1-cell embryos using demecolcine. 1-cell embryos (12 h post-activation) were cultured in 1 μg/ml demecolcine (vehicle control) for 6-8 h, and HCO_3^-/Cl^- exchanger assessed using the Cl^- removal assay. Shown are the mean rates of alkalinization (± s.e.m) upon Cl^- removal, which were not significantly different (Student's t-test; $p>0.05$). Note that at the time of Cl^- removal the vehicle group had progressed to the 2-cell stage, while the demecolcine-treated group remained arrested at the 1-cell stage. Numbers above points/bars as in Fig. 23.

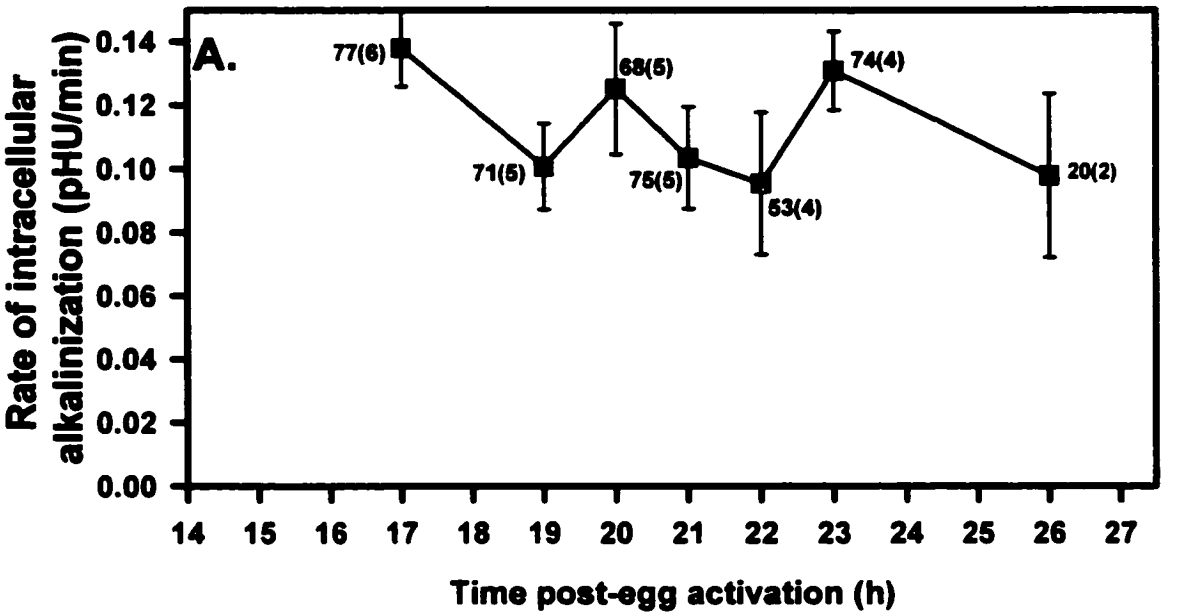
A.
Rate of intracellular alkalinization (pHU/min)
0.14
0.12
0.10
0.08
0.06
0.04
0.02
0.00
77(6)
71(5)
68(5)
75(5)
53(4)
74(4)
20(2)
14 15 16 17 18 19 20 21 22 23 24 25 26 27
Time post-egg activation (h)

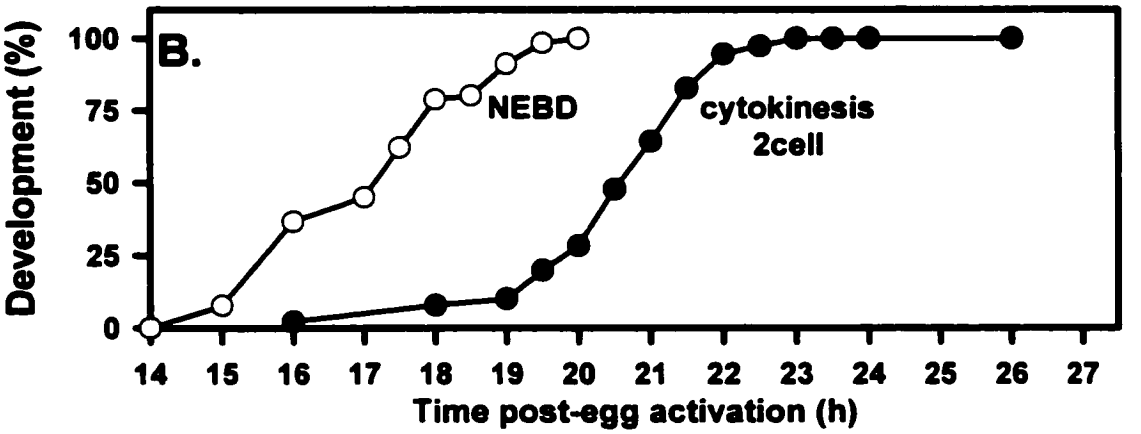
B.
Development (%)
100
75
50
25
0
NEBD
cytokinesis
2cell
14 15 16 17 18 19 20 21 22 23 24 25 26 27
Time post-egg activation (h)

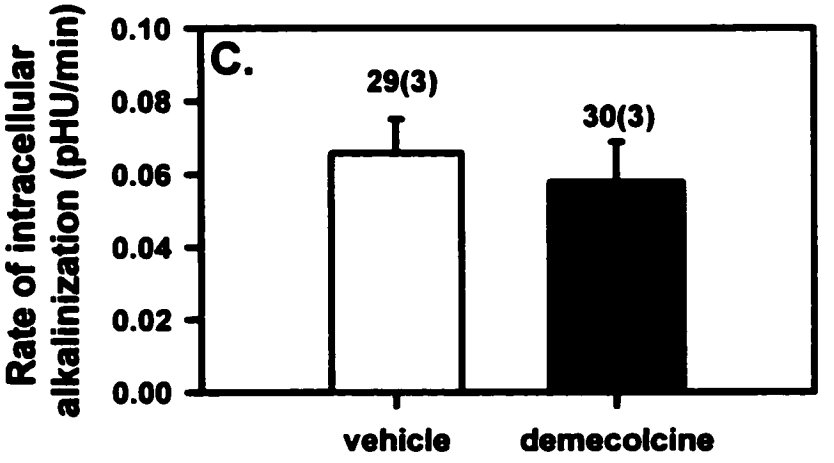
C.
Rate of intracellular alkalinization (pHU/min)
0.10
0.08
0.06
0.04
0.02
0.00
29(3)
30(3)
vehicle
demecolcine

mitotic metaphase did not, however, reduce HCO_3^-/Cl^- exchanger activity (Fig. 37C; p=0.42; Student's t-test).

V. HCO_3^-/Cl^- EXCHANGER ACTIVITY IN GV OOCYTES AND DURING MEIOTIC MATURATION

HCO_3^-/Cl^- exchanger activity is downregulated during meiotic maturation in vitro

The HCO_3^-/Cl^- exchanger could either be quiescent throughout oocyte maturation, or its activity could alternatively be downregulated prior to MII arrest. To investigate the status of HCO_3^-/Cl^- exchanger activity prior to MII arrest, HCO_3^-/Cl^- exchanger activity was measured using the Cl^- removal assay in GV oocytes and during meiotic maturation. GV oocytes were obtained and maintained in GV arrest where appropriate with 0.3 mM dbcAMP or allowed to mature in vitro through MI to MII (Fig. 38B). The rate of alkalinization upon Cl^- removal in freshly-obtained GV oocytes in the presence of dbcAMP indicated significant HCO_3^-/Cl^- exchanger activity (Fig. 38A; 0.077 ± 0.006; n=22; N=4) which was appropriately DIDS sensitive (data not shown). HCO_3^-/Cl^- exchanger activity in GV eggs was at a level comparable to that seen in zygotes obtained 8-12 h post-fertilization (Fig. 23A).

Separate groups of GV oocytes were cultured in the absence of dbcAMP to determine the timing of GVBD and to produce in vitro-matured MI and MII eggs (Fig. 38B). HCO_3^-/Cl^- exchanger activity in GV oocytes immediately prior to GVBD, in the absence of dbcAMP, was significantly higher (mean ± s.e.m.; 0.064 ± 0.008; n=54; N=6) than exchanger activity exhibited by in vitro matured MII eggs (0.028 ± 0.005; n=56; N=6; Student's t-test; p=0.003) and comparable to activity in GV oocytes in the presence

Figure 38. HCO_3^-/Cl^- exchanger activity is downregulated during meiotic maturation. A. The mean rate of intracellular alkalization (± s.e.m) upon Cl^- removal was measured in GV oocytes, maintained in prophase I arrest by 0.3 mM dbcAMP, immediately following retrieval or at various time points up to 16 h (cultured in dbcAMP, ●). Some GV oocytes were maintained in culture in the absence of dbcAMP for maturation in vitro. GV (■), MI (◒) or MII (○) oocytes were removed from culture and the mean rates of intracellular alkalization (± s.e.m) measured at various time points up to 16 h. B. Time-course of GVBD and emission of the first polar body (MI-MII transition) in GV (■), MI (●) or MII (○) oocytes matured in vitro and in GV oocytes cultured in dbcAMP (●). Numbers at points as in Fig. 23.

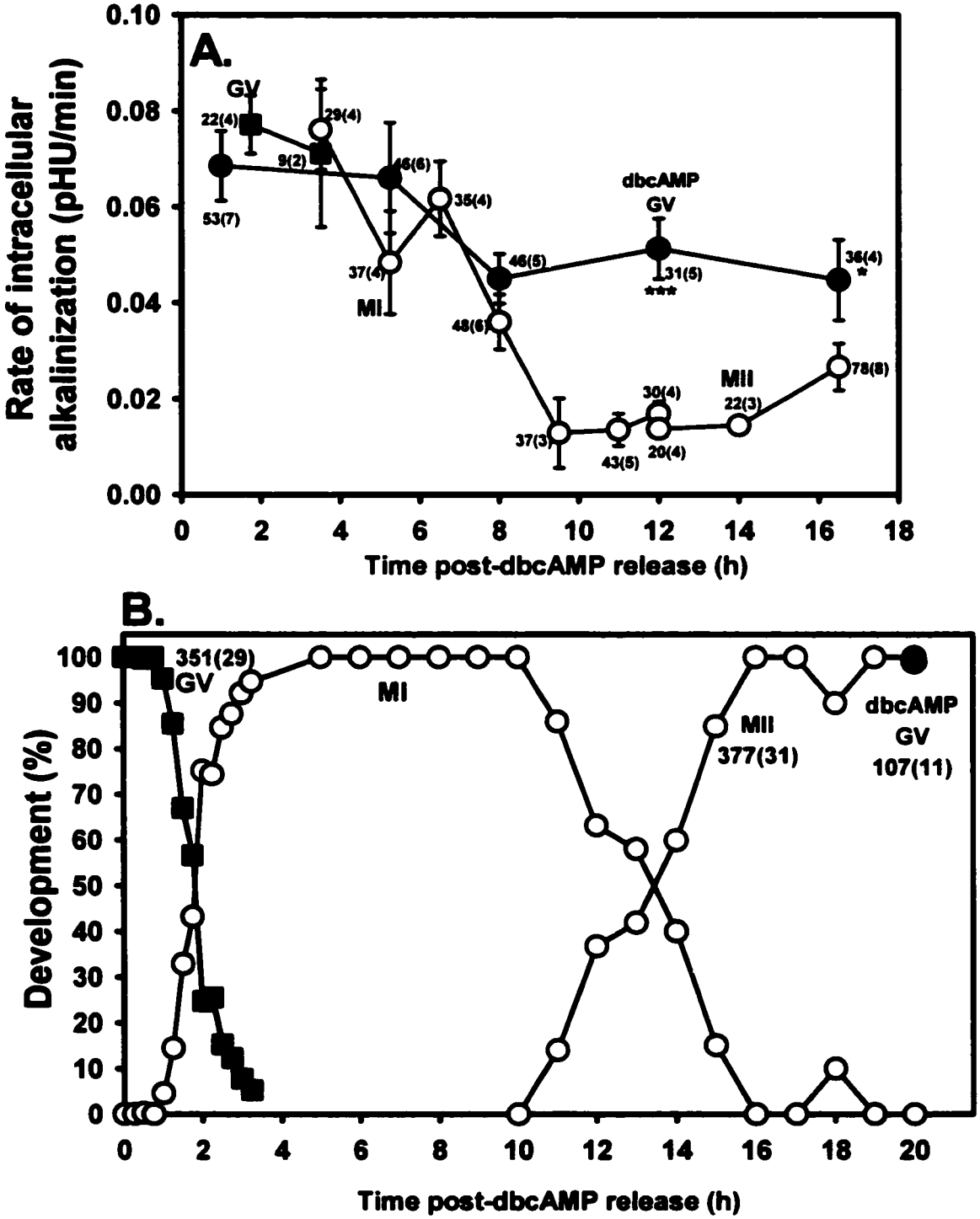
A.
Rate of intracellular alkalinization (pHU/min)
0.10
0.08
0.06
0.04
0.02
0.00
GV
22(4)
29(4)
9(2)
46(6)
53(7)
35(4)
37(4)
MI
46(5)
48(6)
dbcAMP
GV
31(5)
***
36(4)
*
MII
30(4)
22(3)
78(8)
37(3)
43(5)
20(4)
0 2 4 6 8 10 12 14 16 18
Time post-dbcAMP release (h)
B.
Development (%)
100 90 80 70 60 50 40 30 20 10 0
351(29)
GV
MI
MII
377(31)
dbcAMP
GV
107(11)
0 2 4 6 8 10 12 14 16 18 20
Time post-dbcAMP release (h)

of dbcAMP (above). HCO_3^-/Cl^- exchanger activity of in vitro-matured MII eggs was very similar to that of in vivo-matured ovulated eggs, indicating that HCO_3^-/Cl^- exchanger activity is similarly downregulated at some point after GVBD both in vivo and in vitro. To determine the time-course of this downregulation, HCO_3^-/Cl^- exchanger activity was measured in oocytes matured in vitro following removal of GV oocytes from dbcAMP (Fig. 38A). GVBD was complete within 2.5-3 h following removal from dbcAMP, yielding MI eggs with no germinal vesicle and no polar body (Fig. 2-MI). Cytokinesis began at 11-12 h following removal from dbcAMP and was completed at 17-18 h, yielding MII eggs with one polar body (Fig. 2-MII). In contrast, GV oocytes cultured in the continued presence of dbcAMP remained arrested at the GV stage for up to 20 h (Fig. 2-GV). HCO_3^-/Cl^- exchanger activity was high in GV oocytes and early MI eggs, with activity decreasing between 6-8 h following removal from dbcAMP. HCO_3^-/Cl^- exchanger activity then remained low in late MI eggs and MII eggs. Oocytes cultured in the presence of dbcAMP and thus arrested at the GV stage, maintained high HCO_3^-/Cl^- exchanger activity for up to 16.5 h following culture (Fig. 38A).

VI. UPREGULATION OF HCO_3^-/Cl^- EXCHANGER IS CELL CYCLE - DEPENDENT AND MAY INVOLVE MAPK

Disruption of the metaphase II spindle prevents upregulation of HCO_3^-/Cl^- exchanger activity following Sr^{2+}-induced egg activation

To disrupt resumption of the cell cycle upon egg activation, eggs were pretreated with 1 μg/ml demecolcine for 1 h prior to Sr^{2+}-activation (Fig. 39). Eggs were activated and maintained in culture in the presence of demecolcine for up to 7-9 h and timing of

Figure 39. HCO_3^-/Cl^- exchanger activity following egg activation with or without disruption of the MII spindle. To determine whether an intact spindle was required for Sr^{2+} to trigger HCO_3^-/Cl^- exchanger upregulation, eggs were pretreated for 1 h with demecolcine or vehicle, followed by exposure to Sr^{2+} for 2 h (demecolcine or vehicle present) and then cultured in demecolcine or vehicle for an additional 7-9 h, whereupon HCO_3^-/Cl^- exchanger activity was assessed using the Cl^- removal assay. A. Mean rates of intracellular alkalization (± s.e.m) in vehicle (Sr^{2+}) and demecolcine groups (Sr^{2+} + deme). B. Average rates of second polar body extrusion (PB2) and pronuclear development (PN). Numbers above bars/points as in Fig. 23.

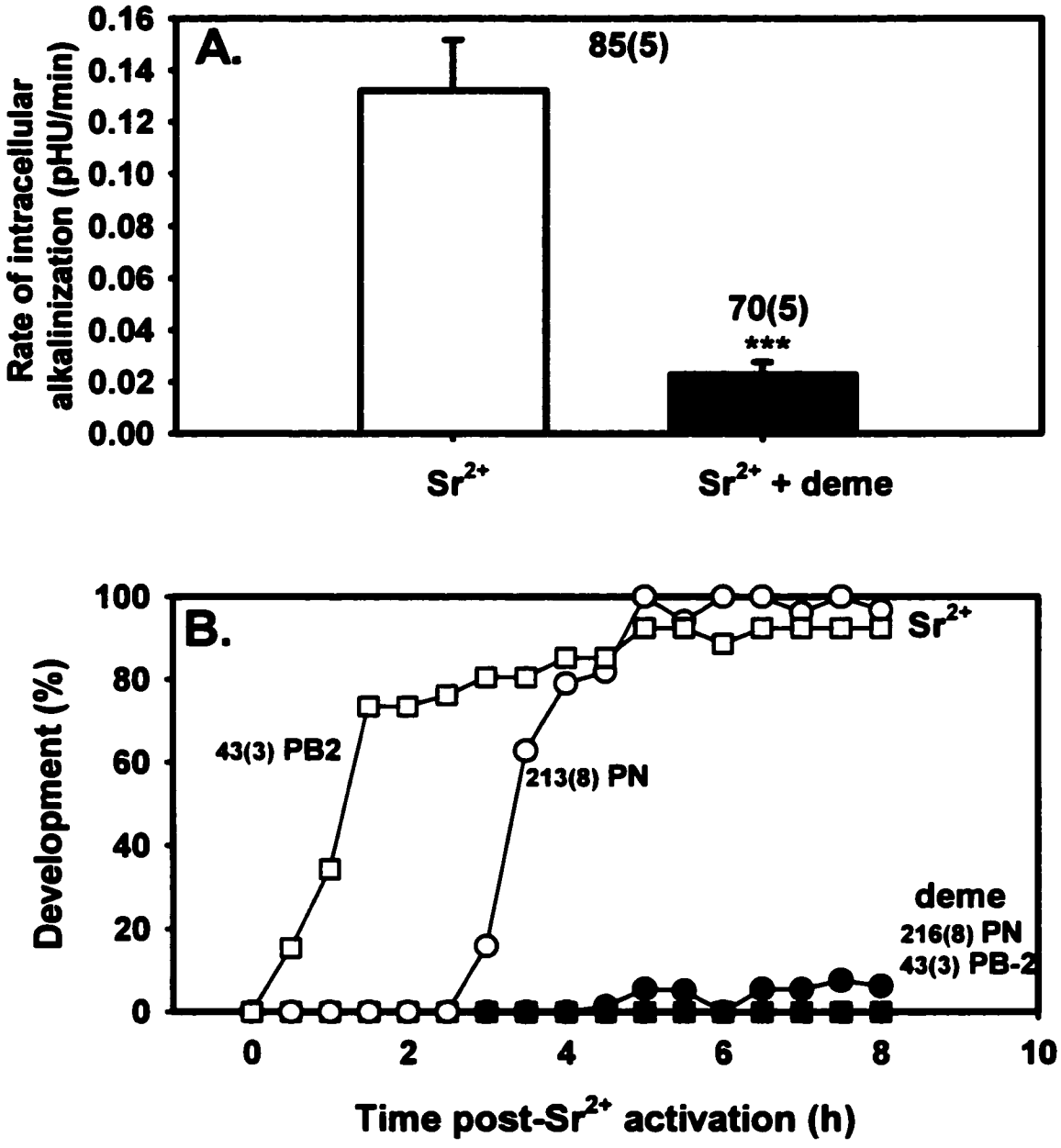
A.
85(5)
70(5)
***
Rate of intracellular alkalinization (pHU/min)
0.16
0.14
0.12
0.10
0.08
0.06
0.04
0.02
0.00
Sr2+
Sr2+ + deme
B.
Sr2+
43(3) PB2
213(8) PN
deme
216(8) PN
43(3) PB-2
Development (%)
100
80
60
40
20
0
0
2
4
6
8
10
Time post-Sr2+ activation (h)

pronuclear development was assessed (Fig. 39B). As discussed, demecolcine disrupts microtubules, thereby dismantling the metaphase II spindle. Exit from metaphase is dependent on an intact spindle (Verlhac et al., 1993; Moos et al., 1996). Ca^{2+}_i transients occurred normally in demecolcine-treated eggs upon Sr^{2+}- activation (assessed with Fura-2; data not shown). However, pronuclear development was completely inhibited by demecolcine treatment (Fig. 39B). HCO_3^-/Cl^- exchanger activity was measured using the Cl^- removal assay 7-9 h post Sr^{2+} activation (Fig. 39A). Demecolcine significantly inhibited the upregulation of HCO_3^-/Cl^- exchanger activity (0.023 ± 0.005) compared to control (0.13 ± 0.02; Student's t-test, p=0.004), maintaining it at a level comparable to that in unfertilized eggs.

Okadaic acid treatment prevents upregulation of HCO_3^-/Cl^- exchanger activity

Eggs were cultured with okadaic acid (OA), an inhibitor of protein phosphatases PP1 and PP2A (Cohen et al., 1990), and previously shown to maintain high MAPK activity in fertilized eggs (Schwartz and Schultz, 1991; Moos et al., 1996). OA (2.5 μM) was added at various times either before, during, or following Sr^{2+} activation and remained present throughout the culture period. OA inhibits pronuclear development or cause precocious pronuclear envelope breakdown (NEBD) in mouse zygotes following fertilization (Schultz et al., 1991; Moos et al., 1996). Thus, the presence of pronuclei was assessed throughout the culture period. For most experiments, HCO_3^-/Cl^- exchanger activity was assessed 7-9 h post-Sr^{2+} activation. When OA was introduced 15 min prior to or coincident with Sr^{2+} activation (t=0 h), pronuclear development was completely inhibited compared to vehicle controls (Fig. 40B). When OA was introduced following Sr^{2+} activation (1.5 h, 3 h, 8 h) pronuclei formed but premature nuclear envelope

Figure 40. HCO_3^-/Cl^- exchanger activity following okadaic acid (OA) treatment. Eggs were activated with Sr^{2+} and exposed to 2.5 μM OA (vehicle control) at various times (-15 min, 0, 1.5, 3, 8 or 24 h) post-Sr^{2+} introduction. When OA was introduced up to 3 h post-Sr^{2+} activation, eggs were cultured up to 7-9 h post-activation and HCO_3^-/Cl^- exchanger activity assessed. When OA was introduced at 8 h (mature 1-cell embryo) or 24 h (2-cell embryo), embryos were cultured for an additional 8 h in the presence of OA followed by assessment of HCO_3^-/Cl^- exchanger using the Cl^- removal assay. A. Mean rates of intracellular alkalinization (± s.e.m). B. Average rates of pronuclear/nuclear formation and breakdown with OA added at t=0. Numbers above bars as in Fig. 23.

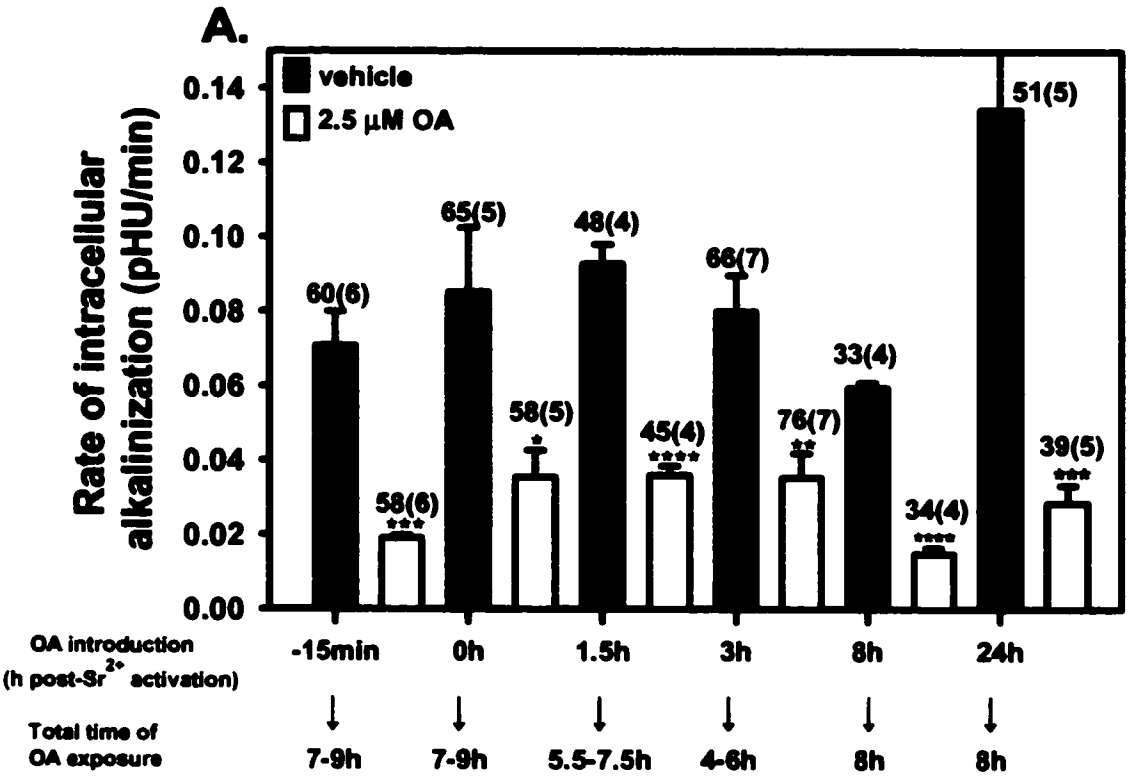
A.
vehicle
2.5 µM OA
Rate of intracellular alkalinization (pHU/min)
0.14
0.12
0.10
0.08
0.06
0.04
0.02
0.00
60(6)
58(6)
65(5)
58(5)
48(4)
45(4)
66(7)
76(7)
33(4)
34(4)
51(5)
39(5)
OA introduction (h post-Sr2+ activation)
-15min
0h
1.5h
3h
8h
24h
Total time of OA exposure
7-9h
7-9h
5.5-7.5h
4-6h
8h
8h

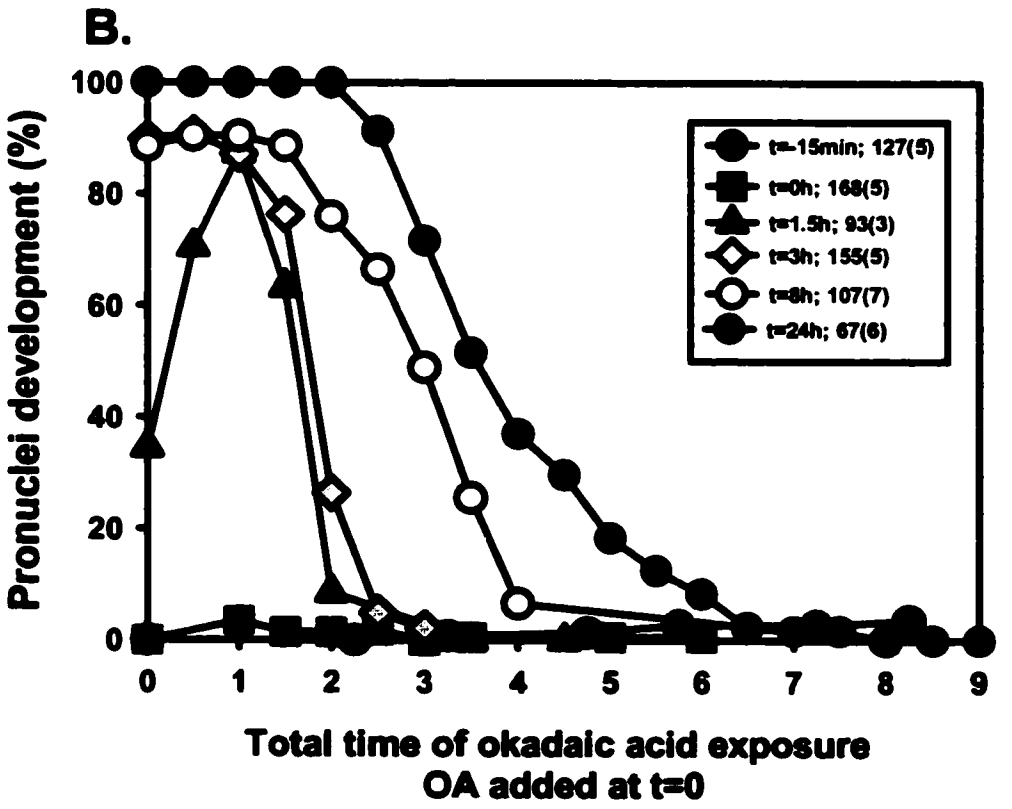
B.
Pronuclei development (%)
100
80
60
40
20
0
0
1
2
3
4
5
6
7
8
9
t=-15min; 127(5)
t=0h; 168(5)
t=1.5h; 93(3)
t=3h; 155(5)
t=8h; 107(7)
t=24h; 67(6)
Total time of okadaic acid exposure
OA added at t=0

breakdown (NEBD) then occurred. OA significantly inhibited the development of HCO_3^-/Cl^- exchanger activity when added 15 min before activation (Fig. 40A; OA: 0.019 ± 0.0007; n=58, N=6; control: 0.071 ± 0.009; n=60, N=6; Student's t-test; p=0.0002), coincident with Sr^{2+}-activation (t=0 h; OA: 0.035 ± 0.007; n=58, N=5; control: 0.085 ± 0.017; n=65, N=5; Student's t-test; p=0.029), 1.5 h post-activation (OA: 0.036 ± 0.003; n=45, N=4; control: 0.093 ± 0.005; n=48, N=4; Student's t-test; p=0.00007) and 3 h post-activation (0.035 ± 0.007; n=76, N=7; control 0.080 ± 0.010; n=66, N=7; Student's t-test; p=0.003). OA was introduced in these experiments during the period of development of HCO_3^-/Cl^- exchanger activity. OA treatment, at least in part, acts to prevent the upregulation of HCO_3^-/Cl^- exchanger activity.

To determine whether OA treatment could inhibit fully active HCO_3^-/Cl^- exchanger activity, OA was introduced 8 h following Sr^{2+}-activation. Sr^{2+}-produced zygotes were treated with OA for 4 h followed by assessment of HCO_3^-/Cl^- exchanger activity by the Cl^- removal assay. However, HCO_3^-/Cl^- exchanger activity was not significantly reduced by a 4 h OA treatment in mature Sr^{2+}-produced zygotes (OA: 0.077 ± 0.011, n=107, N=9; control: 0.10 ± 0.015; n=104, N=9; Student's t-test; p=0.16; not shown). It was possible that the brief 4 h OA treatment was insufficient to inhibit the fully active HCO_3^-/Cl^- exchanger, present 8 h post-Sr^{2+}-activation. The experiment was repeated again, this time with OA exposure extended from 4 h to 8 h. The extended OA exposure (8 h OA treatment) was sufficient to significantly downregulate HCO_3^-/Cl^- exchanger activity in zygotes (OA: 0.015 ± 0.0016; n=34, N=4; control: 0.060 ± 0.0014; n=33, N=4; Student's t-test; $p<10^{-6}$; Fig. 40A).

To investigate further whether fully active HCO_3^-/Cl^- exchange is refractory to

downregulation by OA, eggs were activated by Sr^{2+} and cultured for 24 h (to the 2-cell stage) whereupon OA was introduced for an additional 8 h. Nuclear envelope breakdown (NEBD) was observed in OA-treated embryos but not control (vehicle-treated) embryos. OA treatment significantly decreased HCO_3^-/Cl^- exchanger activity in 2-cell embryos (Fig. 40A; OA: 0.029 ± 0.005; n=39, N=5; control: 0.13 ± 0.017; n=51, N=5; Student's t-test; p=0.00035).

MEK inhibitor U0126 parthenogenetically activates unfertilized eggs

Eggs were cultured in the presence of the MEK inhibitor U0126 (50 μM) for up to 9 h (Fig. 41). A much higher proportion of unfertilized MII eggs treated with U0126 were parthenogenetically activated (71%; n=167; N=14) compared to vehicle-treated eggs (11%; n=178; N=16; Fisher's Exact test, p<0.0001; Fig. 41A). Parthenogenotes were classified at 7-9 h following U0126 treatment on the basis of morphology and assigned to one of three classes (Fig. 7) which were first used by Hirao and Eppig (1997) to classify parthenogenotes derived from $mos^{-/-}$ oocytes. Class I included activated eggs that exhibited second polar body emission or pronuclear development, Class II included activated eggs that exhibited abnormal cleavage or fragmentation and Class III included activated eggs that immediately cleaved to the 2-cell stage. U0126 treatment produced all three types, but primarily Class I parthenogenotes (58%; Fig. 14D) compared to Class II (4%) or Class III (8%) parthenogenotes (Fig. 41A). The timing of PB2 emission and PN development in Class I parthenogenotes (Fig. 41B) was similar to that in oocytes following IVF (Fig. 27C) or in Sr^{2+} activated eggs (Fig. 34C). Developmental potential of these U0126-activated eggs was limited to precocious cleavage during the first 12 h

Figure 41. Parthenogenetic activation by the MEK inhibitor U0126. Unfertilized eggs were treated with 50 μM U0126 (n=167, N=14) or vehicle (control; n=178, N=16) for up to 9 h. A. Average incidence of parthenogenesis measured at 7-9 h following U0126 or vehicle (control) exposure. For parthenogenetic activation following U0126 treatment, parthenogenotes were assigned to one of three parthenogenetic classes (Class I, II or III, inset) established by Hirao and Eppig (1997; see Fig. 7). **** represents statistical significance, $p<0.0001$; Fisher's Exact Test). B. Shown is average seond polar body (PB2) emission and pronuclear development (PN) in U0126- ( ) or vehicle-treated eggs (□○). Numbers above bars as in Fig. 23.

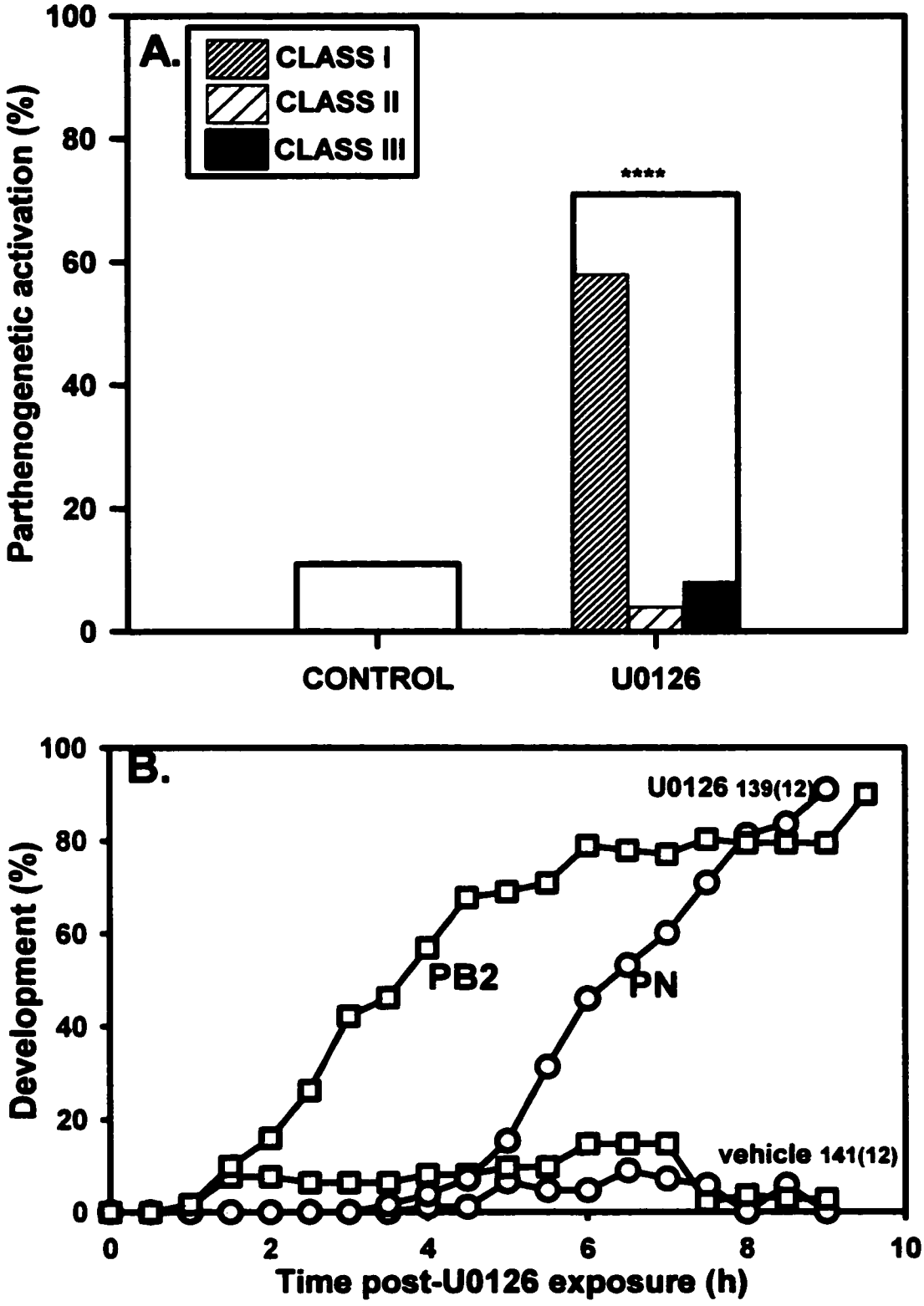
A.
CLASS I
CLASS II
CLASS III
****
Parthenogenetic activation (%)
100
80
60
40
20
0
CONTROL
U0126
B.
U0126 139(12)
PB2
PN
vehicle 141(12)
Development (%)
100
80
60
40
20
0
0
2
4
6
8
10
Time post-U0126 exposure (h)

following U0126 exposure followed by degeneration after 24-36 h (data not shown).

U0126 treatment of unfertilized eggs activates HCO_3^-/Cl^- exchanger activity

U0126-treated eggs (see above) were assessed for HCO_3^-/Cl^- exchanger activity using the Cl^- removal assay at 7-9 h following U0126 exposure (Fig. 42). HCO_3^-/Cl^- exchanger activity was significantly higher in U0126-activated eggs (0.072 ± 0.0053) compared to vehicle treated eggs (0.027 ± 0.0004; Student's t-test; p=0.00014), reaching a level similar to that seen in IVF- or Sr^{2+}-activated eggs.

U0126 may stimulate activation of HCO_3^-/Cl^- exchanger activity in unfertilized eggs, independent of cell cycle resumption

To attempt to separate the effects of cell cycle resumption from MEK/MAPK inhibition on HCO_3^-/Cl^- exchanger activity, eggs were pretreated with demecolcine followed by U0126 activation in the continued presence of demecolcine for up to 11 h ("deme + U0126"; Fig. 43). Some eggs were pretreated with the vehicle for demecolcine (ethanol) followed by continued culture with both U0126 and the vehicle for demecolcine ("U0126"). A second control group was pretreated with the vehicle for demecolcine followed by continued culture with the vehicles for both demecolcine (ethanol) and U0126 (DMSO; "control"). Parthenogenetic activation was assessed as described above in all three groups for up to 9 h. Total parthenogenetic activation by U0126 following a 1 h vehicle pretreatment (ethanol) was reduced (37%; n=226; N=21) compared to U0126-treated eggs with no pretreatment (71%, see above). However, even with these experimental manipulations, parthenogenetic activation following U0126 treatment was

Figure 42. Activation of HCO_3^-/Cl^- exchanger activity by the MEK inhibitor U0126. Unfertilized eggs were exposed to the MEK inhibitor U0126 (50 μM) or vehicle for 7-10 h followed by measurement of HCO_3^-/Cl^- exchanger by Cl^- removal assay. Shown are mean rates of intracellular alkalinization (± s.e.m). ****; $p<0.0001$; Student's t-test. Level of HCO_3^-/Cl^- exchanger activity (measured by Cl^- removal assay) in eggs represented by dotted line (Fig. 27A) and in Sr^{2+} activated eggs represented by dashed line (Fig. 34A). Numbers above bars as in Fig. 23.

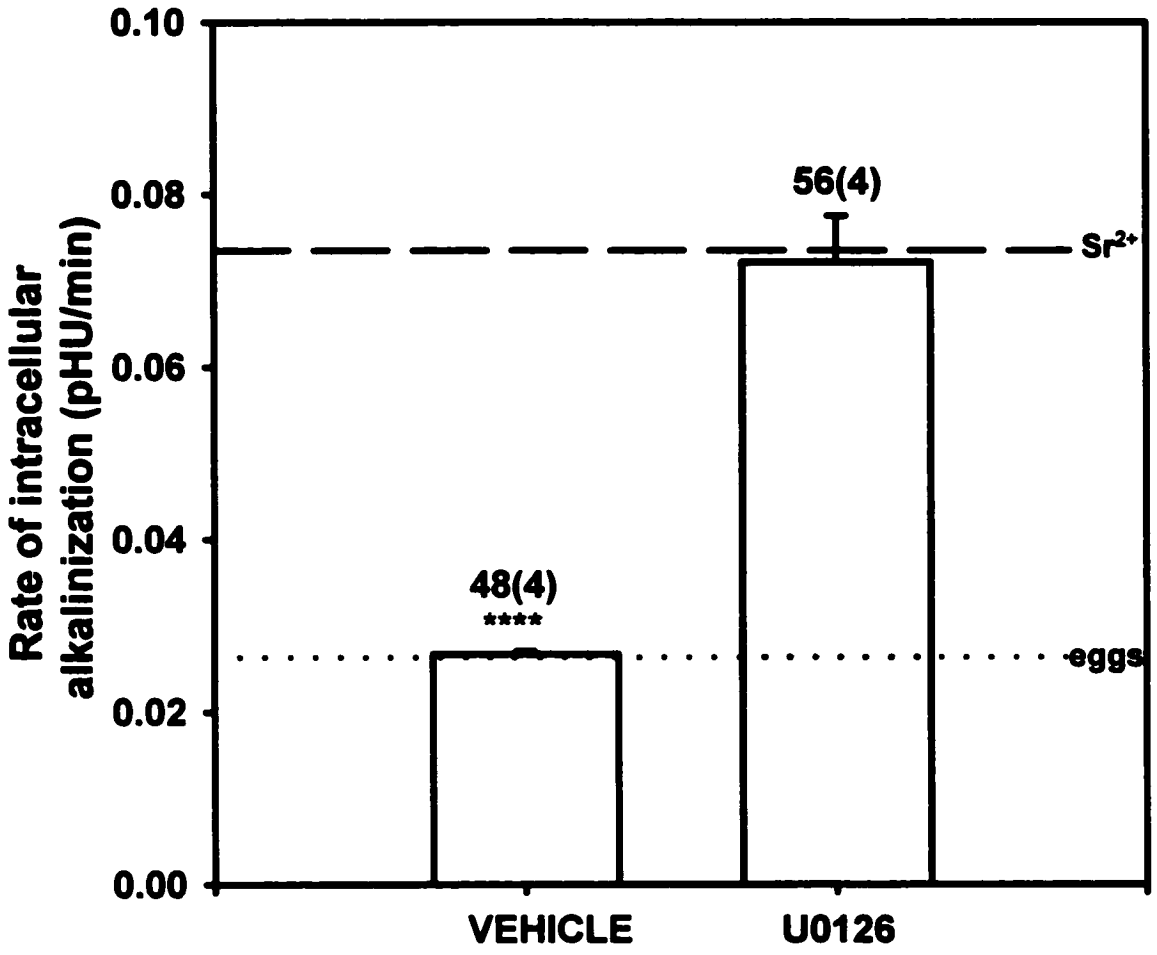
0.10
0.08
0.06
0.04
0.02
0.00
Rate of intracellular alkalinization (pHU/min)
56(4)
Sr2+
48(4)
****
eggs
VEHICLE
U0126

Figure 43. Parthenogenetic activation following disruption of the MII spindle combined with U0126 treatment. Average incidence of parthenogenesis in eggs treated with demecolcine or vehicle for 1 h, followed by demecolcine + U0126 treament (DEME + U0126; n=150, N=14), vehicle treatment (CONTROL; n=77, N=8) or vehicle + U0126 treatment (U0126; n=226; N=21) for 7-9 h. Total parthenogenetic activation was significantly lower in the DEME + U0126 and CONTROL groups compared to the U0126 group ($p<0.05$ nonparametric ANOVA; Dunn's Multiple Comparisons Test). For parthenogenetic activation in the U0126 group, parthenogenotes were assigned to one of three parthenogenetic classes (Class I, II or III, inset) established by Hirao and Eppig (1997; see Fig. 7).

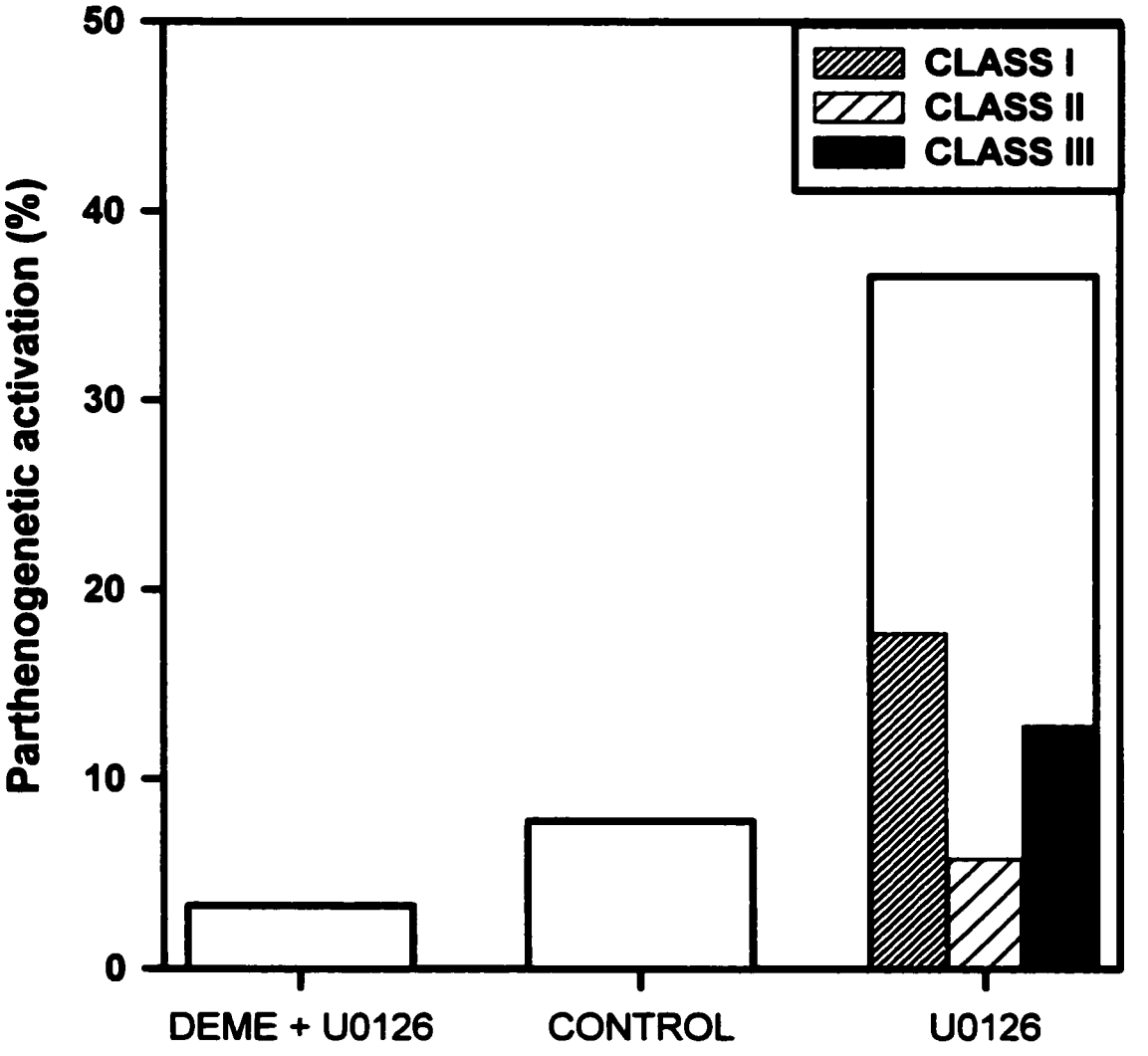
50
40
30
20
10
0
Parthenogenetic activation (%)
CLASS I
CLASS II
CLASS III
DEME + U0126
CONTROL
U0126

significantly higher than in demecolcine-treated eggs (3%; n=150; N=14; $p<0.001$) or vehicle-treated eggs (8%; n=77; N=8; nANOVA; Dunn's Multiple Comparisons Test; $p<0.05$). Following vehicle pretreatment, U0126-treated eggs exhibited a higher proportion of Class II (16%) and Class III parthenogenotes (35%) than U0126-treated eggs without pretreatment (see above; Class II: 6%; Class III: 12% of total activated). The additional manipulations (i.e., even vehicle pretreatment) required to arrest eggs in metaphase prior to U0126 exposure reduced the incidence of total parthenogenetic activation and the proportion of Class I parthenogenotes (U0126 with vehicle pretreatment: 49% of total activated) compared to the previous experiments, wherein eggs were treated with U0126 alone (82% Class I parthenogenotes of total activated) immediately after isolation from the female reproductive tract.

Because U0126-treated eggs without these additional manipulations exhibited very high HCO_3^-/Cl^- exchanger activity (Fig. 42) and corresponding high rates of parthenogenetic activation (71%), parthenogenetic activation was used as a bioassay for the efficacy of U0126 in a given experiment. Thus, only experiments where the U0126 group parthenogenetically activated to at least 50% (total activation) at 8 h post-U0126 exposure were used for measurement of HCO_3^-/Cl^- exchanger activity (Fig. 44). For each experiment demecolcine + U0126 treatments were performed in parallel to U0126 treatment, and HCO_3^-/Cl^- exchanger activity measurements performed only if parthenogenetic activation in the U0126 group exceeded 50%. For these experiments, HCO_3^-/Cl^- exchanger activity was measured in all embryos within each group (deme + U0126, U0126, control) by the Cl^- removal assay with no preselection for activation. In addition, HCO_3^-/Cl^- exchanger activity was measured in these paired groups (deme +

Figure 44. HCO_3^-/Cl^- exchanger activity following disruption of the MII spindle combined with U0126 treatment. Eggs were pretreated with demecolcine or vehicle for 1 h, followed by culture with demecolcine + U0126, vehicle + U0126 or vehicle + vehicle (CONTROL) for 7-9 h. Only groups with at least 50% activation were used for HCO_3^-/Cl^- exchanger activity measurements (see text for details). Vehicle-pretreated, U0126 activated (n=96, N=10) and demecolcine-pretreated, U0126 activated (n=90, N=10) groups were treated as paired experiments (●) such that HCO_3^-/Cl^- exchanger activity (measured by the Cl^- removal assay) for each experiment was correlated. A linear regression was fitted to the data (solid line) with 95% confidence intervals shown as dashed lines. HCO_3^-/Cl^- exchanger activity for each experiment in the CONTROL treatment group is also shown (○; n=49, N=6).

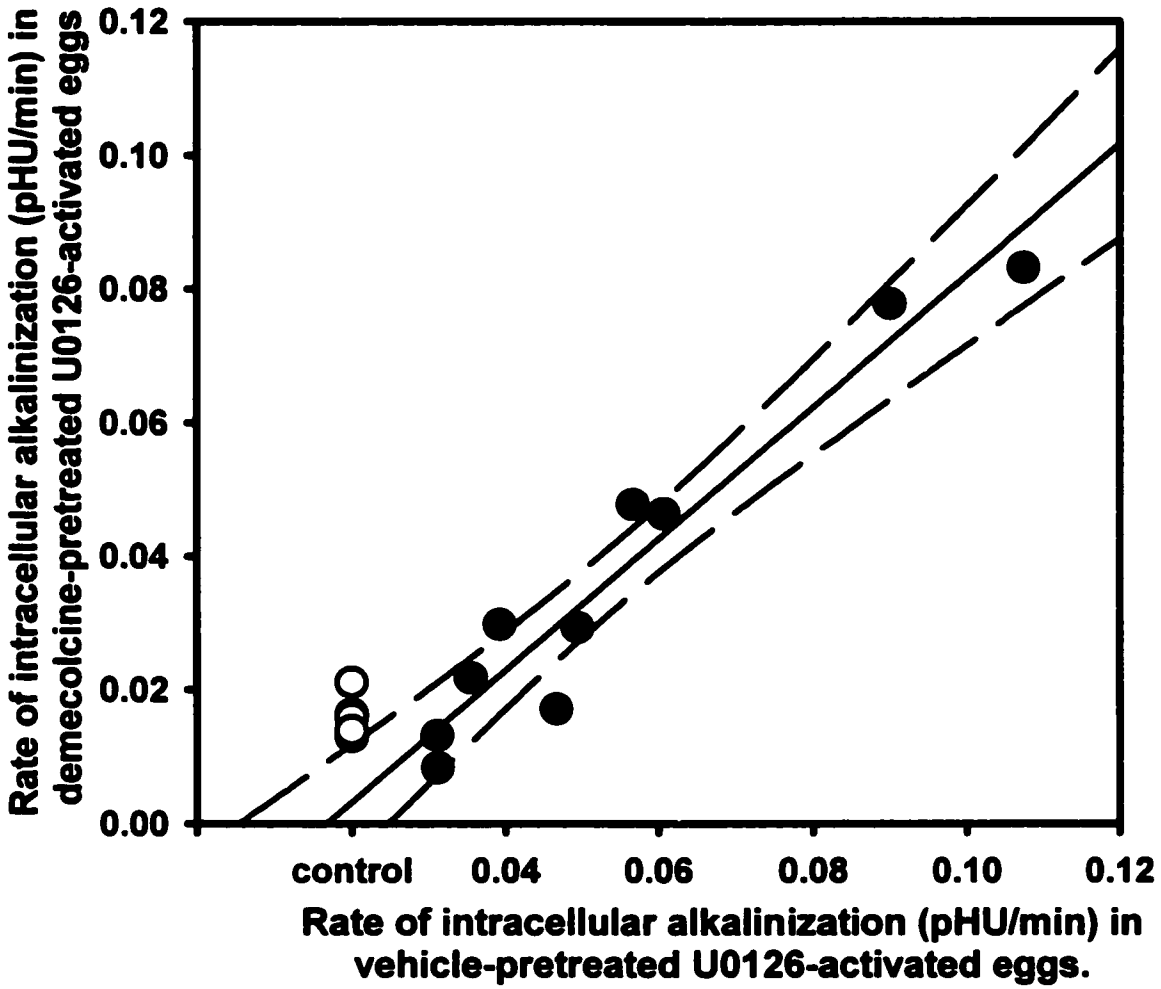
Rate of intracellular alkalinization (pHU/min) in demecolcine-pretreated U0126-activated eggs
0.12
0.10
0.08
0.06
0.04
0.02
0.00
control
0.04
0.06
0.08
0.10
0.12
Rate of intracellular alkalinization (pHU/min) in vehicle-pretreated U0126-activated eggs.

U0126 vs. U0126) simultaneously. In contrast to the previous set of experiments (see above) where demecolcine inhibited HCO_3^-/Cl^- exchanger upregulation in Sr^{2+} activated eggs, demecolcine did not inhibit the development of HCO_3^-/Cl^- exchanger activity in U0126-treated eggs. HCO_3^-/Cl^- exchanger activity in paired demecolcine + U0126-treated and U0126-treated eggs was positively correlated (0.99). The mean rate of intracellular alkalinization upon Cl^- removal was 0.038 ± 0.008 (n=90; N=10) in demecolcine + U0126-treated eggs, 0.055 ± 0.008 (n=96; N=10) in U0126-treated eggs and 0.016 ± 0.001 (n=49; N=6) in vehicle-treated eggs.

DISCUSSION

I. Very little change in pH_i accompanies GVBD or egg activation in the mouse

Studies of sea urchin fertilization identified two major events at fertilization; an increase in Ca^{2+}_i and an increase in pH_i. A transient increase in Ca^{2+}_i has thus far proven to be a universal feature of fertilization (Yanagamachi, 1988). In several species examined, GVBD or fertilization is accompanied by a pH_i increase (sea urchin, Johnson et al., 1976; *Xenopus,* Webb and Nuccitelli, 1981; *Urechis caupo*, Paul, 1975; bivalves, Brassard et al., 1988; limpets, Dubé et al., 1985; Guerrier et al., 1986). The phenomenon of a pH_i increase upon cell activation is also seen in somatic cells (e.g. fibroblasts; Mendoza, 1988), where it can also follow a transient increase in Ca^{2+}_i. While the role of Ca^{2+}_i at fertilization in mammals had been well examined (Whitaker and Irvine, 1984; Swann and Whitaker, 1986; Swann and Whitaker, 1990; Miyazaki, 1991), it was not known whether mammalian fertilization was accompanied by changes in pH_i. Thus, a role for pH_i or changes in pH_i regulatory mechanisms had not been investigated in any mammalian model and indeed, in only one vertebrate, the frog.

pH_i was measured here in mouse eggs during parthenogenetic activation, and before and after in vivo fertilization. No change in pH_i accompanied parthenogenetic activation, suggesting that egg activation did not involve immediate changes in pH_i (Fig. 22A). Similarly, in the nominal absence of HCO_3^-/CO_2 no change in pH_i accompanied parthenogenetic egg activation (Fig. 22C). While I was investigating pH_i changes during mammalian parthenogenetic egg activation, there was a report that showed that no change in pH_i accompanied in vitro fertilization of mouse eggs (Kline and Zagray, 1994). As pH_i

did not change during fertilization (Kline and Zagray, 1994; 1995) or parthenogenetic activation (Fig. 22A), this suggested that mouse eggs do not exhibit an increase in pH_i in the period immediately following sperm-egg fusion, unlike in sea urchin eggs where a pH_i increase occurs within a few minutes.

It was possible, however, that any increase in pH_i following fertilization in mammals followed a slower time-course compared to animals which exhibit a more rapid progression of egg activation and embryo development (e.g. sea urchin, *Xenopus*). This would not have been detected by the technique used by Kline and Zagray, which addressed the possibility of an increase relatively soon after fertilization, or by my investigation of parthenogenetic activation, which spanned a similarly short period. Steady-state pH_i of unfertilized eggs was therefore compared to that of zygotes approximately 6 h after in vivo fertilization. Measurement of steady-state pH_i of zygotes fertilized in vivo also precludes the possibility that artificially activating the egg through techniques such as ethanol-induced parthenogenetic activation may act through a separate pathway that does not include a pH_i change. However, no difference in pH_i was found between unfertilized and fertilized eggs (Fig. 22B).

In the absence of external HCO_3^-/CO_2, there was a significantly lower pH_i (<0.1 pH unit) in zygotes compared to eggs (Fig. 22D). This small change is probably not physiologically relevant, since HCO_3^-/CO_2 is present in the female reproductive tract. Thus, unlike in marine invertebrates and *Xenopus*, fertilization in the mouse (Kline and Zagray, 1994; Phillips and Baltz, 1996) is not accompanied by an increase in pH_i. A lack of change in pH_i at fertilization has since been confirmed in the rat (Ben-Yosef et al., 1996) and human (Dale et al., 1998). In the pig oocyte, however, a small pH_i increase

(0.1-0.2 pH) has recently been reported to accompany parthenogenetic activation by ethanol or A23187 and a larger pH_i increase was found upon thimerosol exposure (Ruddock et al., 2000). However, each method of parthenogenetic activation appears to act via a different pH_i-perturbing pathway (Ruddock et al., 2000), making it unlikely that these pH_i increases are normal physiological responses to egg activation.

It was also possible that mammalian oocytes resembled those of the limpet-*Patella vulgata*, in which an increase in pH_i accompanies the release from prophase I (GVBD), rather than at fertilization, which occurs in metaphase I in this species (Dubé et al., 1985). Therefore, I measured steady-state pH_i in GV oocytes (Fig. 22B). There was no significant difference between the pH_i of GV oocytes and ovulated eggs, indicating that there is no sustained increase in pH_i in mouse eggs following GVBD. Similarly, pH_i of GV oocytes and unfertilized eggs was identical in the absence of HCO_3^-/CO_2 (Fig. 22D). Indeed, pH_i remains virtually unchanged from the GV oocyte through preimplantation embryo development: pH_i of the embryo from the 1-cell through blastocyst stages is approximately the same as that of the egg (Zhao et al., 1995). pH_i of human oocytes is also not different in GV oocytes compared to MII oocytes (Dale et al., 1998; Phillips et al., 2000; see Appendix). Rat GV oocytes, however, exhibit significantly lower pH_i (by 0.2 units) compared to unfertilized rat eggs (Ben-Yosef et al., 1995). The conflicts between these reports may be due to species variation between mice and rats or due to the conditions used for each study, but this has not been investigated.

II. HCO_3^-/Cl^- exchanger activity appears following fertilization

An increase in the fertilized egg's ability to regulate pH_i, rather than a net change

in pH_i, may be a more important consequence of mammalian fertilization. Opposing pH_i regulatory systems (e.g. Na^+/H^+ antiporter and HCO_3^-/Cl^- exchanger, Fig. 15), simultaneously activated at fertilization, would not necessarily result in a net change in pH_i but would provide more robust pH_i regulation. Such an activation without a net change in pH_i is observed following vasopressin activation of renal mesangial cells, in which both HCO_3^-/Cl^- exchanger and Na^+/H^+ antiporter become activated (Ganz et al., 1989). As HCO_3^-/Cl^- exchanger activity exists in all preimplantation mouse embryos (1-cell through blastocyst; Baltz et al., 1991; Zhao et al., 1995), I investigated whether HCO_3^-/Cl^- exchanger activity was present in unfertilized mouse eggs and whether HCO_3^-/Cl^- exchanger activity increased as a consequence of fertilization.

HCO_3^-/Cl^- exchanger activity was first investigated in unfertilized eggs and zygotes by the Cl^- removal assay during which changes in pH_i or Cl^- were detected using fluorescent imaging. Removal of external Cl^- causes any HCO_3^-/Cl^- exchanger present to run in reverse, resulting in Cl^- efflux coupled to HCO_3^- influx. The influx of HCO_3^- thus produces a marked intracellular alkalinization only if active HCO_3^-/Cl^- exchangers are present (Nord et al., 1988). It has been shown that such alkalinization upon Cl^- removal in mouse embryos is due solely to HCO_3^-/Cl^- exchanger activity (Baltz et al., 1991; Zhao et al., 1995).

Zygotes, obtained 8-12 h following fertilization in vivo exhibited a large intracellular alkalinization upon removal of external Cl^- that was appropriately DIDS-sensitive, indicating the presence of HCO_3^-/Cl^- exchanger activity (Fig. 23A, C). However, unfertilized eggs exhibited a very small intracellular alkalinization upon removal of external Cl^- (Fig. 23A, B). Furthermore, this small alkalinization was not

inhibitable by 500 μM DIDS, which is sufficient to completely inhibit HCO_3^-/Cl^- exchanger activity (Lee et al., 1991; Humphreys et al., 1994; Zhao and Baltz, 1996). Therefore, significant HCO_3^-/Cl^- exchanger activity is absent from the unfertilized egg but is maximally activated in pronuclear-stage zygotes obtained several hours following fertilization.

Upon removal of external Cl^-, intracellular Cl^- will exit the cell via available anion transport pathways. In mouse eggs and zygotes, Cl^- efflux pathways potentially include at least HCO_3^-/Cl^- exchangers and Cl^- channels, the latter shown to be present in both eggs and zygotes by patch-clamp electrophysiological recording (Kolajova and Baltz, 1999; and unpublished). Thus, total Cl^- efflux upon Cl^- removal would be expected to occur via several routes. Total Cl^- efflux in eggs and zygotes was detected by monitoring changes in the intensity of the Cl^--sensitive fluorophore, MQAE. In measuring total Cl^- efflux, I initially assumed that the proportion of Cl^--efflux via Cl^- channels would be essentially the same between eggs and zygotes, but that the robust HCO_3^-/Cl^- exchanger activity exhibited by zygotes would contribute more significantly to the total rate of Cl^- efflux in zygotes, thereby resulting in a much faster rate of Cl^- efflux in zygotes compared to eggs. As expected, the total rate of Cl^- efflux, measured by decreased MQAE intensity, occurred at a greater rate in zygotes than in eggs (about 2-fold faster after subtracting the small H_2DIDS-resistant component; Fig. 24-inset). This is consistent with a stable component of Cl^- efflux via Cl^- channels which remains unchanged after fertilization, and an additional pathway appearing after fertilization which could represent the appearance of HCO_3^-/Cl^- exchanger activity.

Unfortunately, Cl^- efflux measured by MQAE could not be attributed specifically

to HCO_3^-/Cl^- exchanger activity or Cl^- channels. Attempts to isolate HCO_3^-/Cl^--dependent Cl^-efflux included the use of the nominally specific Cl^- channel inhibitor IAA-94, but it also was found to inhibit HCO_3^-/Cl^- activity measured by alkalinization upon Cl^- removal. Cl^- measurements in the absence of HCO_3^- were unsuccessful, as MQAE fluorescence was unstable in the absence of HCO_3^- for unknown reasons (not shown). $^{36}Cl^-$ measurements were also attempted, but the specific activity of the isotope was too low (data not shown).

I found that MQAE, the fluorophore used to detect Cl^-, was somewhat toxic in eggs and embryos. MQAE, necessarily loaded at high concentrations, slows pronuclear development following IVF and reduces subsequent cleavage (Phillips et al., 1998). However, short-term Cl^- efflux, measured here with MQAE, was appropriately sensitive to H_2DIDS and IAA-94, indicating that specific Cl^- transporters were functioning. In addition, mouse blastocysts expand normally in the presence of 20 mM MQAE, indicating minimal short-term toxicity (Zhao et al., 1997). Thus, the increased rate of total Cl^- efflux coupled with high rates of intracellular alkalinization in zygotes compared to eggs is consistent with the appearance of HCO_3^-/Cl^- exchanger activity after fertilization, but a component due to increased Cl^- channel activity cannot be ruled out. As the sole Cl^- channel detected electrophysiologically in eggs and zygotes is activated only upon cell swelling (Kolajova and Baltz, 1999) this would seem to preclude fertilization-induced activation of Cl^- channels, as eggs and embryos assessed here were not swelled.

Unfertilized eggs also lacked the ability to specifically regulate pH_i against intracellular alkalosis in the pH_i range examined (7.1 - 7.5; Fig. 25A). Recovery from

intracellular alkalosis produced by exposure to NH_4^+: NH_3 was slow and incomplete in eggs (Fig. 25C), while it occurred quickly in zygotes (Fig. 25D). The absence of external Cl^-, required for HCO_3^-/Cl^-exchanger-mediated recovery from alkalosis, had no effect on the rate of recovery in eggs (Fig. 25A) in contrast to the marked inhibition of recovery in zygotes (Fig. 25B). Similarly, the HCO_3^-/Cl^- exchanger inhibitor DIDS had no effect on the recovery in eggs but significantly reduced recovery in zygotes.

Taken together, these data indicate that unfertilized eggs lack significant HCO_3^- /Cl^-exchanger activity while zygotes demonstrate specific pH_i regulatory activity that is appropriately DIDS-sensitive, Cl^--dependent, and with a defined pH_i set-point (7.1). HCO_3^-/Cl^- exchanger activity in unfertilized eggs was consistently low in both freshly ovulated eggs and in eggs cultured for up to 9 h (Fig. 27A). Characterization of this very low activity as specific HCO_3^-/Cl^- exchange was difficult and at times beyond the sensitivity of these measurements. Eggs cultured for 8 h exhibited a small DIDS-sensitive intracellular alkalinization upon Cl^- removal, but DIDS inhibition was not significant for freshly ovulated eggs. As zygotes and early cleavage stage embryos have the highest HCO_3^-/Cl^- exchanger activity in the preimplantation period (Zhao et al., 1995; Zhao and Baltz, 1996), robust HCO_3^-/Cl^- exchanger activity and the ability to regulate pH_i against alkalosis must develop following fertilization in the mouse.

Upregulation of Na^+/H^+ antiporter activity at fertilization is responsible for the increase in pH_i in sea urchin eggs (Swann and Whitaker, 1985), and thus activation of pH_i regulatory mechanisms may be a general feature of fertilization, similar to the universal increase in Ca^{2+}_i. Following my initial finding that HCO_3^-/Cl^- exchanger activity was upregulated following fertilization in the mouse in the absence of a net change in pH_i,

Na^+/H^+ antiporter activity was examined in hamster oocytes before and after egg activation by another laboratory in collaboration with our laboratory (M. Lane, B.D. Bavister and J.M. Baltz). Na^+/H^+ antiporter activity was similarly found to be upregulated in hamster eggs following egg activation with no apparent change in pH_i (Lane et al., 1999a). Hamster embryos, in contrast to mouse embryos, exhibit robust Na^+/H^+ antiporter activity with a set-point of pH_i 7.14 which contributes to the maintenance of steady-state pH_i. The development of embryos, cultured under acidic conditions when Na^+/H^+ antiporter activity has been specifically inhibited, is significantly compromised, suggesting that Na^+/H^+ antiporter activity is important for embryo survival during intracellular acidosis (Lane et al., 1998). Na^+/H^+ antiporter activity in mice is variable and strain-dependent (Baltz et al., 1991; Gibb et al., 1997, C.L., Steeves, M. Lane, B.D. Bavister, K.P. Phillips and J.M. Baltz, unpublished). Recently, robust HCO_3^-/Cl^- exchanger activity has also been reported for hamster embryos, which becomes similarly upregulated in hamster eggs at fertilization (Lane et al., 1999b). Thus, mammalian embryos do appear to upregulate pH_i regulatory mechanisms at fertilization which are then sustained through preimplantation development, although no net change in steady-state pH_i apparently occurs. Because marine invertebrates lack pH_i regulatory mechanisms to decrease pH_i (e.g. HCO_3^-/Cl^- exchanger; Alper, 1991; 1994), upregulation of pH_i regulation at fertilization (e.g. Na^+/H^+ antiporter activity) results in a net increase in pH_i in these species.

III. HCO_3^-/Cl^- exchanger upregulation is not dependent on changes in intracellular or extracellular pH

Rapid regulation of HCO_3^-/Cl^- exchange occurs by a shift in the pH_i set-point (Alper, 1991, 1994). The pH_i set-point of HCO_3^-/Cl^- exchange in mouse embryos does not vary significantly throughout the preimplantation period (set-point pH_i 7.0-7.2; Zhao and Baltz, 1996) and is comparable to the values for activated exchangers in other cells (Alper et al., 1991; 1994). It is conceivable that the pH_i set-point in unfertilized eggs is much higher than in zygotes, and that the appearance of activity which follows fertilization is a consequence of a shift of the pH_i set-point to a lower pH_i. If a shift in pH_i set-point were to explain the results obtained here, the set-point in eggs would have to be above about 7.5, since the intracellular alkalinization experiments achieved elevated pH_i to at least this level without revealing any HCO_3^-/Cl^- exchange-mediated recovery (Fig. 25A, C). Increased steady-state pH_i in unfertilized eggs would be consistent with a higher pH_i set-point for HCO_3^-/Cl^- exchanger activity. However, as previously discussed, steady-state pH_i in the presence of HCO_3^-/CO_2 is not significantly different between eggs and zygotes (Fig. 22B). Moreover, comparisons of steady-state pH_i immediately prior to measurements of HCO_3^-/Cl^- exchanger activity revealed no significant difference between eggs and zygotes. Furthermore, as unfertilized eggs are unable to regulate pH_i between pH_i 7.1-7.5, as demonstrated by the lack of significant HCO_3^-/Cl^- exchanger activity in this pH_i range, this suggests that HCO_3^-/Cl^-exchange plays no role in the regulation of steady-state pH_i in unfertilized eggs (Fig. 25A), while HCO_3^-/Cl^- exchanger activity contributes significantly to the maintenance of steady-state pH_i in zygotes (Fig. 25B). It is therefore unlikely that HCO_3^-/Cl^- exchanger upregulation at fertilization is regulated by

changes in steady-state pH_i.

Upregulation of HCO_3^-/Cl^- exchanger activity at fertilization may be due to changes in external pH (pH_o) such as exposure to alkaline oviductal fluid which could in turn affect pH_i. Exposure to alkaline pH_o might be expected to stimulate HCO_3^-/Cl^- exchanger activity whereas acid pH_o might be inhibitory. To investigate the role of pH_o during culture, am-zygotes, 3-5 h post-fertilization (low HCO_3^-/Cl^- activity), were cultured in acidic or alkaline pH_o by altering $[HCO_3^-]$ or ambient CO_2 with HCO_3^-/Cl^- exchanger activity assessed at the 2-cell stage (Fig. 26). Neither acid nor alkaline conditions affected upregulation of HCO_3^-/Cl^- exchanger activity, indicating that pH_o alone does not seem to play a role in regulation of the exchanger.

IV. HCO_3^-/Cl^- exchanger activity develops gradually following egg activation

In vivo-fertilized zygotes exhibited higher HCO_3^-/Cl^- exchanger activity when they were removed from the oviduct and measurements were made at 8-12 h post-fertilization than at 3-5 h post-fertilization. This implied that the development of activity might occur relatively slowly after fertilization. Following IVF, used to more precisely time fertilization, HCO_3^-/Cl^- exchanger activity developed slowly, requiring more than 7 h to reach the maximal level (Fig. 27A). In contrast, unfertilized eggs, under the same culture conditions, showed little or no increase in HCO_3^-/Cl^- exchanger activity, even if they were cultured for up to 9 h. Thus, it appears that the development of HCO_3^-/Cl^- exchanger activity occurs via a mechanism which requires a significant amount of time. From the timing (Fig. 27A), it is evident that HCO_3^-/Cl^- exchanger activity is gradually activated during the G1 phase of the first cell cycle, and maximal activity is reached prior

to the first round of DNA synthesis, which begins several hours after pronuclear development is complete (Fig. 13; Bolton and Howlett, 1986).

To further examine the development of HCO_3^-/Cl^- exchanger activity, eggs were parthenogenetically activated by ethanol exposure and HCO_3^-/Cl^- exchanger activity measured using the Cl^- removal assay. Activation of eggs (assessed by pronuclear development) was delayed compared to IVF eggs, with HCO_3^-/Cl^- exchanger activity becoming upregulated between 15 and 25 h following activation (Fig. 28). HCO_3^-/Cl^- exchanger upregulation also followed parthenogenetic activation by Sr^{2+} exposure (Fig. 34A) or by exposure to the protein synthesis inhibitor cycloheximide (Fig. 36A), although the timing of HCO_3^-/Cl^- exchanger upregulation and egg activation appeared to be similar to IVF rather than the delayed activation observed following ethanol activation. The development of HCO_3^-/Cl^- exchanger activity in parthenogenetically-activated eggs is significant as it indicates that HCO_3^-/Cl^- exchanger activity is independent of sperm factors or the male genome, and is therefore under maternal control.

V. Egg activation appears to activate pre-existing HCO_3^-/Cl^- exchangers

HCO_3^-/Cl^- exchanger upregulation following fertilization could result from synthesis of new HCO_3^-/Cl^- exchangers. Alternatively, posttranslational modifications to presynthesized exchangers, or transport of these exchangers to the plasma membrane, may be required for upregulation. To investigate these scenarios, two approaches were used. First, RT-PCR was used to examine the presence of AE2 mRNA in unfertilized eggs. Although the presence of AE2 mRNA would not necessarily indicate protein

expression, together with the functional studies, AE2 mRNA expression would be highly indicative of the presence of AE2 exchangers. Previous studies of HCO_3^-/Cl^- exchange activity in preimplantation mouse embryos have indicated that the principle exchanger responsible for pH_i regulation in the alkaline range is encoded by AE2 in zygotes and early cleavage state embryos (Zhao et al., 1995). The expression of AE2 mRNA in unfertilized eggs (Fig. 29) in addition to the pattern of mRNA expression in preimplantation embryos (AE3 expressed from 2-cell stage through blastocyst) suggests that AE2 message is expressed by both the maternal and embryonic genomes while AE3 may to be a product of the embryonic genome only (expressed post-zygotic gene activation; Telford et al., 1990; Zhao et al., 1995). The presence of AE2 mRNA in the unfertilized egg is consistent with the presence of inactive AE2 protein. Alternatively, it is possible that the AE2 mRNA detected in unfertilized eggs was translated upon fertilization, thereby resulting in upregulation of HCO_3^-/Cl^- exchanger activity.

The second approach involved the use of standard pharmacological agents to disrupt protein synthesis, the Golgi apparatus, and the cytoskeleton in newly-fertilized eggs (Fig. 30). IVF-eggs were exposed to each of the agents following the end of the 1 h sperm-egg incubation and cultured for 7-9 h. HCO_3^-/Cl^- exchanger activity was then assessed using the Cl^- removal assay. The development of HCO_3^-/Cl^- exchanger activity following IVF was not inhibited by cycloheximide (Fig. 30A) at concentrations previously shown to inhibit protein synthesis in zygotes (Siracusa et al., 1978; De Sousa et al., 1993). Furthermore, trafficking of proteins from the Golgi to the plasma membrane was not required for upregulation, since neither brefeldin A (Fig. 30B), which disrupts the Golgi (Fujiwara et al., 1998; Invessa et al., 1995), nor demecolcine (Fig. 30D), which

disrupts microtubule-based vesicle transport from the Golgi, had any effect (Gordon et al., 1989; Schatten et al., 1989). In addition, cytochalasin D was without effect (Fig. 30C), eliminating any mechanism dependent on actin-based transport or an intact cytoskeleton (Schatten et al., 1989). Thus, HCO_3^-/Cl^- exchanger proteins, which mediate robust HCO_3^-/Cl^- exchanger activity in the zygote, are likely to be present in the plasma membranes of unfertilized eggs in an inactive form and become activated following fertilization.

VI. HCO_3^-/Cl^- exchanger activity is independent of PKA or PKC

HCO_3^-/Cl^- exchangers, present in the plasma membrane in an inactive form, could be activated following fertilization by an intracellular signalling pathway. The activity of pH_i regulatory mechanisms, including HCO_3^-/Cl^- exchange, is regulated by complex stimuli and signalling pathways often involving phosphorylation-dependent events (Olsnes et al., 1986; Ganz et al., 1989; Jiang et al., 1994; Orlowski and Grinstein, 1997). Many pH_i regulatory systems are modulated by phosphorylation (Orlowski and Grinstein, 1997; Alper, 1991). Studies have demonstrated that HCO_3^-/Cl^- exchange in Vero cells, for example, is regulated by both cAMP-dependent protein kinase (PKA) and protein kinase C (PKC). Other exchangers, such as the Na^+/H^+ antiporter, are modified by PKC activation (Vigne et al., 1988). Both PKA and PKC are proposed to play significant roles during meiotic maturation and fertilization. PKA, for example, has been suggested to be involved in the maintenance of meiotic arrest prior to GVBD in mouse oocytes (Schultz et al., 1983b; Bornslaeger et al., 1986). PKC is proposed to play a role in cortical granule exocytosis, ZP2 to ZP2f modification (Raz et al., 1998), and events in later embryo

development such as compaction (Bloom, 1989). PKC is also involved in the upregulation of Na^+/H^+ antiporter activity in the sea urchin at fertilization (Swann and Whitaker, 1985; Shen and Buck, 1990).

Neither PKA or PKC activation alone, however, seems sufficient to stimulate significant HCO_3^-/Cl^- exchanger activity in eggs (Fig. 32A, C). In addition, inhibition of PKA (Fig. 32B) or PKC (Fig. 32D) immediately following IVF does not prevent the upregulation of activity 7-9 h post-IVF. These results seem to preclude a role for either PKA or PKC regulation of HCO_3^-/Cl^- exchanger activity at fertilization. This is in contrast to the apparent PKC regulation of Na^+/H^+ antiporter upregulation at egg activation in the hamster (Lane et al, 1999a). Na^+/H^+ antiporter activity develops gradually following hamster egg activation, similar to HCO_3^-/Cl^- exchanger upregulation in the mouse. Na^+/H^+ antiporter upregulation occurs following parthenogenetic activation and is independent of protein synthesis and protein trafficking, similar to HCO_3^-/Cl^- exchanger upregulation in the mouse. However, Na^+/H^+ antiporter activity appears to be activated by a PKC-dependent mechanism as upregulation was significantly inhibited by sphingosine. Na^+/H^+ antiporter activity was also partially induced in unfertilized hamster eggs by prolonged phorbol ester treatment (Lane et al., 1999a). This is consistent with regulation of Na^+/H^+ antiporter by PKC in sea urchin eggs at fertilization (Lau et al., 1986; Ciapa et al., 1989) and in somatic cells (Counillon and Poussegur, 2000). Regulation of HCO_3^-/Cl^- exchanger activity following fertilization in the mouse, however, does not appear to involve a PKA or PKC-dependent pathway.

VII. Role of Ca^{2+} transients in upregulation of HCO_3^-/Cl^- exchanger activity

At fertilization in the sea urchin, the earliest ionic event is a transient increase in intracellular Ca^{2+} which occurs within seconds of sperm-egg contact and triggers activation of the egg (Mazia, 1937). This Ca^{2+} increase appears to be a universal feature of fertilization, conserved not only in all animals examined to date including mammals (Miyazaki et al., 1992; Kline and Kline, 1994), but apparently in plants as well (Digonnet et al., 1997). Chelation of intracellular Ca^{2+} using BAPTA inhibits many Ca^{2+}-dependent events at egg activation in the mouse. At concentrations greater than 5 μM, intracellular BAPTA introduced prior to IVF inhibits Ca^{2+} transients, cortical granule exocytosis and resumption of meiosis following A23187 or Sr^{2+} activation of eggs (Kline and Kline, 1992). Lower concentrations (≤ 1 μM BAPTA) inhibit second polar body formation (Kline and Kline, 1992). Elimination of $Ca^{2+}{}_i$ transients (Fig. 33D) by BAPTA loading of eggs immediately following a 1 h sperm-egg incubation caused an almost 50% reduction in the rate of intracellular alkalinization upon Cl^- removal at 7-9 h after fertilization (Fig. 33A). These results indicated that $Ca^{2+}{}_i$ transients may be required for HCO_3^-/Cl^- exchange upregulation, that other types of Ca^{2+} signaling may be involved, or that a permissive levels of Ca^{2+} must be maintained to support upregulation. Similarly, HCO_3^-/Cl^- exchanger upregulation in eggs loaded with BAPTA 2.5 h post-sperm-egg incubation was significantly reduced. In contrast, when zygotes with fully developed HCO_3^-/Cl^- exchanger activity were loaded with BAPTA (4.5 h and 6.5 h post-IVF) HCO_3^-/Cl^- exchanger upregulation was not significantly affected, showing that chelation of $Ca^{2+}{}_i$ did not affect already existent HCO_3^-/Cl^- exchanger activity. These experiments revealed

a critical window, prior to formation of pronuclei, during which the upregulation of HCO_3^-/Cl^- exchanger activity appears to be sensitive to chelation of Ca^{2+}_i. This window was consistent with the timing of Ca^{2+}_i transients, which have been shown to persist until pronuclear formation (Jones et al., 1995b).

To further examine the possible dependence of HCO_3^-/Cl^- exchanger activity on Ca^{2+}_i transients, eggs were parthenogenetically activated by exposure to 10 mM $SrCl_2$. Unlike other methods of parthenogenetic activation, Sr^{2+} activation induces repetitive Ca^{2+}_i transients which persist as long as external Sr^{2+} is present (Cheek et al., 1993; Bos-Mikich et al., 1995). Sr^{2+}, a divalent cation, substitutes for Ca^{2+}_i by binding to the stimulatory Ca^{2+}_i binding site of the IP_3R at intracellular stores, resulting in the release of Ca^{2+} from the stores. In rat hepatocytes, Ca^{2+}_i oscillations occur in response to IP_3 and are sustained in the presence of either external Ca^{2+} or Sr^{2+} (Hajnoczky and Thomas, 1997).

In Sr^{2+}-activated eggs, HCO_3^-/Cl^- exchanger activity gradually increased around the time of pronuclear formation (Fig. 34A,C), becoming fully active 7-9 h post-activation, similar to IVF eggs (Fig. 26A). Sr^{2+} activation did produce repetitive Ca^{2+}_i transients (Fig. 34B). Although Sr^{2+}-produced Ca^{2+}_i transients were smaller in amplitude, the frequency was similar compared to transients produced following IVF (Fig. 27B). As the frequency and magnitude of Ca^{2+}_i transients produced even following IVF is reported to be somewhat variable (Kline and Kline, 1994; Jones et al., 1995b), the low amplitude of the Sr^{2+}-produced Ca^{2+}_i transients was still nevertheless sufficient to induce rates of egg activation (89%) comparable to IVF (74%).

To further investigate the role of Ca^{2+}_i transients in the upregulation of HCO_3^-/Cl^- exchanger activity, Sr^{2+} activation was used to produce a single Ca^{2+}_i transient. Exposure

to a brief Sr^{2+} pulse (5 min) generated a single, large Ca^{2+}_i transient (Fig. 35B). Eggs activated by a single Sr^{2+} pulse developed HCO_3^-/Cl^- exchanger activity (Fig. 35) with the same timing as IVF and Sr^{2+}-activated eggs (i.e. 7-9 h). Eggs activated by ethanol also produce a single increase in Ca^{2+}_i (Fig. 28B; Kono et al., 1995; Winston et al., 1995b) and subsequently develop HCO_3^-/Cl^- exchanger activity. Thus, as a single Ca^{2+}_i transient is sufficient to upregulate HCO_3^-/Cl^- exchanger activity, this would seem to suggest that repetitive Ca^{2+}_i transients are not required during exchanger upregulation.

Cycloheximide, a protein synthesis inhibitor, activates eggs by preventing the continuous synthesis of new cyclins resulting in the loss of MPF activity and exit from metaphase. This activation produces pronuclear eggs without inducing any changes in Ca^{2+}_i (Moos et al., 1996). Cycloheximide activation was therefore used to determine if any Ca^{2+}_i transients were required for upregulation of HCO_3^-/Cl^- exchanger activity. In cycloheximide-activated eggs, pronuclear development occurred with a similar time course as IVF and Sr^{2+} activated eggs. No changes in Ca^{2+}_i were observed when Fura-2 measurements were obtained during cycloheximide activation (Fig. 36). HCO_3^-/Cl^- exchanger activity did, however, fully develop within the same time-frame as IVF and Sr^{2+} activated eggs. This appears to preclude any required role for Ca^{2+}_i transients in the development of HCO_3^-/Cl^- exchanger activity at egg activation.

Chelation of Ca^{2+}_i using BAPTA prevents resumption of the cell cycle in parthenogenetically activated eggs, as inactivation of MPF requires a certain threshold increase in Ca^{2+}_i. The first Ca^{2+}_i transient induced by fertilization of mouse eggs has an average amplitude of 300 nM, which is sufficient to cause resumption of the cell cycle and entry into interphase (Winston et al., 1995b). The 1 h sperm-egg incubation used here

was sufficient to produce fertilized eggs and the initiation of Ca^{2+}_i transients. Thus, loading fertilized eggs with BAPTA immediately following this 1 h sperm-egg incubation would not have prevented this initial Ca^{2+}_i transient and subsequent resumption of the cell cycle, as shown by the development of pronuclei following BAPTA loading (Fig. 33B).

Why BAPTA, loaded either immediately or 2.5 h following the 1 h sperm-egg incubation, significantly inhibited the subsequent upregulation of HCO_3^-/Cl^- exchanger activity is puzzling. As HCO_3^-/Cl^- exchanger activity is consistently upregulated following activation protocols that either produce repetitive Ca^{2+}_i transients (IVF, Sr^{2+}), single Ca^{2+}_i transients (Sr^{2+} pulse, ethanol) or no Ca^{2+}_i transients (cycloheximide), this would seem to suggest that it is cell cycle resumption and not the appearance of Ca^{2+}_i transients that triggers HCO_3^-/Cl^- exchanger upregulation. However, eggs loaded with BAPTA immediately following sperm-egg incubation did become activated, as shown by pronuclear development, yet developed only partial HCO_3^-/Cl^- exchanger activity. Cytotoxic effects of BAPTA are unlikely, as evidenced by the normal extrusion of the second polar body and pronuclear development. The possibility that the timing of BAPTA addition was sufficient to only block the initiation of the 'late events' of fertilization would also be precluded by the development of pronuclei. Mouse 2-cell embryos, exposed to BAPTA, develop to the blastocyst stage, although development is significantly lower than control embryos (Emerson et al., 2000). Chelation of Ca^{2+}_i would certainly impair long term development of mouse embryos but the normal development of pronuclei and second polar body only a few hours prior to measurement of HCO_3^-/Cl^- exchanger activity would appear to preclude acute cytotoxicity. As HCO_3^-/Cl^- exchanger

activity was measured only at one time-point (7-9 h post-sperm-egg incubation), it is possible that the BAPTA merely delayed full activation of HCO_3^-/Cl^- exchanger such that measurements of exchanger activity obtained much later may have revealed full upregulation. Alternatively, inhibition of upregulation of HCO_3^-/Cl^- exchanger activity following early BAPTA exposure may have been due to chelation of Ca^{2+}_i and general inhibition of all Ca^{2+}_i-dependent pathways or Ca^{2+}-dependent enzymes rather than specific inhibition of the repetitive Ca^{2+}_i transients. This result does, however, indicate that Ca^{2+}-dependent signalling of some type other than the repetitive Ca^{2+}_i transients may be involved in upregulation of HCO_3^-/Cl^- exchanger activity.

VIII. HCO_3^-/Cl^- exchanger upregulation is dependent on cell cycle resumption

As egg activation was sufficient to produce robust HCO_3^-/Cl^- exchanger activity regardless of the method used (ethanol, Sr^{2+}, cycloheximide, U0126) this suggests that exchanger upregulation always occur after the unfertilized egg re-enters the cell cycle. Low HCO_3^-/Cl^- exchanger activity could be feature of meiotic metaphase during oocyte maturation with upregulation triggered by the release from meiotic arrest. Following GVBD, oocytes are in either MI or MII for several hours, characterized by high MPF activity, except during the brief MI-MII transition. Exit from MII at fertilization or egg activation is accompanied by a decrease in MPF activity through increased destruction of cyclin B (Verlhac et al., 1993). Degradation of cyclin B is dependent on an intact spindle (Kubiak et al., 1993) and thus disruption of the metaphase II spindle by microtubule depolymerizing agents prior to egg activation prevents cell cycle resumption (Winston et al., 1995b). Here, pretreatment of eggs with demecolcine (depolymerizes microtubules)

followed by Sr^{2+} activation significantly inhibited egg activation (Fig. 37A). Pretreatment with demecolcine is necessary since the spindle must be disrupted before Sr^{2+}-activation in order to maintain metaphase II arrest. Demecolcine pretreatment completely inhibited development of pronuclei and the second polar body, indicating that metaphase arrest was sustained by demecolcine exposure. Maintenance of metaphase arrest using demecolcine significantly inhibited the upregulation of HCO_3^-/Cl^- exchanger activity in these Sr^{2+} activated embryos (Fig. 37B). This suggests that HCO_3^-/Cl^- exchanger upregulation is dependent on exit from metaphase II. It also further rules out Ca^{2+}_i transients as sufficient for upregulation, since Ca^{2+}_i transients were induced by Sr^{2+} even though the eggs remained arrested in MII in the presence of demecolcine.

IX. HCO_3^-/Cl^- exchanger activity is downregulated during meiotic maturation

As HCO_3^-/Cl^- exchanger upregulation occurred upon exit from metaphase II, I decided to examine HCO_3^-/Cl^- exchanger activity during meiotic maturation- prior to metaphase II. As oocytes following GVBD remain arrested in metaphase for several hours (MI or MII) prior to fertilization, HCO_3^-/Cl^- exchanger activity was measured in GV oocytes and during meiotic maturation to determine whether low HCO_3^-/Cl^- exchanger activity was a general feature of meiotic metaphase (Fig. 38A). GV oocytes, arrested in prophase I, exhibited very high levels of HCO_3^-/Cl^- exchanger activity, similar to in vivo-produced zygotes. This was surprising, given the low HCO_3^-/Cl^- exchanger activity present in MII eggs. However, the discrepancy was resolved when I found that HCO_3^-/Cl^- exchanger activity gradually decreased following GVBD with a very slow time course (Fig. 38B) that was similar to the timing of upregulation of HCO_3^-/Cl^-

exchanger activity at fertilization (Fig. 27A). HCO_3^-/Cl^- exchanger activity had decreased to basal levels by 9-10 h following GVBD (MI eggs) and remained low during the MI-MII transition and in metaphase II eggs. This explained the low activity observed in in vivo produced, ovulated MII eggs. As HCO_3^-/Cl^- exchanger activity decreased upon entry into metaphase I, this seems to indicate that HCO_3^-/Cl^- exchanger activity is cell cycle dependent and that low HCO_3^-/Cl^- exchanger activity may be a feature of meiotic metaphase.

To investigate the possibility that low HCO_3^-/Cl^- exchanger activity was a feature of metaphase in general, exchanger activity was measured during metaphase of the first cell cycle following Sr^{2+} activation. HCO_3^-/Cl^- exchanger activity, however, remained high during metaphase and cytokinesis of the first mitotic cell cycle in Sr^{2+}activated eggs (Fig. 39A, B). As oocytes remain arrested in metaphase (MI or MII) for several hours following GVBD, an extended duration of metaphase arrest may be required for low HCO_3^-/Cl^- exchanger activity. Sr^{2+}-produced zygotes were maintained in an extended metaphase arrest using demecolcine (Fig. 39C). Prolonged mitotic metaphase arrest, however, was still not sufficient to downregulate or inhibit fully active HCO_3^-/Cl^- exchanger activity, suggesting that low HCO_3^-/Cl^- exchanger activity is a feature of meiotic metaphase only.

As HCO_3^-/Cl^- exchanger activity decreases to basal levels during meiotic metaphase but remains high during mitotic metaphase, regulation of exchanger activity seems a feature of meiotic metaphase. During meiosis, but not mitosis, HCO_3^-/Cl^- exchanger activity appears to be cell cycle-dependent with high exchanger activity present in the prophase-arrested GV oocyte, decreasing and remaining low during meiotic

metaphase, and then increasing again after release from metaphase and remaining high thereafter independent of subsequent cell cycle transitions.

In identifying potential regulatory pathways which might participate in downregulation of HCO_3^-/Cl^- exchanger activity in meiotic metaphase and subsequent upregulation after progression into zygotic interphase, one clear candidate is MPF. As MPF is inactive in both GV oocytes and zygotes, which both exhibit high HCO_3^-/Cl^- exchanger activity (Fig. 38A, Fig. 23A), this suggests that low MPF activity might be required for robust HCO_3^-/Cl^- exchanger activity. However, the MI-MII transition during meiotic maturation is associated with high HCO_3^-/Cl^- exchanger activity (Fig. 38A) during a period when MPF activity decreases (Verlhac et al., 1994) indicating that a brief drop in MPF activity does not induce HCO_3^-/Cl^- exchanger activity at this time. Similarly, metaphase of the first mitosis (prior to cleavage to the 2-cell stage) is characterized by high MPF activity, but HCO_3^-/Cl^- exchanger activity remains high in metaphase 1-cell embryos (Fig. 39). Thus, an increase in MPF activity alone is not sufficient to downregulate HCO_3^-/Cl^- exchanger activity.

An alternative candidate for a regulatory pathway involved in upregulation of HCO_3^-/Cl^- exchanger may be the activation of mos→MEK→ERK1/2. ERK1/2 activity is low in GV oocytes, becomes gradually activated during meiotic maturation, and is then subsequently inactivated following fertilization (Fig. 45; Verlhac et al., 1993; Moos et al., 1995). Importantly, ERK1/2 appears to be maintained in an inactive state during metaphase of the first cell cycle in the mouse (between 1-cell and 2-cell stages) distinguishing mitotic and meiotic metaphase (Haraguchi et al., 1998).

From my measurements of HCO_3^-/Cl^- exchanger activity and reports of ERK1/2

Figure 45. Appearance of MAPK activity is inversely correlated with HCO_3^-/Cl^- exchanger activity. *Timing of MAPK activity taken from Verlhac et al., 1993; Moos et al., 1995, Haraguchi et al., 1998.* MAPK activity is upregulated very slowly following GVBD, remains high in metaphase I and II and subsequently becomes downregulated with a very slow time-course following egg activation, remaining low through metaphase of the first cell cycle. HCO_3^-/Cl^- exchanger activity is downregulated very slowly following GVBD (Fig. 38A), becoming gradually activated upon egg activation (Fig. 27A, Fig. 34A). HCO_3^-/Cl^- exchanger activity remains high during metaphase of the first cell cycle and in 2-cell embryos (Fig. 37A). Thus, the timing of MAPK inactivation following egg activation correlates with the appearance of pronuclei (Moos et al., 1995), cessation of Ca^{2+}_i transients (Jones et al., 1995b) and upregulation of HCO_3^-/Cl^- exchanger activity.

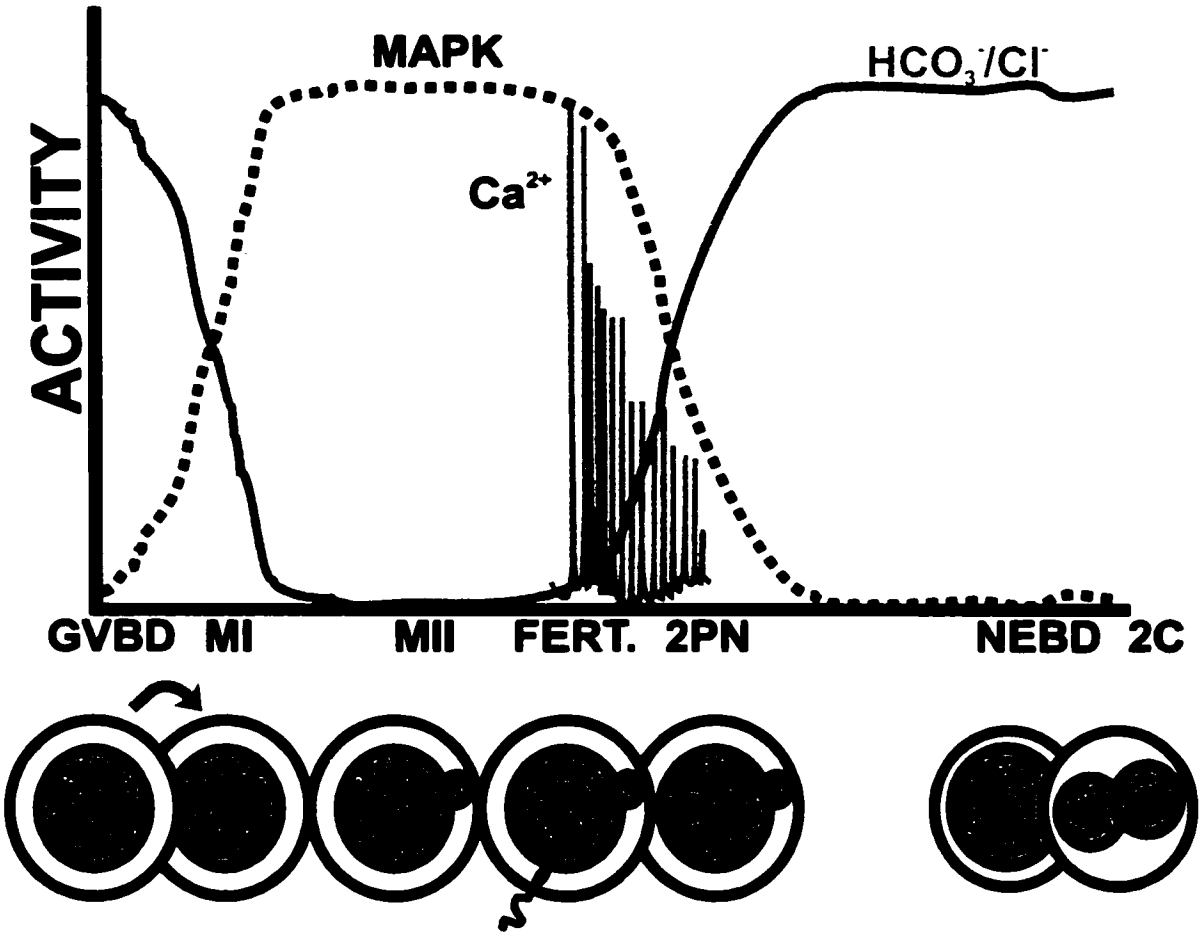
MAPK
HCO3-/Cl-
Ca2+
ACTIVITY
GVBD MI
MII
FERT. 2PN
NEBD 2C

activity in the literature (Verlhac et al., 1993; Moos et al., 1995; Haraguchi et al., 1998), there is a strong inverse correlation between ERK1/2 activity and HCO_3^-/Cl^- exchanger activity during meiotic maturation, fertilization, and through the first cell cycle (Fig. 45) consistent with the hypothesis that HCO_3^-/Cl^- exchanger activity may be inhibited by active ERK1/2 in oocytes and early embryos.

X. Okadaic acid prevents upregulation of HCO_3^-/Cl^- exchanger activity following Sr^{2+} activation

OA was used because previous work has shown that this protein phosphatase inhibitor modulates MAPK activity in mouse zygotes (see below). There are essentially four types of protein phosphatases; PP1 (ATP-Mg^{2+}-dependent), PP2A (polycation stimulated), PP2B (Ca^{2+}-calmodulin dependent) and PP2C (Mg^{2+}-dependent; Cohen et al., 1990). OA has been demonstrated to be a specific inhibitor of PP1 and PP2A (IC_{50} ~0.1 and 10 nM, respectively) with less specificity for PP2B (IC_{50} ~ 5 μM) and little effect on PP2C (Cohen et al., 1990; Schwartz and Schultz, 1991). Protein phosphatases 1 and 2A are present following GVBD and regulate ERK1/2 activation during maturation (Zernicka-Goetz et al., 1997).

OA was introduced at various times following Sr^{2+} activation to determine whether protein phosphatases PP1 and PP2A were involved in upregulation or maintenance of HCO_3^-/Cl^- exchanger activity. When OA was introduced prior to, coincident with or following Sr^{2+} activation, HCO_3^-/Cl^- exchanger upregulation was inhibited (Fig. 40A). This suggests that that HCO_3^-/Cl^- exchanger upregulation may

require dephosphorylation of a regulatory component, such as MAPK, another regulatory protein, or possibly the exchanger itself.

OA inhibits protein synthesis in rat oocytes, with almost total inhibition after 3 h of exposure (Zernicka-Goetz et al., 1997). For all experiments (Fig. 40A), total OA exposure was between 3 and 8 h, which would therefore have inhibited protein synthesis (Zernicka-Goetz et al., 1997). However, specific inhibition of protein synthesis (by cycloheximide) does not inhibit upregulation of HCO_3^-/Cl^- exchanger activity (Fig. 30A), suggesting that OA-induced downregulation of exchanger activity is most likely not due to any effects on protein synthesis.

Treatment of mouse eggs with OA prior to fertilization maintains high ERK1/2 activity and to prevent the formation of pronuclei after egg activation (Moos et al., 1995), whiles OA addition subsequent to fertilization and the decrease in MAPK activity leads to the reactivation of ERK1/2 and precocious NEBD (Schwartz and Schultz, 1991). Thus, one important consequence of OA treatment is the activation of ERK1/2. ERK1/2 inactivation is necessary for the formation of the pronuclear envelope (Moos et al., 1995; Moos et al., 1996), and thus inhibition of pronuclear development or precocious NEBD following OA exposure can be used as a bioassay for active ERK1/2. Here, pronuclear development was completely inhibited and precocious NEBD occurred depending on the timing of OA addition (Fig. 42B), which is consistent with OA activation of ERK1/2 (Moos et al., 1995). Thus, the inhibition of HCO_3^-/Cl^- exchanger upregulation following OA exposure is consistent with a regulatory role for the MAPK pathway.

OA addition to zygotes 8 h post-insemination restores ERK1/2 activity to levels similar to those in unfertilized eggs within 4 h of OA addition (Moos et al., 1995).

However, when OA was added to zygotes 8 h post-Sr^{2+} activation, HCO_3^-/Cl^- exchanger activity was not downregulated by a 4 h OA exposure (see Results) but was significantly reduced by an 8 h OA exposure (Fig. 40A). In both cases, NEBD was completed within 4 h of OA treatment, which suggests that ERK1/2 was fully reactivated by 4 h. As OA exposure between 4 and 8 h was required to downregulate HCO_3^-/Cl^- exchanger activity, much longer than the time reported to reactivate ERK1/2 (Moos et al., 1995), this suggests that HCO_3^-/Cl^- exchanger downregulation is not directly and quickly inhibited by ERK1/2 activity. However this does not preclude regulation by a signaling pathway downstream of ERK1/2. Interestingly, fully-active HCO_3^-/Cl^- exchanger activity in zygotes and 2-cell embryos was significantly downregulated by OA treatment and accompanied by precocious NEBD (Fig. 40A). This suggests that fully-active HCO_3^-/Cl^- exchanger activity is not refractory to modulation following the initial activation of exchanger activity at fertilization. This also suggests that both upregulation of HCO_3^-/Cl^- exchanger activity following egg activation and maintenance of HCO_3^-/Cl^- exchanger activity in 1-cell and 2-cell embryos are regulated by the same OA-sensitive pathway, which may be MAPK.

XI. HCO_3^-/Cl^- exchanger is activated by the MEK inhibitor U0126 in unfertilized eggs

HCO_3^-/Cl^- exchanger activity, fully active in zygotes and 2-cell embryos, is downregulated by OA exposure, conditions which hyperphosphorylate ERK1/2 in mouse eggs following fertilization (Moos et al., 1995). Unfertilized eggs have high ERK1/2 activity (Verlhac et al., 1993) and very low HCO_3^-/Cl^- exchanger activity (Fig. 23). To determine whether HCO_3^-/Cl^- exchanger activity could be induced prior to fertilization or

egg activation solely by a decrease in ERK1/2 activity, unfertilized eggs were cultured with the MEK inhibitor U0126.

U0126 is a noncompetitive inhibitor (K_i ~ 41-109 nM) of MEK1/2 with binding sites distinct from ATP and ERK. U0126 is considered a specific inhibitor of MEK and is able to bind and inhibit active MEK at concentrations which do not inhibit PKC, Raf or ERK1/2 (Favata et al., 1998; Hoffert et al., 2000).

HCO_3^-/Cl^- exchanger activity was significantly upregulated in unfertilized eggs following treatment with the MEK inhibitor U0126 (Fig. 42). Pronuclear development and emission of the second polar occurred following U0126 treatment of unfertilized eggs with similar timing to IVF and Sr^{2+} activated eggs. However, U0126 exposure also resulted in parthenogenetic egg activation (Fig. 14D; 41A) and thus it could not be concluded that deactivation of MAPK alone is sufficient for HCO_3^-/Cl^- exchanger upregulation. The phenomenon of parthenogenetic egg activation upon disruption of the MAPK pathway has been described previously in $mos^{-/-}$ oocytes. These oocytes undergo GVBD and emission of the first polar body normally but do not arrest in metaphase II. This indicates that while the mos→MEK→MAPK pathway is not required for GVBD or the MI-MII transition, it is required for maintenance of the metaphase II arrest (Colledge et al., 1994; Hashimoto et al., 1994). Similarly, injection of double-stranded RNA designed to 'knock-out' mos function in mouse oocytes also resulted in parthenogenetic activation with precocious cleavage observed (Wianny and Zernicka-Goetz, 2000). Parthenogenetic activation has been observed following U0126 treatment of *Urechis* oocytes. U0126 did not affect the timing of GVBD but did produce abnormally large polar bodies followed immediately by entry into interphase and formation of pronuclei

(Gould and Stephano, 1999). However, parthenogenetic activation by U0126 is a likely consequence of disruption to the MAPK pathway, and hence, loss of CSF activity, in unfertilized eggs.

Although HCO_3^-/Cl^- exchanger activity appears to be inversely correlated with MAPK activity, the possibility that some event, dependent on egg activation and temporally correlated with ERK1/2 inactivation, may be responsible for exchanger activation cannot be precluded. As ERK1/2 is the only known target of MEK1/2, U0126 activation of HCO_3^-/Cl^- exchanger activity in unfertilized eggs is consistent with regulation by ERK1/2. However, the parthenogenetic activation of eggs by U0126 precluded ERK1/2 activity from being assessed separately from egg activation using this drug. Thus, I attempted to find conditions where eggs could be maintained in MII arrest in the presence of U0126.

In an attempt to separate the effects of egg activation from perturbations to the MAPK pathway, cell cycle resumption was prevented by demecolcine in U0126-treated eggs. Parthenogenetic activation was observed in the control group but the incidence of parthenogenesis was greatly reduced compared to the previous experiments. One difference here was that control eggs had been pretreated with the vehicle for demecolcine (ethanol) for 1 h followed by U0126 treatment for up to 9 h. Pretreatment with demecolcine is necessary since the spindle must already be disrupted before egg activation, or the egg will exit from MII arrest. Therefore demecolcine must be added prior to addition of the parthenogenetic agent, in this case U0126. In addition to decreased incidence of parthenogenesis, U0126 treatment after a pretreatment period produced different proportions of the classes of parthenogenotes (Fig. 43). Hirao and

Eppig described three classes of parthenogenotes obtained from $mos^{-/-}$ mice (Hirao and Eppig, 1997; Fig. 7). This classification system was used here to describe the morphology exhibited by different U0126 parthenogenotes. U0126 treatment with no preincubation period produced primarily Class I parthenogenotes and a high incidence of parthenogenesis (Fig. 41A). However, U0126 treatment after experimental manipulations produced a lower incidence of parthenogenesis but a higher proportion of Class II and Class III parthenogenotes (Fig. 43). Why the incidence of parthenogenesis decreased following vehicle exposure is unknown. Preliminary attempts to determine the effect of vehicle exposure time has revealed that the incidence of parthenogenesis decreases with increased vehicle exposure time (data not shown). However, the vehicle (ethanol) was not itself the cause since this same protocol, using a 1 h vehicle (ethanol) pretreatment, was used with Sr^{2+} activation (Fig. 37B) without decreased incidence of parthenogenesis or loss of HCO_3^-/Cl^- exchanger activity. It may be that the target of U0126, the MEK pathway, is particularly sensitive and labile, such that a period of in vitro culture reduces the ability of U0126 to act as a parthenogenetic agent. This remains to be investigated.

U0126 treatment of freshly-ovulated eggs resulted in both parthenogenetic activation and HCO_3^-/Cl^- exchanger upregulation (Fig. 41, 42). This suggested that parthenogenetic activation was correlated with HCO_3^-/Cl^- exchanger upregulation. As U0126 treatment after a period in culture greatly reduced the incidence of parthenogenesis, only groups with at least 50% activation were selected for measurement of HCO_3^-/Cl^- exchanger activity. Treatment groups were paired, such that demecolcine and vehicle/U0126 groups were measured simultaneously. Following demecolcine treatment, parthenogenetic activation in U0126-treated eggs was not observed, indicating

that cell cycle resumption had been successfully inhibited in the presence of U0126 (Fig. 43). These demecolcine-treated eggs did, however, upregulate HCO_3^-/Cl^- exchanger activity in the same proportion as the paired U0126-activated eggs (Fig. 44). This is in contrast to demecolcine treatment of Sr^{2+} activated eggs (Fig. 37), which significantly inhibited the upregulation of HCO_3^-/Cl^- exchanger activity. Disruption of the metaphase II spindle prior to egg activation maintains MPF activity but does not prevent the decrease in MAPK activity associated with egg activation (Moos et al., 1996). So, in the presence of demecolcine, U0126-treated eggs would be identically arrested in MII except that with U0126 MEK and MAPK activities would be low, while with Sr^{2+} they would be high. Thus, U0126-treatment appears to activate HCO_3^-/Cl^- exchanger in unfertilized eggs by disruption of the MAPK pathway and not by activation of the cell cycle.

I propose that the MAPK pathway regulates HCO_3^-/Cl^- exchanger activity during fertilization. Once fertilization occurs and ERK1/2 is deactivated, the regulatory 'brake' for HCO_3^-/Cl^- exchanger activity is removed, such that high HCO_3^-/Cl^- exchanger activity is present in early embryo development. There is evidence to support MAPK regulation of pH_i transporters. In renal epithelial cells, Na^+-HCO_3^- cotransporter (NBC1) activity is upregulated in response to acute CO_2 elevation. This activation is dependent on Src activation of ERK1/2 (Ras → Raf → MEK1/2 → ERK1/2). ERK1/2 activity mediates growth factor and arginine vasopressin activation of Na^+/H^+ antiporter activity (NHE1; Ruiz et al., 1999). During meiotic maturation *Xenopus* oocytes upregulate Na^+/H^+ antiporter activity via a Raf-1-dependent mechanism (Kang et al., 1998). Previous studies of pH_i regulation in *Xenopus* oocytes have shown that microinjection of c-mos also upregulates Na^+/H^+ antiporter activity, suggesting that MAPK may be involved in pH_i

regulation in *Xenopus* (Rezai et al., 1994). Thus, there are several examples of MAPK regulation of pH_i transporters, although if MAPK is involved in regulating HCO_3^-/Cl^- exchanger activity during fertilization in the mouse, it would be the first instance wherein *in*activation of MAPK resulted in activation of a pH_i regulatory transporter.

CONCLUSION

My investigation of pH_i during egg activation in the mouse has produced several key findings. First, an increase in pH_i is not a feature of mammalian egg activation or meiotic maturation. This is significant, as an increase in pH_i during meiotic maturation and/or fertilization has been described for several species (e.g. sea urchin, *Xenopus*, molluscs, limpets, *Urechis*) and plays an important role in the development of the embryo in these species. In the sea urchin (Swann and Whitaker, 1985) and *Xenopus* (Rezai et al., 1994), pH_i increases following activation of the Na^+/H^+ antiporter.

Although no net change in pH_i accompanies mouse egg activation, at least one pH_i regulatory transporter, HCO_3^-/Cl^- exchanger, is upregulated following fertilization and egg activation. This is my second key finding. HCO_3^-/Cl^- exchanger activity is very low in unfertilized eggs, HCO_3^-/Cl^- exchanger activation becomes activated gradually, becoming maximal by 7-9 h post-egg activation. HCO_3^-/Cl^- exchanger activity remains high from the 1-cell stage to the 2-cell stage, consistent with previous measurements of embryo HCO_3^-/Cl^- exchanger activity (Zhao et al., 1995). The presence of AE2 mRNA in the unfertilized egg is consistent with AE2 being the sole isoform expressed by zygotes and 2-cell embryos (Zhao et al., 1995) as little new transcription occurs until zygotic gene

activation (Telford et al., 1990). HCO_3^-/Cl^- exchanger upregulation is independent of protein synthesis, posttranslational modifications, or transport to the plasma membrane. Exchanger upregulation is also independent of Ca^{2+}_i transients, or cAMP, PKA and PKC signalling pathways.

As HCO_3^-/Cl^- exchanger upregulation was independent of sperm, parthenogenetic activation using ethanol, Sr^{2+}, or cycloheximide was used successfully to further examine HCO_3^-/Cl^- exchange. Sr^{2+} activation proved to be an excellent model for fertilization as Sr^{2+} exposure produces repetitive Ca^{2+} transients and high rates of activation. The timing of the first cell cycle (second polar body formation, pronuclear development, NEBD, cytokinesis) following Sr^{2+} activation has been clearly determined here, such that the kinetics of these developmental events can be compared to other mechanisms of activation, including IVF. These detailed time-courses had not been reported for Sr^{2+} activation thus far.

Upregulation of HCO_3^-/Cl^- exchanger activity was dependent on an intact MII spindle, as pretreatment with demecolcine prior to Sr^{2+} activation significantly inhibited HCO_3^-/Cl^- exchanger activity. This suggests that HCO_3^-/Cl^- exchanger upregulation depends upon entry into the cell cycle.

My third key finding is that HCO_3^-/Cl^- exchanger activity is very high in GV oocytes, becoming subsequently downregulated during meiotic maturation with low activity in the unfertilized egg. Downregulation of HCO_3^-/Cl^- exchanger activity during meiotic maturation requires approximately the same period of time (7-9 h) required to upregulate HCO_3^-/Cl^- exchanger activity following egg activation. Although HCO_3^-/Cl^- exchanger activity is low during meiotic metaphase (MI and MII), HCO_3^-/Cl^- exchanger

activity remains high during metaphase of the first mitosis. Thus, a cell cycle-dependent mechanism, specific to meiotic metaphase, appears to regulate HCO_3^-/Cl^- exchanger activity.

The MAPK pathway becomes activated following GVBD, remains high through the MI-MII transition, and maintains metaphase II arrest in the unfertilized egg (Verlhac et al., 1993; Colledge et al., 1994; Hashimoto et al., 1994). Following egg activation, ERK1/2 becomes inactivated very slowly, becoming significantly reduced at pronuclear formation and fully inactivated by 7-9 h following fertilization (Moos et al., 1995). A signalling pathway normally upstream of ERK1/2 which includes Raf-1, is activated during metaphase of the first mitosis. However, ERK1/2 remains inactive during mitotic metaphase in the mouse zygote (Haraguchi et al., 1998). Thus, ERK1/2 activity is inversely correlated with HCO_3^-/Cl^- exchanger activity in prophase-arrested GV oocytes through to metaphase of the first mitosis (Fig. 49). Several experiments described here provide some evidence to support ERK1/2 regulation of HCO_3^-/Cl^- exchanger activity. First, OA treatment of Sr^{2+} activated eggs and embryos downregulates HCO_3^-/Cl^- exchanger activity. The inhibition of pronuclear development and precocious NEBD is consistent with previous reports wherein OA has been used to hyperphosphorylate ERK1/2 in mouse eggs (Moos et al., 1995; Moos et al., 1996). Second, the MEK inhibitor U0126 activated HCO_3^-/Cl^- exchanger activity in unfertilized eggs in a manner possibly independent of cell cycle resumption. As disruption of the MAPK pathway in unfertilized eggs releases the egg from metaphase II arrest, parthenogenetic activation upon U0126 treatment and the specific morphology exhibited by these U0126 parthenogenotes was consistent with parthenogenetic activation in $mos^{-/-}$ oocytes

(Colledge et al., 1994; Hashimoto et al., 1994, Hirao and Eppig, 1997).

In conclusion, while no net change in pH_i accompanies egg activation in the mouse, there is activation of pH_i regulation which enhances the pH_i regulatory capacity of the embryo. Activation of both pH_i regulatory transporters that correct both alkalosis (HCO_3^-/Cl^- exchanger) and acidosis (Na^+/H^+ antiporter - hamster, Lane et al., 1999a) may be a general feature of mammalian fertilization. As changes in cell cycle in the oocyte and developing embryo are often accompanied by changes in environment, it may be physiologically advantageous for pH_i regulation to be controlled by a cell cycle-dependent pathway, such as the MAPK pathway. The GV oocyte, for example, exhibits robust HCO_3^-/Cl^- exchanger activity and resides in the ovarian follicle until it is recruited for maturation and ovulation, whereas the unfertilized egg is ovulated with its surrounding cumulus mass into the alkaline oviduct where fertilization occurs.

Why would HCO_3^-/Cl^- exchanger activity be downregulated prior to ovulation? Perhaps the absence of HCO_3^-/Cl^- exchanger activity in the unfertilized egg combined with the lifespan of the cumulus mass provide a fertilization window. The cumulus mass is sustained for 15-20 h in the mouse oviduct (Roblero et al., 1989). The cumulus mass, while present, provides a protective microenvironment for the oocyte such that the alkalinity of the oviduct may not be detrimental to the oocyte. The cumulus mass is important for capacitation and acts to positively select the 'best' sperm (Boatman, 1987). In the absence of the cumulus, denuded oocytes would be more susceptible to alkalosis. Oocytes ovulated in scant cumulus masses may have decreased developmental potential and thus, would be subject to degeneration upon prolonged exposure to the oviduct. Oocytes that are not fertilized may be prone to parthenogenetic activation as a natural

result of aging. Again, the absence of both HCO_3^-/Cl^- exchanger activity and a protective cumulus mass would increase the rate of degeneration among such oocytes. The development of HCO_3^-/Cl^- exchanger activity in the fertilized egg occurs coincides with the loss of the cumulus mass, which supports this hypothesis.

FUTURE DIRECTIONS

As there are currently no pharmacological agents available which specifically inhibit ERK1/2, the MAPK pathway has been examined here by inhibition of MEK1/2, the kinase directly upstream of ERK1/2. This introduces variability as to the efficiency and efficacy of the agents in question and the nature of the effects on ERK1/2. Now that a potential pathway has been identified that may regulate HCO_3^-/Cl^- exchanger activity, several experiments would logically follow. The state of ERK1/2 activity would be confirmed following OA, U0126, and Sr^{2+}-treatment. This is currently ongoing in our laboratory. Constitutively-active MEK (Moos et al., 1996b) could be expressed (by microinjecting mRNA) in mouse 1-cell and 2-cell embryos to determine the effects of maintaining high MEK/MAPK activity on the HCO_3^-/Cl^- exchanger. If active MEK downregulates HCO_3^-/Cl^- exchanger activity, as in the unfertilized egg, HCO_3^-/Cl^- exchanger activity should be similarly downregulated in the 1-cell and 2-cell embryo (consistent with the effect of OA).

The mechanism of HCO_3^-/Cl^- exchanger downregulation during meiotic maturation is another avenue of investigation. As MAPK becomes gradually activated during metaphase I, coincident with the downregulation of HCO_3^-/Cl^- exchanger activity,

it is possible that MAPK activity also regulates HCO_3^-/Cl^- exchanger activity during this period of development. My preliminary attempts to determine whether HCO_3^-/Cl^- exchanger activity downregulation was U0126-sensitive, and therefore required MAPK activation, were complicated by the partial inhibition of GVBD by U0126. As GVBD is independent of the mos→MEK→MAPK pathway in both $mos^{-/-}$ oocytes (Colledge et al., 1994; Hashimoto et al., 1994) and following U0126 treatment of *Urechis* oocytes (Gould and Stephano, 1999), it is possible that inhibition of GVBD by U0126 may have been due to U0126 cytotoxicity rather than reflecting a requirement for MAPK in GVBD in the mouse. Further study of HCO_3^-/Cl^- exchanger activity downregulation during meiotic maturation is required.

Na^+/H^+ antiporter activity should also be examined in mouse oocytes to determine whether activity is upregulated in this species as it is in the hamster (Lane et al., 1999a). Although Na^+/H^+ antiporter activity was shown to be regulated by PKC in the hamster (Lane et al., 1999a), it may be possible that PKC acts on the Na^+/H^+ antiporter downstream of the MAPK pathway. It would be interesting to investigate whether both alkaline and acid pH_i regulatory transporters are regulated by the same pathway.

Finally, the serendipitous discovery made here that U0126 parthenogenetically activates mouse eggs producing similar parthenogenetic phenotypes as $mos^{-/-}$ oocytes is interesting. Particularly interesting is the question of why a short period of culture prior to U0126 addition reduces the incidence of parthenogenesis while increasing the proportion of Class II and Class III parthenogenotes, which could be related to the status of ERK1/2 during the culture period.

APPENDIX

pH_i regulation in human preimplantation embryos.

The study of pH_i regulation in human preimplantation embryos was undertaken to complement the larger investigation of pH_i regulation in mouse eggs and embryos, discussed in the body of the Thesis. Because of the limitations of human embryo research, which preclude obtaining high numbers of stage-specific human eggs and embryos, the premise of this investigation was simple; I wanted to determine whether human eggs and embryos regulated pH_i by the same mechanisms described for other mammalian embryos (ie. mouse, hamster, rat). Rather than discuss these results in the body of the Thesis, my study of pH_i regulation in human embryos is appended here to avoid species confusion (human vs. mouse) and to better emphasize the importance of this smaller project. When this project was first undertaken little was known about how human embryos regulate pH_i; a subject that has important clinical implications for the field of human reproductive technology.

I. INTRODUCTION

Intracellular pH (pH_i) regulation is an important component of mammalian cell homeostasis. There are three major pH_i-regulatory mechanisms in mammals: HCO_3^-/Cl^- exchanger, which alleviates alkalosis, and Na^+/H^+ antiporter and $Na^+,HCO_3^-/Cl^-$ exchanger, both of which alleviate acidosis. pH_i regulation has been well-examined in some mammalian embryos, such as those of mouse (Zhao et al., 1995; Phillips and Baltz,

1999) and hamster (Lane et al., 1998, 1999a,1999b), but little is known about the mechanisms of pH_i regulation in the human preimplantation embryo. Using methods which have been successfully employed in mouse and hamster embryos to reveal the identity and active ranges of pH_i-regulatory mechanisms present, pH_i regulation was examined in human embryos.

II. MATERIALS AND METHODS

I. Patients

Immature and mature eggs and cleavage-stage embryos, excess to requirements for standard in vitro fertilization (IVF) or intracytoplasmic sperm injection (ICSI) protocols at the Human IVF Clinic, Ottawa Hospital, were obtained for research with written patient consent. Use of human eggs and embryos for research was approved by the Ottawa Hospital Research Ethics Board. Treatment of patients for infertility, including superovulatory protocols, oocyte retrievals and embryo transfers, were carried out by the medical staff of the Human IVF Clinic. Laboratory manipulations of gametes and embryos were performed by the laboratory staff (embryologists) of the Human IVF Clinic. I have been on staff part-time at the Human IVF Clinic as an embryologist and was therefore an active participant in the clinical laboratory procedures outlined below, with the exception of ICSI.

II. Ovarian stimulation, egg retrieval

Patients were stimulated to produce supernumerary follicles using standard

ovarian stimulation protocols which included downregulation of endogenous gonadotropin production by suppressing GnRH production using a GnRH analogue (Lupron; Abbott Pharmaceuticals, Montreal, QC). This was followed by ovarian stimulation with hMG (Humegon; Organon Canada; Scarborough, ON) or recFSH (recombinant FSH, Puregon; Organon Canada) with dose adjusted according to follicular response and serum estradiol (E_2) levels (Rattanachaiyanont et al., 1999). Egg retrieval or "oocyte pick-up" (OPU) was performed 36 h following intramuscular administration of 10,000 IU human chorionic gonadotropin (hCG-Pregnyl®, Organon Canada). This is conceptually similar to the superovulation protocol described for mice in the main body of the Thesis, with hMG or recFSH playing the role of PMSG, and hCG using in both cases. However, in humans the endogenous gonadotropin pathway must be first suppressed as well, necessitating the use of GnRH analogue for downregulation.

III. Fertilization

A. IVF: Each cumulus-enclosed egg was inseminated with 0.125 million/ml motile sperm following standard sperm washing procedures. 17-19 h post-insemination, eggs were stripped of cumulus cells and assessed for the presence of pronuclei.

B. ICSI: For ICSI, eggs were stripped of cumulus cells using 80 IU/ml hyaluronidase (Type VIII-Bovine Testes; H-3757, Sigma, St. Louis, MO) in Hepes-buffered "Human Tubal Fluid" medium (a simple, artificial culture medium like KSOM) with 0.5 % bovine serum albumin added (HTF-BSA) (HTF; Meditech 1ST Canada Inc, Montreal, QC) 2-4 h post-egg retrieval and assessed as immature if there was a germinal vesicle or no polar

body (metaphase I- MI), or mature (metaphase II- MII) if there was no germinal vesicle and one polar body. Only MII eggs were used for ICSI. ICSI was performed on an inverted microscope at 400x magnification using Hoffman Modulation Contrast optics. 1-2 µl washed sperm were placed in Hepes-buffered HTF-BSA containing 10% polyvinylpyrrolidone (PVP K-90; Irvine Scientific, Santa Ana, CA) and injected using standard techniques. Following injection, each egg was cultured individually in a 20 µl drop of HTF-BSA covered with paraffin oil at 37°C, 5% O_2/5% CO_2/90% N_2 for about 17-19 h. Embryos were then assessed for the presence of pronuclei.

IV. Embryo development

Embryos were maintained in culture for 2-4 days post-IVF/ICSI during which time embryo cleavage was assessed. Embryos were graded from 1-5 (Rattanachaiyanont et al., 1999) according to the quality of blastomeres and the presence of fragmentation, with 5 indicating the best-quality embryos.

V. Human eggs and embryos used for this research

Some immature eggs and mature eggs (MII) were released for research (within 24 h of OPU) without having been exposed to sperm. One immature egg (MI) matured to MII after several hours in culture after release for research as assessed by the appearance of the first polar body. In total, 4 GV eggs, 9 MI eggs and 9 MII eggs (including the MI-MII egg) were released for research and available for this study.

96 embryos used for this study were obtained following IVF while 126 embryos were obtained following ICSI. Pronuclei (PN) detected in embryos donated for research

included (assessed 17-19 h post-IVF/ICSI): 0PN, 26 embryos; 1PN, 43 embryos; 2PN, 120 embryos; 3 PN, 23 embryos; 4 PN, 1 embryo. Embryos used for this study included 11 Grade 1; 53 Grade 2; 122 Grade 3; 21 Grade 4; and 6 Grade 5 embryos. Eggs were not rated.

VI. pH_i measurements

For detailed protocols describing solutions, pH_i measurements, Cl^- removal assay and the induction of intracellular alkaline load, please see Materials and Methods in the body of the Thesis.

Recovery from induced acid load

To determine whether embryos were able to recover from a decrease in pH_i, intracellular acidosis was induced using a pulse of the permeant weak base NH_4Cl followed by (Zhao and Baltz, 1996). $H^+ + NH_3$ is in equilibrium NH_4^+ such that upon initial exposure to NH_4Cl, the more permeable NH_3 enters the egg/embryo rapidly, resulting in an intracellular alkalinization (Fig. 46). This is followed by the slower entry of the much less permeable NH_4^+ which continues throughout the period when NH_4Cl is present. The abrupt removal of external NH_4Cl, upon replacement by KSOM, results in the rapid exit of the permeable species, NH_3 from the cytoplasm. Not only does all the NH_3 which entered exit, but all the NH_4^+ which had entered gives up a H^+ as the equilibrium shifts, and also exits as NH_3. This leaves behind the H^+ which had been carried in by NH_4^+, causing an intracellular acidification (Boron and DeWeer, 1976; Roos and Boron, 1981). Upon acidification of the cytoplasm, any pH_i regulatory transporters

Figure 46. Recovery from induced acidosis. A. Intracellular acidosis can be induced by brief exposure (10 min) to NH_4Cl^--containing solution followed by removal of NH_4Cl (KSOM). At the start of the NH_4Cl pulse, NH_3 (a weak base) rapidly enters the egg/embryo resulting in a very fast intracellular alkalinization. This is followed by the slower entry of NH_4^+ (weak acid) which is reflected by a gradual acidification of pH_i. At the end of the pulse, upon removal of NH_4Cl, NH_3 rapidly exits the egg/embryo leaving behind trapped H^+ which had entered as NH_4^+. This results in rapid intracellular acidification. B. Na^+/H^+ antiporter depicted schematically. Na^+ influx is coupled to H^+ efflux. Na^+/H^+ antiporter is inhibited by the absence of external Na^+ and by amiloride and its derivatives.

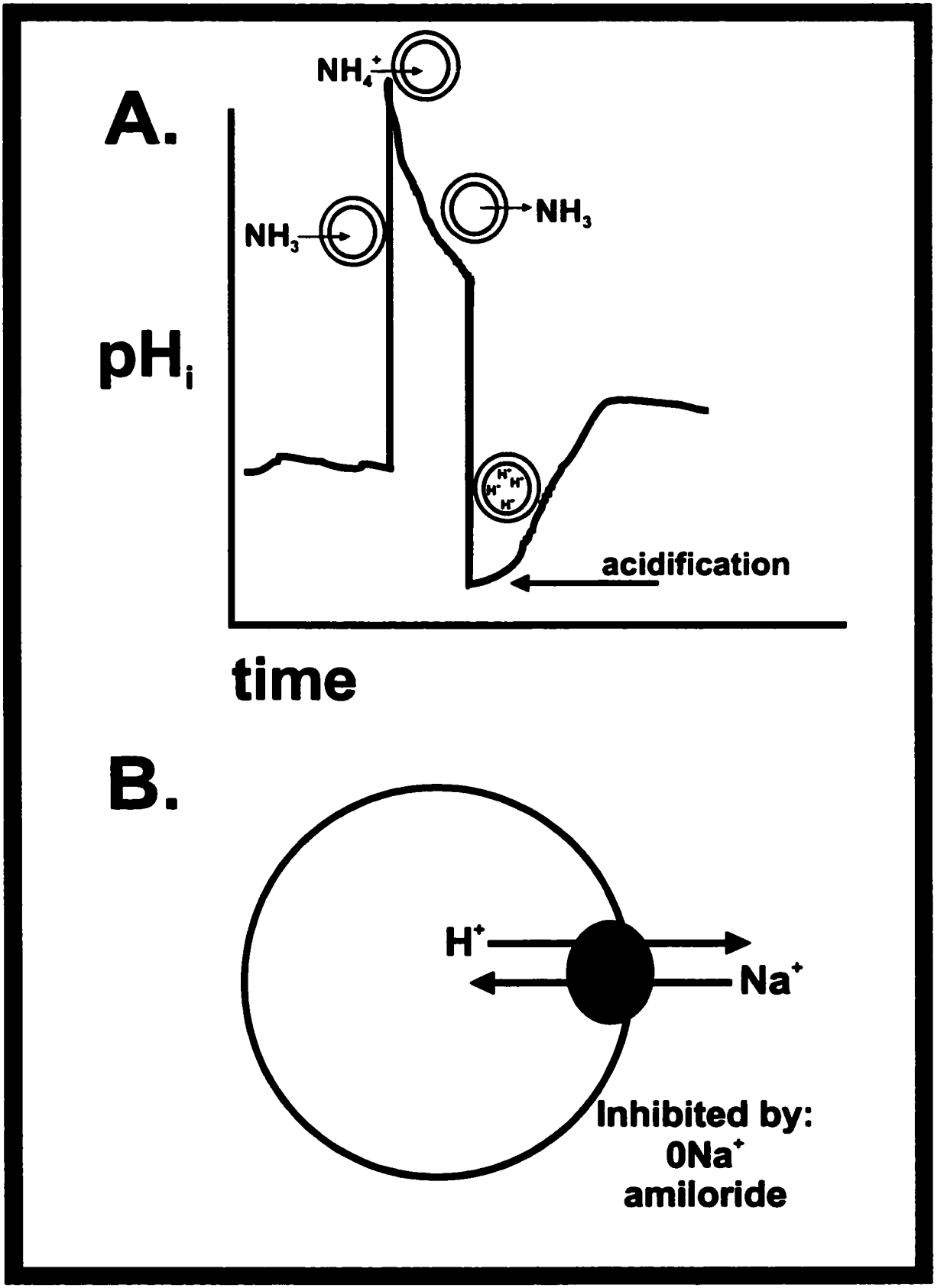
A.
NH_4^+
NH_3
NH_3
pH_i
acidification
time
B.
H^+
Na^+
Inhibited by:
$0Na^+$
amiloride

present, such as Na^+/H^+ antiporter or Na^+-HCO_3^-/Cl^- exchanger, could mediate recovery of pH_i from the induced acidosis.

Steady-state pH_i measurements were obtained in KSOM for 10 min at the onset of each experiment. Following steady-state pH_i measurements, the solution was changed to NH_4Cl-KSOM (25 mM HCO_3^-) for 10 min followed by replacement of NH_4Cl by KSOM or Na^+-free KSOM for 15 min. As the rate of recovery from intracellular acidosis by either mechanism should be enhanced by Na^+ unloading, some embryos were acid-loaded by NH_4Cl pulse, and then the medium switched to Na^+-free KSOM for 15 min followed by Na^+ reintroduction (KSOM). These experiments were referred to as 'Na^+ replacements'. For some experiments, following the Na^+-free period, embryos were exposed to KSOM containing either 1 mM amiloride, 500 μM DIDS, 50 μM EIPA, or Na^+-free KSOM again for an additional 15 min. For some Na^+-replacement experiments, HCO_3^- in all solutions was replaced by Hepes as described for Hepes-KSOM (see Materials and Methods, body of the Thesis). The inclusion of the Na^+/H^+ antiporter inhibitor amiloride, or Na^+-HCO_3^-/Cl^- exchanger inhibitor DIDS, or the exclusion of HCO_3^- was intended to help determine the identity of any acidosis-alleviating mechanisms present in the human cleavage stage embryo.

III. RESULTS

Steady-state pH_i in human eggs and embryos.

Steady-state pH_i was measured in KSOM (5%CO_2, 37°C) in eggs (GV, MI and MII) and cleavage-stage embryos (2-8 cell). pH_i ranged from about 6.9 to 7.55 among

different eggs and embryos with no significant difference between stages ($p>0.05$; nANOVA) or fertilization protocol (ICSI vs. IVF; Welch's t-test; $p>0.05$). Embryo morphology rating generally had no effect on pH_i, although pH_i of embryos rated 2 or 3 was significantly lower than pH_i of embryos rated 5, likely due to variation and small sample size in the latter group (nANOVA; $p<0.05$). Mean pH_i (± s.e.m.) were as follows: GV oocytes: 7.04 ± 0.07 (n=4), MI eggs: 7.03 ± 0.04 (n=9); MII eggs: 6.98 ± 0.02 (n=9) and cleavage-stage embryos: 7.12 ± 0.008 (n=199).

Recovery from intracellular alkalosis in human embryos

Cleavage-stage embryos were alkalinized by exposure to NH_4Cl to assess whether embryos could recover from intracellular alkalosis (Fig. 47A). Recovery rates were determined by fitting a single exponential to the recovery by non-linear regression for every 0.1 pH_i increment between pH_i 7.1 and 7.7 (Fig. 47C). There was no significant difference in recovery rates between stages of embryo development (compared at pH_i 7.6; $p>0.05$; nANOVA), and thus, the recovery rates for cleavage-stage embryos were pooled (n=15; Fig. 47A). When embryos (n=8) were alkalinized in the absence of external Cl^- (Fig. 47B,C) recovery from alkalosis was significantly inhibited ($p=0.001$, Welch's t-test).

Assessment of HCO_3^-/Cl^- exchanger activity in human embryos by Cl^- removal assay

Cleavage-stage embryos exhibited rapid intracellular alkalinization upon Cl^- removal (Fig. 48A,B). There was no significant difference in rate of alkalinization between cleavage stages, morphology rating, or fertilization protocol ($p>0.05$;

Figure 47. Recovery from intracellular alkaline load in human embryos. *Adapted from Phillips et al., 2000.* A, B. Representative traces of cleavage-stage embryo pH_i measured in KSOM (○) followed by recovery from NH_4^+-induced alkaline load in the presence (A: □) and absence (B: ■) of external Cl^-. C. Mean rate of recovery (± s.e.m.) from NH_4^+-induced alkaline load was calculated from exponential fits to recovery data as described in the text for every 0.1 pH unit between 7.1 and 7.7 for cleavage-stage embryos (2- 8-cell) in the presence (□) or absence (■) of external Cl^-. *** indicates statistical significance ($p<0.0001$; Welch's t-test). Numbers as in Fig. 23.

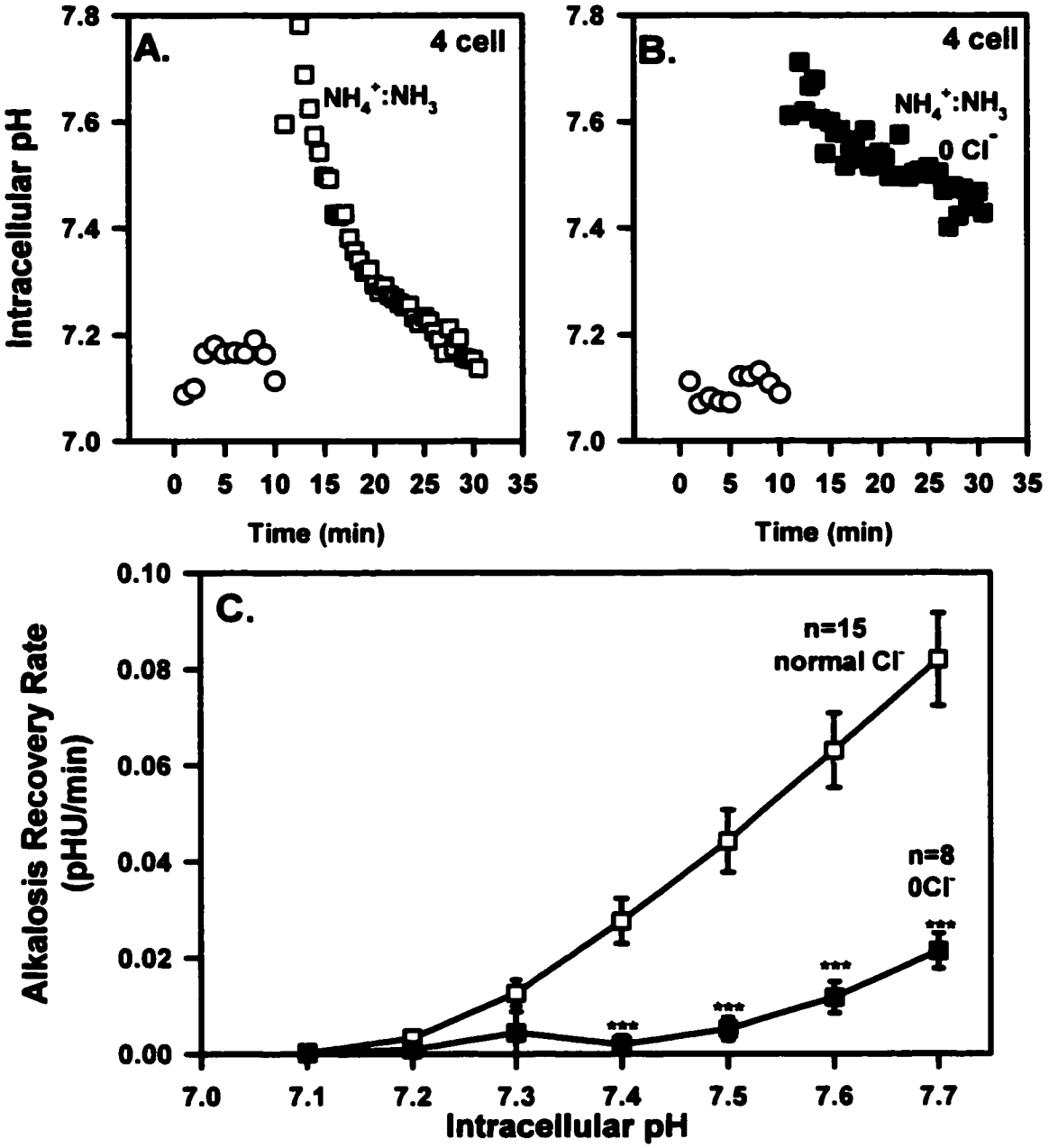
A.
4 cell
NH_4^+:NH_3
Intracellular pH
Time (min)
B.
4 cell
NH_4^+:NH_3
0 Cl^-
Time (min)
C.
n=15
normal Cl^-
n=8
0Cl^-
***
Alkalosis Recovery Rate
(pHU/min)
Intracellular pH

Figure 48. HCO_3^-/Cl^- exchanger activity measured by intracellular alkalinization in human embryos upon Cl^- removal. *Adapted from Phillips et al., 2000.* A, B. Representative traces of embryo pH_i measured in KSOM (●) followed by two consecutive Cl^- removals (○) with the second in the presence (●) or absence (○) of DIDS. C. Mean rates of intracellular alkalinization (± s.e.m.) upon initial (1^{st}) Cl^- removal and subsequent (2^{nd}) Cl^- removal in the absence or presence of 500 μM DIDS. *** indicates statistical significance ($p<0.001$; paired Student's t-test). Numbers as in Fig. 23.

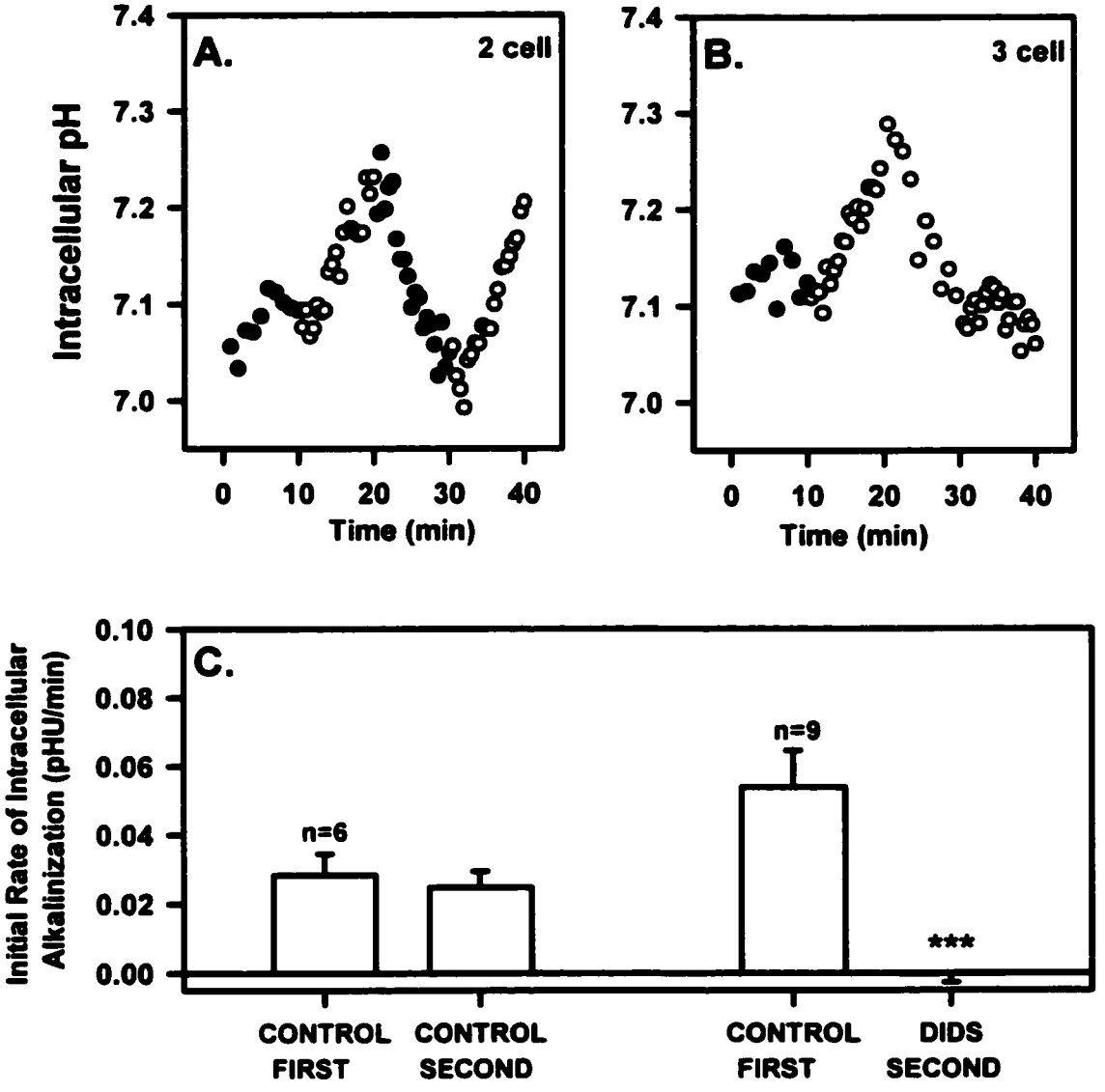
A.
2 cell
B.
3 cell
Intracellular pH
7.4
7.3
7.2
7.1
7.0
0
10
20
30
40
Time (min)
C.
Initial Rate of Intracellular Alkalinization (pHU/min)
0.10
0.08
0.06
0.04
0.02
0.00
n=6
n=9
***
CONTROL FIRST
CONTROL SECOND
CONTROL FIRST
DIDS SECOND

nANOVA). The mean rate (± s.e.m.) of intracellular alkalinization for pooled cleavage-stage embryos was 0.053 ± 0.008 (n=32). For some embryos, a second Cl^- removal was performed in which Cl^- was replaced following the first Cl^- removal and then removed again (Fig. 48A,B). There was no significant difference between the initial rate of intracellular alkalinization (first Cl^- removal) and the rate upon the second Cl^- removal (Fig. 48A,C; Paired Student's t-test, $p>0.05$; n=6). However, there was a significant inhibition of the rate of intracellular alkalinization when the anion transport inhibitor DIDS was present during the second Cl^- removal (Fig. 48B,C; Paired Student's t-test; $p=0.0016$; n=9).

Recovery from intracellular acidosis in human embryos

Recovery from induced acidosis was measured for 15 min following an NH_4Cl pulse. For some experiments, embryos were maintained in Na^+-free solution following an NH_4Cl pulse and then Na^+ was replaced for an additional 15 min (Fig. 49). Recovery rates from induced acidosis were determined by non-linear regression for every 0.1 pH_i unit increment spanning the pH_i range from the initial acidification pH_i to the final pH_i value measured at the end of 15 min. This pH_i range was specific for each embryo as there was considerable variation between embryos in the initial acidification pH_i and the final pH_i value. Cleavage-stage, morphology rating and fertilization protocol had no significant effect on the initial rate of recovery from acidosis ($p>0.05$; nANOVA); thus the data were pooled. Comparing the rates of recovery from acidosis within the same pH_i range, there was no significant difference between recoveries following acidification directly into Na^+-containing solutions or the recoveries acidified first in the absence of

external Na^+, followed by Na^+ replacement ($p>0.05$; linear regression). Thus, the rates obtained from the two protocols were pooled for analysis of rate as a function of pH_i. Rates obtained by linear regression (i.e., when recovery was inhibited and there was thus very little change in pH_i during 15 min period) are reported at the initial acidification pH_i to the nearest 0.1 pHU (e.g. the amiloride point in Fig. 49B and all 0 Na^+ points).

Embryos recovered from induced acidosis in the absence of external HCO_3^- (Fig. 49A, B). The absence of external Na^+ completely abolished this recovery (Fig. 49A, B; $p<0.0001$; nANOVA; Welch's t-test). Amiloride also significantly inhibited the recovery (Fig. 49A, B; $p<0.0001$; nANOVA). This Na^+-dependent, HCO_3^--independent recovery dropped to non-specific levels at pH_i 6.8, indicating activity only below this pH_i (Fig. 49B; $p>0.05$; Welch's t-test).

Embryos also recovered from acidosis in the presence of external HCO_3^- (Fig. 49A, C). Recovery from acidosis in the pH_i range 6.5-6.9 was significantly inhibited by the absence of external Na^+ (Fig. 49A, C; $p<0.0001$; nANOVA). However, neither inhibition of Na^+/H^+ antiporter by amiloride (1 mM) nor the presence of the anion transport inhibitor DIDS (500 μM) significantly reduced the recovery rate (Fig. 49A,C; $p>0.05$; nANOVA). As recovery from acidosis in the presence of HCO_3^- was inhibited by the absence of external Na^+ at pH_i 6.9 but not at pH_i 7.1 (Fig. 49C), this suggests that the set-point for this HCO_3^--dependent transporter is between pH_i 6.9 and 7.1. As cleavage-stage embryos recovered to approximately pH_i 7.0 following recovery of acidosis in the presence of HCO_3^-, this is consistent with a set-point of pH_i 7.0. (Fig. 49A).

pH_i regulation in human eggs

HCO_3^-/Cl^- exchanger activity and recovery from acidosis were only assessed in the few eggs available to us, and thus no statistical tests were performed. HCO_3^-/Cl^- exchanger activity in eggs was assessed by the Cl^- removal assay (Fig. 50A). The mean rate of intracellular alkalinization during Cl^- removal (± s.e.m.) was 0.075 ± 0.025 pHU/min in GV oocytes (n=2), 0.028 ± 0.010 pHU/min for MI eggs (n=3), and 0.017 ± 0.002 pHU/min in MII eggs (n=5) which appear similar to the rates observed in cleavage-stage embryos although there is a trend towards a decrease in activity from GV to MII. For MI eggs, a second Cl^- removal was performed in which Cl^- was replaced following the first Cl^- removal (Fig. 50C). Results suggest that the initial rate of intracellular alkalinization (0.028 pHU/min) was reduced when the anion transport inhibitor DIDS was present during the second Cl^- removal (0.003 ± 0.001 pHU/min).

Intracellular acidosis was induced in MI and MII eggs by a pulse of NH_4^+-KSOM, followed by a 15 min period in Na^+-free KSOM, with any recovery from acidosis measured during subsequent Na^+ replacement (Fig. 50B, D). The mean rates (± s.e.m.) of recovery from acidosis were as follows: MI eggs: 0.006 ± 0.002 pHU/min; $0Na^+$: 0.004 ± 0.003 pHU/min (n=4) and MII eggs: 0.028 ± 0.013 pHU/min and $0Na^+$: 0.003 ± 0.002 pHU/min (n=4). These recovery rates from acidosis appear to suggest only non-specific activity in MI eggs, and possibly a low Na^+-dependent activity in MII eggs compared to embryos.

Figure 50. pH_i regulation in human eggs. *Adapted from Phillips et al., 2000.* A. Mean rates of intracellular alkalinization (± s.e.m.) upon single Cl^- removal or upon Cl^- removal followed by a second Cl^- removal in the presence of 500 μM DIDS (MI eggs; n=3). B. MI and MII eggs were first acidified in the absence of external Na^+ followed by replacement of Na^+. C. Representative trace of pH_i measured in KSOM (●) followed by two consecutive Cl^- removals in the absence (○) and then presence (▲) of DIDS. D. Representative trace of pH_i during recovery from intracellular acid load in the presence of external HCO_3^-/CO_2 (KSOM (○) followed by NH_4Cl-KSOM (●), $0Na^+$-KSOM (●) and KSOM (○)). Numbers above bars as in Fig. 23.

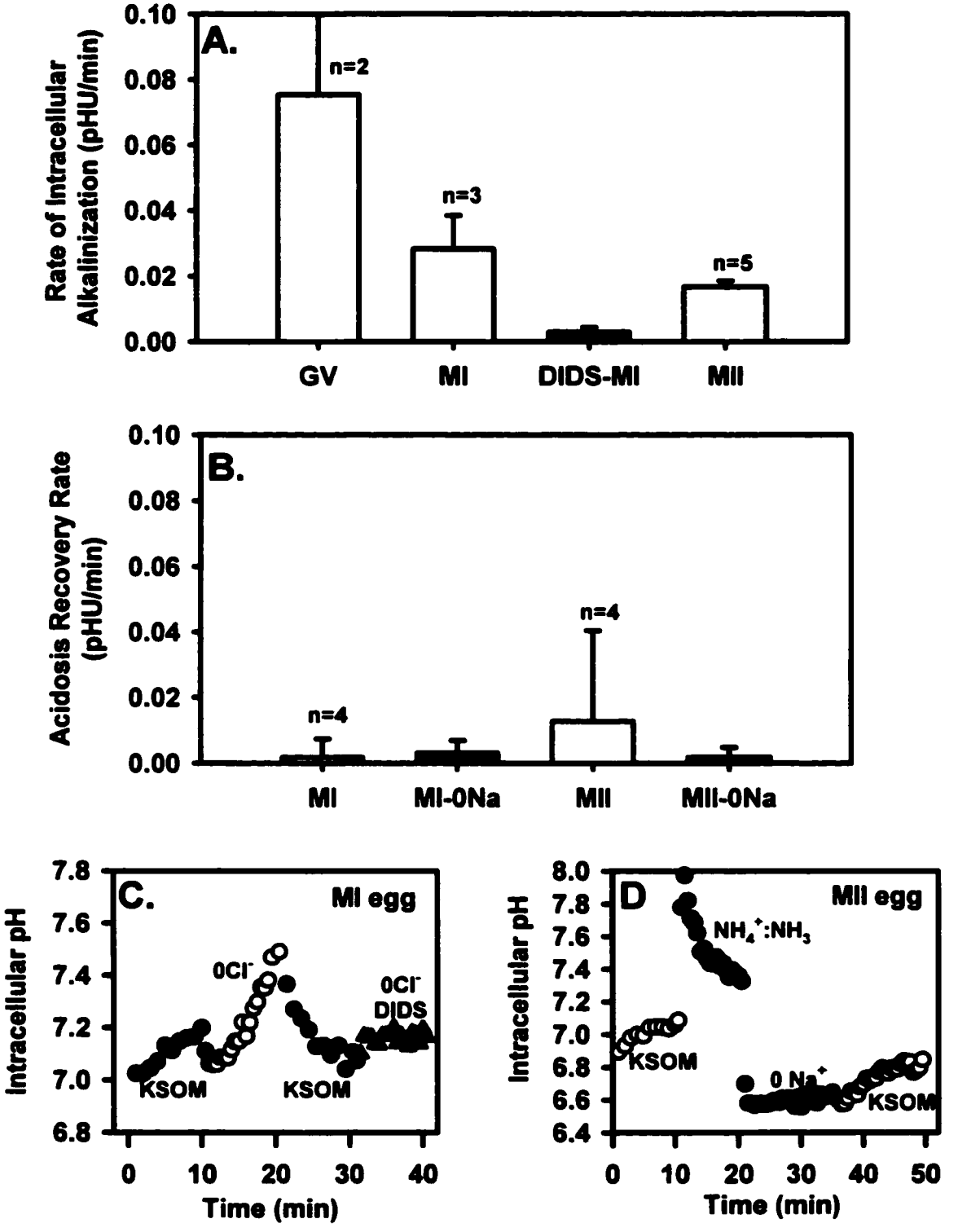
A.
Rate of Intracellular Alkalinization (pHU/min)
0.10
0.08
0.06
0.04
0.02
0.00
n=2
n=3
n=5
GV
MI
DIDS-MI
MII
B.
Acidosis Recovery Rate (pHU/min)
0.10
0.08
0.06
0.04
0.02
0.00
n=4
n=4
MI
MI-0Na
MII
MII-0Na
C.
MI egg
Intracellular pH
7.8
7.6
7.4
7.2
7.0
6.8
0Cl-
0Cl- DIDS
KSOM
KSOM
0
10
20
30
40
Time (min)
D
MII egg
Intracellular pH
8.0
7.8
7.6
7.4
7.2
7.0
6.8
6.6
6.4
NH4+:NH3
KSOM
0 Na+
KSOM
0
10
20
30
40
50
Time (min)

IV. DISCUSSION

During this investigation, Dale et al (1998) published results indicating that human preimplantation embryos, at all stages from zygote to blastocyst, have the ability to recover from an intracellular alkalosis induced by increased external pH. In contrast, they could not detect any recovery from mild acidosis induced by decreased external pH in human embryos until the blastocyst stage. Thus, they concluded that preimplantation human embryos lack mechanisms needed for recovery from intracellular acidosis until the blastocyst stage, but possess a mechanism such as HCO_3^-/Cl^- exchanger for alleviating alkalosis throughout preimplantation development. My investigation into pH_i regulation of human embryos has provided a more comprehensive examination of pH_i regulation using standard manipulations to perturb pH_i over a broader range. I have found that human preimplantation embryos, like mouse (Zhao et al; 1996, Phillips and Baltz, 1999) and hamster (Lane et al., 1999b) embryos, appear to alleviate intracellular alkalosis by HCO_3^-/Cl^- exchanger activity (Fig. 47). Recovery of human cleavage-stage embryos from NH_4^+-induced alkalosis depended on the presence of external Cl^-, as expected for mediation by HCO_3^-/Cl^- exchange. HCO_3^-/Cl^- exchanger activity was also evidenced upon external Cl^- removal, whereupon an intracellular alkalinization occurred which was inhibited by the HCO_3^-/Cl^- exchanger inhibitor DIDS (Fig. 48).

I also found that human cleavage-stage embryos rapidly recovered from acidosis (Fig. 49). Recovery from acidosis, induced by NH_4Cl pulse in the absence of external HCO_3^- and CO_2, was Na^+-dependent and completely inhibited by the presence of the Na^+/H^+ antiporter inhibitor amiloride. This suggests that Na^+/H^+ antiporter activity is

present in the human cleavage-stage embryo. Such regulation by Na^+/H^+ antiporter activity in human embryos is consistent with the presence of Na^+/H^+ antiporter activity in hamster (Lane et al., 1998) and mouse embryos of various strains (Gibb et al., 1997; C.L. Steeves, M. Lane, B.D. Bavister, K.P. Phillips, and J.M. Baltz, unpublished).

To determine whether any HCO_3^--dependent mechanisms mediating recovery from acidosis were also present in cleavage-stage embryos, recoveries from acidosis were measured in the presence of external HCO_3^- with CO_2 present (Fig. 49A,C). In the presence of HCO_3^-/CO_2, human embryos exhibited a rapid, Na^+-dependent recovery from acidosis to a slightly higher pH_i (about 6.9-7.0) than in the absence of external HCO_3^-/CO_2 where pH_i recovered to only about 6.8 (Fig. 49A, B). This suggests that a second, Na^+-dependent mechanism, which requires HCO_3^-, contributes to the alleviation of acidosis in human cleavage-stage embryos. The presence of a second system is also suggested by the inability of amiloride to significantly inhibit recovery from acidosis in the presence of external HCO_3^-/CO_2, in contrast to the complete inhibition seen in HCO_3^-/CO_2-free medium. Such Na^+ and HCO_3^- -dependent, but amiloride-insensitive, recovery would seem to implicate Na^+, HCO_3^-/Cl^- exchanger activity. No component of the recovery in the presence of HCO_3^-/CO_2 could be detected which was DIDS-sensitive, although DIDS would be expected to partially inhibit recovery by eliminating the contribution of Na^+, HCO_3^-/Cl^- exchange, leaving only Na^+/H^+ antiporter activity. It is possible, however, that the variability in recovery rates seen with human embryos precluded detection of such partial inhibition just as partial inhibition by amiloride in the presence of HCO_3^-/CO_2 was not observed.

These data indicate that human cleavage-stage embryos have the ability to

effectively maintain pH_i within a range between about 7.0 to 7.3. The embryo's HCO_3^-/Cl^- exchanger appears to be activated when pH_i rises above about 7.2-7.3 (Fig. 49C), which therefore prevents pH_i from increasing beyond this level. I also found that, in the presence of HCO_3^-/CO_2, there appear to be two mechanisms which will prevent pH_i from becoming too low. Na^+/H^+ antiporter activity becomes activated below a threshold of about 6.8 (Fig. 49B), while a second HCO_3^--dependent mechanism which may be a Na^+-HCO_3^-/Cl^- exchanger, is activated below 7.0 (Fig. 49C). Together, these would effectively maintain pH_i above 7.0. The hypothesis that pH_i is maintained within a range of 7.0-7.3 by the concerted activities of these mechanisms is consistent with the baseline pH_i of about 7.1 measured for cleavage-stage human embryos under the conditions used here.

In the absence of HCO_3^-/CO_2, my data indicate that human embryos would be less able to regulate pH_i. Since defense against alkalosis by HCO_3^-/Cl^- exchanger requires intracellular HCO_3^-, alkalosis could not be opposed in media without HCO_3^-/CO_2 where there would be little intracellular HCO_3^-. Acidosis would still be opposed, but only below about 6.8 where the Na^+/H^+ antiporter is active (Fig. 49B); the second HCO_3^--dependent mechanism which maintains pH_i above 7.0 (Fig. 49C) would be inactive since it appears to require external HCO_3^-. This has implications for the handling of human embryos in vitro, which are routinely manipulated in Hepes-buffered media at atmospheric CO_2 in vitro. This would be predicted to impair the ability of embryos to maintain pH_i, and thus, media containing HCO_3^-/CO_2 is preferable.

Dale et al (1998) found that the baseline pH_i of human eggs and zygotes was about 7.4 in HCO_3^-/CO_2-buffered medium. This value for eggs is different from the 7.0-

7.1 which we found here; the reason for this discrepancy is unknown. They probed the ability of cleavage-stage embryos to recover from an alkalosis produced by exposing them to pH 8.0 medium (Medium 199) buffered with Hepes at atmospheric CO_2. Although the low CO_2, and hence intracellular HCO_3^-, might be expected to reduce HCO_3^-/Cl^- exchanger activity, the amount of intracellular HCO_3^- remaining under their conditions (apparently embryos were assessed soon after removal from CO_2-buffered medium) was sufficient to permit HCO_3^-/Cl^- exchanger activity. Using this method, recovery from alkalosis was detected at every stage of embryo development, which is consistent with my findings. In contrast, Dale et al (1998) did not detect an ability in human cleavage-stage embryos to recover from acidosis until the blastocyst stage, using a protocol in which pH_i was reduced to about 7.0 by decreasing external pH to the same level, again in Hepes-buffered medium at atmospheric CO_2. This is also consistent with my findings, which indicated that the Na^+/H^+ antiporter in human embryos, although it would be active under their conditions, is quiescent in the absence of HCO_3^- until pH_i falls below 6.8 and thus would not have been detected with their protocol. The HCO_3^--dependent mechanism described here, however, should have been revealed in preimplantation embryos following intracellular acidification to pH_i 7.0, as the I was able to detect Na^+-dependent, HCO_3^-- recovery of pH_i up to pH_i 7.2. The use of Hepes-buffered medium at atmospheric CO_2 may not have contained sufficient levels of HCO_3^- to support the Na^+- and HCO_3^--dependent transporter revealed here. No measurements were performed here on later stage human embryos (morulae and blastocysts) since none were available at the time this study was done, and thus I can only speculate that a change in transport kinetics occurs after blastocyst formation, allowing HCO_3^--independent

recovery from mild acidosis in blastocysts.

pH_i regulation was also examined in a few available human eggs. pH_i of GV, MI and MII eggs was not significantly different from cleavage-stage embryos, with pH_i ranging from 7.0-7.1. All egg stages examined exhibited intracellular alkalinization upon Cl^- removal, similar to cleavage-stage embryos although the rate appeared to decreased from GV to MII (Fig. 50A). The rate of alkalinization in MI eggs appeared to be reduced by DIDS, which suggests that HCO_3^-/Cl^- exchanger activity is also present in eggs. This is in contrast to the recent finding that HCO_3^-/Cl^- exchanger activity in the mouse and hamster is activated upon egg activation or fertilization, with eggs (MII) having very low or barely detectable HCO_3^-/Cl^- exchanger activity (Phillips and Baltz, 1999; Lane et al., 1999b). However, the data are consistent with the finding by Dale et al (1998) that fresh MII eggs recovered from alkalosis and that recovery was inhibited by DIDS. In contrast, recovery from induced acidosis, measured in the presence of external HCO_3^-, was barely detectable in MI eggs and did not appear to be Na^+-dependent (Fig. 50B). MII eggs exhibited low rates of recovery from acidosis that appeared Na^+-dependent (Fig. 50D), although the recovery appeared to be much slower compared to the rates measured in cleavage-stage embryos. This is consistent with the recent finding that Na^+/H^+ antiporter activity is low in unfertilized hamster eggs (MII) and is subsequently activated upon fertilization (Lane et al., 1999a). Thus, it appears that although human eggs may regulate pH_i against alkalosis, they lack robust pH_i regulation in the acid range.

Robust pH_i regulation may be particularly important for the developing cleavage-stage embryo, as the fallopian tube has been reported to be quite alkaline in several mammalian species (rhesus: pH 7.7; Maas et al., 1977, rabbit: pH 7.9; Maas et al., 1987;

rat: 8.0-8.2; Ben-Yosef et al; 1996; mouse: pH 7.7; Y. Zhao, P.J-P Chauvet and J.M. Baltz, unpublished). Acid-alleviating systems may also be required by the growing embryo during this period of development to correct perturbations in pH_i due to increased metabolism and the production of intracellular protons resulting from processes such as ATP hydrolysis. I have demonstrated that human cleavage-stage embryos correct deviations in steady-state pH_i by HCO_3^-/Cl^- exchanger activity, Na^+/H^+ antiporter activity and a Na^+, HCO_3^--dependent system which together maintain embryo pH_i between 7.0-7.3. Thus, cleavage-stage human embryos possess the ability to maintain pH_i within a narrow physiological range, but this ability requires the presence of HCO_3^- and CO_2.

LITERATURE CITED

Aharonovitz, O. and Granot, Y. 1996. Stimulation of mitogen-activated protein kinase and Na^+/H^+ exchanger in human platelets. Differential effect of phorbol ester and vasopressin. J. Biol. Chem. 271:16494-16499.

Alper, S.L. 1991. The band 3-related HCO_3^-/Cl^- exchanger (AE) gene family. Ann. Rev. Phys. 53:549-564.

Alper, S.L. 1994. The band 3-related HCO_3^-/Cl^- exchanger gene family. Cell Phys. Biochem. 4:265-281.

Alper, S.L., Kopito, R.R., Libresco, S.M., and Lodish, H.F. 1988. Cloning and characterization of a murine band 3-related cDNA from kidney and from a lymphoid cell line. J. Biol. Chem. 263:17092-17099.

Araki, K., Naito, K., Haraguchi, S., Suzuki, R., Yokoyama, M., Inoue, M., Aizawa, S., Toyoda, Y. and Sato, E. 1996. Meiotic abnormalities of c-mos knockout mouse oocytes: activation after first meiosis or entrance into third meiotic metaphase. Biol. Reprod. 55:1315-1324

Aronson, P.S., Nee, J. and Suhm, M.A. 1982. Modifier role of internal H^+ in activating the Na^+-H^+ exchanger in renal microvillus membrane vesicles. Nature. 299:161-163.

Aronson, P.S. 1985. Kinetic properties of the plasma membrane Na^+-H^+ exchanger. Annu Rev Physiol. 47:545-560.

Baltz, J.M., Biggers, J.D., Lechene, C. 1990. Apparent absence of Na^+-H^+ antiport activity in two-cell mouse embryos. Dev. Biol. 138:421-429.

Baltz, J.M., Biggers, J.D., and Lechene, C. 1991a. Two-cell stage mouse embryos appear to lack mechanisms for alleviating intracellular acid loads. J. Biol. Chem. 266:6052-6057.

Baltz, J.M., Biggers, J.D., and Lechene, C. 1991b. Relief from alkaline load in two-cell stage mouse embryos by bicarbonate/chloride exchange. J. Biol. Chem. 266:17212-17217.

Baltz, J.M., and Phillips, K.P. 1999. Intracellular ion measurements in single eggs and embryos using ion-sensitive fluorophores. In, Advances in Molecular Biology, A Comparative Methods Approach to the Study of Oocytes and Embryos (ed. JD Richter). Oxford University Press, Oxford.

Barr K.J., Garrill A., Jones D.H., Orlowski J., and Kidder G.M. 1998. Contributions of Na^+/H^+ exchanger isoforms to preimplantation development of the mouse. Mol. Reprod. Dev. 50:146-153

Batten, B.E., Albertini, D.F., and Ducibella, T. 1987. Paterns of organelle distribution in mouse embryos during preimplantation development. Am. J. Anat. 178:204-213.

Bell, S.M., Schreiner, C.M., Shultheis, P.J., Miller, M.L., Evans, R.L., Vorhees, C.V., Shull, G.E., and Scott, W.J. 1999. Targeted disruption of the murine Nhe1 locus induces ataxia, growth retardation, and seizures.Am. J. Physiol. 276:C788-C795.

Bellier, S. , Chastant, S., Adenot, P., Vincent, M., Renard, J.P. and Bensaude, O. 1997. Nuclear translocation and carboxyl-terminal domain phosphorylation of RNA polymerase II delineate the two phases of zygotic gene activation in mammalian embryos. EMBO J. 16:6250-6262.

Benos, D.J. 1982. Amiloride: a molecular probe of sodium transport in tissues and cells. Am. J. Physiol. 242:C131-145.

Bensaude, O., Babinet, C., Morange, M., and Jacob, F. 1983. Heat-shock proteins, first major products of zygotic gene activity in mouse embryo. Nature. 305:331-333.

Ben-Yosef, D., Oron, Y., and Shalgi, R. 1996. Intracellular pH of rat eggs is not affected by fertilization and the resulting calcium oscillations. Biol. Reprod. 55:461-468.

Ben-Yosef, D., Oron, Y., and Shalgi, R. 1995. Low temperature and fertilization-induced Ca^{2+} changes in rat eggs. Mol. Reprod. Dev. 42:122-9.

Bertrand, B., Wakabayashi, S., Ikeda, T., Pouyssegur, J. and Shigekawa, M. 1994. The Na^+/H^+ exchanger isoform 1 (NHE1) is a novel member of the calmodulin-binding proteins. Identification and characterization of calmodulin-binding sites. J. Biol. Chem. 269:13703-13709.

Bhatt, R.R., and Ferrell Jr., J.E. 1999. The protein kinase $p90^{Rsk}$ as an essential mediatory of cytostatic factor activity. Science. 286:1362-1365.

Bianchini, L., L'Allemain, G. and Pouyssegur, J. 1997. The p42/p44 mitogen-activated protein kinase cascade is determinant in mediating activation of the Na^+/H^+ exchanger (NHE1 isoform) in response to growth factors. J. Biol. Chem. 272(1):271-9.

Bigler, D., Takahashi, Y., Chen, M.S., Almeida, E.A.C., Osbourne, L., and White, J.M. 2000. Sequence-specific interaction between the disintegrin domain of mouse ADAM 2 (fertilin β) and murine eggs. J. Biol. Chem. 275:11576-11584.

Bleil, J.D. and Wassarman, P.M. 1980. Mammalian sperm-egg interaction: identification of a glycoprotein in mouse egg zonae pellucidae possessing receptor activity for sperm. Cell. 20(3):873-82.

Bloom, T.L. 1989. The effects of phorbol ester on mouse blastomeres: a role for protein kinase C in compaction? Develop. 106:159-171.

Boatman, D.E. 1997. Responses of gametes to the oviductal environment. Hum. Reprod. 12:133-149

Bolton, V.N., Oades, P.J., and Johnson, M.H. 1984. the relationship between cleavage, DNA replication and gene expression in the mouse 2-cell embryo. J. Embryol. exp. Morph. 79:139-163.

Bookstein, C., Musch, M.W., DePaoli, A., Xie, Y., Rabenau, K., Villereal, M., Rao, M.C. and Chang, E.B. 1996. Characterization of the rat Na^+/H^+ exchanger isoform NHE4 and localization in rat hippocampus. Am. J. Physiol. 271:C1629-38.

Bookstein, C., Xie, Y., Rabenau, K., Musch, M.W., McSwine, R.L., Rao, M.C., and Chang, E.B. 1997. Tissue distribution of Na^+/H^+ exchanger isoforms NHE2 and NHE4 in rat intestine and kidney. Am. J. Physiol. 273:C1496-C1505.

Borland, R.M., Biggers, J.D., and Lechene, C.P. 1977. Studies on the composition and formation of mouse blastocoele fluid using electron probe microanalysis. Dev. Biol. 55(1):1-8.

Borland, R.M., Biggers, J.D., Lechene, C.P., and Taymor, M.L. 1980. Elemental composition of fluid in the human Fallopian tube. J Reprod Fertil. 58(2):479-82.

Boron, W.F., Roos, A., and de Weer, P. 1978. NH_4Cl and other weak bases in the activation of sea urchin eggs. Nature. 274:190.

Bornslaeger, E.A., Mattel, P., and Schultz, R.M. 1986. Involvement of cAMP-dependent protein kinase and protein phosphorylation in regulation of mouse oocyte maturation. Dev. Biol. 114:453-462.

Boron, Walter F. 1986. Intracellular pH regulation. Membrane Transport Processes in Organized Sygstems. ed. Andreoli, Th. E. et al. Plenum Med. Book Co.

Bos-Mikich, A., Swann, K., and Whittingham, D.G. 1995. Calcium oscillations and protein synthesis inhibition synergistically activate mouse oocytes. Mol. Reprod. Dev. 41:84-90.

Bos-Mikich, A., Swann, K., Ozil, J.P., McCarthy, A., and Whittingham, D.G. 1993. Parthenogenic activation of mouse eggs by strontium. J. Reprod. Fert. Abs.11:24

Boyarsky, G., Ganz, M.B., Sterzel, R.B., and Boron, W.F. 1988. pH regulation in single glomerular mesangial cells. I. Acid extrusion in absence and presence of HCO_3^-. Am. J. Physiol. 255:C844-C856.

Boyarsky, G., Ganz, M.B., Sterzel, R.B., and Boron, W.F. 1988b. pH reguation in single glomerular mesangial cells. II. Na^+-dependent and -independent Cl^--HCO_3^- exchangers. Am. J. Physiol. 255:C857-C869.

Brassard, M., Duclohier, H., Moreau, M., and Guerrier, P. 1988. Intracellular pH change does not appear as a prerequisite for triggering activation of *Barnea candida* (Mollusca, Pelecypoda) oocytes. Gam. Res. 20:43-52.

Brison, D.R. and Leese, H.J. 1993. Role of chloride transport in the development of the rat blastocyst. Biol. Reprod. 48:692-702.

Brison, D.R., and Schultz, R.M. 1998. Increased incidence of apoptosis in transforming growth factor alpha-deficient mouse blastocysts. Biol. Reprod. 59:136-144.

Bronson, R.A., Fusi, F.M., Calzi, F., Doldi, N., and Ferrari, A. 1999. Evidence that a functional fertilin-like ADAM plays a role in human sperm-oolemmal interactions. Mol. Hum. Reprod. 5:433-440.

Brosius, F.C., Alper, S.L., Garcia, A.M., and Lodish, H.F. 1989. The major kidney band 3 gene transcript predicts an amino-terminal truncated band 3 polypeptide. J. Biol. Chem. 264:7784-7787.

Brunton, W.J., and Brinster, R.L. 1971. Active chloride transport in the isolated rabbit oviduct. Am. J. Physiol. 221:658-661.

Brunton, W.J. 1972. Beta-adrenergic stimulation of transmembrane potential and short circuit current of isolated rabbit oviduct. Nature New Biol. 1:236:12-24.

Chambers, E.L. 1976. Na^+ is essential for activation of the inseminated sea urchin egg. J. Exp. Zool. 197:149-154.

Chambers, E.L., and McCulloh, D.H. 1990. Excitation, activation and sperm entry in sea urchin eggs. J. Reprod. Fert. (Suppl.) 117-132.

Cheek, T.R., McGuinness, O.M., Vincent, C., Moreton, R.B., Berridge, M.J., and Johnson, M.H. 1993. Fertilisation and thimerosal stimulate similar calcium spiking patterns in mouse oocytes but by separate mechanisms. Develop. 119:179-189.

Chen, Y., Cann, M.J., Litvin, T.N., Iourgenko, V., Sinclair, M.L., Levin, L.R., and Buck, J. 2000. Soluble adenylyl cyclase as an evolutionarily conserved bicarbonate sensor. Science. 289:625-628

Cherr, Gary N., and Ducibella, Thomas. 1990. Activation of the Mammalian Egg. Fertilization in Mammals. ed. Barry D. Bavister et al. Serono Symposia.

Cheung, A., Swann, K., and Carroll, J. 2000. The ability to generate normal Ca^{2+} transients in response to spermatozoa develops during the final stages of oocyte growth and maturation. Hum. Reprod. 15:1389-1395.

Chini, E.N., Liang, M., and Dousa, T.P. 1998. Differential effect of pH upon cyclic-ADP-ribose and nicotinate-adenine dinucleotide phosphate-induced Ca^{2+} release systems. Biochem. J. 335:499-504.

Cho, W.K., Stern, S., and Biggers, J.D. 1974. Inhibitory effect of dibutyryl cAMP on mouse oocyte maturation in vitro. J. Exp. Zool. 187:383-386.

Choi, I., Romero, M.F., Khandoudi, N., Bril, A. and Boron, W.F. 1999a. Cloning and characterization of a human electrogenic Na^+-HCO_3^- cotransporter isoform (hhNBC). Am. J. Physiol. 276: C576-C584.

Cicirelli, Michael F., Robinson, K.R., and Smith, L.D. 1983. Internal pH of *Xenopus* oocytes: A study of the mechanism and role of pH changes during meiotic maturation. Dev. Biol. 100:133-146.

Cognard, C., and Raymond, G. 1985. The strontium-induced calcium-release process and its implication in contractility of skeletal muscle of *Rana ridibunda*. Proc. R. Soc. Lond. Biol. Sci. 224:489-509.

Colledge, W.H., Carlton, M.B.L., Udy, G.B., and Evans, M.J. 1994. Disruption of *c-mos* causes parthenogenetic development of unfertilized mouse eggs. Nature. 370:65-67.

Collins, J.L., and Baltz, J.M. 1999. Estimates of mouse oviductal fluid tonicity based on osmotic responses of embryos. Biol. Reprod. 60:1188-1193.

Conover, J., Temeles, G.L., Zimmermann, J.W., Burke, B., and Schultz, R.M. 1991. Stage-specific expression of a family of proteins that are major products of zygotic gene activation in the mouse embryo. Dev. Biol. 114:392-404.

Coulter, K.L., Perier, F., Radeke, C.M., and Vandenberg, C.A. 1995. Identification and molecular localization of a pHi-sensing domain for the inward rectifier potassium channel HIR. Neuron. 15:1157-1168.

Counillon, L., Scholz, W., Lang, H.J., and Pouyssegur, J. 1993. Pharmacological characterization of stably transfected Na^+/H^+ antiporter isoforms using amiloride analogs and a new inhibitor exhibiting anti-ischemic properties. Mol. Pharmacol. 44:1041-5.

Counillon, L., and Pouysségur, J. 2000. The expanding family of eukaryotic Na^+/H^+ exchangers. J. Biol. Chem. 275:1-4.

Coupaye-Gerard, B., Bookstein, C., Duncan, P., Chen, X.Y., Smith, P.R., Musch, M., Ernst, S.A., Chang, E.B., and Kleyman, T.R. 1996. Biosynthesis and cell surface delivery of the NHE1 isoform of Na^+/H^+ exchanger in A6 cells. Am. J. Physiol. 271:C1639-C1645.

Cox, G.A., Lutz, C.M., Yang, C.L., Biemesderfer, D., Bronson, R.T., Fu, A., Aronson, P.S., Noebels, J.L., and Frankel, W.N. 1997. Sodium/hydrogen exchanger gene defect in slow-wave epilepsy mutant mice. Cell. 91:139-148.

Crow, J., Amso, N.N., Lewin, J., and Shaw, R.W. 1994. Morphology and ultrastructure of fallopian tube epithelium at different stages of the menstrual cycle and menopause. Hum. Reprod. 9(12):2224-33

Dale, B., Marino, M., and Wilding, M. 1999. Sperm-induced calcium oscillations. Soluble factor, factors or receptors? Mol. Hum. Reprod. 5:1-4.

Dale, B., Menezo, Y., Cohen, J., DiMatteo, L. and Wilding, M. 1998. Intracellular pH regulation in the human oocyte. Hum. Reprod. 13:964-970.

Dale, B., DeFelice, L., and Ehrenstein, G. 1985. Injection of a soluble sperm extract into sea urchin eggs triggers the cortical reaction. Experientia. 41:1068-1070.

Davis, W., De Sousa, P.A., and Schultz, R.M. 1996. Transient expression of translational initiation factor eIF4C during the 2-cell stage of the preimplantation mouse embryo: identification by mRNA differential display and the role of DNA replication in zygotic gene activation. Dev. Biol. 174:190-201.

Demuth, D.R., Showe, L.C., Ballantine, M., Palumbo, A., Fraser, P.J., Cioe, L., Rovera, G., and Curtis, P.J. 1986. Cloning and structural characterization of a human nonerythroid band 3-like protein. EMBO J. 5:1205-1214.

Deng, M.Q. and Shen, S.S. 2000. A specific inhibitor of p34(cdc2)/cyclin B suppresses fertilization-induced calcium oscillations in mouse eggs. Biol Reprod. 62(4):873-8.

de Vantéry, C., Stutz, A., Vassall, J.D., and Schorderet-Slatkine, S. 1997. Acquisition of meiotic competence in growing mouse oocytes is controlled at both translational and posttranslational levels. Dev. Biol. 187:43:54.

DeSousa, P., Valdimarsson, G., Nicholson, B.J. and Kidder, G.M. 1993. Connexin trafficking and the control of gap junction assembly in mouse preimplantation embryos. Develop. 117:1355-1367.

De Souza, L.R., Moore, H., Raha, S., and Reed, J.K. 1995. Purine and pyridimine nucleotides activate distinct signalling pathways in PC12 cells. J. Neurosci. Res. 41:753-763.

Dickens, C.J.m and Leese, H.J. 1994. The regulation of rabbit oviductal fluid. J. Reprod. Fert. 100(2):5777-581.

Digonnet, C., Aldon, D., Leduc, N., Dumas, C. and Rougier, M. 1997. First evidence of a calcium transient in flowering plants at fertilization. Develop. 124:2867-2874.

Ding, Y., Kobayashi, S., and Kopito, R. 1991. Mapping of ankyrin binding determinants on the erythroid exchanger, AE1. J. Biol. Chem. 271:22494-22498.

Dhanasekaran, N., Prasad, M.V., Wadsworth, S.J., Dermott, J.M., van Rossum G. 1994. Protein kinase C-dependent and -independent activation of Na^+/H^+ exchanger by G alpha 12 class of G proteins. J Biol Chem. 269(16):11802-6.

Dubé, F., and Eckberg, W.R. 1997. Intracellular pH increase driven by an Na^+/H^+ exchanger upon activation of surf clam oocytes. Dev. Biol. 190:41-54.

Dubé, François. 1988. The relationship between early ionic events, the pattern of protein synthesis, and oocyte activation in the surf clam, Spisula solidissima. Dev. Biol. 126:233-241.

Dubé, François, Schmidt,Tobias, Johnson, Carl Hirschie, and Epel, David. 1985. The hierarchy of requirements for an elevated intracellular pH during early development of sea urchin embryos. Cell. 40:657-666.

Ducibella, T., Albertini, D.F., Anderson, E., and Biggers, J.D. 1975. The preimplantation mammalian embryo: characterization of intercellular junctions and their appearance during development. Dev. Biol. 45(2):231-50.

Ducibella, T., Ukena, T., Karnovsky, M., and Anderson, E. 1977. Changes in cell surface and cortical cytoplasmic organization during early embryogenesis in the preimplantation mouse embryos. J. Cell Biol. 74:153-167.

Ducibella, T., and LeFevre, L. 1997. Study of protein kinase C antagonists on cortical granule exocytosis and cell-cycle resumption in fertilized mouse eggs. Mol. Reprod. Dev. 46(2):216-26.

Dudeja, P.K., Rao, D.D., Syed, I., Joshi, V., Dahdal, R.Y., Gardner, C., Rish, M.C., Schmidt, L, Bavishi, D., Kim, K.E., Harig, J.M., Goldstein, J.L., Layden, T.J., and Ramaswamy, K. 1996. Intestinal distribution of human Na^+/H^+ exchanger isoforms NHE-1, NHE-2, and NHE-3 mRNA. Am. J. Physiol. 271:G438-G493.

Dudeja, P.K., Hafez, N., Tyagi, S., Gailey, C.A., Toofanfard, M., Alrefai, W.A., Nazir, T.M., Ramaswamy, K., and Al-Bazzaz, F.J. 1999. Expression of the Na^+/H^+ and Cl^-/HCO_3^- exchanger isoforms in proximal and distal human airways. Am. J. Phys. 276:971-978.

Dyban, A.P., and Noniashvili, E.M. 1990. Parthenogenetic development in response to the treatment of mouse oocytes with a weak alkali. Experiments with methylamine. [abstr.] Ontogenez 21(3):280-285.

Emerson, M., Travis, A.R., Bathgate, R., Stojanov, T., Cook, D.I., Harding, E., Lu, D.P., and O'Neill, C. 2000. Characterization and functional significance of calcium transients in the 2-cell mouse embryo induced by an autocrine growth factor. J. Biol. Chem. 275:21905-21913.

Eppig, J.J. 1979. FSH stimulates hyaluronic acid synthesis by oocyte-cumulus cell complexes from mouse preovulatory follicles. Nature. 281(5731):483-4.

Eppig, J.J. 1982. The relationship between cumulus cell-oocyte coupling, oocyte meiotic maturation, and cumulus expansion. Dev. Biol. 89:268-272.

Eppig, J.J., O'Brien, M., and Wigglesworth, K. 1996. Mammalian oocyte growth and development in vitro. Mol. Reprod. Develop. 44:260-273.

Eppig, J.J., O'Brien, J., Pendola, F.L., and Watanabe, S. 1998. Factors affecting the developmental competence of mouse oocytes grown in vitro: follicle-stimulating hormone and insulin. Biol. Reprod. 59:1445-1453.

Epel, D. 1988. The role of Na^+/H^+ exchange and intracellular pH changes at fertilization. In: Na^+/H^+ exchange. Ed: S. Grinstein.

Evans, J.P. 2000. Getting sperm and egg together: Things conserved and things diverged. Biol. Reprod. 63:355-360.

Favata, M.F., Horiuchi, K.Y., Manos, E.J., Daulerio, A.J., Stradley, D.A., Feeser, W.S., Van Dyk, D.E., Pitts, W.J., Earl, R.A., Hobbs, F., Copeland, R.A., Magolda, R.L., Scherle, P.A., and Trzaskos, J.M. 1998. Identification of a novel inhibitor of mitogen-activated protein kinase kinase. J. Biol. Chem. 273:18623-18632.

Ferrell Jr., J.E. 1999. *Xenopus* oocyte maturation: new lessons from a good egg. Bioessays. 21:833-842.

Fleming, T.P., Cannon, P.M., and Pickering, S.J. 1986. The cytoskeleton endocytosis and cell polarity in the mouse preimplantation mouse embryo. Dev. Biol. 113:406-419.

Fliegel, L., Dyck, J.R., Wang, H., Fong, C., and Haworth, R.S. 1993. Cloning and analysis of the human myocardial Na^+/H^+ exchanger. Mol Cell Biochem. 125(2):137-43.

Fliegel, L., and Frohlich, O. 1993. The Na^+/H^+ exchanger: an update on structure, regulation and cardiac physiology. Biochem J. 296(Pt 2):273-85.

Fraser, Lynn R. 1987. Strontium supports capacitation and the acrosome reaction in mouse sperm and rapidly activates mouse eggs. Gam. Res. 18:363-374.

Freeman, G. and E.B. Ridgway. 1993. The role of intracellular calcium and pH during fertilization and egg activation in the hydrozoan *Phialidium*. Dev. Biol. 156(1):176-90.

Frelin, C., Vigne, P., and Lazdunski, M. 1983. The amiloride-sensitive Na^+/H^+ antiport in 3T3 fibroblasts. J. Biol. Chem. 258(10):6272-6.

Fujiwara, T., Takami, N., Misumi, Y. and Ikehara, Y. 1998. Nordihydroguaiaretic acid blocks protein transport in the secretory pathway causing redistribution of Golgi proteins into the endoplasmic reticulum. J. Biol. Chem. 273:3068-3075.

Fulton, B.P., and Whittingham, D.G. 1978. Activation of mammalian oocytes by intracellular injection of calcium. Nature. 273:149-151.

Fudner, J., Tosteson, D.C., and Wieth, J.O. 1978. Effects of bicarbonate on lithium. J. Gen. Physiol. 71:721-746.

Galione, A., and White, A. 1994. Ca^{2+} release induced by cyclic ADP-ribose. Trends Cell Biol. 4:431-437.

Gallicano, G.I., McGaughey, R.W., and Capco, D.C. 1997. Activation of protein kinase C after fertilization is required for remodeling the mouse egg into the zygote. Mol. Reprod. Develop. 46:587-601.

Ganz, M.B., Boyarsky,G., Sterzl, R.B. and Boron, W.F. 1989. Arginine vasopressin enhances pH_i-regulation in the presence of HCO_3^- by stimulating three acid-base transport systems. Nature. 337:648-651.

Gavin, A-C, Ainle, A.N., Chierici, E., Jones, M., and Nebreda, A.R. 1999. A $p90^{rsk}$ mutant constitutively interacting with MAP kinase uncouples MAP kinase from $p34^{cdc2}$/cyclin B activation in *Xenopus* oocytes. Mol. Biol. Cell. 10:2971-2986.

Gianaroli, L., Tosti, E., Magli, C., Iaccarino, M., Ferraretti, A.P., and Dale, B. 1994. Fertilization current in the human oocyte. Mol. Reprod. Dev. 38:209-214.

Gibb, C.A., Poronnik, P., Day, M.L., and Cook, D.I. 1997. Control of cytosolic pH in two-cell mouse embryos: roles of H^+-lactate cotransport and Na^+/H^+ exchange. Am. J. Physiol. 273:C404-C419.

Girard, J.-P., Payan, P., and Sardet, C. 1982. Changes in intracellular cations following fertilization of sea urchin eggs. Na^+/H^+ and Na^+/K^+ exchanges. Exp. Cell Res. 142:215-221.

Gordon J.W., Grunfeld, L., Garrisi, G.J., Navot, D., and Laufer, N. 1989. Successful microsurgical removal of a pronucleus from tripronuclear zygotes. Fert. Steril. 52(3):367-372.

Gould, M.C., and Stephano, J.L. 1999. MAP kinase, meiosis, and sperm centrosome suppression in *Urechis caupo*. Dev. Biol. 216:348-358.

Gould, M.C., and Stephano, J.L. 1993. Nuclear and cytoplasmic pH increase at fertilization in *Urechis caupo*. Dev. Biol. 159(2):608-17.

Gould, Meredith, and Holland,Linda Z. 1984. Fertilization acid release in *Urechis* eggs. II. The stoichiometry of Na^+ uptake and H^+ release. Dev. Biol. 104:329-335.

Grainger, J.L., Winkler, M.M., Shen, S.S., and Steinhardt, R.A. 1979. Intracellular pH controls protein synthesis rate in the sea urchin egg and early embryo. Dev. Biol. 68:396-406.

Grandin, N. and M. Charbonneau. 1991a. Intracellular pH and intracellular free calcium responses to protein kinase C activators and inhibitors in *Xenopus* eggs. Develop. 112:461-470.

Grandin, N. and M. Charbonneau. 1991b. Changes in intracellular free calcium activity in *Xenopus* eggs following imposed intracellular pH changes using weak acids and weak bases. Biochim. Biophys. Acta. 1091(2):242-50.

Grandin, N. and M. Charbonneau. 1992. The increase in intracellular pHi associated with *Xenopus* egg activation is a Ca^{2+}-dependent wave. J. Cell Sci. 101:55-67.

Green, J., Yamaguchi, D.T., Kleeman, C.R., and Muallem, S. 1990. Cytosolic pHi regulation in osteoblasts. Regulation of anion exchange by intracellular pHi and Ca^{2+} ions. J. Gen. Physiol. 95:121-45.

Grichtchenko, I.I., Choi, I., Zhong, X., Bray-Ward, P., Russell, J.M., and Boron, W.F. 2001. Cloning, characterization and chromosomal mapping of a human electroneutral Na^+-driven Cl^--HCO_3^- exchanger. J. Biol. Chem. In press.

Grinstein, S., Ship, S., and Rothstein, A. 1978. Anion transport in relation to proteolytic dissection of band 3 protein. Biochim. Biophys. Acta. 507:294-304.

Grinstein, S., and Foskett, J.K. 1990. Ionic mechanisms of cell volume regulation in leukocytes. Annu Rev Physiol. 52:399-414.

Grøndahl, C., Lessl, M., Færge, I., Hegele-Hartung, C., Wassermann, K., and Ottesen, J.L. 2000. Meiosis-activating sterol-mediated resumption of meiosis in mouse oocytes in vitro is influenced by protein synthesis inhibition and cholera toxin. Biol. Reprod. 62:775-780.

Gross, S.D., Schwab, M.S., Lewellyn, A.L., and Maller, J.L. 1999. Induction of metaphase arrest in cleaving *Xenopus* embryos by the protein kinase $p90^{Rsk}$. Science. 286:1365-1367.

Gross, S.D., Schwab, M.S., Taieb, F.E., Lewellyn, A.L., Qian, Y.W., and Maller, J.L. 2000. The critical role of the MAP kinase pathway in meiosis II in *Xenopus* oocytes is mediated by p90(Rsk). Curr. Biol. 10(8):430-8

Guerrier, P., Brassard, M., David, C., and Moreau, M. 1986. Sequential control of meiosis reinitiation by pH and Ca^{2+} in oocytes of the prosobranch mollusk *Patella vulgata*. Dev. Biol. 114:315-324.

Grynkiewicz, G., Poenie, M., and Tsien, R.Y. 1985. A new generation of Ca^{2+} indicators with greatly improved fluorescence properties. J Biol Chem. 260(6):3440-50.

Hajnóczky, G., and Thomas, A.P. 1997. Minimal requirements for calcium oscillations driven by the IP3 receptor. EMBO J. 16:3533-3543.

Hampl, A., and Eppig, J.J. 1995. Analysis of the mechansism(s) of metaphase I arrest in maturing mouse oocytes. Develop. 121:925-933.

Hannun, Y.A., Loomis,C.R., Merrill Jr., A.H. and Bell, R.M. 1986. Sphingosine inhibition of protein kinase C activity and of phorbol dibutyrate binding in vitro and in human platelets. J. Biol. Chem. 261:12604-12609.

Haraguchi, S., Naito, K., and Sato, E. 1998. MAP kinase cascade, but not ERKs, activated during early cleavage of mouse embryos. Mol. Reprod. Dev. 51:148-155.

Hashimoto, N., Watanabe, N., Furuta, Y., Tamemoto, H., Sagata, N., Yokoyama, M., Okazaki, K., Nagazyoshi, M., Takeda, N., Ikawa, Y., and Alzawa, S. 1994. Parthenogenetic activation of oocytes in *c-mos*-deficient mice. Nature. 370:68-71.

Haugland, RP. 1996. Handbook of Fluorescent Probes and Research Chemicals. 6th ed. Eugene, OR: Molecular Probes, Inc.

He, X., Wu, X., Knauf, P.A., Tabak, L.A., and Melvin, J.E. 1993. Functional expression of the rat anion exchanger AE2 in insect cells by a recombinant baculovirus. Am. J. Physiol. 264:C1075-C1079.

Hegele-Hartung, C., Kuhnke, J., Lessl, M., Grondahl, C., Ottesen, J., Beier, H.M., Eisner, S., and Eichenlaub-Ritter, U. 1999. Nuclear and cytoplasmic maturation of mouse oocytes after treatment with synthetic meiosis-activating sterol in vitro. Biol. Reprod. 61:1362-1372.

Heinecke, J.W., and Shapiro, B.M. 1990. Protein kinase C activates the respiratory burst of fertilization, but not cortical granule exocytosis, in ionophore-stimulated sea urchin eggs. Dev. Biol. 142:216-223.

Hirao, Y., and Eppig, J.J. 1997. Parthenogenetic development of Mos-deficient mouse oocytes. Mol Reprod Dev. 48:391-6.

Hoffert, J.D., Leitch, V., Agre, P., and King, L.S. 2000. Hypertonic induction of aquaporin-5 expression through an ERK-dependent pathway. J. Biol. Chem. 275:9070-9077.

Hogan, Brigid, Frank Costantini and Elizabeth Lacy. 1986. Manipulating the Mouse Embryo. Cold Springs Harbor Laboratory.

Hoogerwerf, W.A., Tsao, S.C., Devuyst, O., Levine, S.A., Yun, C.H., Yip, J.W., Cohen, M.E., Wison, P.D., Lazenby, A.J., Tse, C.M., and Donowitz, M. 1996. NHE2 and NHE3 are human and rabbit intestinal brush-border proteins. Am. J. Physiol. 270:G29-F41.

Hooley, R., Yu, C.Y., Symons, M., and Barber, D.L. 1996. G alpha 13 stimulates Na^+-H^+ exchange through distinct Cdc42-dependent and RhoA-dependent pathways. J. Biol. Chem. 271:6152-8.

Houliston, E., Pickering, S.J., and Maro, B. 1987. Redistribution of microtubules and pericentriolar material during the development of polarity in mouse blastomeres. J. Cell Biol. 104:1299-1308.

Houliston, E., and Maro, B. 1989. Posttranslational modification of distinct microtubule subpopulations during cell polarization and differentiation in the mouse preimplantation embryo. J. Cell Biol. 108:543-551.

House, C.R. 1994. Confocal ratio imaging of intracellular pH in unfertilized mouse oocytes. Zygote. 2:37-45.

Howlett, S.K., and Bolton, V.N. 1985. Sequence and regulation of morphological and molecular events during the first cell cycle of mouse embryogenesis. J.Embryol. Exp. Morph. 87:175-206.

Humphreys, B.D., Jiang, L., Chernova, M.N. and Alper, S.L. 1994. Functional characterization and regulation by pH of murine AE2 HCO_3^-/Cl^- exchanger expressed in *Xenopus* eggs. Am. J. Phys. 267:C1295-C1307.

Igarashi, H., Takahashi, E., Hiroi, M., and Doi, K. 1997. Aging-related changes in calcium oscillations in fertilized mouse oocytes. Mol. Reprod. Develop. 48:383-390.

Invessa, N.E., De Lemos-Chiarandin, C., Gravotta, D., Sabatini, D.D., and Kreibich, G. 1995. The brefeldin A-induced retrograde transport from the Golgi apparatus to the endoplasmic reticulum depends on calcium sequestered to intracellular stores. J. Biol. Chem. 270:25960-25967.

Jaffe, L.A. 1990. First messengers at fertilization. J. Reprod. Fert. Suppl. 42:107-16.

Jarolim, P., Shayakul, C., Prabakaran, D., Jiang, L., Stuart-Tilley, A., Rubin, H.L., Simova, S., Zavadil, J., Herrin, J.T., Brouillette, J., Somers, M.J., Seemanova, E., Brugnara, C., Guay-Woodford, L.M., and Alper, S.L. 1998. Autosomal dominant distal renal tubular acidosis is associated in three families with heterozygosity for the R589H mutation in the AE1 (band 3) Cl-/HCO3- exchanger. J Biol Chem. 273(11):6380-8

Jennings, M.L., and Smith, J.S. 1992. Anion-proton cotransport through the human red blood cell band 3 protein. Role of glutamate 681. J. Biol. Chem. 267:13964-13971.

Jiang, L., Stewart-Tilley, A., Parkash, J., and Alper, S.L. 1994. pH_i and serum regulate AE2-mediated Cl^-/HCO_3^- exchange in CHOP cells of defined transient transfection status. Am. J. Phys. 267:C845-C856.

Johnson, J.D., Epel, D., and Paul, M. 1976. Intracellular pH and activation of sea urchin eggs after fertilization. Nature. 262:661-664.

Johnson, M.H., and Maro, B. 1984. The distribution of cytoplasmic actin in mouse 8-cell blastomeres. J. Embryol. Exp. Morphol. 82:97-117.

Johnson, M.H., Pickering, S.J., Braude, P.R., Vincent, C., Cant, A., and Currie, J. 1990. Acid Tyrode's solution can stimulate parthenogenetic activation of human and mouse oocytes. Fert. Steril. 53(2):266-70.

Jones, K.T., Carroll, J., and Whittingham, D.G. 1995a. Ionomycin, thapsigargin, ryanodine, and sperm induced Ca^{++} release increase during meiotic maturation of mouse oocytes. J. Biol. Chem. 270:6671-6677.

Jones, K.T., Carroll, J., Merriman, J.A., Whittingham, D.G., and Kono, T. 1995b. Repetitive sperm-induced Ca^{2+} transients in mouse oocytes are cell cycle dependent. Develop. 121:3259-3266.

Kalab, P., Kubiak, J.Z., Verlhac, M.H., Colledge, W.H., and Maro, B. 1996. Activation of p90rsk during meiotic maturation and first mitosis in mouse oocytes and eggs: MAP kinase-independent and -dependent activation. Develop. 122(6):1957-64.

Kang, M.G., Kulisz, A., and Wasserman, W.J. 1998. Raf-1 kinase, a potential regulator of intracellular pH in Xenopus oocytes. Biol. Cell. 90:477-85.

Kaplan, D.L., and Boron, W.F. 1994. Long-term expression of c-H-ras stimulates Na^+-H^+ and Na^+-dependent Cl--HCO3 exchange in NIH-3T3 fibroblasts. J. Biol. Chem. 269:4116-4124.

Kaufman, 1978. The experimental production of mammalian parthenogenetic embryos. In: Methods in Mammalian Reproduction. Ed. J.C. Daniel, Jr. Academic Press. pp. 21-46.

Kaufman, M.H. 1982. The chromosome complement of single-pronuclear haploid mouse embryos following activation by ethanol treatment. J. Embryol. exp. Morph. 71:139-154.

Kemp, B.E., and Pearson, R.B. 1990.Protein kinase recognition sequence motifs. Trends Biochem Sci. 15(9):342-6.

Klanke, C.A., Su, Y.R., Callen, D.F., Wang, Z., Meton, P., Baird, N., Kandasamy, R.A., Orlowski, J., Otterud, B.E., Leppert, M et al. 1995. Molecular cloning and physical and genetic mapping of a novel human Na^+/H^+ exchanger (NHE5/SLC9A5) to chromosome 16q22.1. Genomics. 25:615-622.

Kline, D., and Kline, J.T. 1992. Thapsigargin activates a calcium influx pathway in the unfertilized mouse egg and suppresses repetitive calcium transients in the fertilized egg. J. Biol. Chem. 267:17624-17630.

Kline, J.T., and Kline, D. 1994. Regulation of intracellular calcium in the mouse egg: Evidence for inositol trisphosphate-induced calcium release, but not calcium-induced calcium release. Biol. Reprod. 50:193-203.

Kline, D., and Stewart-Savage, J. 1994. The timing of cortical granule fusion, content dispersal, and endocytosis during fertilization of the hamster egg: an electrophysiological and histochemical study. Dev Biol. 162(1):277-87.

Kline, D., and Zagray, J. 1994. Absence of a significant change in intracellular pH at fertilization of the mouse egg. Mol. Biol. Cell 5(suppl.):460a.

Kline, D., and Zagray, J.A. 1995. Absence of an intracellular pH change following fertilization of the mouse egg. Zygote. 3:305-311.

Kobayashi, S., Morgans, C.W., Casey, J.R., and Kopito, R.R. 1994. AE3 anion exchanger isoforms in the vertebrate retina: developmental regulation and differential expression in neurons and glia. J. Neuro. 14:6266-6279.

Kolajova, M., and Baltz, J.M. 1999. Volume-regulated anion and organic osmolyte channels in mouse zygotes. Biol. Reprod. 60:964-972.

Kollert-Jons, A., Wagner, S., Hubner, S., Appelhans, H., and Drenckhahn, D. 1993. Anion exchanger 1 in human kidney and oncocytoma differs from erythroid AE1 in its NH2 terminus. Am. J. Physiol. 265:F813-F821.

Kono, T., Carroll, J., Swann, K., and Whittingham, D.G. 1995. Nuclei from fertilized mouse embryos have calcium-releasing activity. Develop. 121:1123-1128.

Kopito, R.R., and Lodish, H.F. 1985. Primary structure and transmembrane orientation of the murine anion exchange protein. Nature. 316:234-238.

Kopito, R.R., Lee, B.S., Simmons, D.M., Lindsey, A.E., Morgans, C.W., and Schneider, K. 1989. Regulation of intracellular pH by a neuronal homolog of the erythrocyte anion exchanger. Cell. 59:927-937.

Kubiak, J.Z., Weber, M., de Pennart, H., Winston, N.J., and Maro, B. 1993. The metaphase II arrest in mouse oocytes is controlled through microtubule-dependent destruction of cyclin B in the presence of CSF. EMBO J. 12:3773-3778.

Kubota, H.Y., Yoshimoto, Y., and Hiramoto, Y. 1993. Oscillation of intracellular free calcium in cleaving and cleavage-arrested embryos of *Xenopus laevis*. Dev. Biol. 160:512-518.

Kudrycki, K.E., and Shull, G.E. 1989. Primary structure of the rat kidney band 3 anion exchange protein deduced from a cDNA. J. Biol. Chem. 264:8185-8192.

Kudrycki, K.E., Newman, P.R., and Shull, G.E. 1990. cDNA cloning and tissue distribution of mRNAs for two proteins that are related to the band 3 Cl^-/HCO_3^- exchanger. J. Biol. Chem. 265:462-471.

Kudrycki, K.E., and Shull, G.E. 1993.Rat kidney band 3 Cl-/HCO3- exchanger mRNA is transcribed from an alternative promoter. Am J Physiol. 264:F540-F547.

Kurtz, I., and Golchini, K. 1987. Na^+- independent Cl^--HCO_3^- exchange in Madin-Darby canine kidney cells. J. Biol. Chem. 262:4516-4520.

L'Allemain, G., Paris, S., and Pouyssegur, J. 1984. Growth factor action and intracellular pH regulation in fibroblasts. Evidence for a major role of the Na^+/H^+ antiport. J. Biol. Chem. 259:5809-5815.

Lane, M., Baltz, J.M., and Bavister, B.D. 1998. Regulation of intracellular pH in hamster preimplantation embryos by the sodium hydrogen (Na^+/H^+) antiporter. Biol. Reprod. 59:1483-1490.

Lane, M., Baltz, J.M., and Bavister, B.D. 1999a. Na^+/H^+ antiporter activity in hamster embryos is activated during fertilization. Dev Biol. 208:244-252.

Lane, M., Baltz, J.M., and Bavister, B.D. 1999b. Bicarbonate/chloride exchange regulates intracellular pH of embryos not oocytes of hamster. Biol. Reprod. 61:452-457.

Latham, K.E., Rambhatla, L., Hayashizaki, Y., and Chapman, V.M. 1995. Stage-specific induction and regulation by genetic imprinting of the imprinted mouse U2afbp-rs gene in the preimplantation mouse embryo. Dev. Biol. 168:670-676.

Lau, A.F., Rayson, T.C., and Humphreys, T. 1986. Tumor promoters and diacylglycerol activate the Na^+/H^+ antiporter of sea urchin eggs. Exp. Cell Res. 166:23-30.

Law, F.Y., Steinfeld, R., and Knauf, P.A. 1983. K562 cell anion exchange differs markedly from that of mature red blood cells. Am. J. Physiol. 244:C68-C74.

Lawitts, J.A., and Biggers, J.D. 1993. Culture of Preimplantation Embryos. Methods in Enzymology. 225:153-164.

Lee, B.S., Gunn, R.B., and Kopito, R.R. 1991. Functional differences among nonerythroid HCO_3^-/Cl^- exchangers expressed in a transfected human cell line. J. Biol. Chem. 266:11448-11454.

Lee, S.C., and Steinhardt, R.A. 1981. pH changes associated with meiotic maturation in oocytes of *Xenopus laevis*. Dev. Biol. 85:358-69.

Leese, H. 1988. The formation and function of oviduct fluid. J. Reprod. Fertil. 82:843-856.

Levasseur, M., and McDougall, A. 2000. Sperm-induced calcium oscillations at fertilization in ascidians are controlled by cyclin B1-dependent kinase activity. Develop. 127:631-641.

Lindsey, A.E., Schneider, K., Simmons, D.M., Baron, R., Lee, B.S., and Kopito, R.R. 1990. Functional expression and subcellular localization of an anion exchanger cloned from choroid plexus. Proc. Natl. Acad. Sci. 87:5278-5282.

Lin, X., and Barber, D.L. 1996. A calcineurin homologous protein inhibits GTPase-stimulated Na-H exchange. Proc. Natl. Acad. Sci. 93:12631-12636.

Linn, S.C., Kudrycki, K.E., and Shull, G.E. 1992. The predicted translation product of a cardiac AE3 mRNA contains an N terminus distinct from that of the brain AE3 Cl^-/HCO_3^- exchanger. Cloning of a cardiac AE3 cDNA, organization of the AE3 gene, and identification of an alternative transcription initiation site. J. Biol. Chem. 267:7927-7935.

Loeb, J. 1906. Weiter Beobachtungen über den Einfluss der Befruchtung und der Zahl der Zellkerne auf die Saurefildung im Ei. Biochem. Z. 2:34.

Loeb, J. 1913. Artificial Parthenogenesis. University of Chicago Press, Chicago.

Lopo, Alina and Victor D. Vacquier. 1977. The rise and fall of intracellular pH of sea urchin eggs after fertilization. Nature 269:590-592.

Lorca, T., Galas, S., Fesquet, D., Devault, A., Cavadore, J.C. and Dorée, M. 1991. Degradation of the proto-oncogene product p39mos is not necessary for cyclin proteolysis and exit from meiotic metaphase: requirement for a Ca^{2+} calmodulin dependent event. EMBO J. 10:2087-2093.

Luna, E.J., and Hitt, A.L. 1992. Cytoskeleton-plasma membrane interactions. Science. 258(5084):955-64.

Maas, D.H., Stein, B., Metzger, H., and Schneider, U. 1987. Influence of microsurgical reanastomosis of the fallopian tube on luminal pH and PO_2 and on the fertilization rate and embryo development in the rabbit oviduct. Eur. J. Obstet. Gynecol. Reprod. Biol. 24:73-83.

Maas, D., Storey, B., and Mastroianni, L. 1977. Hydrogen ion and carbon dioxide content in the oviductal fluid of the rhesus monkey. Fert. Steril. 28:981-985.

Maas, D.H., Stein, B., and Metzger, H. 1984. PO_2 and pH measurements within the rabbit oviduct following tubal microsurgery: reanastomosis of previously dissected tubes. Adv. Exp. Med. Biol. 169:561-70

Macháty, Z., Bonk, A.J., Kühholzer, B., and Prather, R.S. 2000. Porcine oocyte activation induced by a cytosolic sperm factor. Mol. Reprod. Develop. 57:290-295.

MacPhee, D.J., Jones, D.H., Barr, K.J., Betts, D.H., Watson, A.J., and Kidder, G.M. 2000. Differential involvement of Na^+,K^+-ATPase isozymes preimplantation development of the mouse. Dev. Biol. 222:486-498.

Manejwala, F.M., Cragoe Jr., E.J., and Schultz, R.M. 1989. Blastocoel expansion in the preimplantation mouse embryo: Role of extracellular sodium and chloride, and possible apical routes of their entry. Dev. Biol. 133:210-20.

Maro, B., Johnson, M.H., and Pickering S.J. 1985. Changes in the distribution of membranous organelles during mouse early development. J. Embryol. Exp. Morphol. 90:287-309.

Masui, Y., and Markert, C.L. 1971. Cytoplasmic control of nuclear behavior during meiotic maturation of frog oocytes. J. Exp. Zool. 177:129-146.

Mazia, D. 1937. The release of calcium in *Arbacia* eggs upon fertilization. J. Cell Comp. Phys. 10:291-304.

McCulloh, D.H., and Chambers, E.L. 1992. Fusion of membranes during fertilization: increases of sea urchin egg's membrane capacitance and membrane conductance at the site of contact with the sperm. J. Gen. Physiol. 99:137-175.

McGuinness, O.M., Moreton, R.B., Johnson, M.H., and Berridge, M.J. 1996. A direct measurement of increased divalent cation influx in fertilised mouse oocytes. Develop. 122:2199-206.

Michaely, P., and Bennett, V. 1995a. The ANK repeats of erythrocyte ankyrin form two distinct but cooperative binding sites for the erythrocyte anion exchanger. J. Biol. Chem. 270(37):22050-7.

Michaely, P., and Bennett, V. 1995b. Mechanism for binding site diversity on ankyrin. Comparison of binding sites on ankyrin for neurofascin and the Cl-/HCO3- anion exchanger. J. Biol. Chem. 270:31298-31302.

Miyazaki, S. 1990. Cell signalling at fertilization of hamster eggs. J. Reprod. Fert.Suppl. 42:163-175.

Miyazaki, S., Yuzaki, M., Nakada, K., Shirakawa, H., Nakanishi, S., Nakade, S., and Mikoshiba, K. 1992. Block of Ca^{++} wave and Ca^{++} oscillation by antibody to the inositol 1,4,5-triphosphate receptor in fertilized hamster eggs. Science. 257:251-256.

Miyazaki, S. 1991. Repetitive calcium transients in hamster oocytes. Cell Calcium. 12:205-216.

Moolenaar, W.H., Tsien, R.Y., van der Saag, P.T., and de Laat, S.W. 1983. Na^{+}/H^{+} exchange and cytoplasmic pH in the action of growth factors in human fibroblasts. Nature. 304:645-648.

Moore, G.D., Kopf, G.S., and Schultz R.M. 1993. Complete mouse egg activation in the absence of sperm by stimulation of an exogenous G protein-coupled receptor. Dev. Biol. 159:669-678.

Moos, J., Visconti, P.E., Moore, G.D., Schultz, R.M. and Kopf, G.S. 1995. Potential role of mitogen-activated protein kinase in pronuclear envelope assembly and disassembly following fertilization of mouse eggs. Biol. Reprod. 53:692-699.

Moos, J., Kopf, G.S., and Schultz, R.M. 1996. Cylcoheximide-induced activation of mouse eggs: effects on cdc2/cyclin B and MAP kinase activities. J. Cell Sci. 109:739-748.

Moos, J., Xu, Z., Schultz, R.M., and Kopf, G.S. 1996b. Regulation of nuclear envelope assembly/disassembly by MAP kinase. Dev. Biol. 175:358-361.

Néant, I., and Guerrier, P. 1988. Meiosis reinitiation in the mollusc *Patella vulgata*. Regulation of MPF, CSF and chromosome condensation activity by intracellular pH, protein synthesis and phosphorylation. Develop. 102:505-516.

Noel, J., Roux, D., and Pouyssegur, J. 1996. Differential localization of Na^+/H^+ exchanger isoforms (NHE1 and NHE3) in polarized epithelial cell lines. J. Cell Sci. 109:929-939.

Nord, E.P., Brown, S.E.S. and Crandall, E.D. 1988. Cl^-/HCO_3^- exchange modulates intracellular pH in rat type II alveolar epithelial cells. J. Biol. Chem. 263:5599-5606.

Oh, B., Hampl, A., Eppig, J.J., Solter, D., and Knowles, B.B. 1998. SPIN, a substrate in the MAP kinase pathway in mouse oocytes. Mol. Reprod. Dev. 50:240-249.

Ohsugi, M., Ohsawa, T., and Yamamura, H. 1993. Involvement of protein kinase C in nuclear migration during compaction and the mechanism of the migration: analyses in two-cell mouse embryos. Dev. Biol. 156:146-154.

Olsnes, S., Tonnesen, T.I., and Sandvig, K. 1986. pH-regulated anion antiport in nucleated mammalian cells. J. Cell Biol. 102:967-971.

Olsnes, S., Tonnessen, T.I., Ludt, J., and Sandvig, K. 1987. Effect of intracellular pH on the rate of chloride uptake and efflux in different mammalian cell lines. Biochem. 26:2778-2785.

Orlowski, J. 1993. Heterologous expression and functional properties of amiloride high affinity (NHE-1) and low affinity (NHE-3) isoforms of the rat Na^+/H^+ exchanger. J. Biol. Chem. 268(22):16369-16377.

Orlowski, J., and Kandasamy, R.A. 1996. Delineation of transmembrane domains of the Na^+/H^+ exchanger that confer sensitivity to pharmacological antagonists. J. Biol. Chem. 271:19922-19927.

Orlowski, J. and Grinstein, S. 1997. Na^+/H^+ exchangers of mammalian cells. J. Biol. Chem. 272:22373-22376.

Palmer, A., Gavin, A.-C., and Nebreda, A.R. 1998. A link between MAP kinase and $p34^{cdc2}$/cyclin B during oocyte maturation: $p90^{rsk}$ phosphorylates and inactivates the $p34^{cdc2}$ inhibitory kinase Myt1. EMBO J. 17:5037-5047.

Paris, S., and Poussegur, J. 1983. Biochemical characterization of the amiloride-sensitive Na^+/H^+ antiport in Chinese hamster lung fibroblasts. J. Biol. Chem. 258:3503-3508.

Pauken, C.M., and Capco, D.G. 1999. Regulation of cell adhesion during embryonic compaction of mammalian embryos: roles for PKC and beta-catenin. Mol Reprod Dev. 54(2):135-44.

Paul, Miles. 1975. Release of acid and changes in light-scattering properties following fertilization of Urechis caupo eggs. Dev. Biol. 43:299-312.

Payan, P., Girard, J.-P., Christen, R., and Sardet, C. 1981. Na^+ movements and their oscillations during fertization and the cell cycle in sea urchin eggs. Exp. Cell Res. 134:339-344.

Payan, P., Girard, J.-P., and Ciapa, B. 1983. Mechanisms regulating intracellular pH in sea urchin eggs. Dev. Biol. 100:29-38.

Pelech, S.L., and Sanghera, J.S. 1992. MAP kinases: charting the regulatory pathways. Science. 257:1355-1356.

Peter, M., Sanghera, J.S., Pelech, S.L., and Nigg, E.A. 1992. Mitogen-activated protein kinases phosphorylatenulcear lamins and display sequence specificity overlapping that of mitotic protein kinase $p34^{cdc2}$. Eur. J. Biochem. 205:287-294.

Petronilli, V., Nicolli, A., Costantini, P., Colonna, R., and Bernardi, P. 1994. Regulation of the permeability transition pore, a voltage-dependent mitochondrial channel inhibited by cyclosporin A. Biochim. Biophys. Acta. 1187:255-259.

Phillips, K.P. and Baltz, J.M. 1996. An intracellular pH increase does not accompany egg activation in the mouse. Mol. Reprod. Develop. 45:52-60.

Phillips, K.P., Zhou, W.L. and Baltz, J.M. 1998. Fluorophore toxicity in mouse eggs and embryos. Zygote. 6:113-123.

Phillips, K.P., and Baltz, J.M. 1999. Intracellular pH regulation by HCO_3^-/Cl^- exchange is activated during early mouse zygote development. Dev. Biol. 208:392-405.

Phillips, K.P., Léveillé, M-C, Claman, P.C., and Baltz, J.M. 2000. Intracellular pH regulation in the human preimplantation embryo. Hum. Reprod. 15:896-904.

Poenie, M., Alderton, J., Tsien, R.Y., and Steinhardt, R.A. 1985. Changes in free calcium with stage of the cell division cycle. Nature. 315:147-149.

Pucéat, M., Clement, O, and Vassort, G. 1991. Extracellular MgATP activates the Cl^-/HCO_3^- exchanger in single rat cardiac cells. J. Physiol. 444:241-256.

Pucéat, M., Korichneva, I., Cossoly, R. and Vassort, G. 1995. Identification of band 3-like proteins and Cl^-/HCO_3^- exchange in isolated cardiomyocytes. J. Biol. Chem. 270:1315-1322.

Pucéat, M., Roche, S., and Vassort, G. 1998. Src family tyrosine kinase regulates intracellular pH in cardiomyocytes. J. Cell Biol. 141:1637-1646.

Putnam, Robert. 1988. Basic principles of pH regulation. Na^+/H^+ Exchange. ed. Sergio Grinstein. C.R.C. Press. Boca-Raton, USA.

Qu, J., Godin, P.A., Nisolle, M., and Donnez, J. 2000. Distribution and epidermal growth factor receptor expression of primordial follicles in human ovarian tissue before and after cryopreservation. Hum. Reprod. 15:302-310.

Ramamoorthy, S., Tirruppathi, C., Nair, C.N., Mahesh, V.B., Leibach, F.H., and Ganapathy, V. 1991. Relative sensitivity to inhibition by cimetidine and clonidine differentiates between the two types of Na^+-H^+ exchangers in cultured cells. Biochem. J. 280:317-322.

Rattanachaiyanont, M., Leader, A. and Léveillé, M-C. 1999. Lack of correlation between oocyte-corona-cumulus complex morphology and nuclear maturity of oocytes collected in stimulated cycles for intracytoplasmic sperm injection. Fertil.Steril. 71:937-940.

Reithmeier, R.A.F. 1994. Mammalian exchangers and co-transporters. Curr. Opion. Cell Biol. 6:583-594.

Reuss, L. 1987.Cyclic AMP inhibits Cl^-/HCO_3^- exchange at the apical membrane of *Necturus* gallbladder epithelium. J. Gen. Physiol. 90:173-196.

Rezai, K., Kulisz, A., and Wasserman, W.J. 1994. Protooncogene product, c-mos kinase, is involved in upregulating Na^+/H^+ antiporter in *Xenopus* oocytes. Am. J. Physiol. 267:C1717-22

Rezai, K., and Wasserman, W.J. 1994. Forskolin and methylxanthines block the increase in intracellular pH during meiosis in *Xenopus laevis* oocytes. Biochem. Biophys. Res. Commun. 205:979-83.

Rimon, A., Gerchman, Y., Olami, Y., Schuldiner, S., and Padan, E. 1995. Replacements of histidine 226 of NhaA-Na^+/H^+ antiporter of *Escherichia coli*: cysteine (H226C) or serine (H226S) retain both normal activity and pH sensitivity, aspartate (H226A) inactivates the carrier at all pH values. J. Biol. Chem. 270:26813-26817.

Roblero, L.S., Riffo, M.D., and Croxatto, H.B. 1989. Cumulus cell dispersion induced by estradiol in mouse oviduct in vitro. Gam. Res. 23:467-473.

Roos, A., and Boron, W.F. 1981. Intracellular pH. Phys. Rev. 61:296-434.

Rose-Hellekant, T.A., and Bavister, B.D. 1996. Precocious oocyte maturation is induced by an inhibitor of cAMP-dependent protein kinase in the intact golden hamster. Mol. Reprod. Develop. 44:250-255.

Ruddock, N.T., Macháty, Z., Milanick, M., and Prather, R.S. 2000. Mechanism of intracellular pH increase during parthenogenetic activation of in vitro matured porcine oocytes. Biol. Reprod. 63:488-492.

Ruiz, O.S., Brooks Robey, R., Qiu, Y-Y., Wang, L., Li, C., Ma, J., and Arruda, J.A.L. 1999. Regulation of the renal Na^+-HCO_3^- cotransporter. XI. Signal tranduction underlying CO_2 stimulation. Am. J. Physiol. 277:F580-F586.

Sahai, E., Alberts, A.S., and Treisman, R. 1998.RhoA effector mutants reveal distinct effector pathways for cytoskeletal reorganization, SRF activation and transformation. EMBO J. 17:1350-1361.

Sardet, C., Fafournoux, P., and Pouyssegur, J. 1991. Alpha-thrombin, epidermal growth factor, and okadaic acid activate the Na^+/H^+ exchanger, NHE-1, by phosphorylating a set of common sites. J Biol Chem. 266:19166-19171.

Sardet, C., Counillon, L., Franchi, A., and Pouyssegur, J. 1990. Growth factors induce phosphorylation of the Na^+/H^+ antiporter, glycoprotein of 110 kD. Science. 247:723-726.

Schatten, H., Simerly,C., Maul G., and Schatten, G. 1989. Microtubule assembly is required for the formation of the pronuclei, nuclear lamin acquisition, and DNA synthesis during mouse, but not sea urchin, fertilization. Gam. Res. 23:309-322.

Schultheis, P.J., Clarke, L.L., Meton, P., Harline, M., Boivin, G.P., Stemmermann,G., Duffy, J.J., Doetschman, T., Miller, M.L., and Shull, G.E. 1998. Targeted disruption of the murine Na^+/H^+ exchanger isoform 2 gene causes reduced viability of gastric parietal cells and loss of net acid secretion. J. Clin. Invest. 101:1243-1253.

Schultz, R.M, and Wassarman, P.M. 1977. Specific changes in the pattern of protein synthesis during meiotic maturation of mammalian oocytes in vitro. Proc. Natl. Acad. Sci. 74:538-41.

Schultz, R.M., Montgomery, R.R., Ward-Bailey, P.F. and Eppig, J.J. 1983a. Regulation of oocyte maturation in the mouse: posssible roles of intercellular communication, cAMP, and testosterone. Dev. Biol. 95:294-304.

Schultz, R.M., Montgomery, R.R., and Belanoff, J.R. 1983b. Regulation of mouse oocytes meiotic maturation, implication of a decrease in oocyte cAMP and protein dephosphorylation in commitment to resume meiosis. Dev. Biol. 97:264-273.

Schultz, R.M., and Worrad, D.M. 1995. Role of chromatin structure in zygotic gene activation in the mammalian embryo. Semin. Cell Biol. 6:201-208.

Schuster, V.L., and Stokes, J.B. 1987. Chloride transport by the cortical and outer medullary collecting duct. Am. J. Physiol. 253:F203-212.

Schwartz, D.A., and Schultz, R.M. 1991. Stimulatory effect of okadaic acid, an inhibitor of protein phosphatases, on nuclear envelope breakdown and protein phosphorylation in mouse oocytes and one-cell embryos. Dev. Biol. 145:119-127.

Séguin, D.G., and Baltz, J.M. 1997. Cell volume regulation by the mouse zygote: mechanism of recovery from a volume increase. Am. J. Cell Phys. 41:C1854-C1861.

Sekler, I., Lo, R.S., Mastrocola, T., and Kopito, R.R. 1995a. Sulfate transport mediated by the mammalian anion exchangers in reconstituted proteoliposomes. J. Biol. Chem. 270(19):11251-6.

Sekler, I., Lo, R.S., and Kopito, R.R. 1995b. A conserved glutamate is responsible for ion selectivity and pH dependence of the mammalian anion exchangers AE1 and AE2. J. Biol. Chem. 270(48):28751-8.

Sekler, I., Kobayashi, S., and Kopito, R.R. 1996. A cluster of cytoplasmic histidine residues specifies pH dependence of the AE2 plasma membrane exchanger. Cell. 86:929-935. ***retracted; Cell. 1997. 90:6****

Shamsadin, R., Adham, I.M., Nayernia, K., Heinlein, U.A.O., Oberwinkler, H., and Engel, W. 1999. Male mice deficient for germ-cell cyritestin are infertile. Biol. Reprod. 61:1445-1451.

Shen, S.S., and Steinhardt, R.A. 1979. Intracellular pH and the sodium requirement at fertilization. Nature. 282:87-89.

Shen, S.S., and Steinhardt, R.A. 1980. Intracellular pH controls the development of new potassium conductance after fertilization of the sea urchin egg. Exp. Cell Res. 125:55-61.

Shen, S.S. 1989. Na^+/H^+ antiport during fertilization of the sea urchin egg is blocked by W-7 but is insensitive to K52a and H-7. Biochem. Biophys. Res. Comm. 161:1100-1108.

Shen, S.S., and Buck, W.R. 1990. A synthetic peptide of the pseudosubstrate domain of protein kinase C blocks cytoplasmic alkalinization during activation of the sea urchin egg. Dev. Biol. 140(2):272-80.

Shirayoshi, Y., Okada, T.S., and Takeichi, M. 1983. The calcium-dependent cell-cell adhesion system regulates inner cell mass formation and cell surface polarization in early mouse development. Cell. 35:631-8.

Silva, N.L., Haworth, R.S., Singh, D., and Fliegel, L. 1995. The carboxyl-terminal region of the Na^+/H^+ exchanger interacts with mammalian heat shock protein. Biochemistry. 34(33):10412-20.

Siracusa, G., Whittingham, D.G., Molinaro, M., and Vivarelli, E. 1978. Parthenogenetic activation of mouse oocytes induced by inhibitors of protein synthesis. J. Embrol. exp. Morph. 43:157-166.

Smith, R.K.W., and Johnson, M.H. 1986. Analysis of the third and fourth cell cycles of mouse early development. J. Reprod. Fert. 76:393-399.

Soleimani, M., Singh, G., Bizal, G.L., Gullens, S.R., and McAteer, J.A. 1994. Na^+/H^+ exchanger isoforms NHE-2 and NHE-1 in inner medullary collecting duct cells. Expression, functional localization, and differential regulation. J. Biol. Chem. 269:27973-27978.

Steeves, C.L., Lane, M., Bavister, B., Phillips, K.P., and Baltz, J.M. Intracellular pH regulation in mouse 2-cell embryos by the Na^+/H^+ antiporter. Biol. Reprod. (Accepted with revisions).

Sterling D. and Casey, J.R. 1999. Transport activity of AE3 chloride/bicarbonate anion-exchange proteins and their regulation by intracellular pH. Biochem. J. 344:221-229.

Stice, S.L., Keefer, C.L, and Matthews, L. 1994. Bovine nuclear transfer embryos: oocyte activation prior to blastomere fusion. Mol. Reprod. Develop.38:61-68.

Summers, M.C., Bhatnagar, P.R., Lawitts, J.A., and Biggers, J.D. 1995. Fertilization in vitro of mouse ova from inbred and outbred strains: complete preimplantation embryo development in glucose-supplemented KSOM. Biol. Reprod. 53:431-437.

Sun, A.M., Liu, Y., Dworkin, L.D., Tse, C.M., Donowitz, M., and Yip, K.P. 1997. Na/H exchanger isoform 2 (NHE2) is expressed in the apical membrane of the medullary thick ascending limb. J. Membr. Biol. 160:85-90.

Suprenant, Kathy A. 1989. Alkaline pH favors microtubule self-assembly in surf clam, *Spisula solidissima*, oocyte extracts. Exp. Cell Res.184:167-180.

Swann, Karl, and Whitaker, M.J. 1985. Stimulation of the Na^+/H^+ exchanger of sea urchin eggs by phorbol ester. Nature. 314:274-277.

Swann, K., and Whitaker, M.J. 1986. The part played by inositol trisphosphate and calcium in the propagation of the fertilizing wave in sea-urchin eggs. J. Cell Biol. 103:2332-2342.

Swann, K., and Whitaker, M.J. 1990. Second messengers at fertilization in sea-urchin eggs. J. Reprod. Fert. (Suppl.). 42:141-153.

Swann, K. 1990. A cytosolic sperm factor stimulates repetitive calcium increases and mimics fertilization in hamster eggs. Develop. 110(4):1295-1302.

Taieb, F., Thibier, C., and Jessus, C. 1997. On cyclins, oocytes, and eggs. Molec. Reprod. Develop. 48:397-411.

Takahashi, E., Abe, J., Gallis, B., Aebersold, R., Spring, D.J., Krebs, E.G., and Berk, B.C. 1999. $p90^{RSK}$ is a serum-stimulated Na^+/H^+ exchanger iosoform-1 kinase. Regulatory phosphorylation of serine 703 of Na^+/H^+ exchanger isoform-1. J. Biol. Chem. 274:20206-20214.

Tang, X.B., Fujinaga, J., Kopito, R., and Casey, J.R. 1998. Topology of the region surrounding Glu681 of human AE1 protein, the erythrocyte anion exchanger. J. Biol. Chem. 273(35):22545-53.

Tatone, Carla, van Eekelen, Christina Grietje, and Colonna, Rosella. 1994. Plasma membrane block to sperm entry occurs in mouse eggs upon parthenogenetic activation. Mol. Reprod. Develop. 38:200-208.

Telford, N.A., Watson, A.J. and Schultz, G.A.1990. Transition from maternal to embryonic control in early mammalian development: a comparison of several species. Mol. Reprod. Dev. 26:90-100.

Tesarik, J. 1998. Sperm-induced calcium oscillations. Oscillin - reopening the hunting season. Mol. Hum. Reprod. 4:1007-1012.

Tesarik, J., Sousa, M., and Testart, J. 1994. Human oocyte activation after intracytoplasmic sperm injection. Hum. Reprod. 9:511-518.

Thomas, J.A., Buchsbaum, R.N., Zimniak A., and Racker, E. 1979. Intracellular pH measurements in erhlich ascites tumor cells utilizing spectroscopic probes generated in situ. Biochem. 18:2210-2218.

Tombes, R.M., Simerly, C., Borisy, G.C., and Schatten, G. 1992. Meiosis, egg activation, and nuclear envelope breakdown are differentially reliant on Ca^{2+}, whereas germinal vesicle breakdown is Ca^{2+}-independent in the mouse. J. Cell Biol. 117:799-811.

Tonnessen, T.I., Sandvig, K., and Olsnes, S. 1990. Role of Na^+/H^+ and Cl^- HCO^- antiports in the regulation of cytoplasmic pH near neutrality. Am. J. Physiol. 258:C1117-C1126.

Van Winkle, Lon J. 1999. Selected techniques in membrane transport. In: Biomembrane Transport. Academic Press. San Diego. CA. pg. 338-339.

Vaughn-Jones, R.D. 1986. Anion exchange in sheep Purkinje fibers. J. Physiol. 379:377-406.

Verkman, A.S. 1990. Development and biological applications of chloride-sensitive fluorescent indicators. Am. J. Phys. 259: C375-C388.

Verlhac, M.H., De Pennart, H., Maro, B., Cobb, M.H., and Clarke, H.J. 1993. MAP kinase becomes stably activated at metaphase and is associated with microtubule-organizing centers during meiotic maturation of mouse oocytes. Dev. Biol. 158:330-340.

Verlhac, M.H., Kubiak, J.Z., Clarke, H.J., and Maro, B. 1994. Microtubule and chromatin behavior follow MAP kinase activity but not MPF activity during meiosis in mouse oocytes. Develop. 120:1017-1025.

Verlhac, M.H., Kubiak, J.Z., Weber, M., Geraud, G., Colledge, W.H., Evans, M.J. and Maro, B. 1996. Mos is required for MAP kinase activation and is involved in microtubule organization during meiotic maturation in the mouse. Develop. 122:815-822.

Vestweber, D., Gossler, A., Boller, K., and Kemler R. 1987. Expression and distribution of cell adhesion molecule uvomorulin in mouse preimplantation embryos. Dev Biol. 124:451-6.

Vigne, P., Frelin, C., Audinot, M., Borsotto, M., Cragoe Jr, E.J., and Lazdunski, M. 1984. [3H]ethylpropylamiloride, a radio-labelled diuretic for the analysis of the Na^+/H^+ exchange system. Its use with kidney cell membranes. EMBO J. 3:2647-51.

Vigne, P., Breittmayer, J-P., Frelin C., and Lazdunski, M. 1988. Dual control of the intracellular pH in aortic smooth muscle cells by a cAMP-sensitive HCO_3^-/Cl^- antiporter and a protein kinase C-sensitive Na^+/H^+ antiporter. J. Biol. Chem. 263,18023-18029.

Vincent, C., Cheek, T.R., and Johnson, M.H. 1992. Cell cycle progression of parthenogenetically activated mouse oocytes to interphase is dependent on the level of internal calcium. J. Cell Sci. 103:389-396.

Visconti, P.E., Bailey, J.L., Moore, G.D., Pan, D., Olds-Clarke, P., and Kopf, G.S. 1995a. Capacitation of mouse spermatozoa. I. Correlation between the capacitation state and protein tyrosine phosphorylation. Develop. 121:1129-1137.

Visconti, P.E., Moore, G.D., Bailey, J.L., Leclerc, P., Connors, S.A., Pan, D., Olds-Clarke, P., and Kopf, G.S. 1995b. Capacitation of mouse spermatozoa. II. Protein tyrosine phosphorylation and capacitation are regulated by a cAMP-dependent pathway. Develop. 1139-1150.

Wakabayashi, S., Fafournoux, P., Sardet, C., and Pouyssegur, J. 1992. The Na^+/H^+ antiporter cytoplasmic domain mediates growth factor signals and controls "H^+-sensing". Proc. Natl. Acad. Sci. 89(6):2424-8.

Wakabayashi, S., Ikeda, T., Noel, J., Schmitt, B., Orlowski, J., Pouyssegur, J., and Shigekawa, M. 1995. Cytoplasmic domain of the ubiquitous Na^+/H^+ exchanger NHE1 can confer Ca^{2+} responsiveness to the apical isoform NHE3. J. Biol. Chem. 270:26460-5.

Wandji, S.-A., Sršeň, V., Nathanielsz, P.W., Eppig, J.J., and Fortune, J.E. 1997. Initiation of growth of baboon primordial follicles in vitro. Hum. Reprod. 12:1993-2001.

Wang, Z., Schultheis P.J. and Shull. G.E.1996. Three N-terminal variants of the AE2 Cl^-/HCO_3^- exchanger are encoded by mRNAs transcribed from alternative promoters. J. Biol. Chem. 271:7835-7843.

Watanabe, N., Vande Woude, G.F., Ikawa, Y., and Sagata, N. 1989. Specific proteolysis of the c-mos proto-oncogene product by calpain on fertilization of Xenopus eggs. Nature. 342:505-511.

Watson, A.J., Pape, C., Emanuel, J.R., Levenson, R., and Kidder, G.M. 1990. Expression of Na, K-ATPase α and β subunit genes during preimplantation development of the mouse. Dev. Genet. 11:41-48.

Webb, D.J., and Nuccitelli, R. 1981. Direct measurement of intracellular pH changes in Xenopus eggs at fertilization and cleavage. J. Cell Biol. 91:562-7.

Wenzl, E., and Machen, T. 1989. Intracellular pH dependence of buffer capacity and anion exchange in the parietal cell. Am. J. Physiol. 257:G741-G747.

Whitaker, M., and Patel, R. 1990. Calcium and cell cycle control. Develop. 108:525-542.

Whitaker, M.J., and Steinhardt, R.A. 1981. The relation between the increase in reduced nicotinamide nucleotides and the initiation of DNA synthesis in sea urchin eggs.Cell. 25:95-103.

Whitaker, M.J., and Irvine, R.F. 1984. Inositol-1,4,5 trisphosphate microinjection activates sea urchin eggs. Nature, Lond. 312:636-639.

Wianny, F., and Zernicka-Goetz, M. 2000. Specific interference with gene function by double-stranded RNA in early mouse development. Nat. Cell Biol. 2(2):70-5.

Winkel, G.K., Ferguson, J.E., Takeichi, M., and Nuccitelli, R. 1990. Activation of protein kinase C triggers premature compaction in the four-cell stage mouse embryo. Dev. Biol. 138:1-15.

Winkler, M.M., and Grainger, J.L. 1978. Mechanism of action of NH_4Cl and other weak bases in the activation of sea urchin eggs. Nature. 273:536-538.

Winston, N., Johnson, M., Pickering, S., and Braude, P. 1991. Parthenogenetic activation and development of fresh and aged human oocytes. Fert. Steril. 56(5):904-12.

Winston, N.J., McGuinness, O., Johnson, M.H. and Maro, B. 1995a. The exit of mouse oocytes from meiotic M-phase requires an intact spindle during intracellular calcium release. J. Cell Sci. 108:143-151.

Winston, N.J., and Maro, B. 1995b. Calmodulin-dependent protein kinase II is activated transiently in ethanol-stimulated mouse oocytes. Dev Biol. 170(2):350-2.

Xu, Z., Kopf, G.S., and Schultz, R.M. 1994. Involvement of inositol 1,4,5-trisphosphate-mediated Ca^{2+} release in early and late events of mouse activation. Develop. 120:1851-1859.

Yanagimachi, R. 1988. Mammalian Fertilization. The Physiology of Reproduction. ed. E.Knobil and J. Neill et al. Raven Press, Ltd. New York.

Yannoukakos, D., Stuart-Tilley, A., Fernandez, H.A., Fey, P., Duyk, G., and Alper, S.L. 1994. Molecular cloning, expression, and chromosomal localization of two isoforms of the AE3 anion exchanger from human heart. Circ. Res. 75:603-614.

Yu, F.H., Shull, G.E., and Orlowski, J. 1993. Functional properties of the rat Na/H exchanger NHE-2 isoform expressed in Na/H excahnger deficient Chinese hamster ovary cells. J. Biol. Chem. 268:25536-25541.

Yu, H., and Ferrier, J. 1995. Osteoclast ATP receptor activation leads to a transient decrease in intracellular pH. J. Cell Sci. 108:3051-3058.

Zernicka-Goetz, M., Ciemerych, M.A., Kubiak, J.Z., Tarkowski, A.K. and Maro, B. 1995. Cytostatic factor inactivation is induced by a calcium-dependent mechanism present until the second cell cycle in fertilized but not in parthenogenetically activated mouse eggs. J. Cell Sci. 108:469-474.

Zernicka-Goetz, M., Verlhac, M-H, Géraud, G., and Kubiak, J.Z. 1997. Protein phosphatases control MAP kinase activation and microtubule organization during rat oocyte maturation. Eur. J. Cell Biol. 72:30-38.

Zhang, Y., Chernova, M.N., Stuart-Tilley, A.K., Jiang L., and Alper, S.L. 1996. The cytoplasmic and transmembrane domains of AE2 both contribute to regulation of anion exchange by pH. J. Biol. Chem. 271(10):5741-5749.

Zhao, Y., Chauvet, P.J-P., Alper, S.L. and Baltz, J.M. 1995. Expression and function of bicarbonate/chloride exchangers in the preimplantation mouse embryo. J. Biol. Chem. 270:24428-24434.

Zhao, Y., and Baltz, J.M. 1996. Characterization of bicarbonate/chloride exchange during preimplantation mouse embryo development. Am. J. Phys. 271:C1512-C1520.

Zhao, Y., Doroshenko, P.A., Alper, S.L., and Baltz, J.M. 1997. Routes of Cl^- transport across the trophectoderm of the mouse blastocyst. Dev. Biol. 189:148-160.

Zhu, X., Bansal, N.P., and Evans, J.P. 2000. Identification of key functional amino acids of the mouse fertilin β (ADAM2) disintegrin loop for celll-cell adhesion during fertilization. J. Biol. Chem. 275:7677-7683.

BIBLIOGRAPHY

Steeves, C.L., Lane, M., Bavister, B., **Phillips, K.P.**, and Baltz, J.M. Intracellular pH regulation in mouse 2-cell embryos by the Na^+/H^+ antiporter. Biol. Reprod. (In press).

Phillips, K.P., Léveillé, M-C, Claman, PC and Baltz, J.M. 2000. Intracellular pH regulation in the human preimplantation embryo. Hum. Reprod. 15:896-904.

Karen P. Phillips, M-C Léveillé, P Claman and Jay M. Baltz. (2000). Intracellular pH regulation in human preimplantation embryos. Fert. Steril. **72**(3) Suppl.1:S228. Abstract P-427.

Phillips, K.P. and Baltz, J.M. 1999. Intracellular pH regulation by HCO_3^-/Cl^- exchange is activated during early mouse zygote development. Dev. Biol. 208:392-405.

Baltz, J.M., and **Phillips, K.P.** 1999. Intracellular ion measurements in single eggs and embryos using ion-sensitive fluorophores. In, Advances in Molecular Biology, A Comparative Methods Approach to the Study of Oocytes and Embryos (ed. JD Richter). Oxford University Press, Oxford. pp. 39-82.

Phillips, K.P., Zhou, W.L. and Baltz, J.M. 1998. Fluorophore toxicity in mouse eggs and embryos. Zygote. 6:113-123.

Phillips, K.P. and Baltz, J.M. 1996. An intracellular pH increase does not accompany egg activation in the mouse. Mol. Reprod. Develop. 45:52-60.

Phillips, K.P. and Baltz, J.M. 1996. Possible activation of pH regulatory bicarbonate/chloride exchange following fertilization in the mouse. Biol. Reprod. 54(1):72. Abstract 62.

Baltz, J.M., Zhao, Y., and **Phillips, K.P.** 1995. Intracellular pH and its regulation during fertilization and early embryogenesis. Theriogenology. 44:1133-1144.